TECHNISCHE UNIVERSITÄT
ILMENAU

Optimizing the neuroplastic effects of cathodal transcranial direct current stimulation over the primary motor cortex and transferability to prefrontal cortex

Dissertation

zur Erlangung des akademischen Grades

Doktor-Ingenieur

(Dr.-Ing)

vorgelegt der

Fakultät für Infurmatik und Automatisierung der

Technischen Universität Ilmenau

von

M. Sc. Mohsen Mosayebi Samani

geboren am 11.09.1985 in Saman, IRAN

Datum der Einreichung: 14.10.2020

Datum der wissenschaftlichen Aussprache: 07.01.2021

Gutachter: 1. Prof. Dr.-Ing. habil. Jens Haueisen

2. Prof. Dr. med. Michael Nitsche

3. Prof. Dr. Adam Woods

urn:nbn:de:gbv:ilm1-2021000014

To Avicenna

c. 980 – June 1037

Acknowledgements

The completion of this thesis would not have been possible without the dedication and encouragement of many persons, who deserve my sincere gratitude.

I would like to give my thanks to Prof. Dr.-Ing. habil. Jens Haueisen, for his support, valuable advice and constructive criticism, throughout the whole work which helped me to proceed and complete this thesis; to Prof. Dr.-med. Michael A. Nitsche, for his scientific knowledge, ideas, constant support, honest feedback, patience and encouragements, throughout the whole work; to my colleagues and those who scientifically support me: Dr. Min-Fang Kuo, Dr. Asif Jamil, Dr. Giulio Ruffini, Dr. Ricardo Salvador, Dr. Tuomas Mutanen, Desmond Agboada, Lorena Melo, Tobias Blanke, Nina Abich, Ludger Blanke; AND to my lovely family.

The output of the thesis has already been released in three original research papers:

Mosayebi Samani, M., D. Agboada, A. Jamil, M.-F. Kuo and M. A. Nitsche (2019)**.** "*Titrating the neuroplastic effects of cathodal transcranial direct current stimulation (tDCS) over the primary motor cortex.*" Cortex 119: 350-361.

Mosayebi Samani, M., D. Agboada, M. F. Kuo and M. A. Nitsche (2020)**.** "*Probing the relevance of repeated cathodal transcranial direct current stimulation over the primary motor cortex for prolongation of after-effects.*" The Journal of Physiology 598(4): 805-816.

Mosayebi-Samani, M., L. Melo, D. Agboada, M. A. Nitsche and M. F. Kuo (2020)**.** " *Ca2+ channel dynamics explain the nonlinear neuroplasticity induction by cathodal transcranial direct current stimulation over the primary motor cortex*". European Neuropsychopharmacology. In Press

This work was supported by a research grant from the German Federal Ministry of Education and Research (BMBF) (GCBS grant 01EE1501, TRAINSTIM grant 01GQ1424E).

Abstract

Major advances have been made in treatment of neurological and neuropsychiatric disorders; they have however still significant limitations. A vast body of evidence shows a dysregulation or disruption of neuroplasticity in mental and brain disorders. Here, non-invasive brain stimulation techniques come into play, which modulate brain plasticity without disrupting the integrity of the skull. One of those, transcranial direct current stimulation (tDCS), has shown promising results in several pilot clinical studies to improve symptoms of central nervous system disorders; but, in general, effects are often moderate, show nonlinear dosage-dependency, and interindividual variability. For improving the efficacy of this tool, more sustained, and homogeneous effects are required. This requires novel, improved intervention strategies. In addition, neuromodulatory effects of tDCS over the primary motor cortex were largely taken as a template so far for the use of this intervention over other brain regions, whereas a direct exploration of the physiological effects of tDCS on non-motor regions is largely missing.

The thesis aims to address these challenges, by utilizing advanced neurophysiological and computational techniques, aiming to improve the efficacy of cathodal tDCS over the primary motor cortex, but also to explore the transferability of the results to the prefrontal cortex. To this end, we at the ***first step*** systematically titrated cathodal tDCS parameters for the human motor cortex model with different intensities (1, 2, and 3mA) and durations (15, 20 and 30 min). The results revealed intensity-dependent nonlinear effects, in which stimulation with 1 mA induced a significant motor evoked potentials (MEP) amplitude diminution, while stimulation with 2 mA resulted in a significant corticospinal excitability enhancement. Protocols with higher stimulation intensity (specifically stimulation with 3 mA) induced again a significant excitability diminution lasting for about one and half hour after stimulation, and thus were more efficient than the other protocols. At the ***second* step**, we explored if repeated tDCS protocols with different intervals can prolong the after-effects. We compared the impact of single interventions of conventional (1mA for 15min) and optimized cathodal tDCS (3mA for 20min) with the effects of repeated application with intervals of 20 min and 24 hours on primary motor cortex excitability, based on the assumption derived from animal models that short, but not long intervals induce late phase plasticity. The results revealed that the duration of

after-effects of repeated conventional and optimized protocols with short intervals remained nearly unchanged, as compared to the respective single intervention protocols. For the long interval (24 h), stimulation with the conventional protocol did not significantly alter respective after-effects, while it reduced the efficacy of the optimized protocol, as compared with respective single interventions.

One important outcome of the first study were the observed nonlinear intensity-dependent effects of tDCS, which might be an explanation for sometimes heterogeneous outcomes of cathodal stimulation, and are not well explained at the neurophysiological level. At the ***third step*** we therefore explored the underlaying mechanisms of this nonlinearity. Since tDCS generates NMDA receptor-dependent neuroplasticity, which has calcium channel properties, such non-linearity can likely be explained by different levels of calcium concentration induced by the intervention, which control for the directionality of plasticity. We therefore administrated the calcium channel blocker flunarizine in low (2.5 mg), medium (5 mg) or high (10 mg) dosages before cathodal motor cortex tDCS of 3mA for 20min. The results revealed that the inhibitory after-effects induced by high intensity cathodal tDCS were unchanged, diminished, or converted to excitability enhancement with low, medium and high dosages of a calcium blocker, respectively, which confirms the calcium-dependent directionality of tDCS-induced neuroplasticity.

The outcome of the first and second studies showed also relevant inter-individual variability of tDCS effects, which could be another source of limited efficacy of this intervention. Recent human *in-vivo* experiments and computational studies indicated that the tDCS-induced electrical field (EF) depends strongly on individual brain anatomy and tissue conductivity properties. EF variability might thus be an important factor for heterogeneous outcomes of tDCS. At the ***fourth step***, based on neurophysiological data obtained in former studies of our group, which explored tDCS-altered MEP (induced by transcranial magnetic stimulation (TMS)) and cerebral blood flow (CBF; measured by functional magnetic resonance imaging (MRI) via arterial spin labeling), we investigated the association between individual anatomical factors and tDCS-induced EF, and the respective physiological outcomes at the level of the individual. To this end, for each participant, a MRI-based realistic head model was designed to 1) calculate anatomical factors and 2) simulate the tDCS- and TMS-induced electrical fields (EF). We then investigated at the regional

level which individual anatomical factors explain the simulated EFs. Finally, we explored which specific anatomical and/or EF factors predicted the neurophysiological outcomes of tDCS. The results indicated that, of the included anatomical factors, higher EF values were associated with lower electrode to cortex distance (ECD), and cerebrospinal fluid (CSF) thickness. In addition, CSF thickness, and ECD were negatively correlated, whereas EFs were positively correlated with tDCS-induced physiological changes.

Finally, at the ***fifth step***, we explored the transferability of cathodal tDCS-induced neuroplasticity from the motor to the prefrontal cortex. Neurophysiological effects of tDCS have been extensively studied over the primary motor cortex. Much less is however known for its effects over non-motor areas, such as the prefrontal cortex, which is the neuronal foundation for many high-level cognitive functions, and involved in neuropsychiatric disorders. To this end, cathodal tDCS was applied with low, medium, and high dosages, or as sham stimulation, and applied over the primary motor and dorsolateral prefrontal cortex. After-effects of tDCS were evaluated via TMS-electroencephalography (EEG), and TMS-MEP at the regional level, for the outcome parameters TMS-evoked potentials (TEP), TMS-evoked oscillations, and MEP amplitude alterations. The results indicated a dosage-dependent nonlinear neurophysiological effect of motor cortex tDCS, which was not one-to-one transferable to the results of prefrontal tDCS. Low and high dosages of motor cortex tDCS reduced early positive TEP peaks, and MEP amplitudes, while an enhancement was observed for medium dosage motor cortex tDCS (early positive TEP peak and MEP amplitudes). In contrast, prefrontal low, medium and high dosage tDCS uniformly reduced the early positive TEP peak amplitudes. Furthermore, for both cortical areas, tDCS-induced neuromodulatory effects were not observed for late TEP peaks (with the exception of low-dosage prefrontal tDCS), nor TMS-evoked oscillations.

Taken together, using advanced neurophysiological, computational and neuroimaging techniques, this thesis has addressed important challenges regarding tDCS-induced neuroplastic effects, and thus provides new insight for future applications of tDCS in basic and clinical studies.

Zusammenfassung

Die Behandlungsmöglichkeiten neurologischer und neuropsychiatrischer Erkrankungen haben sich in den letzten Jahrzehnten deutlich verbessert, sind aber immer noch eingeschränkt. Eine Dysregulation oder Störung der Neuroplastizität ist bei vielen psychischen und Hirnfunktionsstörungen beteiligt. Hier sind nicht-invasive Hirnstimulationstechniken relevant, die die Plastizität des Gehirns modulieren, ohne die physische Integrität des Schädels zu beeinträchtigen. Eine davon, die transkranielle Gleichstromstimulation (tDCS), hat in mehreren klinischen Pilotstudien vielversprechende Ergebnisse zur Verminderung von Symptomen auf der Grundlage von Störungen des Zentralnervensystems gezeigt. Diese Effekte sind jedoch häufig moderat, zeigen eine nichtlineare Dosisabhängigkeit und eine interindividuelle Variabilität. Um die Wirksamkeit dieses Verfahrens zu verbessern, sind länger anhaltende und homogenere Effekte erforderlich. Dies erfordert neuartige, verbesserte Interventionsstrategien. Darüber hinaus wurden die neuromodulatorischen Wirkungen von tDCS auf den primären motorischen Kortex bisher weitgehend als Grundlage für die Anwendung dieser Intervention auf andere Hirnregionen herangezogen, während eine direkte Untersuchung der physiologischen Wirkungen von tDCS auf nichtmotorische Regionen weitgehend fehlt.

Die Arbeit zielt darauf ab, diese Herausforderungen durch den Einsatz innovativer neurophysiologischer und mathematischer Techniken anzugehen, um die Wirksamkeit des kathodalen tDCS über dem primären motorischen Kortex zu verbessern, aber auch die Übertragbarkeit der Ergebnisse auf den präfrontalen Kortex zu untersuchen. Zu diesem Zweck titrierten wir im ersten Schritt systematisch kathodale tDCS-Parameter für das humane motorische Kortexmodell mit unterschiedlichen Intensitäten (1, 2 und 3 mA) und Stimulationsdauern (15, 20 und 30 min). Die Ergebnisse zeigten intensitätsabhängige nichtlineare Effekte, bei denen die Stimulation mit 1 mA eine signifikante Verringerung der Amplitude der motorisch evozierten Potentiale (MEP) induzierte, während die Stimulation mit 2 mA zu einer signifikanten Erhöhung der kortikospinalen Erregbarkeit führte. Protokolle mit höherer Stimulationsintensität (insbesondere Stimulation mit 3 mA) induzierten erneut eine signifikante Verringerung der Erregbarkeit, die etwa eineinhalb Stunden nach der Stimulation andauerte, und waren daher effizienter als die anderen Protokolle. Im zweiten Schritt haben wir untersucht, ob wiederholte tDCS-Protokolle mit unterschiedlichen Intervallen die Nacheffekte verlängern

können. Wir verglichen die Auswirkungen von Einzelinterventionen mit konventioneller (1 mA für 15 Minuten) und optimierter kathodaler tDCS (3 mA für 20 Minuten) mit den Auswirkungen einer wiederholten Anwendung in Intervallen von 20 Minuten und 24 Stunden auf die Erregbarkeit des primären motorischen Kortex, basierend auf tierexperimentellen Befunden, dass kurze, aber nicht lange Intervalle zwischen einzelnen Interventionen eine langanhaltende Plastizität erzeugen. Die Ergebnisse zeigten, dass die Dauer der Nacheffekte wiederholter konventioneller und optimierter Protokolle mit kurzen Intervallen im Vergleich zu den jeweiligen Einzelinterventionsprotokollen nahezu unverändert blieb. Für das lange Intervall (24 h) veränderte die Stimulation mit dem herkömmlichen Protokoll die jeweiligen Nachwirkungen nicht signifikant, während sie die Wirksamkeit des optimierten Protokolls im Vergleich zu den jeweiligen Einzelinterventionen verringerte.

Ein wichtiges Ergebnis der ersten Studie waren die beobachteten nichtlinearen intensitätsabhängigen Effekte von tDCS, die eine Erklärung für teilweise heterogene Ergebnisse der kathodalen Stimulation bieten können, allerdings hinsichtlich ihrer neurophysiologischen Grundlagen bisher nur unzureichend untersucht waren. Im dritten Schritt haben wir daher die zugrunde liegenden Mechanismen dieser nonlinearen Effekte untersucht. Da tDCS eine NMDA-Rezeptor-abhängige Neuroplastizität erzeugt, die Kalzium-abhängig ist, kann eine solche Nichtlinearität möglicherweise durch unterschiedliche durch die Intervention induzierte Kalziumkonzentrationen erklärt werden, die die Richtung der Plastizität steuern. Wir verabreichten daher den Kalziumkanalblocker Flunarizin in niedrigen (2,5 mg), mittleren (5 mg) oder hohen (10 mg) Dosierungen vor der kathodalen tDCS des motorischen Kortex mit 3 mA für 20 Minuten. Die Ergebnisse zeigten, dass die durch kathodale tDCS hoher Intensität induzierten inhibitorischen Nachwirkungen bei niedrigen, mittleren bzw. hohen Dosierungen eines Kalziumblockers nicht verändert, verringert oder in eine Erregbarkeitserhöhung modifiziert wurden, was die Kalzium-abhängige Direktionalität von tDCS-induzierter Neuroplastizität bestätigt.

Das Ergebnis der ersten und zweiten Studie zeigten eine relevante interindividuelle Variabilität der tDCS-Effekte, die eine weitere Quelle für die begrenzte Wirksamkeit dieser Intervention sein könnte. Jüngste In-vivo-Experimente und Computerstudien am Menschen zeigten, dass das tDCS-induzierte elektrische Feld (EF) stark von der individuellen Anatomie des Gehirns und den Leitfähigkeitseigenschaften des Gewebes abhängt. Die EF-Variabilität könnte daher ein wichtiger Faktor für

heterogene Ergebnisse der tDCS sein. Im vierten Schritt, basierend auf neurophysiologischen Daten, die in früheren Studien unserer Gruppe erhoben wurden, die tDCS-induzierte MEP- (induziert durch transkranielle Magnetstimulation (TMS)) und zerebrale Blutfluss-Veränderungen (CBF; gemessen durch funktionelle Magnetresonanztomographie (MRT) über arterielles Spin-Labelling) erfaßten, untersuchten wir den Zusammenhang zwischen einzelnen anatomischen Faktoren, tDCS-induziertem EF und den jeweiligen physiologischen Parametern auf der Ebene des Individuums. Zu diesem Zweck wurde für jeden Teilnehmer ein MRT-basiertes realistisches Kopfmodell entworfen, um 1) anatomische Faktoren zu berechnen und 2) die tDCS- und TMS-induzierten elektrischen Felder (EF) zu simulieren. Anschließend untersuchten wir auf regionaler Ebene, welche einzelnen anatomischen Faktoren die simulierten EFs erklären. Schließlich untersuchten wir, welche spezifischen anatomischen und / oder EF-Faktoren die neurophysiologischen Ergebnisse der tDCS vorhersagten. Die Ergebnisse zeigten, dass von den untersuchten anatomischen Faktoren höhere EF-Werte mit einem geringeren Abstand zwischen Elektrode und Kortex (ECD) und einer geringeren Dicke des Liquor cerebrospinalis (CSF) verbunden waren. Zusätzlich waren CSF-Dicke und ECD negativ korreliert, während EFs positiv mit tDCS-induzierten physiologischen Veränderungen korreliert waren.

Schließlich untersuchten wir im fünften Schritt die Übertragbarkeit der durch kathodale tDCS induzierten Neuroplastizität vom motorischen auf den präfrontalen Kortex. Die neurophysiologischen Wirkungen von tDCS auf den primärmotorischen Kortex wurden bereits in einer vielzahl von Studien untersucht. Viel weniger ist jedoch hinsichtlich physiologischer Effekte der tDCS auf nichtmotorische Bereiche wie den präfrontalen Kortex bekannt, der eine wichtige Basis für vielfältige kognitive Funktionen darstellt und dessen Dysfunktionen an neuropsychiatrischen Störungen beteiligt sind. Zu diesem Zweck wurde kathodale tDCS mit niedrigen, mittleren und hohen Dosierungen oder eine Placebo-Stimulation über dem primärmotorischen und dorsolateralen präfrontalen Kortex appliziert. Die Nacheffekte der tDCS wurden mittels TMS-Elektroenzephalographie (EEG) und TMS-MEP auf regionaler Ebene für die Ergebnisparameter TMS-evozierte Potentiale (TEP), TMS-evozierte Oszillationen und MEP-Amplitudenänderungen bewertet. Die Ergebnisse zeigten eine dosisabhängige nichtlineare neurophysiologische Wirkung der tDCS über dem motorischen Kortex, die nicht vollständig auf die Ergebnisse der tDCS über dem präfrontalen tDCS übertragbar war. Niedrige und hohe Dosierungen der tDCS über dem motorischen Kortex

reduzierten frühe positive TEP-Peaks und MEP-Amplituden, während eine Erhöhung der Amplituden dieser Potentiale für primärmotorische tDCS mit mittlerer Dosierung beobachtet wurde. Im Gegensatz dazu reduzierte präfrontale tDCS mit niedriger, mittlerer und hoher Dosierung die frühen positiven TEP-Amplituden gleichermaßen. Darüber hinaus wurden für beide kortikalen Bereiche keine tDCS-induzierten neuromodulatorischen Effekte auf späte TEP-Amplituden (mit Ausnahme präfrontaler tDCS mit niedriger Dosierung) oder TMS-evozierte Oszillationen beobachtet.

Zusammengenommen hat diese Arbeit unter Verwendung innovativer neurophysiologischer, Computer-gestützter und bildgebender Verfahren wichtige Aspekte in Bezug auf tDCS-induzierte neuroplastische Effekte untersucht, und liefert neue Erkenntnisse für zukünftige Anwendungen von tDCS in Grundlagen- und klinischen Studien.

Table of Contents

1 Introduction

1.1. Motivation

Neurological and neuropsychiatric disorders are leading the list of highly prevalent disorders, causing a major individual burden of disease (clinical symptoms, impairment of social functioning and quality of life, mortality) and high direct and indirect economic costs [1-4]. Despite major advances in treatments, including pharmaco-, physical or psychotherapy, these have significant limitations, such as nonspecific effects, insufficient tailoring to the individual, and moderate to severe adverse effects [5]. Stroke survivors are often left with significant and permanent residual motor impairments [6-8]. In Parkinsonian patients the clinical utility of medications tends to become limited over the years, often due to adverse effects such as dyskinesias [9]. Of all, 20 to 30% of patients with mood or anxiety disorders, and up to 50% of patients with schizophrenia do not sufficiently respond to standard therapeutic interventions, and 22–50% of major depressive disorder (MDD) patients suffer from recurrent episodes within 6 months after recovery [1-3, 10]. *Thus, there is a need for novel effective treatment strategies in order to ameliorate the course of disease, to improve life quality and to elevate the level of individual functioning.*

Based on a large body of neurobiological evidence, neurological disorders are not simply the consequence of an initial insult, injury, inflammation or dysfunction of a specific compartment of the brain; they also reflect the attempt of the entire nervous system to adapt to the insult [5], and psychiatric disorders are conceptualized as system-level disorders of the brain. A number of lines of evidence point to a dysregulation or disruption of neuroplasticity, which refers to structural and functional alteration of the strength of synaptic connections in response to environmental or internal demands [11, 12], as a main contributor to the pathophysiology of neurological and neuropsychiatric disorders [5, 13, 14]. For example, stroke accompanied by motor deficits, in which the interhemispheric interaction between the primary motor cortices is impaired, is typically characterized by weakening of the excitability, and functionality of the motor cortex of the lesioned hemisphere and dysfunctional strengthening of the non-lesioned hemisphere [15]. For a second example, major depressive disorder has been shown to be accompanied by profound alterations of neural structure and function. An imbalance between the activity of the left and right dorsolateral prefrontal cortex (DLPFC), namely hypoactivity of the left, and hyperactivity of the right DLPFC, has been suggested as important factor in MDD [16]. *The targeted modulation of plasticity might therefore be suited to improve the symptoms of neurological and psychiatric disorders.*

Considering these sources of evidence, research has focused on novel approaches that induce enduring changes of cortical excitability and neuroplasticity, using non-invasive brain stimulation (NIBS) techniques [17, 18]. One of those tools, transcranial direct current stimulation (tDCS), has been shown to modulate cortical excitability in a polarity-dependent way, by delivering weak direct electrical currents through the scalp via two electrodes placed on the head. Anodal tDCS, which refers to surface inward current over the target area, enhances cortical excitability, while cathodal tDCS, which refers to outward current over the target area, results in excitability reduction with standard protocols at the circuit level [19, 20]. Respective after-effects can last for 1 h or longer.

Promising research lines have provided sound preclinical and clinical data supporting the application of tDCS as treatment for neurological and psychiatric disorders in order to overrule treatment-resistance and chronicity [18, 21, 22]. For the improvement of motor functions, the mode of application of tDCS is based on diverse neuroimaging and electrophysiological data, indicating that a distributed neural network, including the primary motor, premotor and supplementary motor cortices, the cerebellum, thalamic nuclei and the striatum, are associated with motor skill learning, acquisition, early consolidation phases of motor learning, but also long-term skill consolidation [23-26]. Accordingly, anodal tDCS of the primary motor cortex improved motor learning as evaluated by the serial reaction time task, while cathodal stimulation decreased the rate of motor sequence learning [27, 28]. In addition, neuroimaging and electrophysiological data have further shown an involvement of the prefrontal cortex as neuronal basis for many high-level cognitive functions. Here, the DLPFC has been shown to be involved in positive mood, negative affect, and specific emotional processes [16, 29], as well as working memory, and other cognitive processes [30, 31]. In accordance, tDCS of the left DLPFC improved emotional face recognition, most markedly for emotionally positive faces [32], while tDCS over the right DLPFC enhanced fear memories, possibly by influencing the prefrontal cortex-amygdala circuit underlying fear memory [33], and anodal tDCS of the left DLPFC improved working memory [34], while no effects were observed for cathodal tDCS [35]. Improvement of the symptoms of neurological disorders by motor tDCS were reported in clinical studies for stroke [36, 37], and Parkinson's disease [38], and improvement of symptoms of psychiatric disorders by prefrontal tDCS were reported in clinical studies for MDD [13, 39], schizophrenia [40], anxiety [41], and Alzheimer's disease [42]. *Despite these and other encouraging results of pilot studies, the overall efficacy of the technique is currently limited.*

Multiple reasons might cause the limited efficacy of current tDCS protocols. First and probably most importantly, a relevant interindividual variability of tDCS outcomes has been reported [43, 44], which is one of the major challenges regarding its applicability for basic research, and clinical purposes. However, given the variation and complexity of the individual factors (including physical, physiological, and functional) proposed to affect outcomes, it is very difficult to simultaneously measure or examine the independent contribution of each factor to the response to interventions [45]. In addition, the direct measurement of electrical currents in the human brain is complex and not feasible as a routine procedure [46]. From the bioelectromagnetic point of view, tDCS alters brain functions by its effects on neurons, likely via shifting their operating point, which depends strongly on the induced electrical field (EF) strength and direction, but also stimulation duration [47, 48]. At the microscopic level, computational, as well as *in vivo* and *in vitro* studies, have shown that the tDCS-induced EF alters neural membrane polarization, with a contribution of all neuronal compartments, i.e. dendrites, soma and axon, and that EF components oriented parallel to the axonal axes likely contribute to the directionality of stimulation effects [49-51]. These effects alter overall synaptic efficacy at the macroscopic level, if sufficient stimulation intensity/duration is applied [19, 20, 52, 53]. However, apart from this principle mechanism of action of tDCS, recent studies have shown a significant variability of effects between individuals, based on anatomical factors of the head, including head shape, tissues thickness, as well as cortical morphology [54, 55]. In addition, in vivo, as well as electrical impedance tomography studies have shown relevant differences of head tissue electrical conductivity between humans [56, 57]. With this in mind, recently developed computational simulation techniques, based on MR-derived detailed realistic head models, provide the opportunity to estimate the individual tDCS-induced EF [47, 48, 58], and have highlighted a strong contribution of individual anatomical and/or electrical properties of the head for shaping the EF induced by tDCS. Accordingly, respective studies have shown a significant EF variability between humans, when one-size-fits-all tDCS protocols are used [59, 60]. Thus taken together, EF variability might be an important factor for heterogeneous outcomes of tDCS. Despite this, a few computational studies have so far investigated the association between individual physical factors, and neurophysiological effects of tDCS [59, 61-63]; *it is however still unclear whether and to what extent individual physical factors explain the neurophysiological outcome of tDCS, at the level of the*

individual. A systematic investigation of the impact of these parameters on the neuroplastic effects of tDCS is therefore required.

Secondly, knowledge about protocols which induce optimal effects is scant; this might also partially explain limitations of clinical outcomes of tDCS, caused by application of suboptimal stimulation protocols, and also the large inhomogeneity between studies with respect to the used stimulation parameters. Indeed, earlier studies suggested a linear enhancement of tDCS efficacy by increasing the stimulation intensity and/or duration [19, 20]. Later works have however shown dosage-dependent non-linear effects of tDCS, both in human healthy [34, 64-70] and clinical populations [38, 40, 71], when stimulation duration and/or intensity exceed a certain limit, thus implying that enhancing stimulation dosage by simply increasing stimulation intensity, and duration, might have its limitations for efficacy improvement. *This suggests the necessity of a systematic investigation of the neuroplastic effects induced by different tDCS dosages, aiming to decipher the neurophysiological effects of widely used tDCS protocols, but also to identify optimal tDCS parameter at the group level.*

Finally, neuromodulatory effects of tDCS over the primary motor cortex were largely taken as a template so far for the use of this intervention over non-motor regions, whereas a direct exploration of the physiological effects of tDCS of these brain areas is largely missing; this is of critical importance, as previous findings show only a gradual comparability of stimulation effects between the primary motor cortex and other cortical regions [72-74], due likely to anatomical, as well as receptor, and neurotransmitter differences between distinct cortical areas. A one-to-one transferability of motor cortex tDCS effects to other cortical regions can therefore not be taken for granted, but direct physiological tests of tDCS effects over respective target areas are required.

Collectively, these factors very likely explain the moderate and partially inhomogeneous effects of tDCS. To improve the efficacy of the technique, and understand its underlying mechanisms, these need to be addressed.

As the ultimate goal, this dissertation is dedicated to:

1. The improvement of the efficacy of cathodal tDCS to induce neuroplastic effects over the primary motor cortex by:

1.1. Titrating cathodal tDCS parameters for the human motor cortex model with different stimulation intensities, and durations, to explore the impact of these parameters on tDCS after-effects, and to identify a protocol that induces optimized effects.
1.2. Exploring if repeated cathodal tDCS protocols with different intervals prolong the stimulation after-effects.
1.3. Investigating if the dosage-dependent nonlinear effects of cathodal tDCS on cortical excitability, as potential sources of limited tDCS efficacy, can be explained by calcium channel dynamics as a main contributor.
1.4. Testing another relevant aspect of limited efficacy of stimulation, i.e. interindividual variability. Here we aimed to explore whether and to which extent the neurophysiological outcome of tDCS, at the individual level can be explained by considering individual anatomical, and resulting electrical field factors.

2. Explore if the cathodal tDCS results obtained over the primary motor cortex are transferable to non-motor areas.

1.2. Structure and contribution of the Thesis

The thesis is organized as follows: Following this introductory chapter, **Chapter 2** addresses the first aim of the thesis. It consists of five parts including 1) an introduction part, in which the previous literature is reviewed, including knowledge gaps, and unsolved questions, and the aim of the study is developed , 2) the methodological part, in which we explain how we titrated cathodal tDCS parameters for the human motor cortex model with different stimulation intensities (1, 2 and 3 mA), and durations (15, 20 and 30 min), 3) the results part, in which we show the detailed results of the experiment, 4) the discussion part, in which we explain the proposed mechanisms of the obtained results, limitations of this study and future directions, and 5) a concluding part.

Chapter 3 also addresses the first aim of the thesis, by exploring the effects of repeated tDCS protocols with different intervals, aiming to extend the stimulation after-effects. It encompasses five sub-sections including 1) an introduction part, in which we review previous findings, address their limitations and respective unknown questions, and develop the aim of this study, 2) a methodological part, which

explains study procedures, in which we compared the impact of single interventions of conventional (1mA for 15min) and optimized (identified in the first study; 3mA for 20min) cathodal tDCS with the effects of repeated application of these interventions with intervals of 20 min and 24 h on motor cortex excitability, 3) a results part, in which we show the detailed results of the experiment, 4) a discussion part, in which we discuss the findings, explain the proposed mechanisms of the obtained results, and discuss limitations of this study and future directions, and 5) a concluding part.

Chapter 4 addresses the underlying neurophysiological mechanisms of intensity-dependent nonlinear effects of tDCS-altered corticospinal excitability, which can be considered as a source of tDCS limited efficacy. It consists of five sub-sections including 1) an introduction part, in which we review previous studies that highlight this nonlinearity, explain neurophysiological mechanisms with the main focus on the well-known contributor calcium channel dynamics, and develop the aim of this study, 2) a methodological part, in which we explain the experimental procedures, which include a pharmacological intervention with different dosages of calcium channel blocker flunarizine (low (2.5 mg), medium (5 mg) or high (10 mg)) before cathodal motor cortex tDCS with 3mA for 20min, 3) a results part, in which we present the detailed results of the experiment, 4) a discussion part, in which we discuss the findings in detail, including mechanistic explanations, and discuss limitations of this study and future directions, and 5) a concluding part.

Chapter 5 also addresses the first aim of the study, by focussing on another source of limited efficacy of tDCS, i.e. interindividual variability, via considering the role of individual physical factors (anatomical, and resulting electrical field factors), which affect the tDCS-induced electrical field and therefore potentially its neuroplastic effects. It includes five sub-sections: 1) an introduction part, in which we review previous studies exploring different sources of tDCS interindividual variability, address their limitations and respective solved problems, and develop the aim of this study, 2) a methodological part, in which we explain, based on neurophysiological data obtained in former studies of our group, which explored tDCS-induced MEP (induced by TMS) and CBF (measured by ASL-fMRI) alterations[75], how we explored the association between individual anatomical factors and tDCS-induced EF, and the respective physiological outcomes at the level of the individual. In detail, for each individual, a structural MRI-based realistic head

model was developed, which was used to simulate, based on the finite element method (FEM), the tDCS- and TMS-induced EF. We then explored the contribution of individual anatomical factors to EF variabilities, and we investigated also whether and to which degree the individual anatomical factors and EFs predict the tDCS-induced MEP and CBF changes, 3) a results section, in which we present the detailed results of the experiment, 4) a discussion part, in which we discuss the findings in detail, explain the proposed mechanisms of the obtained results, and discuss limitations of this study and future directions, and 5) a concluding part.

Chapter 6 addresses the second aim of the study, by exploring the transferability of motor cathodal tDCS-induced neuroplasticity to the prefrontal cortex. In encompasses five sections including 1) an introduction, in which we review the previous work regarding the neurophysiological results obtained by tDCS on different brain regions, address their limitations and respective unsolved questions, and state the aim of this study, 2) a methodological part, in which we explain how we evaluated the transferability of the neuromodulatory effects of different dosages of motor cortex cathodal tDCS between the motor, and prefrontal cortex. In detail, in eight randomized sessions, four cathodal tDCS dosages, low, medium, and high, as well as sham stimulation, were applied over the primary motor and dorsolateral prefrontal cortex, and regional after-effects were evaluated via TMS-EEG, and TMS-MEP, for the outcome parameters TMS-evoked potentials (TEP), TMS-evoked oscillations, and MEP amplitude alterations, 3) a results section, in which we present the detailed results of the experiment, 4) a discussion part, in which we discuss the findings, explain mechanistic aspects of the outcome, and limitations of this study as well as future directions, and 5) a concluding part.

Finally, in **Chapter 7,** we describe, and discuss the main outcomes of the conducted studies, and also add suggestions for future research directions.

2 Study 1: Titrating the neuroplastic effects of cathodal tDCS over the primary motor cortex

2.1. Introduction

Alterations of the strength of neuronal connections caused by environmental demands, called neuroplasticity, are the foundation of various cognitive processes [11, 12]. In humans, non-invasive brain stimulation (NIBS) protocols provide an excellent avenue for modulating brain plasticity without disrupting the integrity of the skull [20, 76, 77]. These tools enable further investigation of brain functions, and have been probed to treat associated neurological and psychiatric disorders, in which aberrant cerebral excitability and plasticity play a role [26, 39, 78-81].

One of those tools, tDCS, has been shown to modulate cortical excitability, in a polarity-dependent way, by delivering weak direct electrical currents through the scalp via two electrodes placed on the head. For the primary motor cortex, but also other areas, anodal tDCS, which refers to surface inward current over the target area, results in enhancement of cortical excitability, whereas cathodal tDCS, which refers to outward current over the target area, reduces it. Respective after effects can last for one hour or longer [19, 20]. Directionality of these effects however critically depend on stimulation intensity, duration, and also positioning of the return electrode [64, 82-84].

Regional after-effects of tDCS can be explained by modification of synaptic strength by modulating the activity of N-methyl-D-aspartate (NMDA) receptors and calcium homeostasis [84, 85]. Downregulation of GABA activity might have a gating effect on respective plasticity of glutamatergic synapses [86]. tDCS has also been shown recently to alter cortico-cortical, as well as cortico-subcortical functional network connectivity, as explored by magnetic resonance imaging and electroencephalography [87, 88].

Studies in young healthy human populations show that increasing stimulation intensity and/or duration within certain limits enhances the efficacy of tDCS [19, 20]. However, recent studies also showed non-linearities of tDCS-induced plasticity, when stimulation intensity or duration was increased beyond these limits [64, 66, 82]. While 1mA-13 min anodal stimulation significantly increased cortical excitability, doubling stimulation duration led to excitability diminution [82].

Another study showed a significant increase of MEP amplitudes by applying cathodal tDCS with 2mA for 20min, whereas cathodal tDCS with 1mA for 20min decreased cortico-spinal excitability [64]. These non-linearities of effects have been also shown by other studies [67, 89, 90]. A systematic investigation on the neuroplastic effects of different tDCS dosages is however so far missing.

Because of its relatively low cost and simplicity, tDCS has been widely probed clinically to treat neurological and psychiatric disorders like stroke accompanied by motor deficits, in which the interhemispheric interaction between the primary motor cortices is impaired, typically by weakening of the excitability, and functionality of the motor cortex of the lesioned hemisphere and dysfunctional strengthening of the non-lesioned hemisphere [15]. tDCS (especially in combination with motor training) has shown its capability to improve clinical symptoms probably by rebalancing the activity of targeted areas [6, 91]. Despite these and other encouraging results reported in pilot studies, the overall efficacy of the technique is currently limited, probably caused by sub-optimal stimulation protocols due to the fact that knowledge about protocols which induce optimal effects is limited [92].

In this study, we aimed to systematically explore the dose-dependent effect of cathodal tDCS over the primary motor cortex in healthy subjects, via titrating tDCS intensity from 1 to 3mA, and stimulation duration from 15 to 30 minutes. In accordance with previous studies, we hypothesized a nonlinear modulatory effect of tDCS on motor cortical plasticity, depending on stimulation intensity and duration. The results provide further insights on the dependency of tDCS-induced neuroplasticity from these stimulation parameters, and thereby deliver crucial information for future applications of cathodal tDCS.

2.2. Materials and Methods

2.2.1. Participants

Sixteen healthy, non-smoking participants (7 males, mean age ± standard deviation (SD): 25.12 ± 4.61) were recruited. All participants were right-handed according to the Edinburgh handedness inventory [93] and had no history of neurological and psychiatric diseases, or fulfilled exclusion criteria for non-invasive electrical or magnetic brain stimulation [94, 95]. Central nervous system-acting medication or respective recreational substances served also as exclusion criteria. The study

conformed to the Declaration of Helsinki and was approved by the Ethics Committee of the Leibniz Research Centre for Working Environment and Human Factors. All participants gave informed written consent before starting the study, and were financially compensated for participating.

2.2.2. Transcranial direct current stimulation of the motor cortex

tDCS was applied with a constant-current battery powered stimulator (neuroConn, Ilmenau, Germany), through a pair of saline-soaked surface sponge electrodes (35 cm^2) placed on the scalp. One electrode was fixed over the motor cortex representational area of the right abductor digiti minimi muscle (ADM) as identified by TMS, and the other was placed contralaterally above supraorbital area [19, 96]. Prior to stimulation, a topical anesthetic cream (EMLA®, 2.5% lidocaine + 2.5% prilocaine) was applied to the stimulation site, in order to sufficiently blind the participants [97]. All participants received cathodal tDCS at an intensity of 1.0, 2.0 or 3.0 mA for 15, 20 or 30 min with 10 sec ramp-up and down at the start and end of stimulation. For sham stimulation, 1.0 mA stimulation was delivered for 15 seconds, with a 10 sec ramp up and down followed by 15min with 0.0 mA stimulation. Taking into account all intensity-duration combinations, including sham stimulation, this resulted in 10 sessions per participant.

2.2.3. Motor cortical excitability assessment

Single pulse TMS at 0.25 Hz ± 10% (random) delivered by a PowerMag magnetic stimulator (Mag&More, Munich, Germany) with a figure-of-eight magnetic coil (diameter of one winding, 70mm; peak magnetic field, 2T) which was held tangentially to the skull, with the handle pointing backwards and laterally at 45° from the midline was applied to the left primary motor cortex. Surface MEPs were recorded from the right ADM with gold cup electrodes in a belly-tendon montage. The signals were amplified, and filtered (1000; 3Hz- 3KHz) using D440-2 (Digitimer, Welwyn Garden City, UK) and were digitized (sampling rate, 5kHz) with a micro 1401 AD converter (Cambridge Electronic Design, Cambridge, UK), controlled by Signal Software (Cambridge Electronic Design, v. 2.13). A waterproof pen was used to mark the position of TMS coil and ADM electrodes.

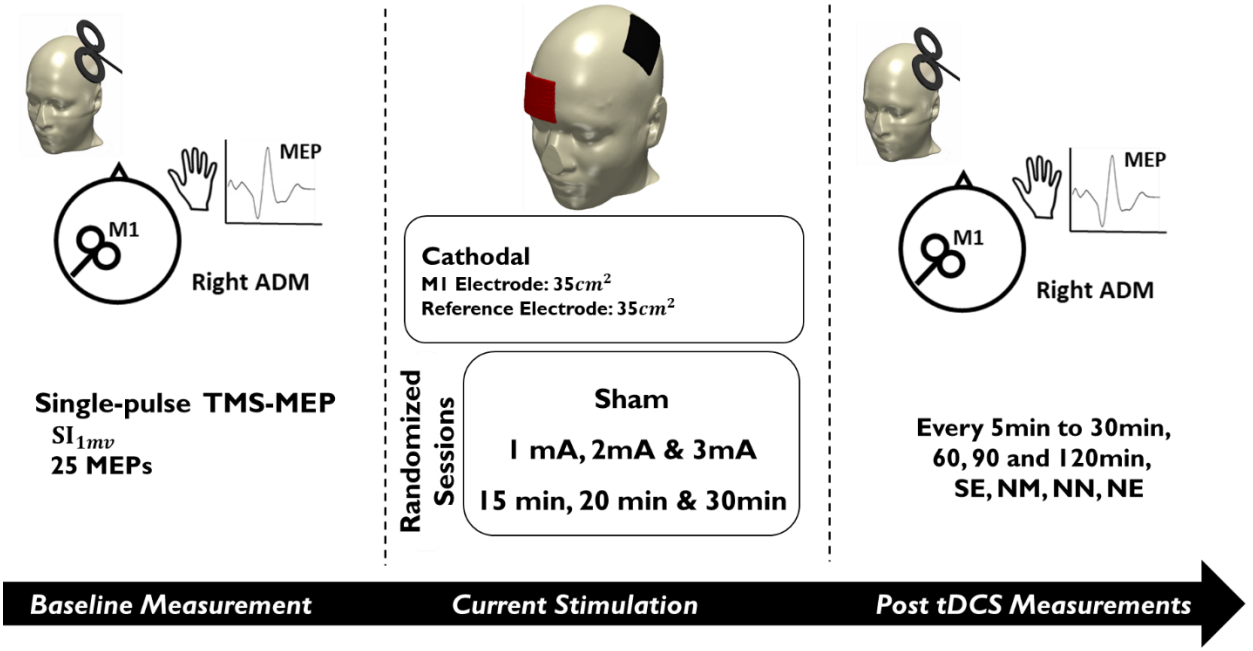

Figure 2.1 Course of the study. Single-pulse TMS was conducted at a frequency of 0.25 Hz to the left motor cortex. The representational area of the right ADM, in which the largest MEPs were produced, was identified first. The intensity of the TMS pulses was adjusted to elicit MEPs with a peak-to-peak amplitude of on average 1 mV (SI1mV). Finally, baseline cortical excitability was determined by measuring 25 MEPs. Afterwards, cathodal real tDCS was applied in one of three different intensities (1, 2 and 3mA) and durations (15, 20 and 30mins), or sham tDCS was applied, in random order in 16 young healthy subjects. The after-effects were monitored with TMS-induced MEPs (each time point with 25 MEPs) every 5 min up to 30 min and the following time points of 60 min, 90 min, 120 min, same evening (SE, ~ 7 hours after tDCS), next morning (NM, ~ 24 hours after tDCS), next noon (NN, ~ 4-5 hours after next morning time point) and next evening (NE, ~ 4-5 hours after next noon).

2.2.4. Experimental procedures

At the beginning of each session, participants were seated in a comfortable chair with head and arm rests. Then single-pulse TMS was conducted at a frequency of 0.25 Hz to the left motor cortex for identification of the representational area of the right ADM, in which the largest MEPs were produced. The intensity of the TMS pulses was adjusted to elicit MEPs with a peak-to-peak amplitude of on average 1 mV (SI1mV). Finally, baseline cortical excitability was determined by measuring 25 MEPs. Afterwards, tDCS electrodes were mounted onto the head and cathodal tDCS was applied. tDCS with different intensities and durations (as outlined above), which resulted in 10 experimental sessions, was applied in randomized order with a minimum of seven days between each session to avoid carry-over effects [85]. After

finishing the intervention, tDCS electrodes were removed and corticospinal excitability was assessed by TMS measurements (with baseline TMS intensity, 25 stimuli per time point) every 5 min for up to 30 min after tDCS, and 60 min, 90 min, 120 min, same evening (~ 7 hours after tDCS), next morning (~ 24 hours after tDCS), next noon (~ 4-5 hours after the next morning measure) and next evening (~ 4-5 hours after the next noon measure), Figure 2.1.

For simplicity, in the following we indicate each condition, except for sham stimulation, according to the applied stimulation intensity and duration. For example, the condition in which tDCS was applied with 1mA for 15 minutes will be labelled as '1mA-15min', and tDCS application with 2mA for 30-minutes duration is referred to as '2mA-30min'.

2.2.5. Discriminability and qualitative assessment of tDCS protocols

In each session, subjects filled in a questionnaire which contained: 1. Guessed intensity of applied direct current (0, 1, 2 and 3mA), 2. Rating scales for the presence and severity of visual phenomena, itching, tingling and pain during stimulation, and 3. Rating scales for the presence and severity of skin redness, headache, fatigue, concentration difficulties, nervousness and sleep problems within 24 hours after stimulation. The side-effects were rated on a numerical scale from zero to five, zero representing no and five extremely strong sensations.

2.2.6. Calculations and statistics

2.2.6.1. The effect of tDCS intensity and duration

To disentangle the effects of tDCS intensity and duration, first, the individual means of each time point's MEP amplitudes were calculated and then normalized to baseline MEPs (quotient of the averaged MEP amplitudes of each time point vs baseline, MEPs which were contaminated by muscle activity, tiredness, or arousal reactions were excluded from the analysis). A repeated measures ANOVA was then calculated with normalized MEPs as dependent variable, and 'intensity' (3 levels), 'duration' (3 levels), and 'time point' (15 levels) as within-subject factors.

2.2.6.2. Overall tDCS effect vs. sham

To determine if the respective active stimulation conditions effects differ from those of sham stimulation, a repeated measures ANOVA was calculated with normalized MEPs as dependent variable, and 'condition' (10 levels) and 'time point' (15 levels) as within-subject factors.

2.2.6.3. Early-, late-, and very-late- time point of tDCS effects

To compensate for the variability between time-points and better define the time course of plasticity induction by tDCS, the normalized MEP amplitudes of all measured time points were pooled into three time points: the MEPs grand average of first 30 min after stimulation (early-time point after-effects), 60 min-120 min (late-time point after-effects) and same-day evening to next-day evening (very-late-time point after-effects). For these parameters, repeated measures ANOVAs were calculated with normalized MEPs as dependent variable, and 1) with 'intensity' (3 levels), 'duration' (3 levels) and 'time point' (4 levels) as within-subject factors, and 2) with 'condition' (10 levels) and 'time point' (4 levels) as within-subject factors.

2.2.6.4. The effects of baseline measures 'SI1mV' and 'baseline MEP' on tDCS after-effects

To test if baseline measures differed between sessions, two separated one-way repeated measures ANOVA were performed with 'session' as within-subject factor, and 'SI_{1mV}' or 'baseline MEP' as dependent variables.

2.2.6.5. Qualitative assessment of tDCS protocols

To identify if participants correctly guessed the tDCS intensities, chi-square tests were conducted for each tDCS intensity. The presence of side-effects during and after tDCS were analyzed by a repeated measure ANOVA with 'condition' (10 levels) as within-subject factor and rating scores (0-5) as dependent variable. In case of significant effects, follow-up exploratory post-hoc paired t-tests were conducted to examine if an active session resulted in a significant difference sensation relative to sham, and Pearson's correlation coefficients were calculated to test a dependency of tDCS after-effects from respective sensations.

Mauchly's test of sphericity was conducted, and the Greenhouse-Geisser correction was applied when necessary, for all ANOVAs. The critical level of significance was set to p <= 0.05 for all statistics. Post hoc t-tests were exploratory, and conditional on significant results of the ANOVAs, and therefore were not corrected for multiple comparisons. Statistical analysis was performed with SPSS (IBM Corp. Version 24.0).

2.3. Results

The MEP data for one of the subjects' last session (1 mA – 30 min) was not available due to the subject's refusal to attend. Also, data for the one time point of one another participant following right after tDCS (2 mA – 20 min) was not recorded due to a software technical issue. The following results are based on the analysis of all subject's available data. The ratings of the qualitative assessment of tDCS protocols of one participant were also excluded because he stated that he rated completely at random, without reading the items.

2.3.1. The effect of tDCS intensity and duration

The 3-factorial ANOVA ('intensity' - 3 levels, 'duration' - 3 levels, and 'time point' - 15 levels) conducted to discern between intensity and duration effects of stimulation resulted in a significant main effect of intensity (df = 2, F = 8.953, p = 0.001), but no main effects of duration, time point or the respective interactions, Figure 2.2; Table 2.1.A. Post hoc tests revealed a significant difference between 1mA and 2 mA, 2 mA and 3 mA in which 1 mA and 3 mA resulted in LTD-like plasticity induction, while 2 mA intensity induced LTP-like plasticity.

Table 2.1. Results of the ANOVAs conducted for tDCS-induced MEP alterations. A) The 3-factorial repeated-measures ANOVA revealed a significant main effect of stimulation intensity, but no significant main effects of time, and duration, or respective interactions. B) The 2-factorial repeated-measures ANOVA conducted for all separately measured time points revealed a significant effect of stimulation condition, but no significant main effect of the factor time, or the respective interaction. C.1) The 3-factorial ANOVA for the grand averaged MEPs grouped into three time points of early, late and very late effects revealed a significant main effect of intensity and a significant interaction between intensity and time, but no significant main effect of time. C2) The 2-factorial repeated-measures ANOVA for the grand averaged MEPs grouped into three time point of early, late and very late effects revealed a significant effect of stimulation condition and its interaction with time, but no significant main effect of the factor time. Mauchly's test of

sphericity was conducted, and the Greenhouse-Geisser correction was applied when necessary, for all ANOVAs. Asterisks indicate significant results. d.f. = degrees of freedom.

		Factor	d.f.	F value	*p* value
A	**Effects of intensity and duration of tDCS on MEP amplitudes**	**Intensity**	2	8.953	0.001*
		Duration	2	0.287	0.753
		Time	4.774	0.844	0.519
		Intensity × Duration	4	1.749	0.153
		Intensity × Time	7.623	1.865	0.077
		Duration × Time	8.122	0.919	0.505
		Intensity× Duration × Time	9.050	1.098	0.369
B	**Effects of different tDCS conditions on MEP amplitudes**	**Condition**	4.554	3.714	0.007*
		Time	4.666	0.749	0.582
		Condition × Time	10.509	1.280	0.245
C.1	**Early, late and very late effects of different intensity and duration of tDCS on MEP amplitudes (Pooled MEPs)**	**Intensity**	2	8.617	0.001*
		Duration	2	0.328	0.723
		Time	2.219	1.768	0.185
		Intensity × Duration	4	1.839	0.134
		Intensity × Time	6	4.405	0.001*
		Duration × Time	6	0.728	0.628
		Intensity× Duration × Time	4.811	1.935	0.103
C.2	**Early, late and very late effects of tDCS on MEP amplitudes (Pooled MEPs)**	**Condition**	4.605	3.561	0.008*
		Time	2.235	1.432	0.254
		Condition × Time	7.230	2.469	0.021*

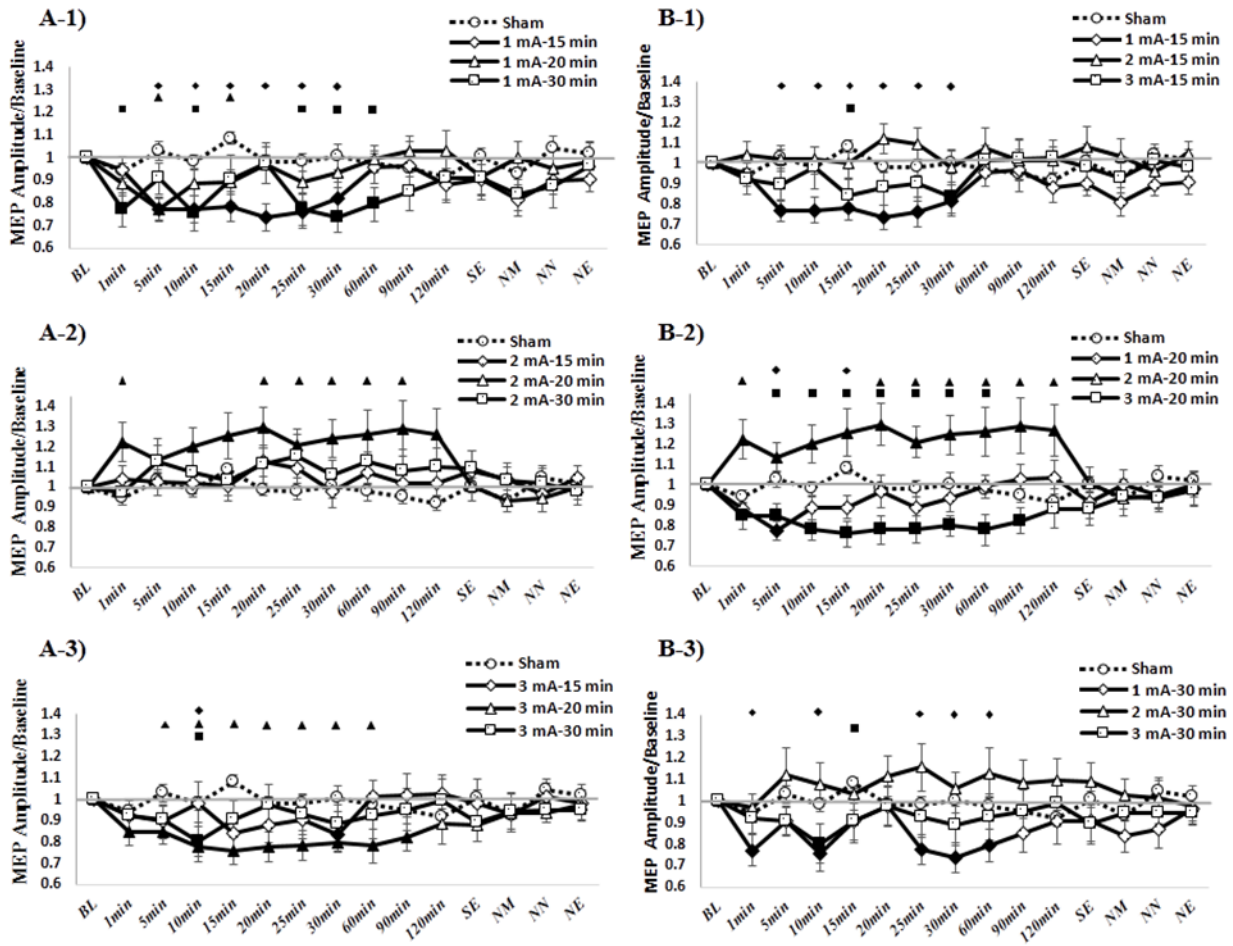

Figure 2.2 Post-tDCS excitability alterations including 10 different levels of stimulation intensity/duration. (A) Based on stimulation intensities: sham, 1 mA, 2 mA and 3 mA with (A-1) fixed tDCS duration of 15 min; 20 min (A-2) and 30 min (A-3). (B) Based on stimulation duration: 15 min, 20 min and 30 min with (B-1) fixed tDCS intensity of 1 mA; 2mA (B-2) and 3 mA (B-3). 1 mA-15 min, 1 mA-30 min and 3 mA-20 min resulted in a significant excitability diminution, and 2 mA-20 min in a significant excitability enhancement. Sham stimulation did not induce any significant change of cortical excitability. Error bars represent standard error of mean. Filled symbols indicate a significant difference of cortical excitability against the respective baseline values. Floating symbols refer to each sub-figure, and indicate a significant difference between the respective active intensity/duration combination and sham stimulation condition. SE: same evening, NM: next morning, NN: next noon, NE: next evening.

2.3.2. Overall tDCS effect vs. sham

The 2-factorial ANOVA ('condition' - 10 levels, and 'time point' - 15 levels), which was conducted to compare if active stimulation condition effects differ from those of sham stimulation, revealed a significant main effect of tDCS condition (df =

4.554, F = 3.714, p = 0.007), but no main effect of time (df = 4.666, F = 0.749, p = 0.582), or condition × time interaction (df = 10.509, F = 1.180, p = 0.245). Post hoc tests comparing sham tDCS with the respective real stimulation protocols revealed: The 1 mA-15 min (for about 30 min after stimulation) and 1 mA-30 min (for about one hour with a 20 min delay after stimulation) conditions induced a cortical excitability diminution, while 2 mA-20 min (for two hours after stimulation) resulted in a significant cortical excitability enhancement. Higher stimulation intensity (3 mA-20 min) induced a significant excitability diminution lasting for about one and half hour after stimulation. The remaining protocols resulted in no significant effects on motor cortex excitability, Figure 2.2; Table 2.1.B, for results of individual participants, please refer to Figure 2.4.

2.3.3. Early-, late-, and very-late-time points of tDCS effects

The 3-factorial ANOVA ('intensity' - 3 levels, 'duration' -3 levels- and 'time point' - 4 levels) which was conducted to explore the time course of plasticity induction of each tDCS intensity and/or duration, showed a significant main effect of intensity (df = 2, F = 8.617, p = 0.001) and a significant interaction between intensity and time point (df = 6, F = 4.405, p = 0.001), but no significant main effect of duration, time point, or the remaining interactions, Table 2.1.C1). The respective post hoc tests revealed significant differences between 1mA and 2 mA, as well as 2 mA and 3 mA; whereas 1, and 3 mA stimulation intensities reduced MEP amplitudes, 2 mA stimulation had a MEP-enhancing effect, Figure 2.3.

The 2-factorial ANOVA ('condition' - 10 levels, and 'time point' - 4 levels) which was conducted to better define the time course of plasticity induction of each tDCS condition showed a significant main effect of condition (df = 4.605, F = 3.561, p = 0.008) and a significant interaction between condition and time point (df = 7.230, F = 2.469, p = 0.021), but no significant main effect of time point. Post-hoc comparisons between the active protocols and sham for the first 30 min after stimulation (early effects) showed a significant excitability diminution for 1 mA-15 min, 1 mA-20 min, 1 mA-30 min, 3 mA-20 min and a significant excitability enhancement for 2 mA-20 min, while 60-120 min after stimulation (late effects) only 1 mA-30 min, 3 mA-20 min and 2 mA-20 min resulted in a significant cortical excitability diminution or enhancement, respectively. No significant effects were

found for very late effects, including same day evening to next day evening measures, Figure 2.3; Table 2.1.C2.

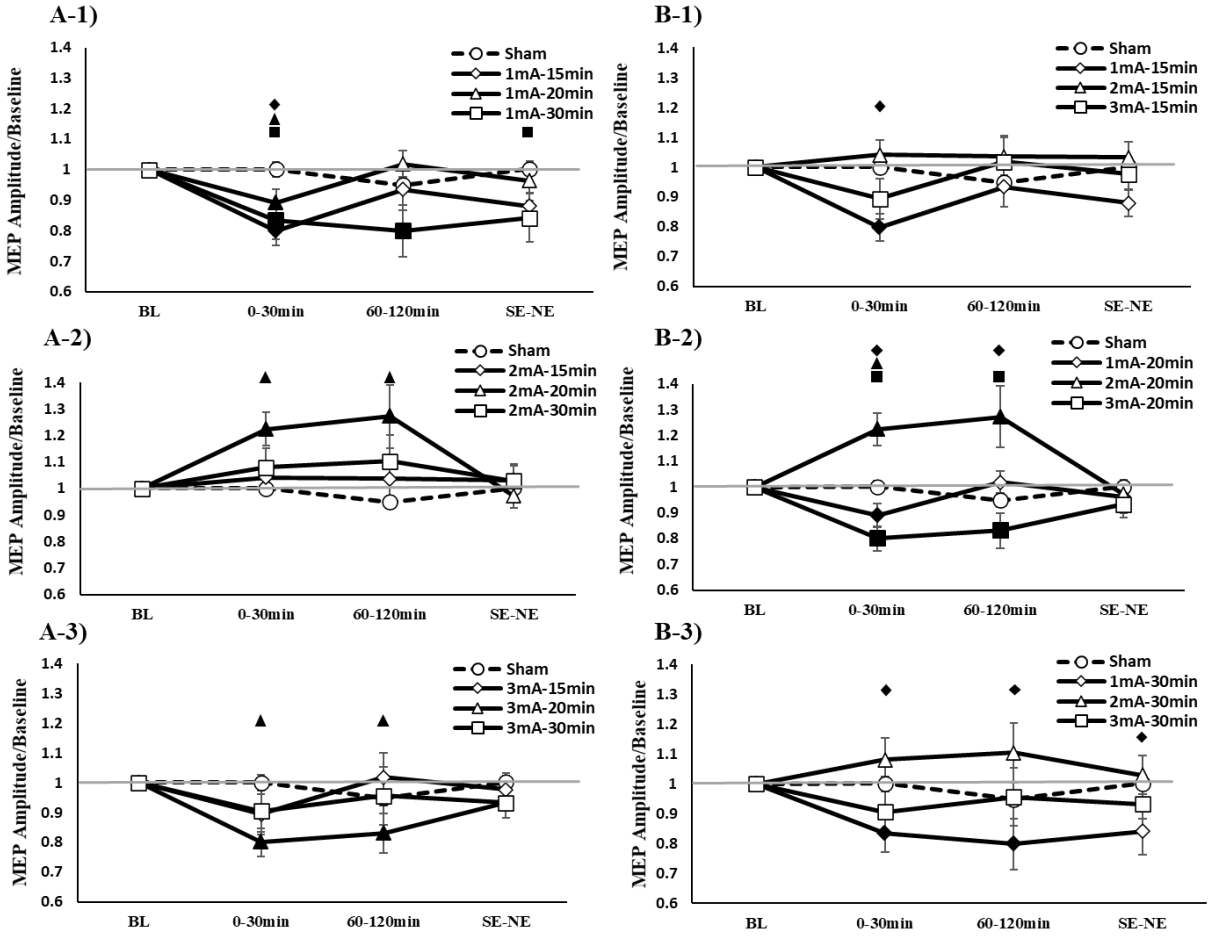

Figure 2.3 Pooled MEP Amplitudes early, late and very late tDCS post stimulation effects. grand-averaged MEPs were pooled into three time points of early (0-30 min), late (60-120 min) and very late (same day evening- next day evening) excitability changes. Error bars represent standard error of means. A) Results for the early time point, for intensities (A-1, 2 and 3) and duration (B-1, 2 and 3). Filled symbols indicate a significant difference of cortical excitability versus the respective baseline values. Floating symbols refer to each sub-figure, and indicate a significant difference between the respective active condition and the sham stimulation condition. SE: same evening, NE: next evening.

2.3.4. No difference of SI1mV and baseline MEPs between conditions

Baseline MEP and $SI1_{mV}$ TMS intensity adjusted to elicit a ~1 mV peak-to-peak amplitude of MEPs ($SI1_{mV}$) are listed in Table 2.2. The ANOVAs showed no

significant differences of baseline MEP and $SI1_{mV}$ across sessions (Baseline MEP: df = 9, F = 0.767, p = 0.647; $SI1_{mV}$: df = 4.095, F = 0.671, p = 0.618).

Table 2.2 Baseline measurements and TMS stimulation intensities. Data are presented as mean ± SD; SI1mV refers to the maximal stimulator output (%MSO) which was required for generating ~1mV MEP. An overall ANOVA showed no significant differences of baseline MEP and SI1mV across sessions.

Experimental Session	SI_{1mv} (%)	Baseline MEP (mV)
Sham	57.15 ± 11.59	1.06 ± 0.16
1mA-15min	56.43 ± 11.70	1.03 ± 0.13
1mA-20min	58.18 ± 13.05	1.03 ± 0.11
1mA-30min	55.93 ± 11.50	0.99 ± 0.09
2mA-15min	55.93 ± 11.93	1.05 ± 0.11
2mA-20min	56.00 ± 10.56	1.08 ± 0.13
2mA-30min	57.53 ± 12.84	1.06 ± 0.14
3mA-15min	57.21 ± 11.87	1.05 ± 0.09
3mA-20min	55.76 ± 11.71	1.03 ± 0.09
3mA-30min	56.25 ± 11.44	1.01 ± 0.10

2.3.5. Qualitative assessment of tDCS protocols

Chi-square tests for each tDCS intensity including sham results indicated a significant effect for 3mA ($\chi2$ = 10.200, p = 0.017) with no significant effects for sham ($\chi2$= 1.600, P = 0.449), 1mA ($\chi2$ = 5.578, P= 0.134) and 2mA ($\chi2$ = 6.111, p = 0.106). Table 2.3 shows the results of guessed intensities vs. actual intensities.

Table 2.3 Participants guess of the actual intensity. In each session, participants were asked to guess the intensity of the actually applied direct current (0, 1, 2 and 3mA). The table contrasts actually applied intensity (rows) with perceived intensity (columns). Differences in the sum of the ratings of each intensity are present, because only one sham stimulation condition was included in the experiments, but three sessions per intensity. The ratings of one participant were excluded because he stated that he rated completely at random, without reading the items.

		Intensity guessed by participants			
		0 mA	**1 mA**	**2 mA**	**3 mA**
Actual tDCS intensity	**Sham**	5	7	3	0
	1 mA	12	12	16	5
	2 mA	9	18	11	7
	3 mA	3	18	12	12

Participant ratings for the presence and intensity of side-effects during and within 24 hours after stimulation are listed in Table 2.4.

Table 2.4 Presence and Intensity of Side Effects Participant ratings of the presence and intensity of side-effects. A) Visual phenomena, itching, tingling and pain during stimulation, and B) skin redness, headache, fatigue, concentration difficulties, nervousness and sleep problems within 24 hours after stimulation. The presence and intensity of the side-effects were rated in a numerical scale from zero to five, zero representing no and five extremely strong sensations. Data are presented as mean ± SD. The ratings of one participant were excluded because he stated that he rated completely at random, without reading the items.

	Side-effects	Sham	*1mA–15min*	*1mA-20min*	*1mA-30min*	*2mA-15min*	*2mA-20min*	*2mA-30min*	*3mA-15min*	*3mA-20min*	*3mA-30min*
During stimulation	**Visual Phenomenon**	0.4 ± 0.71	0.66 ± 1.07	0.6 ± 1.08	0.53 ± 0.88	0.93 ± 1.52	1 ± 1.63	0.46 ± 0.8	0.53 ± 1.08	0.93 ± 1.48	1.3 ± 1.53
	Itching	0.26 ± 0.44	0.33 ± 0.59	0.53 ± 0.71	0.4 ± 0.87	0.6 ± 0.95	0.93 ± 0.92	0.33 ± 0.59	0.53 ± 0.71	0.6 ± 0.87	1.2 ± 1.42
	Tingling	0.53 ± 0.71	0.6 ± 0.8	0.46 ± 0.88	0.8 ± 1.16	0.8 ± 0.9	0.86 ± 0.8	0.6 ± 0.71	0.86 ± 0.71	1.26 ±1.28	1 ± 1.31
	Pain	0.2 ± 0.4	0.53 ± 0.95	0.33 ± 0.78	0.46 ± 0.61	0.33 ± 0.59	0.8 ± 1.2	0.33 ± 0.47	0.33 ± 0.78	0.66 ± 1.13	1.06 ± 1.23
24 hours after stimulation	**Redness**	0.33 ± 1.01	0.46 ± 1.08	0.26 ± 0.57	0.53 ± 0.71	0.6 ± 1.08	0.73 ± 1.18	0.46 ± 0.8	0.4 ± 0.6	0.53 ± 1.2	0.8 ± 0.9
	Headache	0.2 ± 0.4	0.33 ± 0.59	0.4 ± 0.71	0.46 ± 0.61	0.66 ± 0.86	0.66 ± 1.13	0.53 ± 0.71	0.4 ± 0.6	0.66 ± 1.01	0.73 ± 0.99
	Fatigue	0.66 ± 0.78	0.4 ± 0.8	0.6 ± 0.87	0.8 ± 1.2	0.6 ± 0.95	0.73 ± 1.28	0.66 ± 1.13	0.73 ± 0.99	0.8 ± 1.04	0.8 ± 0.97
	Concentration	0.4 ± 0.87	0.46 ± 1.02	0.4 ± 0.87	0.46 ± 0.88	0.46 ± 0.88	0.66 ± 0.94	0.53 ± 0.71	0.26 ± 0.77	0.33 ± 0.78	0.66 ± 1.19
	Nervousness	0 ± 0	0.26 ± 0.77	0.06 ± 0.24	0.33 ± 0.59	0.06 ± 0.24	0.53 ± 0.88	0.2 ± 0.4	0.06 ± 0.24	0.26 ± 0.67	0.4 ± 1.01
	Sleep Problem	0 ± 0	0.06 ± 0.24	0.13 ± 0.49	0.33 ± 0.69	0.26 ± 0.77	0.2 ± 0.54	0.06 ± 0.24	0.13 ± 0.49	0.2 ± 0.74	0.2 ± 0.54

The ANOVAs (‘condition’ - 10 levels) conducted for the side-effect questionnaires showed a significant effect for pain during stimulation, but no significant effects for visual phenomena, itching, tingling, redness, headache, fatigue, concentration, nervousness and sleep problems, Table 2.5. The numerical results indicate that the side-effects were all relatively minor over conditions.

Table 2.5 Statistical Results for Presence and Intensity of Side Effects. The presence and intensity of side-effects were analyzed by one-way repeated-measures ANOVAs. A significant effect of pain, but no significant effects of other side-effects was revealed. Asterisks indicate significant effects (where $p<0.05$). d.f.= degree of freedom. The ratings of one participant were excluded because he stated that he rated completely at random, without reading the items.

	Side-effects	d.f.	*F* Value	*p* Value
During stimulation	Visual Phenomenon	3.337	1.465	0.234
	Itching	4.590	2.375	0.052
	Tingling	4.341	1.155	0.341
	Pain	2.988	2.919	0.045*
24 hours after stimulation	Redness	3.475	0.873	0.475
	Headache	2.820	1.287	0.292
	Fatigue	3.472	0.504	0.708
	Concentration	2.287	0.824	0.462
	Nervousness	1.993	1.915	0.166
	Sleep Problem	1.994	1.187	0.320

Post hoc t-test comparisons between active stimulation sessions and sham for the pain ratings revealed significant differences between sham and 2mA-20min as well as 3mA-30min. However, the Pearson's correlation coefficients, which were calculated to explore a possible dependency of MEP alterations from pain perception, revealed no significant association between tDCS early after-effects and pain sensations for the 2mA-20min (Pearson's $r = 0.268$, $p = 0.315$), as well as 3mA-30min (Pearson's $r = 0.150$, $p = 0.580$).

2.4. Discussion

In this study, we systematically titrated the dose-dependent effect of cathodal tDCS for three different stimulation intensities (1, 2 and 3mA) and durations (15, 20 and 30mins) on motor cortex excitability and observed non-linear after-effects. Both, LTD and LTP-like plasticity were induced by cathodal tDCS, while magnitude, duration, and direction of the effects were determined by specific stimulation intensities.

The 1 mA low intensity protocols resulted in inhibitory effects. 1 mA cathodal tDCS with a duration of 15 min, 20 min and 30 min resulted in a significant reduction of motor cortical excitability for 30 min and about one hour after stimulation respectively. Different patterns of after-effects were observed by increasing tDCS intensity to 2 mA. For tDCS durations of 15 min and 30 min, the results indicate no significant effects on MEP amplitudes, while 20 min of 2mA cathodal tDCS shifted

cortical excitability from LTD- to LTP-like plasticity for about two hours after intervention. Interestingly, in contrast to the facilitatory effect of 2 mA – 20 min, we found again an excitability-diminishing effect of stronger stimulation. 3 mA – 20 min cathodal tDCS again reduced MEP amplitudes for about one and half an hour after stimulation, whereas no significant excitability alterations were observed for 3 mA – 15 min and 3 mA – 30 min.

These results are in accordance with those described in previous studies, in which excitability-diminishing effects of cathodal tDCS were reported for low intensity stimulation (1 mA) with durations of 9 min [96], 15 min [98], 18 min [66] and 20 min [64], and excitability-enhancing effects of 2 mA- 20 min cathodal tDCS [64] with no significant effects for 2 mA- 15 min [98]. No neurophysiological data were so far available for 3 mA stimulation.

2.4.1. Proposed mechanism

A linear neuroplasticity enhancement/reduction by anodal/cathodal stimulation has been reported when tDCS of low intensity/duration was applied over the left motor cortex with a return electrode over the contralateral supraorbital area [20, 96]. Recent studies however revealed nonlinearities of the physiological response for stimulation protocols with stronger intensity and longer duration [64, 82, 98]. Regarding mechanisms of these effects, it has been suggested that bi-directional excitability alterations induced by weak anodal/cathodal tDCS can be explained by glutamatergic plasticity involving NMDA receptors [99, 100]. Here, different levels of activation of NMDA receptors result in different levels of calcium influx, which might result in different effects on synaptic plasticity. It has been shown primarily in animal models so far that low postsynaptic calcium enhancement induces LTD, high calcium increases result in LTP, and calcium overflow again induces LTD/no plasticity; between these plasticity-inducing calcium concentrations so –called no man's lands do exist, which do not result in plasticity [101, 102]; thus one could speculate that 1 mA tDCS resulted in an LTD-inducing low calcium concentration, 2 mA in a calcium concentration sufficient for the induction of LTP-like plasticity, and 3 mA in LTD-like plasticity due to calcium overflow. The discernable effects of stimulation duration within a specific current intensity condition might be due to respective intermediate calcium concentrations, which represent transition zones/no man´s lands. At present, these explanations are speculative, and should be explored

in future studies directly (e.g. by pharmacological interventions which alter calcium neuronal calcium influx). These are supported however by a couple of other tDCS studies, which showed that cathodal tDCS-induced LTD-like plasticity is NMDA receptor-dependent , that calcium dynamics play a role for tDCS-induced plasticity [103], and that non-linearities of tDCS effects can be antagonized by NMDA and calcium channel blockers [82, 104].

Alternative explanations cannot be ruled out at present. Increasing tDCS intensity should strengthen the electric field in deeper cortical layers, which are less affected under the weaker electric field with lower stimulation intensities. This enhanced field strength in deeper regions might then generate plasticity in neurons, which are not relevantly affected by weaker stimulation intensities. Indeed, animal studies using direct cortical stimulation revealed that anodal stimulation deactivated while cathodal stimulation activated neurons in deep cortical layers [105]. In addition, different thresholds for modulation have been reported for different neuronal subgroups, e.g. a physiological impact of DC stimulation on pyramidal neurons required higher total charges than that required for an effect on nonpyramidal neurons [105]. This stresses the important role of stimulation intensity and dosage on tDCS-induced neuromodulatory after-effects, and is a critical issue for future human studies. It might also be speculated that especially stronger protocols may affect not only the cortical regions of the target area, but enhance also recruitment of neighbored non-target brain regions to a larger extent, as suggested by modeling and fMRI studies, which might indirectly affect and strengthen, or change the direction of plasticity in the target regions. Thus, while low intensity (1 mA) cathodal tDCS results in a reduction of MEP amplitudes, doubling and/or tripling the intensity may shift resulting plasticity to an opposite direction by involving additional cortical regions and/ or layers. A slight drawback of this interpretation is the fact that for these stimulation intensities, no respective non-linearities of the respective plasticity direction were seen for anodal tDCS in previous studies [64, 82, 98]. This would however be expected if respective additional neuronal populations would be recruited by stronger stimulation, which because of the dependency of tDCS effects from induced electrical field to neuronal orientation should then result in antagonistic effects of anodal as compared to cathodal tDCS.

The assessment of tolerability and side-effects during stimulation and 24 hours after stimulation indicates that participants tolerated all conditions well and side-effects

were minor. These were moreover largely equivalent between conditions, except for pain perception in higher intensities. In principle, this could have affected our experimental results. This seems however not have been the case, as shown by missing associations between pain ratings and MEP results, as explored by the respective correlations. These results are in accordance with previous studies that characterize tDCS as a well-tolerated technique [95, 106]. For blinding purposes, we used local anesthetics cream which relevantly reduces tDCS-induced sensory perceptions as shown in previous studies [98, 107]. Our results showed reasonable blinding quality, as participants could not correctly guess the intensities of the respective stimulation conditions for sham, 1 mA, and 2 mA stimulation. Only for 3 mA stimulation intensity, "guessing" was not at chance level. This shows that the topical anesthetics cream we used works well with stimulation intensities between 1 and 2 mA, but might have limited efficacy with stronger stimulation. However, the fact that the MEP results differed also within the 3mA condition between stimulation durations argues – together with the missing effects of pain ratings on MEP amplitudes - against a relevant impact of blinding quality under 3 mA tDCS intensity on the results of this study.

2.4.2. Limitations and future directions

While our study mainly focuses on the neurophysiological effects of tDCS at the group level, inter-individual variability in healthy adults has also been reported for tDCS effects, similar to other neuromodulatory brain stimulation interventions [43, 108], and can be seen also in our data (Figure 2.4). Potential contributing factors are anatomical and biophysical differences of the brain, genetics, sex, age, and brain state [109]. Our results did not show significant effects of age and gender on the neurophysiological outcome of tDCS. Anatomical and tissue differences, which affect tDCS outcome by their impact on current distribution, and could be explored by computational modelling, were not explored in this study [110-112]. For personalization of the intervention, with the aim to achieve optimal effects at the individual level, the next step would now be to use these models, and knowledge about other factors affecting the physiological impact of stimulation, and explore their usefulness for physiological, as well as behavioral effects of stimulation.

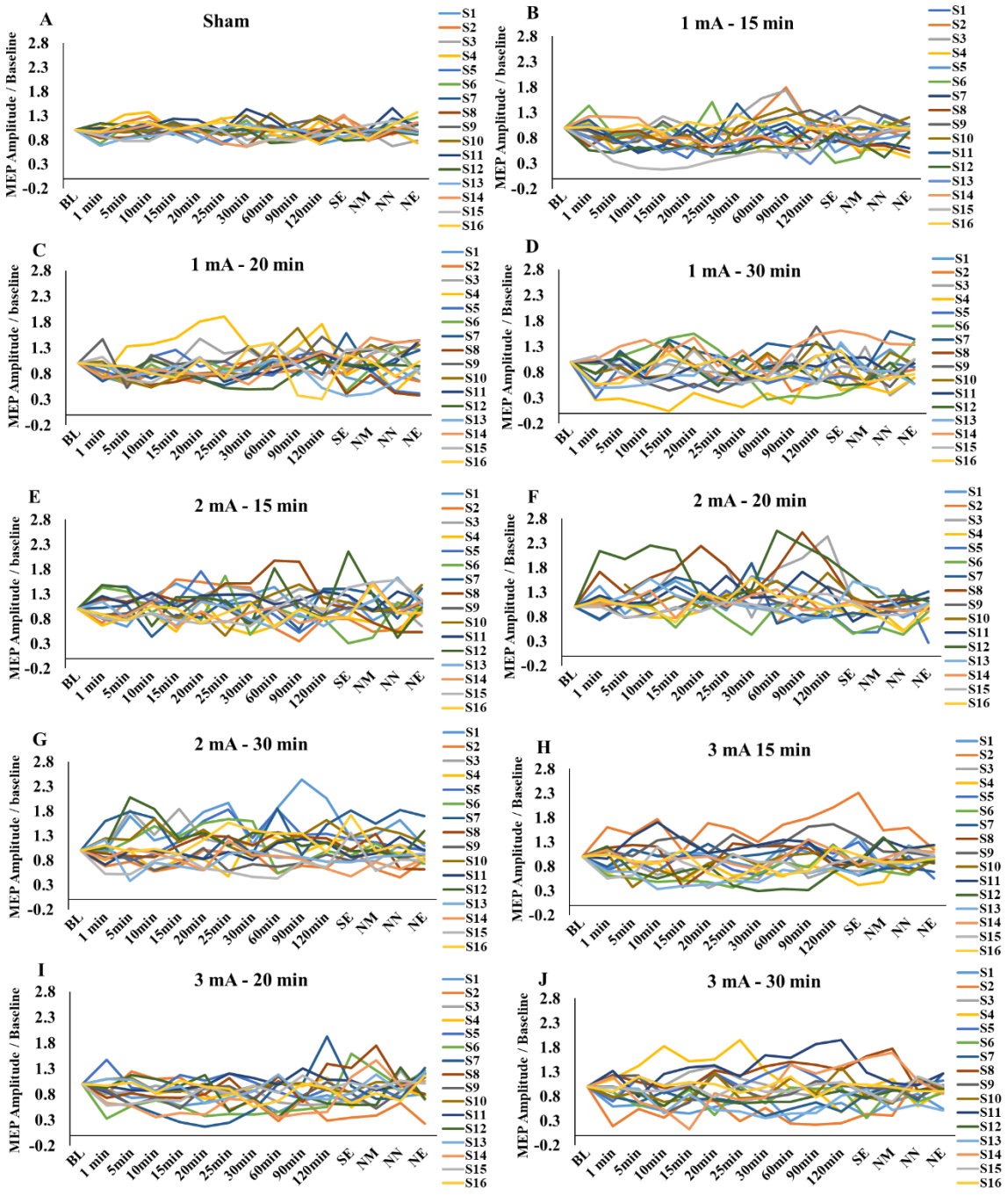

Figure 2.4. Intra-individual motor cortical excitability changes after cathodal transcranial direct current stimulation (tDCS) over the primary motor cortex. Individual excitability alterations after sham (A), 1mA-15min (B), 1mA-20min (C), 1mA-30min (D), 2mA-15min (E), 2mA-20min (F), 2mA-30min (G), 3mA-15min (H), 3mA-20min (I) and 3mA-30min (J) of tDCS are depicted. Each color line of each graph represents MEP values of one participant. MEP

amplitudes are normalized to baseline values individually. Each colored line in each graph represents MEP values of one participant (S1–S16).

The targeted population in this study were healthy young humans. It should not be taken for granted that the results obtained from these participants are one-to-one transferable to different age populations, as well as patient groups. Indeed, it was shown that identical tDCS protocols can have different effects in healthy young adults, children/adolescents, and aged subjects [113-115]. Similarly, differences between healthy participants and neuropsychiatric patients should also be considered with regard to the extension of current results to clinical settings.

Although investigating inter-individual variability was not the main scope of this study, it is possible that the covariates analysed may have been masked due to a relatively low sample size. For future studies which aim to investigate inter-individual variability, larger sample sizes would be beneficial for being able to detect subtle differences.

2.5. Conclusion

This study shows a nonlinear modulatory effect of cathodal tDCS on motor cortical plasticity, depending on stimulation parameters. We titrated cathodal tDCS intensity from 1 to 3mA, and stimulation duration from 15 to 30 minutes. As 1 mA and 3 mA stimulation induced a reduction of MEP amplitudes, but 2 mA resulted in excitability enhancement at the group level, this nonlinearity should be taken into account particularly when an inhibitory effect is aimed for by cathodal tDCS. These nonlinear effects might be due to NMDA receptor-dependent calcium dynamics and/or stimulation intensity-dependent effects of tDCS on cortical layers. The results of the present study give hints for optimally suited tDCS protocols to reduce excitability of the primary motor cortex. They might also help to improve the efficacy of tDCS as therapeutic tool for the treatment of neurological and psychiatric disorders. It should however be noted that a one-to-one transferability of these effects to other cortical areas, and patient populations should not be taken for granted due to state-dependency of tES effects, anatomical differences, and differences of neuromodulator activities and cortical excitability between healthy humans and respective patients.

3 Study 2: Probing the relevance of repeated cathodal tDCS over the primary motor cortex for prolongation of after-effects

3.1. Introduction

Application of a weak direct current via electrodes placed over the scalp (transcranial direct current stimulation, tDCS) can bidirectionally induce neuroplasticity in the targeted area. The direction, magnitude and duration of respective effects depend on stimulation parameters, such as polarity and intensity/duration. Anodal tDCS, which refers to surface inward current over the target area, enhances cortical excitability, while cathodal tDCS, which refers to outward current over the target area, results in excitability reduction with standard protocols at the macroscopic level [20, 96, 116]. These effects alter symptoms of neurological and psychiatric disorders accompanied by pathological alterations of cortical excitability, such as in stroke [117], Parkinson´s disease [118], depression [119], and schizophrenia [40].

However, the overall efficacy of the technique is currently limited, most probably caused by sub-optimal stimulation protocols [120]. Earlier studies indicated that 1 mA tDCS for 4 seconds over the primary motor cortex alters cortical excitability during stimulation [116]. Increasing the duration of stimulation to some minutes induces long term potentiation (LTP)- and long term depression (LTD)-like neuroplastic after-effects, respectively [20, 96]. These results show that stronger and/or longer stimulation extends the neuromodulatory after-effects of tDCS within specific windows of stimulation intensity and duration. However, recent studies revealed a non-linear dosage dependency of tDCS-induced neuroplasticity, when stimulation duration and intensity exceed the limits of these “classic” protocols. While 1mA cathodal tDCS for 15min significantly reduced cortical excitability, no significant effects were observed with 2mA for the same duration [98], and prolongation of 2 mA cathodal tDCS to 20 min resulted in an excitability enhancement [64, 65]. A respective dosage-dependent non-linearity of tDCS after-effects has also been revealed by other studies [67, 89, 90], which can partially be explained by the dependency of the direction of plasticity on the amount of neuronal calcium influx [101, 121]. Thus, for enhancing the efficacy of tDCS, increasing stimulation intensity, and duration, might have its limitations.

Animal studies revealed the possibility of extending neurophysiological after-effects of plasticity-inducing stimulation from early- to late-phase plasticity by means of repeated stimulation protocols with short time intervals [122-124] In accordance, studies in humans have also shown that single intervention cathodal tDCS-induced excitability-reducing after-effects can be extended by repeated tDCS protocols with certain inter-stimulation intervals. In a former study, the excitability-diminishing after-effects of single intervention of cathodal tDCS with 1mA for 9min over the primary motor cortex, which induces after-effects of about 1 h duration, were enhanced by repeating the same protocol with short intervals (3, or 20 min), but abolished when the interval was extended to 3, or 24 hours [66]. In another study however, the excitability-diminishing after-effects of a single intervention of 1mA cathodal tDCS for 5min, which induces short-term depression-like effects, were reversed or unchanged by repeated tDCS protocols with 3 min and 30 min intervals, respectively [125]. These results suggest that an enhanced efficacy of cathodal tDCS to reduce cortical excitability can be induced by repeated stimulation within specific intervals, but that beyond the interval between interventions, also the respective stimulation protocol itself is of critical relevance. It is however also important to mention that in difference to respective results in animal models, so far repeated stimulation in humans has gradually enhanced the efficacy of respective cathodal stimulation protocols, but not resulted in late phase effects, which should last for more than 3h.

In the first study, we systematically titrated cathodal tDCS parameters for the human motor cortex model with different intensities (1, 2, and 3mA) and durations (15, 20 and 30 min), to explore systematically the impact of these parameters on after-effects, and identify most efficient protocols. The results revealed that stimulation with 1 mA for 15 min, and 1 mA for 30 min induced a significant MEP amplitude diminution, while stimulation with 2 mA for 20 min resulted in a significant corticospinal excitability enhancement. Protocols with higher stimulation intensity (specifically stimulation with 3 mA for 20 min) induced again a significant excitability diminution lasting for about one and half hour after stimulation, and thus were more efficient than the other protocols [65]. Since a former cathodal tDCS repetition study with a standard stimulation protocol with 1 mA did not lead to after-effects lasting for more than a few hours, we were interested to explore if repetition of a protocol, whose single application had shown superior effects, would also

induce improved effects with a repeated protocol. Accordingly, in the present study, tDCS with the cathode positioned over M1 was applied with 1mA for 15 min (conventional protocol), and 3 mA for 20 min (optimized protocol). To explore if repeated tDCS protocols with different intervals prolong the after-effects, we compared the impact of single interventions of conventional and optimized cathodal tDCS with the effects of repeated application with intervals of 20 min and 24 hours on motor cortex excitability. These intervals were selected since in a previous study the 20-minute interval prolonged the neuroplastic after-effects as compared to a single intervention protocol, and an interval of 24 h is often used for repeated tDCS, but did reduce the neurophysiological effects of tDCS in that study [126]. In accordance with previous studies, we hypothesized an enhancement of the cathodal tDCS-induced excitability diminution by repeated application of conventional and optimized protocols with the short interval, and a reduction of the efficacy of the respective intervention with the long interval. Furthermore, we hypothesized that the high intensity protocol should improve tDCS-induced neuroplastic after-effects more than the low intensity (1 mA) condition for repeated stimulation. This study aimed to provide further information about the dependency of tDCS-induced neuroplasticity from the respective stimulation parameters, and thereby to deliver crucial information for future applications of cathodal tDCS.

3.2. Materials and Methods

3.2.1. Participants

Sixteen healthy, non-smoking participants (7 males, mean age 25.56 ± 4.96 standard deviation (sd)) were recruited. All participants were right-handed according to the Edinburgh handedness inventory [93]. None of the participants had a history of neurological or psychiatric disease, current or previous drug abuse, alcohol abuse, present pregnancy or metallic head implants, and all fulfilled the exclusion criteria for non-invasive electrical or magnetic brain stimulation [94, 95]. The study conformed to the Declaration of Helsinki and was approved by the local ethics committee. All participants gave written informed consent before starting the study, and were financially compensated for participation.

3.2.2. Transcranial direct current stimulation over the motor cortex

tDCS was applied with a battery-powered constant current stimulator (neuroCare, Ilmenau, Germany), through a pair of saline-soaked surface sponge electrodes (7x5 cm, 35 cm^2) placed on the scalp. The target electrode was fixed over the motor cortex representational area of the right abductor digiti minimi muscle (ADM) as identified by TMS, and the return electrode was placed contralaterally over the right orbit [19, 96]. The participants received two single interventions of cathodal tDCS of conventional (1mA for 15min), and optimized (3mA for 20min) protocols and two additional repeated cathodal tDCS protocols with 20min and 24 h intervals, for each single protocol. Taking into account all single and repeated protocols, including sham stimulation, this resulted in 7 sessions per participant, Figure 3.1. For sham stimulation, 1.0mA stimulation was delivered for 15 seconds followed by 15min with 0.0mA stimulation. All protocols were conducted with 10 seconds ramp-up and down at the start, and end of stimulation.

3.2.3. Motor cortical excitability assessment

Single pulse TMS was delivered by a PowerMAG stimulator (Mag&More, Munich, Germany) to measure excitability changes of the representational motor cortical area of the right ADM, indexed as the amplitude of motor evoked potentials (MEP). The TMS pulses were delivered via a figure-of-eight-shaped coil (diameter of one winding 70 mm; peak magnetic field 2 T) at a frequency of 0.25 Hz with 10% jitter. The coil was held tangentially to the scalp at an angle of 45° to the sagittal plane with the coil handle pointing laterally and posterior. Surface EMG was recorded from the right ADM in a belly-tendon montage. The signals were amplified, and filtered (1000; 3Hz- 3KHz) using D440-2 (Digitimer, Welwyn Garden City, UK), and were digitized (sampling rate, 5kHz) with a micro 1401 AD converter (Cambridge Electronic Design, Cambridge, UK), controlled by Signal Software (Cambridge Electronic Design, v. 2.13).

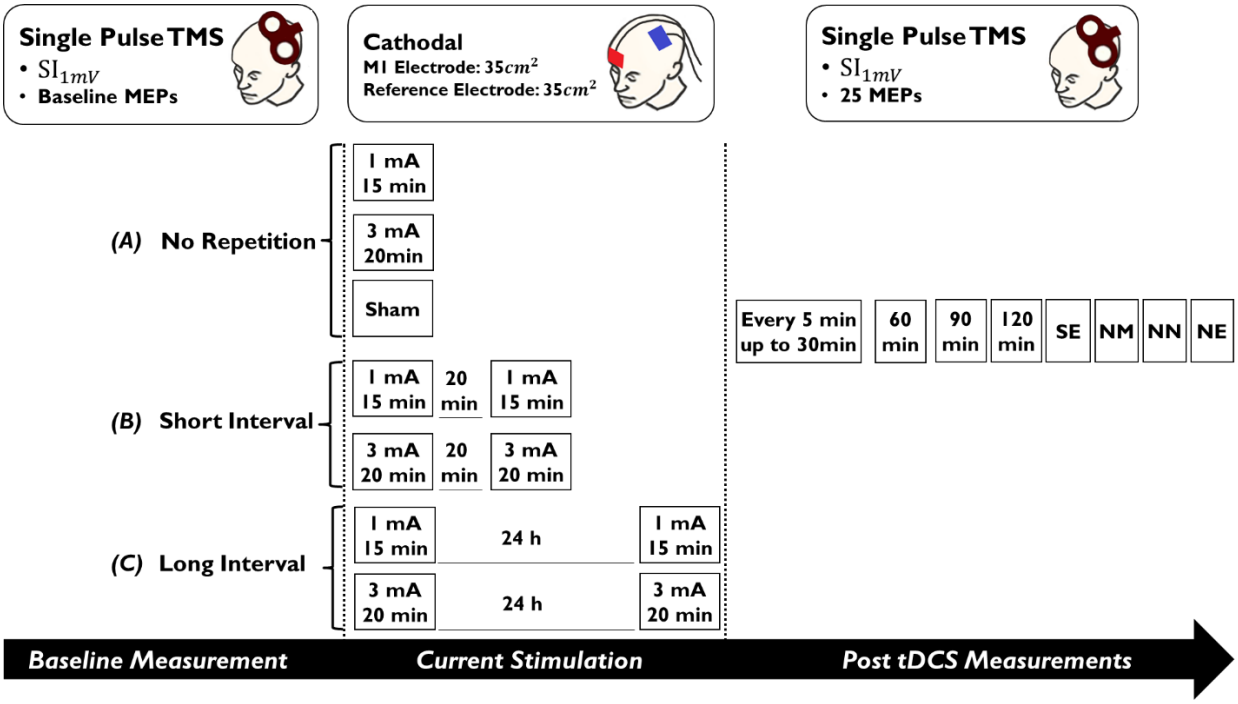

Figure 3.1 Course of Study. To obtain baseline motor cortex excitability, twenty-five single-pulse TMS-generated MEP were recorded from the right ADM. Afterwards, cathodal tDCS was applied as (A) single intervention with the conventional, optimized, or sham protocol (no repetition), or the same stimulation protocols were applied repeated with (B) 20min (short) or (c) 24 hours (long) intervals. The after-effects were monitored with TMS-induced MEPs of baseline intensity every 5 min for up to 30 min and the following time points of 60 min, 90 min, 120 min, same evening (SE, ~ 7 hours after tDCS), next morning (NM, ~ 24 hours after tDCS), next noon (NN, ~ 4-5 hours after next morning time point) and next evening (NE, ~ 4-5 hours after next noon).

3.2.4. Experimental procedures

The study was performed in a cross-over, single-blinded, randomized design. At the beginning of each session, participants were seated in a comfortable chair with head- and arm-rests. Then single-pulse TMS was conducted at a frequency of 0.25 Hz over the left motor cortex for identification of the representational area of the right ADM, in which the largest MEPs were produced by a given TMS intensity (hot spot determination). The TMS intensity (SI1mV) was then adjusted to elicit MEPs with on average 1 mV peak-to-peak amplitudes. Finally, baseline cortical excitability was determined by recording 25 MEPs with that TMS intensity from the right ADM. Prior to intervention, a topical anesthetic cream (EMLA®, 2.5% lidocaine + 2.5% prilocaine) was applied to the stimulation site, in order to decrease somatosensory sensations and sufficiently blind the participants [97, 107]. Afterwards, tDCS electrodes were mounted onto the head, and tDCS was applied. After finishing the

intervention, tDCS electrodes were removed and corticospinal excitability was monitored by 25 MEP obtained by TMS with baseline intensity every 5 min for up to 30 min, and 60 min, 90 min, 120 min, and then same evening, next morning, next noon, and next evening after tDCS (Figure 3.1). A waterproof pen was used to mark the position of the TMS coil on the scalp, as well as EMG electrodes on the hand. Different tDCS protocols were applied in separate sessions and in randomized order with a minimum one-week interval between each session to avoid carry-over effects [85].

3.2.5. Calculations and Statistics

MEP amplitudes were first visually inspected to exclude trials in which background electromyographic activity was present. Then, the individual means of MEP-amplitudes recorded at each time point were calculated for all subjects and all conditions separately. The post-intervention mean MEP amplitudes were then normalized to the respective individual mean baseline MEP-amplitude (quotient of post intervention versus pre-intervention MEP amplitudes).

3.2.5.1. The effects of baseline measures 'SI1mV' and 'baseline MEP' on tDCS after-effects

To investigate if baseline measures differed between sessions, two separate one-way repeated measures ANOVA were performed with 'condition' (7 levels) as within-subject factor and 'SI_{1mV}' or 'baseline MEP' as dependent variables.

3.2.5.2. Overall effects of active tDCS protocols vs sham

To determine if the respective active stimulation conditions altered cortical excitability relative to sham, and if the effects of the real stimulation protocols differed from each other, a repeated measures ANOVA was calculated with normalized MEPs as dependent variable, and 'condition' (7 levels) and 'time point' (15 levels) as within-subject factors.

3.2.5.3. Early-, late-, and very-late-epochs of tDCS effects

To compensate for variability between single time bins, the normalized MEP amplitudes of all time points were grand-averaged and pooled into three epochs: 0-30 min after stimulation (early after-effects), 60-120min (late after-effects) and

same-day evening to next-day evening (very late after-effects). For these parameters, a repeated measures ANOVA was separately calculated with normalized MEPs as dependent variable and 'condition' (7 levels) and 'epoch' (4 levels) as within-subject factors.

3.2.5.4. Qualitative assessment of tDCS protocols

After finishing each session, participants were asked to fill in a questionnaire which contained: 1. Guessed intensity of applied direct current (0, 1 and 3mA), 2. Rating scales for the presence and amount of visual phenomena, itching, tingling and pain during stimulation, and 3. Rating scales for the presence and amount of skin redness, headache, fatigue, concentration difficulties, nervousness and sleep problems within 24 hours after stimulation. The side-effects were rated on a numerical scale from zero to five, zero representing no and five extremely strong sensations.

Mauchly's test of sphericity was conducted, and the Greenhouse-Geisser correction was applied when necessary, for all ANOVAs. Exploratory post hoc t-tests were conducted in case of significant results of the ANOVAs, without correction for multiple comparisons [127]. The critical level of significance was set to $p \leq 0.05$ for all statistics. Statistical analysis was performed with SPSS (IBM Corp. Version 25.0).

3.3. Results

All participants completed the entire study.

3.3.1. No difference of SI1mV and baseline MEPs between conditions

Baseline MEP and $SI1_{mV}$ are listed in Table 3.1. The respective one-way ANOVAs showed no significant differences of baseline MEP and $SI1_{mV}$ across conditions (Baseline MEP: df = 6, F = 0.592, $P = 0.736$; $SI1_{mV}$: df = 3.112, F=0.989, p=0.404).

Table 3.1 MEP baseline measurements and TMS stimulation intensities. Data are presented as mean ± SD; SI1mV refers to the maximal stimulator output (%MSO) which was required for generating ~1mV MEP. The ANOVAs showed no significant differences of baseline MEP and SI1mV across sessions.

Experimental Session	SI_{1mv} (%)	Baseline MEP (mV)
Sham	57.18 ± 15.11	1.01 ± 0.08

Conventional protocol	57.40 ± 16.00	0.98 ± 0.15
Conventional protocol with 20min interval	57.68 ± 16.50	1.01 ± 0.09
Conventional with 24 h interval	58.68 ± 16.82	1.04 ± 0.14
Optimized protocol	57.28 ± 15.30	1.01 ± 0.08
Optimized protocol with 20min interval	58.71 ± 16.62	1.04 ± 0.10
Optimized protocol with 24h interval	56.50 ± 15.91	± 0.01

3.3.2. Overall effects of active vs sham tDCS protocols

The overall ANOVA conducted to test if active tDCS sessions differ from sham stimulation resulted in significant main effects of tDCS condition (df = 6, F = 5.031, $p < 0.001$) and time (df = 3.473, F = 17.989, $p < 0.001$), but a non-significant condition × time interaction, Figure 3.2; Table 3.2.A. Post hoc tests comparing the active tDCS protocols with the respective baseline measures revealed a significant reduction of MEP amplitudes after conventional single intervention tDCS, conventional tDCS with a 20min, and 24 hour interval (all protocols induced after-effects for about 1 hour after stimulation), as well as the optimized single intervention protocol (after-effects for about 2 hours after stimulation), optimized tDCS with a 20min interval (after-effects for about 60min after stimulation) and optimized tDCS with a 24 hours interval (after-effects for about 25min after stimulation). Post hoc comparisons of the respective active tDCS protocols with sham stimulation indicated a significant reduction of MEP amplitudes after conventional single intervention tDCS (for about 60min after stimulation), conventional tDCS with a 20min interval (for about 30 min after stimulation), conventional tDCS with a 24 hour interval (for about 30 min after stimulation), optimized single intervention tDCS (for about 2 hours after stimulation), optimized tDCS with a 20min interval (for about 2 hours after stimulation, but not for all respective time points) and optimized tDCS with a 24 h interval (for the time-points of immediately and 20min after stimulation). Furthermore, post hoc tests comparing MEPs between active protocols indicated that neuroplastic after-effects of the optimized single intervention protocol lasted significantly longer than those following the repeated optimized protocol with a 24 hours interval, Figure 3.2.

Table 3.2 Results of the ANOVAs conducted for tDCS-induced MEP alterations. A) The 2-factorial repeated-measures ANOVA conducted to discern active vs sham protocols revealed a significant effect of stimulation condition and time point, but no significant interaction. B) The 2-factorial repeated-measures ANOVA conducted for grand-averaged pooled MEPs to discern active vs sham protocols revealed significant main effects of stimulation condition, and epoch, and a respective significant interaction. Asterisks indicate significant results. d.f, degrees of freedom.

		Factor	d.f.	*F value*	*p value*
A	**Overall effects of tDCS on MEP amplitudes**	**Condition**	6	5.031	<0.001*
		Time point	3.473	17.989	<0.001*
		Condition × Time point	10.189	1.265	0.256
B	**Early, late and very late effects of tDCS on MEP amplitudes (Pooled MEPs)**	**Condition**	6	4.953	<0.001*
		Epoch	3	28.532	<0.001*
		Condition × Epoch	7.495	2.548	0.016*

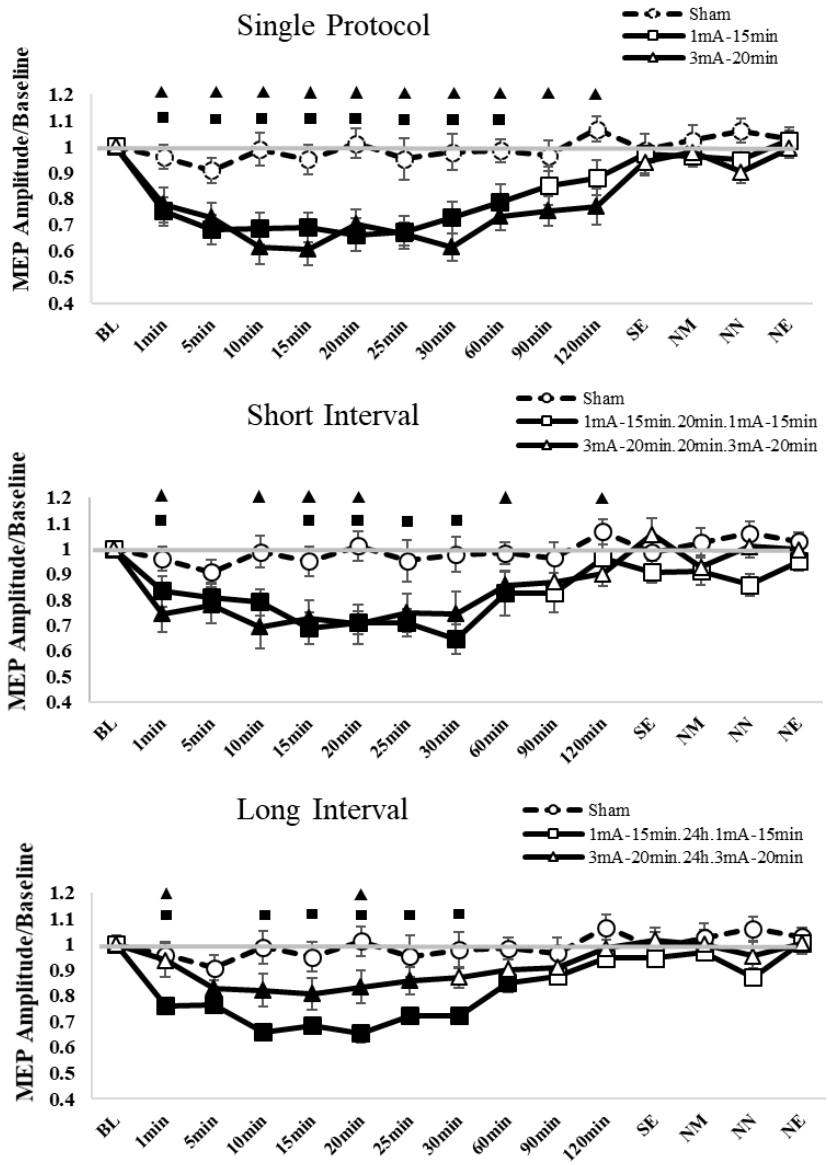

Figure 3.2 Post-tDCS motor cortical excitability alterations. Single intervention protocols with no repetition, repeated tDCS with the short (20 min), and the long interval (24h) are shown for the conventional, and the optimized tDCS protocol. Statistical data indicate a significant difference of all active protocols in comparison with sham tDCS. Error bars represent standard error of mean. Filled symbols indicate a significant difference of cortical excitability after tDCS, as compared to the respective baseline values. Floating symbols indicate a significant difference between the respective active and sham stimulation conditions. SE: same evening, NM: next morning, NN: next noon, NE: next evening.

3.3.3. Early-, late-, and very-late- epochs of tDCS effects

The 2-factorial ANOVA ('condition' - 7 levels, and 'epoch' - 4 levels) revealed significant main effects of condition (df = 6, F = 4.953, $p < 0.001$), epoch (df = 3, F

= 28.532, $p < 0.001$) and the respective interaction (df = 7.495, F = 2.548, $p = 0.016$), Figure 3.3; Table 3.2.B. Exploratory post hoc tests comparing the respective active tDCS protocols with baseline cortical excitability measures for the first 30 min after stimulation (early epoch) revealed a significant reduction of MEP amplitudes after all active protocols. For the late epoch (60-120 min after stimulation), conventional single intervention tDCS, conventional tDCS with a 20min interval, optimized single intervention tDCS and optimized tDCS with a 20min interval results differed significantly from respective baseline values. For the very late epoch, no significant differences versus baseline were revealed. In addition, post-hoc comparisons between the active protocols and sham showed a significant excitability diminution of all active protocols for the early epoch. For the late epoch, the conventional single intervention, the optimized single intervention and the optimized tDCS protocol with a 20min interval induced significant motor cortical excitability diminution. No significant effects were found for the very late epoch (same evening to next day evening). Furthermore, post hoc tests comparing MEPs between active protocols indicated that neuroplastic after-effects of the single intervention conventional (for the early epoch), and optimized protocols (for early and late epochs) were significantly larger than those obtained by the repeated optimized protocol with a 24 hours interval.

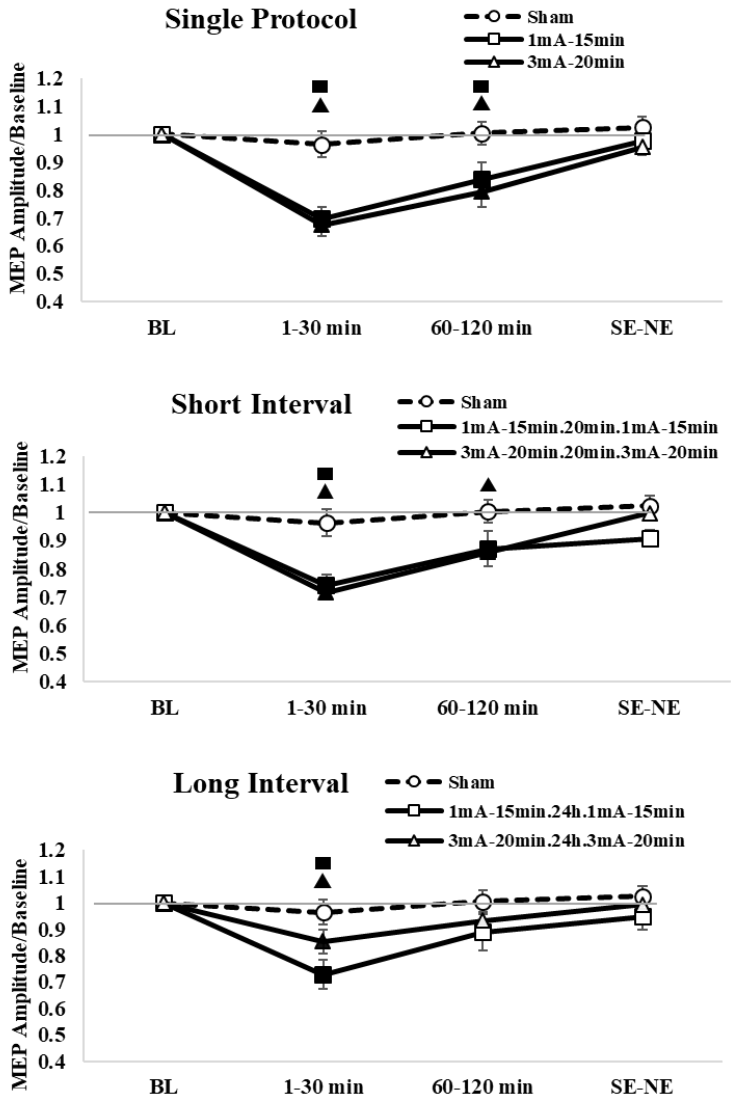

Figure 3.3 MEP amplitudes grand-averaged for early, late, and very late tDCS post stimulation effects. MEP were grand-averaged and pooled into three epochs of early (0-30 min), late (60-120 min) and very late (same day evening- next day evening) excitability changes. Single intervention includes conventional, and optimized tDCS protocols. The short interval includes repeated conventional and optimized tDCS with a 20 min interval. The long interval includes repeated conventional and optimized tDCS with a 24 h interval. Statistical data indicate that in comparison with sham, all protocols significantly reduced MEP amplitudes in the early epoch (0-30min after stimulation). For the late epoch (60-120min after stimulation), only conventional single intervention, optimized single intervention and optimized intervention with a 20min interval induced significant motor cortical excitability diminution. No significant effects were found for the very late epoch. Error bars represent standard error of means. Filled symbols indicate a significant difference of cortical excitability versus the respective baseline values. Floating symbols refer to each sub-figure, and indicate a significant difference between the respective active condition and the sham stimulation condition. SE: same evening, NE: next evening.

3.3.4. Qualitative assessment of tDCS protocols

Chi-square tests for each actual tDCS intensity including sham results indicated a significant effect for 3 mA ($\chi^2 = 27.167$, $p < 0.001$) with no significant effects for sham ($\chi^2 = 0.250$, $p = 0.617$) and 1 mA ($\chi^2 = 4.875$, $p = 0.087$). Table 3.3 shows the results of guessed intensities vs. actual intensities. Participant ratings for the presence and intensity of side-effects during and within 24 h after stimulation are listed in Table 3.4. The ANOVAs ('condition' - 7 levels) conducted for the side-effect questionnaires showed no significant differences between stimulation protocols for visual phenomena, itching, tingling, redness of the skin under the electrodes, pain, headache, fatigue, concentration, nervousness and sleep problems Table 3.5.

Table 3.3 Participants guess of the actual intensity. In each session, participants were asked to guess the intensity of the actually applied direct current (0, 1 and 3mA), merged over all intervals (single intervention, 20 min, and 24h intervals). The table contrasts actually applied intensity (rows) with perceived intensity (columns). Differences in the sum of the ratings of each intensity are present, because only one sham stimulation condition was included in the experiments, but three sessions per intensity for the real tDCS applications.

		Intensity guessed by participants		
		0 mA	**1 mA**	**3 mA**
Actual tDCS intensity	**Sham**	7	9	0
	1 mA	17	21	10
	3 mA	4	24	20

Table 3.4 Participant ratings of the presence and intensity of side-effects. Visual phenomena, itching, tingling and pain during stimulation and skin redness, headache, fatigue, concentration difficulties, nervousness and sleep problems within 24 h after stimulation. The presence and intensity of the side-effects were rated in a numerical scale from zero to five, zero representing no and five extremely strong sensations. Data are presented as mean ± SD.

Side-effects	**Sham**	**1mA-15min**	**1mA-15min with 20min interval**	**1mA-15min with 24h interval**	**3mA-20min**	**3mA-20min with 20min interval**	**3mA-20min with 24h interval**

During stimulation	Visual Phenomenon	0.37 ±0.71	0.62 ±0.71	0.62 ±1.08	0.06 ±0.25	0.56 ±1.09	0.87 ±1.50	1.12 ±1.40
	Itching	0.312 ±0.47	0.50 ±1.03	0.62 ±0.95	0.18 ±0.54	0.56 ±0.72	0.43 ±0.62	1.00 ±1.21
	Tingling	0.62 ±0.80	0.5 ±0.51	0.43 ±0.89	1.12 ±0.88	0.81 ±0.75	1.25 ±1.29	0.93 ±1.34
	Pain	0.25 ±0.44	0.43 ±0.81	0.50 ±1.03	0.75 ±1.12	0.31 ±0.79	0.68 ±1.13	1.06 ±1.23
24 hours after stimulation	Redness	0.31 ±1.01	0.25 ±0.57	0.25 ±0.57	0.43 ±0.89	0.37 ±0.61	0.50 ±1.21	0.75 ±0.93
	Headache	0.25 ±0.44	0.31 ±0.60	0.43 ±0.72	0.75 ±1.18	0.37 ±0.61	0.62 ±1.02	0.56 ±0.81
	Fatigue	0.68 ±0.79	0.31 ±0.47	0.56 ±0.89	0.81 ±1.22	0.68 ±1.01	0.75 ±1.06	0.62 ±0.80
	Concentration difficulties	0.37 ±0.88	0.37 ±0.80	0.37 ±0.88	0.43 ±0.62	0.25 ±0.77	0.31 ±0.79	0.62 ±1.20
	Nervousness	0±0	0.18 ±0.54	0.06 ±0.25	0.50 ±0.73	0.06 ±0.25	0.25 ±0.68	0.37 ±1.02
	Sleep Problem	0±0	0.06 ±0.25	0.12 ±0.50	0.43 ±0.62	0.12 ±0.50	0.18 ±0.75	0.18 ±0.54

Table 3.5 The presence and intensity of side-effects were analyzed by one-way repeated-measures ANOVAs. no significant effects were found for side-effects neither during nor 24 hours after tDCS.

	Side-effects	**d.f.**	***F* Value**	***p* Value**
During stimulation	**Visual Phenomenon**	2.837	2.281	0.096
	Itching	3.574	1.935	0.125
	Tingling	3.541	1.915	0.129
	Pain	3.317	2.066	0.111
24 hours after stimulation	**Redness**	3.031	0.887	0.456
	Headache	2.748	1.304	0.286
	Fatigue	3.623	0.893	0.466
	Concentration difficulties	2.425	0.681	0.540
	Nervousness	2.095	2.199	0.126
	Sleep Problem	2.063	2.143	0.133

3.4. Discussion

In this study, we explored if repetitive stimulation with short or long intervals extends the neuroplastic after-effects of low and high dosages of single interventions of cathodal tDCS. In a sham-controlled repeated measures design, single intervention cathodal tDCS protocols with 1mA for 15min and 3mA for 20min, and two repeated cathodal tDCS protocols with short (20min) and long (24 hours) intervals, for both single intervention protocol parameter combinations, were tested.

In general, the results of the study show that all cathodal tDCS protocols significantly reduced cortical excitability. The respective excitability alterations reflect however early-phase LTD-like neuroplasticity, since the duration of the after-effects was shorter than 3 hours [122, 128]. For repeated stimulation with short intervals, the after-effects of stimulation with conventional and optimized protocols remained nearly unchanged, as compared to the respective single intervention protocols. For the long interval (24 h) protocols, stimulation with the conventional protocol did not significantly alter respective after-effects, while stimulation with the optimized protocol reduced after-effects, as compared with the respective single interventions.

These results are in general accordance with previous findings from other studies conducted in healthy humans, in which late-phase LTD-like plasticity could not be induced by repeated cathodal stimulation with short intervals, and after-effects were reduced with an intervention interval of 24 h [66]. Similarly, repeated continuous theta burst stimulation (cTBS), another non-invasive brain stimulation tool suited to induce LTD-like plasticity, did not induce late phase LTD, when repeated with short intervals, in one study [129]. Other studies using comparable cTBS protocols showed however gradual enhancements of LTD-like plasticity with spaced protocols, which were nevertheless still in the range of early phase plasticity [130, 131]. Interestingly, in the latter study, intensified stimulation- similar to the results of the present study- reduced the excitability reduction in case of repeated stimulation. In contrast, prolonged effects in the range of late phase plasticity were elicited at the behavioral level via spaced theta burst stimulation over the frontal eye field in healthy humans, and the parietal cortex in patients affected by visual neglect, especially when more than 2 interventions were combined [132-134]. Studies in animal models to induce late phase LTD are comparatively rare, but showed a respective potential of slice preparations with repeated pharmacological [135], and also electrical stimulation interventions [124]. Interestingly in these studies, spacing between interventions differed between minutes, and 24h, and the repetition rate was usually larger than one.

3.4.1. Proposed mechanism

The question emerges why repeated plasticity-inducing cathodal tDCS did not generate late-phase LTD-like plasticity in healthy humans in the present, and some previous studies, along with studies in humans, in which related non-invasive brain

stimulation protocols were applied. One explanation might be challenges regarding to the translation of results from animal *in vitro* and/or *in vivo* studies to humans due to differences in stimulation parameters, such as intensity, duration and inter-stimulation intervals as well as differences in spontaneous activity, neuro-transmitter and neuromodulator concentration, among others [136, 137]. Standard animal *in-vivo* stimulation protocols affect relatively small populations of neurons in the target area, while tDCS protocols, in humans, stimulate hundreds of thousands of neurons of diverse origin, including excitatory as well as inhibitory neurons, concurrently. In addition, magnitude and direction of plasticity have been shown to be critically affected by the number of repetition blocks and the inter-stimulation interval. Three stimulation blocks with 10min interval were applied to induce late-phase LTD in the respective animal slice model [124], while in most studies in humans, including the present one, only one repetition was applied. Interestingly, however, larger repetition frequencies might be also more efficient in humans, and should therefore be targeted in future studies [132-134].

With respect to the mechanistic foundation of these effects, it has been shown in animal models, that NMDA receptors, trafficking of AMPA receptors and calcium channel activities are involved in the early and late phase of long term plasticity [12], and modification of gene expression and protein synthesis are required for the maintenance of LTD [138-140]. Similar mechanisms have been described for tDCS-induced cortical excitability alterations in humans [86, 103, 136]. Basic mechanisms of action of tDCS in humans are thus similar to respective mechanisms revealed in animal models. Animal studies have however also described forms of LTD triggered by metabotropic glutamate receptors (mGluRs) [141, 142], including late phase LTD [135]. While these different forms of LTD share similarities, they might have a discernable impact on the direction and rate of LTD plasticity induction. Whereas the contribution of NMDA receptors to tDCS-induced cortical excitability alterations is well-studied [86, 103, 143], a potential impact of metabotropic glutamate receptors, which might be relevant for late phase LTD induction, has not been revealed so far for cathodal tDCS in humans. A potential missing effect of tDCS on these receptors might contribute to the limited efficacy of tDCS to induce late phase LTD. At present, these explanations are however speculative, and should be explored in future studies directly.

Another important feature of the results is that the 24h interval of interventions resulted in diminished LTD-like effects of tDCS. Importantly, this diminution was present only for the intensified stimulation protocol, and observed with the second tDCS intervention applied at a time far beyond the time point when the single intervention resulted in MEP alterations. Homeostatic regulatory mechanisms, which control for the amount of neuroplastic alterations to avoid neuronal network destabilization, might help to explain these results. Here, prior synaptic activity influences the magnitude and direction of subsequently induced plasticity [144]. According to the Bienenstock-Cooper-Munro rule, a prolonged decrease of postsynaptic activity will shift the synaptic modification threshold, reducing the amount of LTD induced by a respective intervention [145]. NIBS studies in humans have shown similar mechanisms [66, 125, 146], and also showed that synergistic or homeostatic effects of repeated stimulation critically depend on the respective intervals. With respect to the latter, the pattern of results obtained in the present study fits nicely to those of a previous one, suggesting that intervals longer than a few minutes are required for the induction of homeostatic effects in case of LTD-inducing protocols [66]. They furthermore suggest that homeostatic counter-regulation is more easily induced by intensified stimulation protocols, which might lead to stronger saturation of the system, and that the mechanism driving these effects is beyond overt excitability alterations observable by MEP alterations.

The failure to induce late phase LTD in the present study does however not imply that it is principally not possible to induce such kind of plasticity in the human brain by tDCS. On the one hand, as outlined above, increasing the number of repetitions could make the intervention more efficient, similar as for other NIBS protocols, such as TBS. On the other hand, it was shown that enhancement of global dopaminergic activity in combination with cathodal tDCS induces late phase LTD-like plasticity [147], and that this effect is at least partially driven by D2 receptors [148]. Respective mechanisms of this synergistic effect are not explored in detail so far, but one possibility might be that NMDA receptor activity diminutions induced by D2 receptor activation reduce spontaneous activity of the stimulated neuronal networks, which might disturb or counteract the effects of cathodal tDCS.

For blinding purposes, we used local anaesthetic cream to decrease tDCS-induced somatosensory sensations, as reported in previous studies for 2 mA tDCS [97]. However, the participants' slightly higher rating of the presence and intensity of side-

effects during stimulation under the high stimulation intensity implies that the topical anaesthetic cream might have limited efficacy at this intensity (here, 3 mA), which might potentially reduce the quality of blinding.

3.4.2. Limitations and future directions

In the present study, we probed the neurophysiological effects of tDCS at the group level, but individual characteristics relevantly affect the outcomes of tDCS and other NIBS protocols [43, 108]. In accordance, the data obtained in the present experiment show some variability, Figure 3.4. Potential contributing factors are anatomical and biophysical differences of individual brains, including genetics, time of day, and brain state [109, 114, 149]. Thus, to improve stimulation efficacy at the level of the individual, an important next step would now be to understand/control for individual factors affecting the physiological and behavioral outcome of tDCS [45]. Moreover, the targeted population in this study was composed of healthy young humans. One-to-one transferability of our results from motor to other cortical areas as well as transferability to different age populations and patient groups should not be taken for granted due to state-dependency of tDCS effects, anatomical differences, and differences of neuromodulator activities and cortical excitability between healthy humans and respective patients, and has to be explored in future studies.

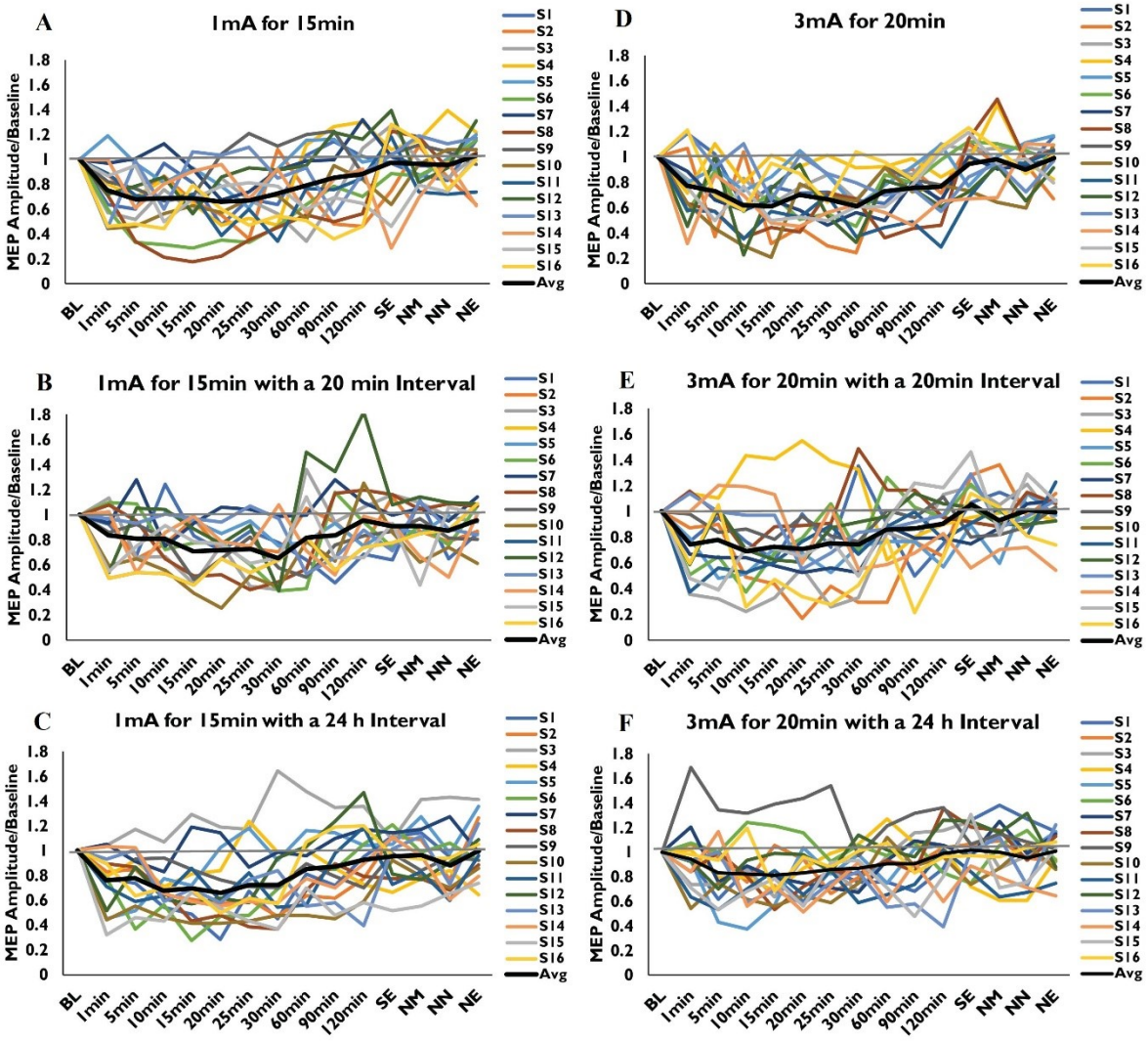

Figure 3.4 Intra-individual motor cortical excitability changes after single and repeated sessions of cathodal transcranial direct current stimulation (tDCS) over the primary motor cortex. The panels show individual excitability alterations after single intervention with the conventional protocol (1 mA for 15 min) (A), repeated intervention with the conventional protocol with a 20 min interval (B), repeated intervention with the conventional protocol with a 24 h interval (C), single intervention with the optimized protocol (3 mA for 20 min) (D), repeated stimulation with the optimized protocol with a 20 min interval (E), repeated intervention with the optimized protocol with a 24 h interval (F). Each colored line in each graph represents MEP values of one participant (S1–S16). MEP amplitudes are normalized to baseline values individually. SE, same evening; NM, next morning; NN, next noon; NE, next evening.

In general, and in difference to the inducibility of late phase LTP-like effects, it seems to be more difficult to induce late phase LTD-like effects in humans, independent from the specific plasticity induction tool. In this line, non-linearities of the effects of cathodal tDCS, dependent largely on stimulation intensity, but possibly

also on other parameters, play a prominent role [65, 98]. Respective mechanisms are largely unexplored, but might be important for the informed development of more efficient stimulation protocols. Based on results of animal, and some human studies, furthermore a promising way might be spaced stimulation with a frequency larger than one, which should be explored systematically in future studies, or combination of stimulation with pharmacological interventions. In this connection, it needs also to be stressed that the results of the present study do not allow to derive assumptions about the physiological effects of multi-session once daily stimulation protocols, which are often used in clinical trials. Finally, a further limitation of this study is that we included only one sham condition, because inclusion of a higher number of sham conditions would have reduced the feasibility of this already relatively laborious study.

3.5. Conclusion

The main results of this study show that late-phase plasticity was not induced by a single repetition of cathodal tDCS with short and/or long intervals by standard, and intensified stimulation protocols. We investigated the effects of repeated stimulation protocols with short (20min), and long intervals (24 hours) for a conventional (1mA for 15min) and a newly developed optimized tDCS protocol (3mA for 20min). Our results revealed that, compared to the single intervention protocols, the duration of after-effects of repeated conventional and optimized protocols remained largely unchanged, or was reduced. The results of the present study are thus not in accordance with the induction of late-phase LTD by a single repetition of cathodal tDCS, but hint for partially non-linear, probably homeostatic counter-regulation. Since more frequent repetition of intervention induced cumulative effects in other studies, and combination of cathodal tDCS with pharmacological interventions induced late-phase effects, these might be promising approaches for future studies.

4 Study 3: Ca2+ channel dynamics explain the nonlinear neuroplasticity induction by cathodal tDCS over the primary motor cortex

4.1. Introduction

Neuroplasticity is suggested to be a fundamental basis for many cognitive functions such as learning and memory formation [11]. At the cellular level, long-term potentiation (LTP) and long-term depression (LTD) have been the major target of plasticity research, which refer to alterations of the strength and/or efficacy of synaptic connections as reaction to internal and environmental demands, involving cascades of molecular reaction in synapses [11, 150, 151]. The induction and direction of long-term plasticity rely on the pre-post synaptic activity, as well as the activation of N-methyl-D-aspartate (NMDA) receptors, which results in calcium influx and thereby triggers biochemical changes that modify the strength of synapses [12].

Stimulation with weak direct currents (transcranial direct current stimulation, tDCS) induces neuroplasticity of the human brain non-invasively [85, 152]. The directionality of tDCS-induced plasticity depends on stimulation parameters: anodal tDCS enhances cortical excitability, while cathodal tDCS has inhibitory effects with conventional protocols of motor cortex stimulation [19, 20]. Similar to the induction of LTP and LTD in animal models, cortical plasticity induced by tDCS has been shown to be NMDA receptor-dependent, and the duration of after-effects can last for more than an hour [20, 96, 143]. Earlier studies revealed a positive association of the magnitude and duration of tDCS effects with stimulation duration/intensity below 20min and 1.5mA [19, 98]. However, non-linear after-effects of tDCS have been reported recently when duration and/or intensity were further increased. The inhibitory effect of 1 mA cathodal tDCS for 20 min was reversed to excitation when the intensity increased to 2 mA [64]. It has also been shown that excitatory effects of 1mA anodal tDCS for 13 min resulted in reduced motor cortical excitability by doubling the duration of the intervention [82].

One likely explanation for these non-linear after-effects might be the calcium-dependency of plasticity. Results of animal studies show that intracellular Ca^{2+} concentration determines the increase or decrease of the synaptic weight, i.e. LTP or

LTD [101, 121]. Hereby the strength of a plasticity induction protocol results in a specific level of NMDA receptor, and calcium channel activation, leading to corresponding amounts of Ca^{2+} influx. Low and prolonged Ca^{2+} influx causes LTD, a moderate increase of calcium influx induces no synaptic modulation, and larger calcium increases result in LTP [101, 121, 153]. Calcium influx beyond the LTP-inducing level might again result in no or excitability-diminishing plasticity due to potassium channel-controlled counter-regulatory mechanisms [102]. With this in mind, earlier tDCS studies in human participants showed that NMDA receptor block, which reduces calcium influx, prevents increased excitability after anodal and decreased excitability after cathodal tDCS [143]. Thus, the non-linear effects of tDCS induced by higher dosages might be caused by respective calcium dynamics. In principal accordance, it was shown that blockage of NMDA receptors abolished the inhibitory after-effects of 1 mA anodal tDCS applied for 26 minutes [82]. Therefore, Ca2+ channel dynamics are a candidate mechanism to explain non-linear after-effects of tDCS.

In the first study conducted for motor cortex tDCS, we systematically titrated cathodal tDCS parameters including different intensities (1, 2 and 3mA) and durations (15, 20 and 30mins) [154]. We observed non-linear after-effects, including induction of LTD- and LTP-like plasticity. While 1 mA cathodal tDCS induced a reduction of MEP amplitudes, 2 mA resulted in excitability enhancement and 3mA induced a secondary motor cortical excitability diminution. We hypothesize that the switch from LTD- to LTP-like plasticity by 20 min cathodal tDCS with 2mA was due to an enhancement of Ca2+ influx to a level sufficient for induction of LTP-like plasticity, and that the further intensified 20 min 3mA protocol resulted in counter-regulatory mechanisms due to calcium overflow, which would cause LTD-like plasticity due to activation of hyperpolarizing potassium channels, which will again reduce calcium influx [102]. To test this hypothesis, in the present study we applied the calcium channel blocker flunarizine in low, medium, and high dosages before cathodal tDCS (3mA, 20min) to induce different levels of intraneuronal Ca2+ concentrations. We expected that depending on the amount of intracellular calcium alteration induced by this substance, LTP- or LTD-like plasticity is induced in a dosage-dependent manner.

4.2. Materials and Methods

4.2.1. Participants

Twelve healthy, non-smoking participants (6 males, mean age ± standard deviation (SD): 25.16 ± 4.98) who participated in our previous study investigating neuroplastic after-effects of different cathodal tDCS dosages [154] were recruited. All participants were right-handed according to the Edinburgh handedness inventory [93]. History of neurological or psychiatric disease, current or previous drug abuse, alcohol abuse, bronchial asthma or allergies to components of the flunarizine (FLU) tablets, present pregnancy or metallic head implants, and fulfilled exclusion criteria for non-invasive electrical or magnetic brain stimulation [94, 95], served as exclusion criteria. The study conformed to the Declaration of Helsinki and was approved by the local ethics committee of the Leibniz Research Center for Working Environment and Human Factors (IfADo). All participants gave written informed consent before starting the study and were financially compensated for participating.

4.2.2. Transcranial direct current stimulation of the motor cortex

tDCS was administered by a battery-driven constant current stimulator (neuroConn GmbH, Ilmenau, Germany), through a pair of rubber electrodes covered by saline-soaked sponges (35 cm^2). The target electrode was placed over the primary motor cortex area representing the right abductor digiti minimi muscle (ADM), with the return electrode over the contralateral supraorbital region. Participants received cathodal motor cortex tDCS of 3mA for 20min, and sham tDCS. Prior to stimulation, topical dermal anesthetic cream (Emla® Creme – Lidocaine 2.5% and Prilocaine 2.5%) was applied on the skin directly under the electrodes, in order to decrease somatosensory sensations caused by tDCS [107]. Sham stimulation was delivered for 15 seconds followed by 20min with 0.0mA stimulation. All protocols were conducted with a 10seconds ramp-up and down at the start, and end of stimulation, Figure 4.1.

4.2.3. Assessing motor cortex excitability

Single pulse TMS was delivered by a PowerMAG stimulator (Mag&More, Munich, Germany) to measure excitability changes of the representational motor cortical area of the right ADM indexed as the amplitude of motor evoked potentials (MEP). The

TMS pulses were conducted via a figure-of-eight-shaped coil (diameter of one winding 70 mm; peak magnetic field 2 T) at a frequency of 0.25 Hz with 10% jitter. The coil was held tangentially to the scalp at an angle of 45° to the sagittal plane with the coil handle pointing laterally and posterior. The optimal coil position on the head was defined as the site where the stimulation results consistently in the largest MEPs with a given TMS intensity. A waterproof pen was used to mark the position of TMS coil on the scalp. The intensity of the TMS pulses was adjusted to elicit MEPs with a peak-to-peak amplitude of 1 mV (SI1mV) on average for baseline recordings. Finally, baseline cortical excitability was determined by measuring 25 MEPs. Surface EMG was recorded from the right ADM in a belly-tendon montage. The signals were amplified, and filtered (1000; 3Hz- 3KHz) using D440-2 (Digitimer, Welwyn Garden City, UK) and were digitized (sampling rate, 5kHz) with a micro 1401 AD converter (Cambridge Electronic Design, Cambridge, UK), controlled by Signal Software (Cambridge Electronic Design, v. 2.13).

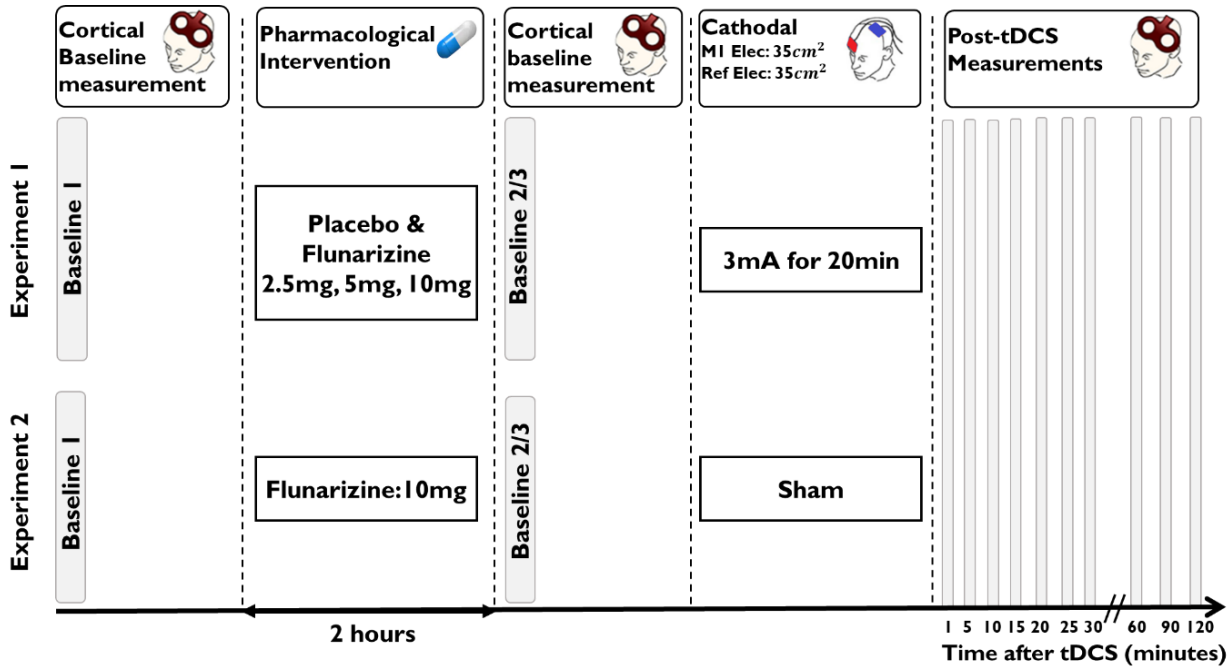

Figure 4.1 Course of the study. ***Experiment 1:*** to investigate the calcium channel dynamics involvement on tDCS-induced nonlinear neuroplasticity induction, 12 volunteers participated in this experiment. In each session, twenty-five single-pulse TMS stimuli were applied over the motor cortex representation area of the right ADM to measure baseline cortical excitability. Afterwards, placebo or FLU was administered in dosages of 2.5, 5 or 10 mg, and two hours later a second baseline was recorded to explore the effect of medication on corticospinal excitability, and TMS intensity was adjusted, if necessary. Then cathodal tDCS was administered with 3mA for 20 min. Immediately after finishing tDCS, after-effects were monitored by TMS-induced MEPs every 5 min for up to 30 min and the following time points of 60 min, 90 min, 120 min. ***Experiment 2:*** to

explore an impact of flunarizine alone on corticospinal excitability monitored by MEP, 8 (out of 12) participants participated in an additional session, in which 10 mg FLU was administered 2 hours before sham tDCS. Cortical excitability alterations were evaluated as in the sessions with active tDCS.

4.2.4. Pharmacological intervention

In each session, FLU in dosages of 2.5, 5, and 10 mg, or a respective placebo medication was administered 2h before tDCS. The substance is a L-type calcium channel antagonist that diminishes intracellular calcium levels. FLU at a dosage of 10 mg has been previously shown to diminish and/or abolish tDCS-induced neuroplastic after-effects; thus, it has relevant effects on neuroplasticity [82, 143]. Maximum plasma levels are reached approximately two hours after oral intake [155].

4.2.5. Experimental Course

Experiment1: The study was performed in a cross-over, double blind and randomized design. At the beginning of each session, subjects were seated in a comfortable chair in a reclined position with head- and arm-rests and were required to relax completely. EMG electrodes were placed over the right ADM as described above. Then TMS was applied over the left motor representation area of the right ADM to measure baseline cortical excitability (baseline 1, bl1), as explained above. After the baseline measurement (bl1), placebo or FLU was administered in dosages of 2.5, 5 or 10 mg in each session. Two hours later, the baseline MEP-amplitude was controlled (baseline 2, bl2), and if needed, TMS-intensity was adjusted to acquire MEP amplitudes of 1 mV on average (baseline 3, bl3). After that, 3mA cathodal tDCS was applied for 20 min, followed by recordings of 25 MEPs at the time-points of 1, 5, 10, 15, 20, 25, 30, 60, 90, and 120 minutes, Figure 1.

Experiment 2: to explore an impact of flunarizine alone on corticospinal excitability monitored by MEP, 8 (out of 12) participants were included in an additional session, in which 10 mg FLU was administered 2 hours before sham tDCS. Cortical excitability alterations were evaluated as in the sessions with active tDCS, Figure 1.

A minimum one-week interval between sessions was obligatory to avoid carry-over effects [85].

4.2.6. Calculations and statistics

MEP amplitudes were first visually inspected to exclude trials in which background electromyographic activity was increased. Then, the individual mean of MEP-amplitudes recorded at each time point were calculated for all subjects and all conditions separately. The post-intervention mean MEP amplitudes were then normalized to the respective individual mean baseline MEP-amplitude (quotient of post intervention versus pre-intervention MEP amplitudes).

4.2.6.1. Impact of 'SI1mV' and 'baseline MEP'

Differences between baseline measures can impact the outcome results. To exclude this, first three repeated measures ANOVAs were performed for values obtained before medication with 'session' (4 levels) as within-subject factor and 'SI1mV' (for bl1) , 'baseline MEPs' (bl1) and 'MEP used for normalization' (bl2/3) as dependent variables, respectively. Then, to test if medication affected baseline cortical excitability, two additional ANOVAs were calculated with 'condition' (3 levels) and 'time-point' (2 levels) as within-subject factors, and 'baseline MEP' (bl1 and bl2) or TMS intensities (measured for bl1 and bl3) as dependent variables.

4.2.6.2. Dose-dependent effect of FLU on tDCS-induced neuroplasticity: overall time course

To determine if the respective stimulation conditions with pharmacological intervention (FLU dosages: 2.5, 5 or 10 mg) effects differ from stimulation with placebo medication, a repeated measures ANOVA was calculated with normalized MEPs as dependent variable, and 'condition' (4 levels) and 'time point' (11 levels) as within-subject factors. In addition, to rule out possible effects of flunarizine itself on MEP amplitudes over the time course of the experiment, another repeated measures one-way ANOVA was calculated for experiment 2 with normalized MEPs as dependent variable, and 'time point' (11 levels) as within-subject factor.

4.2.6.3. Dose-dependent effect of FLU on tDCS-induced neuroplasticity: early and late after-effects

To better define the time course of plasticity induction by tDCS and compensate for variability between time points, the normalized MEP amplitudes of all-time points were pooled into two epochs: the average of MEP measures from the first 30 min after stimulation (early-phase after-effects) and from 60-120 min measurement after tDCS (late-phase after-effects). A repeated measures ANOVA was calculated with

'condition' (4 levels) and 'epoch' (3 levels) as within-subject factors and pooled MEPs as dependent variable. We conducted another repeated measures one-way ANOVA for experiment 2, with normalized MEPs as dependent variable, and 'time point' (3 levels) as within-subject factors, to exclude a possible effect of FLU alone on MEP amplitudes over the time course of the experiment.

We also performed an analysis of covariance (ANCOVA) with order of stimulation sessions (for the two-way ANOVAs in 4.2.6.2 and 4.2.6.3) as covariate to exclude a confounding effect of order on the results.

Mauchly's test of sphericity was conducted, and when necessary, the Greenhouse-Geisser correction was applied, for all ANOVAs. Exploratory post hoc Student´s t-tests (paired samples, two-tailed, $p \leq 0.05$) were conducted to determine significant differences between baseline and post-tDCS MEPs within each medication condition, and between FLU conditions for each time point. Exploratory post-hoc tests were not corrected for multiple comparisons according to Perneger [156]. Statistical analyses were performed with SPSS (IBM Corp. Version 26.0).

4.3. Results

All participants completed the entire study. Two subjects reported slight itching at the beginning and a slight redness of the skin site underneath the return electrode that did not interfere with the experiments. All other subjects tolerated the interventions well and no other adverse effects were reported.

4.3.1. Comparison of 'SI1mV' and 'baseline MEP' between sessions

Baseline MEP and SI1mV are listed in Table 4.1. The one-way repeated measure ANOVA showed no significant differences of baseline MEPs and SI1mV, obtained for bl1 (Baseline MEPs: df = 3, F = 0.907, p = 0.448; SI1mV: df = 3, F = 1.827, p = 0.161) and MEP used for normalization (df = 3, F = 0.186, p = 0.905), across all sessions. The 2-factorial ANOVAs revealed no significant difference between bl1 and bl2 (Condition: df = 3, F = 0.810, p = 0.497, Time point: df = 1, F = 0.144, p = 0.711, Condition × Time point: df = 3, F = 0.564, p = 0.643) and TMS intensities before (for bl1) and after medication (for bl3) (Condition: df = 3, F = 1.761, p = 0.173, Time point: df = 1, F = 0.849, p = 0.377, Condition × Time point: df = 3, F = 0.371, p = 0.774).

Table 4.1 TMS stimulation intensities and baseline measurements. SI1mV refers to the maximal stimulator output (%MSO) which was required for generating ~1mV MEP. bl1 refers to the baseline MEPs measured at the beginning of each session, bl2 refers to the baseline MEPs measurement two hours after medication and bl3 refers to the last baseline measurement if TMS adjustment was needed. The results of the ANOVAs indicate no significant differences of baseline MEP and SI1mV before and after medication between sessions. Data are presented as mean ± SD.

Experimental Session	SI_{1mv} (%MSO)		Baseline MEP (mV)		
	For bl1	For bl3	bl1	bl2	bl3
Placebo	59.37 ± 14.26	59.37 ± 14.06	1.00 ± 0.07	1.03 ± 0.11	1.06 ± 0.09
2.5 mg FLU	58.87 ± 11.81	58.46 ± 11.30	1.08 ± 0.20	1.07 ± 0.19	1.04 ± 0.11
5 mg FLU	59.20 ± 12.24	59.21 ±12.80	1.09 ± 0.28	1.02 ± 0.13	1.02 ± 0.08
10 mg FLU	61.75 ± 13.14	61.60 ± 13.43	1.04 ± 0.11	1.02 ± 0.14	1.03 ± 0.11

4.3.2. Dose-dependent effect of FLU on tDCS-induced neuroplasticity: overall time course

The 2-factorial ANOVA revealed significant main effects of condition (df = 3, F= 3.907, p = 0.017) and time-point (df = 10, F = 2.003, p = 0.040), but no significant effect of the condition × time-point interaction (df = 5.763, F = 1.345, p = 0.225), Figure 4.2; Table 4.2.A. The exploratory post-hoc t-test, comparing the tDCS after-effects with the respective baseline values showed significant alterations of MEP amplitudes with respect to the factor time. MEP amplitudes were significantly reduced in the placebo session for about one hour after stimulation. Administration of low dosage FLU resulted in a significant reduction of MEP amplitudes for about 30min after stimulation, while no significant MEP alteration were observed in the medium dosage FLU session. The results of the post-hoc tests indicate furthermore that the expected cathodal tDCS-induced LTD-like plasticity was initially abolished and later converted into facilitation in the high dosage FLU condition (for 90 min and 120 min time-points after stimulation). With respect to the factor condition, the exploratory post hoc t-tests reveal a significantly higher excitability under high dosage FLU as compared to placebo, and low dosage FLU sessions. In addition, the one-way repeated measures ANOVA calculated to exclude a contribution of FLU itself on cortical excitability (experiment 2) revealed no effect of FLU on cortical excitability over the time course of the experiment (time point: df = 10, F= 0.283, p = 0.983), Figure 4.3.A.

Table 4.2 Results of the ANOVAs conducted for the effect of FLU on tDCS-induced MEP alterations. A) The 2-factorial ANOVA calculated to investigate the overall effects of FLU on tDCS-induced corticospinal excitability alterations reveals significant main effects of condition, and time-point, but no interaction between condition and time-point. **B)** The 2-factorial ANOVA with pooled MEP values reveals a significant main effect of condition, and interaction between condition and epoch, but no significant main effect of epoch. Asterisks indicate significant results. d.f. = degrees of freedom.

		Factors	df	F value	*p value*
A	**Overall effects of FLU on tDCS-induced MEP alterations**	**Condition**	3	3.907	0.017*
		Time-point	10	2.003	0.040*
		Condition × Time-point	5.736	1.345	0.225
B	**Early and Late effects of FLU on tDCS neuroplastic after-effects**	**Condition**	3, 33	4.287	0.012*
		Epochs	2, 22	2.053	0.152
		Condition × Epoch	6, 66	2.774	0.018*

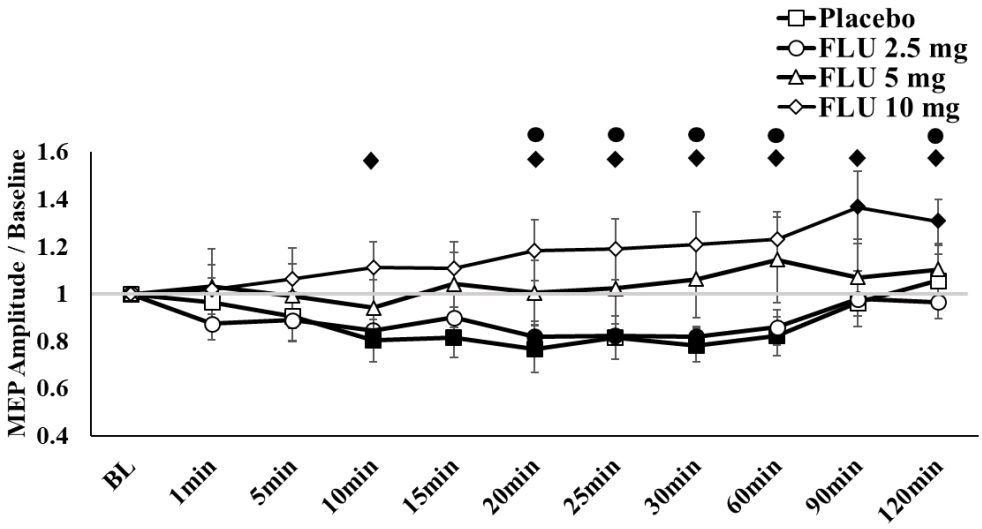

Figure 4.2 Dose-dependent effect of FLU on tDCS-induced neuroplasticity (overall time course). The results of the ANOVA reveal significant main effects of condition and time-point, but no significant effect of condition × time interaction. A dosage-dependency of medication on the tDCS-generated excitability-diminishing after-effects was identified. Medium and high dosage FLU reduced, abolished or converted tDCS-induced excitability diminution to an excitability enhancement. Error bars represent standard error of means. Filled symbols indicate a significant difference of cortical excitability against the respective baseline values. Floating symbols indicate a significant difference between the session with high dosage FLU, and placebo (◆) or low dosage FLU condition (●) in the respective epochs.

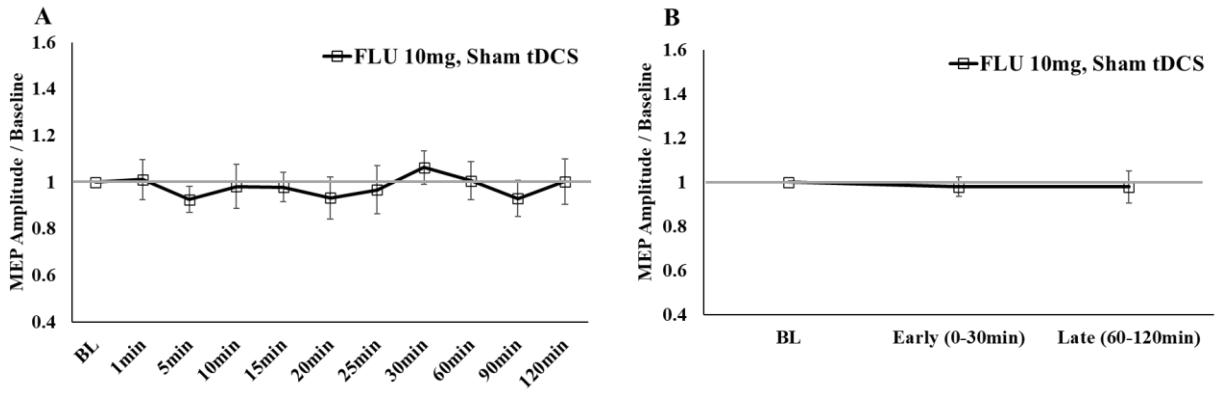

Figure 4.3 No effects of FLU on cortical excitability for prolonged time course measures. To exclude a possible effect of FLU alone on cortical excitability, eight participants (out of 12 from the primary study), participated in a control experiment in which 10 mg FLU was administrated 2 hours before sham tDCS. The results indicate no significant effects of medication on MEP amplitudes, for the overall (A) and pooled MEPs (B: Grand-averaged MEPs were pooled into two epochs of early (0-30 min) and late (60-120 min) excitability changes. Error bars represent standard error of means.

4.3.3. Dose-dependent effect of FLU on tDCS-induced neuroplasticity: early and late after-effects

The 2-factorial ANOVA with pooled MEP values reveals a significant main effect of condition (df = 3, F = 4.287, p = 0.012), and a significant interaction between condition and epoch (df = 6, F = 2.774, p = 0.018), but no significant effect of epoch (df = 2, F = 2.053, , p = 0.152), Figure 4.4; Table 4.2.B. The exploratory post-hoc t-tests, comparing the tDCS after-effects with the respective baseline values showed that MEP amplitudes were significantly reduced in the placebo and low dosage FLU session for the early epoch (first 30 minutes after stimulation), while an excitability enhancement was observed following the session with high dosage of FLU for the late epoch (60-120min after stimulation). Post-hoc tests comparing MEP sizes between conditions for a given time point showed significantly enhanced excitability for the early and late-epoch for the high dosage of FLU, as compared with the placebo session (for early and late epochs), and the session with low dosage of FLU (for early and late epochs). Moreover, the repeated measures ANOVA calculated to investigate effects of medication itself on the plasticity alteration revealed no significant results over the time course of the experiment (df = 2, F = 0.067, p = 0.936), Figure 4.3.B.

The ANCOVA results show no significant effect of session order on tDCS after-effects for both, pooled and non-pooled measures (Pooled MEPs: df = 2, F = 0.198, p = 0.824; non-pooled MEPs: df = 2, F = 0.332, p = 0.762).

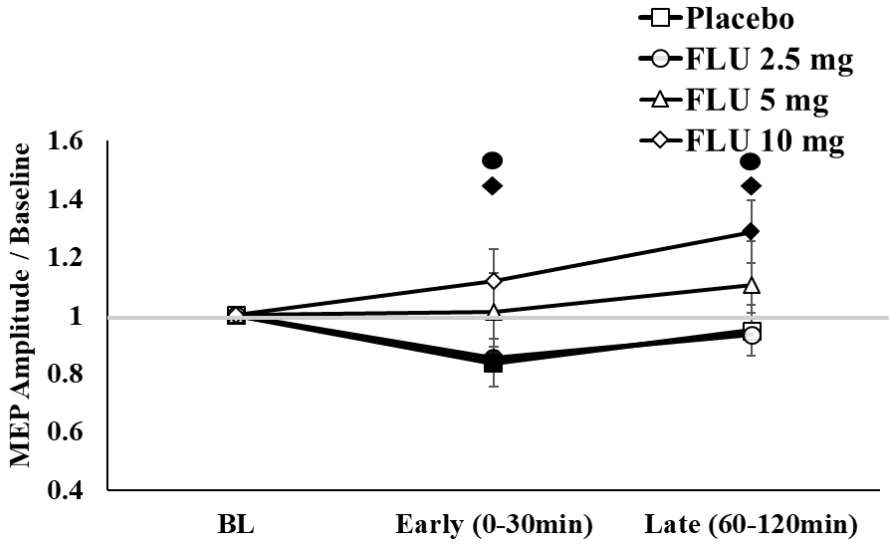

Figure 4.4 Dose-dependent effect of FLU on tDCS-induced neuroplasticity: early and late after-effects. Grand-averaged MEPs were pooled into two epochs of early (0-30 min) and late (60-120 min) excitability changes. Error bars represent standard error of means. Filled symbols indicate a significant difference of cortical excitability versus the respective baseline values. Floating symbols indicate a significant difference between the session with high dosage FLU, and placebo (◆) or low dosage FLU condition (●) in the respective epochs.

4.4. Discussion

In the present study, we explored the effects of calcium influx on tDCS-induced cortical excitability changes in healthy subjects via application of different dosages of a calcium channel blocker. In general, the results of the study show that tDCS-generated neuroplastic alterations are calcium-dependent, and that calcium-dependency can explain the nonlinear dosage-dependency of cathodal tDCS-induced neuroplastic after-effects, which were recently demonstrated.

We administrated low (2.5 mg), medium (5 mg) and high dosages (10 mg) of FLU, and showed that the inhibitory after-effects of 3 mA cathodal tDCS applied for 20 min were dosage-dependently diminished, abolished, or converted into a delayed excitability enhancement. FLU itself did not alter MEP amplitudes, as shown by the additional session with 10mg FLU administrated 2 hours before sham tDCS.

Animal in-vivo experiments revealed that direct current stimulation (DCS) impacts neuronal firing rate by a facilitatory effect under the anode and an inhibitory effect under the cathode, which can modify synaptic efficacy at both, the single cell and network level and thus induce long term effects, dependent on the intensity/duration of stimulation [157-162]. It has been, primarily in animal in-vivo studies and more recently by neuroimaging techniques, revealed that calcium dynamics, which involve NMDA receptors, are relevant for DCS-induced short- and long-term synaptic modifications [12, 103, 163-166].

In accordance, also for tDCS in humans, a glutamatergic process involving NMDA receptors, which have calcium channel properties, has been proposed by a series of studies as a possible mechanism of action of tDCS-induced plasticity. Pharmacological studies show that NMDA receptor block prevents tDCS-induced excitability alterations, both for anodal and cathodal tDCS, whereas NMDA receptor agonists enhance anodal tDCS-induced excitability increases [143, 167]. In line with these pharmacological studies, magnetic resonance spectroscopy (MRS) studies showed reduced glutamate after cathodal and at least trend-wise enhanced glutamate after anodal tDCS [168-170], and anodal tDCS enhances, while cathodal tDCS reduces intracortical facilitation, which depend on glutamatergic mechanisms [171, 172]. It can therefore be assumed that bidirectional plasticity induction via tDCS requires the contribution of NMDA receptors, and is therefore calcium-dependent.

Important for the results of the present study, animal models moreover demonstrated a dependency of the direction of plasticity from the amount of neuronal calcium influx [173]. Low-level Ca^{2+} influx has been shown to induce LTD, whereas a moderate calcium enhancement results in no synaptic modulation, a larger increase induces LTP, and maximum calcium influx might again abolish or convert plasticity due to counter-regulatory mechanisms [101, 102]. Similarly, neuromodulatory after-effects of tDCS in humans are suggested to be Ca2+-dependent, since blocking calcium channels prevents respective plasticity induction. Calcium dynamics are therefore a candidate mechanism to explain the nonlinearities of tDCS effects, which were recently revealed by enhanced tDCS intensity and duration. For cathodal tDCS, 2 mA stimulation for 20 minutes shifted motor cortex excitability from LTD- to LTP-like plasticity, while 1mA with 20 minutes significantly diminished it [64, 154]. In a recently conducted study we have shown that further enhancement of cathodal tDCS intensity again induces an excitability diminution, which provides further

evidence for a complex non-linear dose-dependency of cathodal tDCS-induced neuroplastic after-effects. We hypothesized that this double conversion of cathodal tDCS-induced after-effects depend on calcium dynamics. Based on the model described above, we would expect that stimulation with 1 mA induces LTD-like plasticity due to low calcium influx, 2 mA stimulation enhances calcium level to the LTP-induction range, and 3 mA stimulation results in LTD-like plasticity again due to counter-regulatory mechanisms, which help to avoid calcium overflow. For the 3mA stimulation scenario, which was explored in the present study, this would mean that dependent on the amount of calcium concentration reduction accomplished by calcium channel block, we expect a dosage-dependent reduction, abolishment, or conversion of LTD-like after-effects to LTP-like plasticity. The results of the present experiment fully confirm this hypothesis.

Non-linear cortical plasticity induction is not limited to tDCS effects, but has also been reported for other forms of non-invasive brain stimulation (NIBS). While low-intensity continuous theta burst stimulation (cTBS) at an intensity of 65% resting motor threshold (RMT) induced cortical excitability reduction, an excitability-enhancement was obtained by an otherwise identical protocol at an intensity of 70% RMT [174]. Similarly, for cTBS, which induces LTD-like plasticity at the group level with conventional protocols, enhancement of stimulation intensity beyond the intensity which induced LTD-like plasticity at the level of the individual resulted in LTP-like plasticity [175]. Similar effects have been shown for full spectrum tRNS, and 140 Hz tACS, where 0.4 mA stimulation intensity induced cortical excitability diminution, while stimulation with 1mA resulted in an enhancement of MEP amplitudes [176]. Since plasticity induced by these stimulation techniques is also NMDA receptor-dependent, a calcium-dependency of these effects is also probable [177, 178], and should be explored in future studies.

4.4.1. Limitations and Future Directions

The results of the present study imply that calcium channel dynamics are involved in the non-linear after-effects of high intensity cathodal tDCS. For a full overview about respective dynamics, systematic studies including application of medium (2mA) and lower intensity (1mA) tDCS combined with different flunarizine dosages would be desirable. In addition, increasing tDCS intensity might relevantly affect deeper cortical layers, and also generate plasticity in other types of neurons, which

have a different sensitivity to electrical fields, as indicated in animal models [105]. These mechanisms should be investigated in future research in larger detail.

Furthermore, pharmacological interventions only deliver indirect information on the contribution of calcium dynamics to the effects of tDCS. Studies in which calcium dynamics are directly explored are suggested to confirm these results. Moreover, identical dosages of FLU were administered to all participants; substance dosage was not adjusted to body weight, or body mass index. A respective individualization of medication to reduce variability of efficacy of the intervention should be considered in future studies. Finally, we did not monitor drug concentration levels in individuals. Thus, our experimental results allow to make qualitative statements about dosage-level substance-dependent effects, but deliver no quantitative information.

The results of the present study are relevant for the field, because they offer an explanation why cathodal tDCS results are relatively variable between studies. Furthermore, they might be important for clinical application settings with respect to several aspects. First, they hint to the fact that pharmacological therapy of patients might relevantly alter physiological stimulation effects. Second, they rise the question if a stimulation protocol which might result in secondary, counter-regulatory LTD-like effects, is well suited if primary weakening of synaptic connections is aimed for. The latter question is not easy to answer, and should be explored in larger details in future studies.

Recent advances in computational modeling of neurophysiological phenomena provide an important avenue to investigate tDCS effects ranging from single cell to network and whole brain levels [52, 160, 179, 180]. Computational modeling has also been utilized to link neurophysiological and brain structural properties to further explain tDCS responses at the individual level [62, 170]. However, to the best of our knowledge, current modeling approaches cannot well explain tDCS dosage-dependent nonlinear responses. It thus might be of interest for future modeling approaches to integrate conceptual mechanistic data, such as the proposed calcium-dependency of tDCS effects, for simulating the effects of tDCS on behavioral, cognitive, and neurophysiological outcomes.

4.5. Conclusion

The results of this study suggest a calcium-dependency of non-linear motor cortical plasticity effects of cathodal tDCS in human subjects. Inhibitory after-effects of high-intensity cathodal tDCS were dosage-dependently diminished, decreased, or converted into facilitation by calcium channel block via flunarizine. This improves our understanding of neurophysiological mechanisms underlying tDCS effects, especially with respect to the involvement of calcium dynamics in non-linearities, which may help to improve the efficacy of tDCS for future applications.

5 Study 4: A Comprehensive Study of the Association Between Individual Electrical Field and Anatomical Factors on the Neurophysiological Outcomes of tDCS: a TMS-MEP and MRI Study

5.1. Introduction

In humans, non-invasive brain stimulation (NIBS) provides an excellent avenue for modulating brain plasticity without disrupting the integrity of the skull, and is thus used to shed light on human brain physiology, brain functions underlying cognition and behaviour [76, 181], and probed to alter symptoms of neurological and psychiatric disorders [17, 18]. One of those, transcranial direct current stimulation (tDCS), changes regional cortical excitability in a polarity-dependent way, via delivering weak direct electrical currents, by electrodes placed on the head [22]. Despite promising results reported in pilot studies, effects are however largely moderate, show interindividual variability, and more sustained, and homogeneous effects are required, especially for clinical applications [18, 45].

Recent studies indicate an improvement of tDCS efficacy by manipulating the stimulation parameters at the group level [38, 65, 82, 182-184]. Despite dosage-dependent non-linearities in healthy humans [34, 64-68], and clinical populations [38, 40, 71], these however take not into account another relevant aspect of stimulation effects, which might limit efficacy, i.e. interindividual variability [45]. Indeed, relevant inter-individual variability of outcomes is reported in tDCS studies [43, 44], similar to other NIBS techniques [108, 185], which is one of the major challenges regarding its applicability for basic research, and clinical purposes. Various sources of variability have been identified, including physical (brain anatomy, tissue properties and neural orientation), physiological (genetics, sex- and age-dependency, pharmacology), and functional factors (psychological and behavioral processes) [109].

While causes of variability have yet to be explored in detail [45], recent human *in-vivo* experiments [186, 187], and current-flow simulations [60, 62, 188] indicate that both, spatial distribution and intensity of the tDCS-induced electrical field (EF) depend strongly on individual brain anatomy and tissue conductivity properties;

biophysical factors that can potentially impact the outcome of tDCS [58]. This highlights the importance of understanding and controlling the impact of these biophysical factors on neurophysiological and/or behavioral effects of tDCS at the level of the individual.

To address this, lately analytical, and more recently numerical simulation methods have been developed to estimate the electrical current throughout the head induced by transcranial electrical stimulation. However, analytical methods cannot fully account for the complex brain geometry, which can results erroneous EF analysis [189, 190]. To compensate for this shortcoming, numerical simulation methods, based on MR-derived detailed realistic head models, have been developed to predict the tDCS-induced EF distribution in the individual human brain [48, 58, 187, 191]. Numerical equations are typical solved by finite element (FEM) [192, 193], boundary element [57, 194, 195], or finite difference methods [196]. Despite open questions regarding to the validation [46, 187, 192] , and cost and complexity [48, 197] of these simulation methods, MR-derived realistic FEM simulation is widely used to predict the EF induced by transcranial electrical and/or magnetic stimulation, due to its capability of probing complex brain tissue characteristics such as anisotropy, and considering head models with morphologically realistic cortical neurons, as well as modeling tissues with continuously varying tissue conductivities [112, 198-203]. The results of computational studies have so far highlighted a strong contribution of individual head anatomical and/or electrical properties for the shape of the EF induced by tDCS, and shown further significant EF variability between humans, when one-size-fits-all tDCS protocols are used [59, 60]. Thus taken together, EF variability might be an important factor for heterogeneous outcomes of tDCS. However, despite increasing sophistication of these computational models, much less is known about the association of the individual tDCS-induced EF, and neurophysiological or behavioral effects of tDCS.

Up to now, a few pilot studies have shown an association of neurophysiological or behavioral effects of tDCS and EF differences at the group level. A negative correlation has been shown between the tDCS-induced EF strength under the target electrode and resting motor threshold (RMT) [61]. Furthermore, opposite changes of motor cortical excitability caused by 1mA anodal tDCS for 20min were reported, where individuals with large EFs showed decreased motor evoked potentials (MEPs), whereas volunteers with low EFs showed either no effect or increased MEP,

as compared to sham stimulation [62]. In another study, anodal tDCS (1 mA for 15 min) applied over the sensorimotor cortex altered GABA, and increased functional connectivity to a larger amount in participants with stronger EFs, whereas a negative relationship between EF strength and functional connectivity was observed when the same dosage of cathodal tDCS was applied [63]. Beyond these associations between simulated EF, and physiological parameters, another study suggested also the relevance of individual EF for cognitive effects of tDCS. Here, the magnitude of simulated current density values and improvements in verbal working memory performance were positively correlated for anodal tDCS with 1mA for 20min over the left dorsolateral prefrontal cortex [204]. With respect to the anatomical determinants of respective EF strengths resulting from tDCS, in a small sample size study (n=2), thickness of skull and cerebrospinal fluid (CSF), gyral depth and interelectrode distance accounted for up to 50% of the spatial variation of EF strength [60]. In another study with a larger sample size (n=24), which took the contribution of 11 anatomical factors into consideration, regional CSF thickness was the only single factor influencing EF strength, and explained about one-half of the variation of EFs between subjects [59]. However, it is still unclear whether and to what degree these individual physical factors (including tDCS-induced EF and/or anatomical factors) affect and/or explain the individual neurophysiological outcome of tDCS. A systematic investigation of the impact of these factors on the neuroplastic effects of different tDCS dosages is therefore required.

In addition, the regional neuroplastic after-effects of tDCD have largely been investigated for the motor cortex with TMS. Neuroanatomical studies however indicate that multiple circuits contribute to MEP generation, including afferent pathways from the somatosensory cortex and the dense inhibitory and facilitatory connections between the premotor cortex and M1, resulting in a compound signal with different generators [205, 206]. In principle accordance, computational modeling studies have also highlighted the contribution of the sensorimotor network into TMS-elicited MEP [198, 207-210]. This suggests that a computational model designed to investigate tDCS effects, based on motor cortex excitability measures, should also account for TMS EF distribution.

In two consecutive studies, we systematically titrated the effects of 15min of anodal and cathodal tDCS over the motor cortex at five intensities (sham, 0.5, 1.0, 1.5 and

2.0 mA), evaluated via (1) changes in TMS-induced MEP (Experiment 1: tDCS-*TMS-MEP*) [98], and (2) changes in cerebral blood flow (CBF) measured by fMRI (Experiment 2: tDCS-*fMRI*) [75], for up to 2h after intervention. The results of the tDCS-*TMS-MEP* experiment, at the group level, showed equivalent facilitatory effects at all tested anodal tDCS intensities relative to sham, while for cathodal tDCS, only 1.0mA resulted in a sustained excitability diminution. The outcome of the tDCS-*fMRI* experiment, in which the same participants were involved, revealed an increased CBF under the M1 electrode for all anodal intensities, while all active cathodal conditions, with exception of 0.5mA intensity, showed decreased CBF; tDCS with 2.0mA resulted in the greatest change of CBF in both polarities.

In the present study, we asked based on these data whether and to which extent the neurophysiological outcome of tDCS, at the individual level, can be explained by considering individual anatomical, and resulting EF factors. To this end, for each individual, we designed a structural MRI-based realistic head model, which was then used to simulate, based on the FEM, the tDCS- and TMS-induced EF, for two regions: 1) hand motor knob under the targeted electrode, and 2) TMS-induced effective EF. Based on these individual models, we obtained anatomical factors with potential relevance for the resulting EFs. We then investigated if any of these individual anatomical factors could explain the simulated EF variabilities. We finally explored whether specific anatomical and/or EF factors explained the neurophysiological outcomes of tDCS (including MEP and CBF). Based on previous findings, we anticipated a positive association between the individual EF and tDCS-induced sustained MEP and/or CBF alterations, with larger MEP and/or CBF changes linked with higher EF induction. Accordingly, we expected that anatomical factors resulting in lower EF strengths would also impact negatively on tDCS-induced neurophysiological alterations. The results of the present study would thus enhance comprehension of the dependency of tDCS effects from individual physical factors.

5.2. Materials and Methods

5.2.1. Participants

The neurophysiological, and anatomical data were obtained from Twenty-nine participants (16 males, mean age 25.0 ± 4.44 years) who were involved in our former

experiments ('tDCS-*TMS-MEP* [98] and 'tDCS-*fMRI*' [75]). In these experiments, participants were randomly allotted to two groups of anodal (fifteen participants), or cathodal tDCS (fourteen participants) over the course of five pseudo-randomized experimental sessions of different tDCS intensities (sham, 0.5, 1.0, 1.5, and 2.0mA). All participants were right-handed according to the Edinburgh handedness inventory [93]. None of the participants had a history of neurological or psychiatric disease, and none fulfilled exclusion criteria for non-invasive electrical or magnetic brain stimulation [94, 95]. The study conformed to the Declaration of Helsinki and was approved by the Medical Ethics Committee of the University of Göttingen.

5.2.2. tDCS over the primary motor cortex

For both experiments, tDCS was applied with a MR-compatible battery-powered constant current stimulator (neuroCare, Ilmenau, Germany), through a pair of surface rubber electrodes placed on the scalp. For the 'tDCS-*TMS-MEP*' experiment, electrodes were covered with a saline soaked sponge, and for the 'tDCS-*fMRI'* experiment, a layer of conductive paste (Ten20®, Weaver) was used to make contact between electrodes and scalp. The target electrode (35cm^2) was fixed over the motor cortex representational area of the right abductor digiti minimi muscle (ADM) as identified by TMS ('ADM hotspot'), and the return electrode (100 cm^2) was placed contralaterally over the right orbit. To further reduce any discomfort of the stimulation and to ensure adequate blinding, a topical anesthetic cream (EMLA®, AstraZeneca, UK) was pre-applied to the electrode areas on the scalp and was also layered on the bottom surface of the electrodes [97]. Based on the experimental group and session conditions, anodal or cathodal tDCS at an intensity of 0.5, 1.0, 1.5, 2.0mA, or sham was delivered for 15 min, with a 10 sec ramp at the beginning and end of stimulation. For the sham condition, 1.0mA was delivered for 30sec, with a 20sec ramp, which has been shown to achieve effective stimulation blinding [211, 212].

5.2.3. Motor cortical excitability assessment by TMS-induced MEPs

Monophasic TMS pulses were delivered via a figure-of-eight-shaped coil (diameter of one winding 70 mm; peak magnetic field 2T) at a frequency of 0.25Hz with 10% jitter. The coil was held tangentially to the scalp at an angle of 45° to the sagittal plane with the handle pointing laterally and posterior. MEP signals were sampled

(5kHz), amplified and bandpass filtered at 2Hz–2kHz (Digitimer, Welwyn Garden City, UK), and recorded/controlled with Signal software v.2.13 (CambridgeElectronicDesign, Cambridge, UK).

5.2.4. Structural and Functional MRI acquisition

For the 'tDCS-*fMRI*' experiment, anatomical and functional MR images were conducted in a 3 Tesla Magnetom TrioTim (Siemens Healthcare, Erlangen, Germany) using a 32-channel head coil. Before subjects were placed inside the magnet bore, stimulation electrodes were fitted over the targeted area (as explained in section 5.2.2). Initially, anatomical images based on a T1-weighted 3D turbo fast low angle shot (FLASH) MRI sequence at 1 mm^3 isotropic resolution were recorded (repetition time (TR) 2250 ms echo time (TE) 3.32 ms, inversion time 900 ms, flip angle 9 degrees). Subsequent scans were divided in ten blocks: pre-stimulation (baseline measurement), and then after-effects measurements immediately as well as 15, 30, 45, 60, 75, 90, 105, and 120 minutes after stimulation. For each of the ten blocks, three measurements were obtained: a resting-state blood-oxygen-level-dependent (BOLD) measurement (5 min 51 s), a resting-state arterial spin labeling (ASL) measurement (5 min 8 s), and a gradient echo field mapping scan (1 min). The ordering of the ASL and BOLD scans was counter-balanced evenly between subjects to mitigate any ordering effects. The analysis of the BOLD dataset was not considered within the scope of the current study. ASL images were acquired using a pseudo-continuous ASL (pcASL) sequence with the following parameters: TE 12 ms, TR 3750 ms, 24 slices, in-plane resolution 3x3 mm, slice thickness 4 mm, 20% gap, flip angle 90, FOV 192 mm, labelling time 1484 ms, post-label delay 1 s, RF gap 360 us, RF blocks 80. Each ASL sequence was accompanied by a background-suppressed proton density (PD) reference image using the same parameters, but without ASL labeling, which was used for functional registration and CBF calibration.

5.2.5. tDCS-induced Electrical Field Simulation

Each participant's T1 image was first automatically segmented into seven head tissue compartments, including white matter (WM), gray matter (GM), CSF, skull, scalp, eyeballs and air cavities, using the SPM12 software package [213] including an improved tissue probability map [214]. A custom

MATLAB (R2019a, MathWorks, MA) script was then used to correct for automatic segmentation errors [214]. Afterwards, a 3D head model, based on the segmented images, was developed using Simpleware ® software (Synopsys, Inc., Mountain View, USA) [215], with electrodes (2mm thickness) and Ten20 paste (3mm thickness) precisely located on the head, over the targeted areas, by visual inspection of the structural T1 images, using the render view of MRIcron [216], and a custom Matlab script for electrode placement [214]. The 3D head model was then meshed with tetrahedral elements using adaptive meshing (+ScanFE, Simpleware software). The volume-meshed model was imported to COMSOL Multiphysics software package v.5.5 (COMSOL Inc., MA, USA), and tissue electrical conductivity values were assigned (in S/m): GM:0.276; WM:0.126; CSF:1.65; skull:0.01; scalp:0.465; air:2.5×10^{-14}; Ten20 paste:1.5; electrode rubber: 29 [112, 217]. The EF was then calculated under the quasi-static approximation for 1mA tDCS [191]. Finally, the EF strength, $|E| = \sqrt{{E_x}^2 + {E_y}^2 + {E_z}^2}$, and the component of the EF perpendicular to the interface, $\hat{n}.\vec{E} = \vec{n}_x.\vec{E}_x + \vec{n}_y.\vec{E}_y + \vec{n}_z.\vec{E}_z$ (where $\vec{n}$ is the inner normal vector), on the mesh grids were imported to MATLAB, and interpolated then onto a regular grid similar to the original MR images ($1mm^3$) [191, 214]. All processes were performed on a workstation, with 128GB of RAM and 16 physical AMD-Ryzen-Threadripper 1950X 3.40GHz processors, Figure 5.1C.

5.2.6. TMS-induced Electrical Field Simulation

First, a realistic model of the coil (Magstim 70mm figure-8) was designed using AutoCAD (Autodesk Inc., CA, USA), with two circular wings with nine turns each and a wire cross section of 1.75mm×6mm [218-220], and imported to the Simpleware® software (+ScanCAD). The coil was then precisely placed over the individual head model, with the center placed at the midpoint of the tDCS target electrode and 3mm distance to the scalp, and the handle held 45° to the midline [209, 221]. The head and coil models were then placed inside a spherical surrounding composed of air (r = 0.5m), and the full model was meshed with tetrahedral elements using an adaptive meshing algorithm (+ScanFE, Simpleware®). The volume-meshed model was finally imported to COMSOL Multiphysics software package to

calculate the total EF ($\vec{E} = -\frac{d\vec{A}}{dt} - \vec{\nabla}\varphi$, where $\vec{A}$ and φ represent the magnetic vector potential and the electric scalar potential, respectively [222], for a monophasic pulse (current derivate ($\frac{dI}{dt}$)=67A/µs) delivered by the coil connected with the Magstim 200 stimulator to induce a posterior–anterior current flow in the brain [223, 224], Figure 5.1C. Electrical conductivity of the respective head tissue compartments was assigned as in the tDCS simulation, in addition with an electrical permittivity of 10^4 for all head tissues [220], coil (5.8×10^7S/m) [225], and surrounding air (permittivity of free space, and a conductivity of 2.5×10^{-14}S/m). The EF results were finally imported to MATLAB and interpolated onto a similar regular grid of the MR images ($1mm^3$) [191, 214].

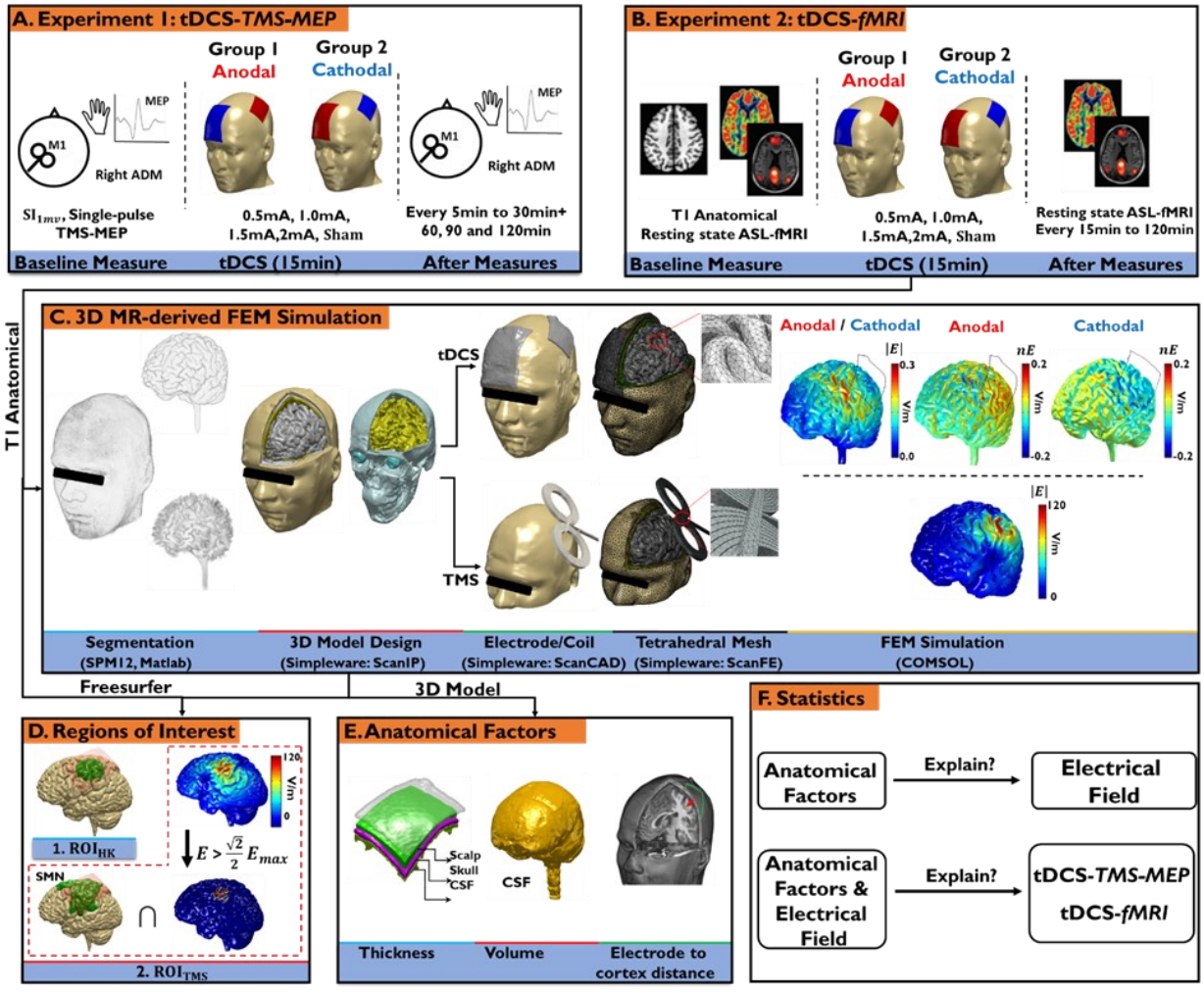

Figure 5.1 Study design. Twenty-nine participants, who took part in two consecutive experiments, ('tDCS-TMS-MEP' and 'tDCS-fMRI'), randomly divided into two groups (Anodal: n=15; Cathodal: n=14). In each group, participants were involved in five randomized sessions, to receive

15min of sham, 0.5, 1.0, 1.5 or 2.0 mA tDCS, with the target electrode(35cm^2) placed over M1 and the reference electrode (100cm^2) positioned contralaterally above the right supraorbital region. **A)** ***Experiment 1- 'tDCS-TMS-MEP'***: The neuroplastic effects of tDCS were obtained by single-pulse TMS-MEP, by comparing the baseline (obtained prior to tDCS) motor cortical excitability of the right ADM, and MEPs obtained every 5 min up to 30min, and 60, 90 and 120min, after tDCS. **B)** ***Experiment 2- 'tDCS-fMRI'***: Scanning acquisition: a high resolution anatomical T1 image (only before tDCS), and resting state ASL-fMRI, as a measure of CBF, were recorded prior to, during, and every 15min up to 120min after motor cortical tDCS, to investigate the tDCS effects on cortical neurovascular activity. **C)** ***3D MR-derived FEM simulation***: the anatomical image was first automatically segmented into scalp, skull, eyeballs, air cavities, CSF, GM and WM, using the SPM12 toolbox, and then corrected for the inherent segmentation errors, using a custom MATLAB script. Segmented-corrected images were then imported to Simpleware software package to: 1) design a 3D model of the head (+ScanIP), 2) locating the tDCS electrode or TMS coil over the targeted area (+ScanCAD), and 3) mesh the model via a tetrahedral adaptive meshing algorithm (+ScanFE). The meshed models were then imported to the COMSOL software package to simulate the EF distribution (tDCS: including the EF strength ($|E|$) and normal component ($\hat{\boldsymbol{n}}.\vec{\boldsymbol{E}}$); TMS:$|E|$) for 1mA anodal (group 1), cathodal tDCS (group 2), and TMS (for both groups). **D)** ***Regions of Interest (ROI)*****:** two ROIs including 1) ROI_{HK}: motor hand knob and 2) ROI_{TMS}: where the total TMS-induced EF meet the predefined condition: $E > \frac{\sqrt{2}}{2} E_{max}$, which refers to the half power region, the region in which the EF is at least 50% of the maximum power for a specific depth. **E)** ***Anatomical Factors*****:** for each individual, the anatomical measures including thickness of scalp, skull and CSF, and CSF volume (without ventricles), were performed by Simpleware measurement tools, in addition to measures of the Euclidian distance from the center of the target electrode to the individual coordinate of the hand motor area. **F)** ***Statistics:*** the objective was to first testify if any of the measured anatomical factors explain individual EF variability. Secondly, we investigated whether and to what extent the individual anatomical factors and/or EFs explain the variability of the neurophysiological outcomes of tDCS (MEP and CBF measures).

5.2.7. Experimental procedure: 'tDCS-TMS-MEP' and 'tDCS- fMRI'

The details of the experimental procedures can be found in our former studies [75, 98]. Briefly, for the 'tDCS-*TMS-MEP*' experiment, subjects were seated in a comfortable chair with head and arm rests. First the ADM hotspot was identified, and TMS intensity adjusted to elicit MEPs with a peak-to-peak amplitude of on average 1mV (SI_{1mV}). Afterwards, baseline cortical excitability was determined by measuring 25 MEPs, following 15min of anodal or cathodal stimulation (in five sessions: sham, 0.5, 1.0, 1.5, and 2.0mA). After finishing the stimulation, cortico-spinal excitability was assessed by TMS measurements, every 5 min for up to 30min, and then 60min, 90min, 120min after tDCS, Figure 5.1.A. Experiment 1. For the *'*tDCS-*fMRI'* sessions*,* stimulation electrodes were first placed over the head with the target electrode positioned over the 'ADM hotspot', as identified by TMS measures, and the return electrode on the right supraorbital region. Subjects were

then situated comfortably inside the scanner, to obtain an initial T1 anatomical scan, followed by baseline measures: resting-state BOLD, ASL sequences, and a Field Mapping sequence in counterbalanced order. Then, anodal or cathodal tDCS was delivered for 15 min in five sessions in randomized order (as explained above); a resting-state block was also recorded during stimulation. After finishing stimulation, the tDCS device was turned off, and the after measures resting-state blocks were acquired in intervals of 15 min until 120 min after the end of stimulation, Figure 5.1.B. Experiment 2.

For both experiments, there was at least 1 week interval between each session to avoid carry-over effects [85].

5.2.8. Calculations

5.2.8.1. Neurophysiological effects of tDCS (TMS-MEP and ASL-fMRI)

Details of the calculations and statistical analyses of the MEP and CBF data are available in our former studies [75, 98]. Briefly, for the first experiment 'tDCS-*TMS-MEP*', individual means of each time point's MEP amplitudes (MEP_t), were calculated and then normalized (Δ) to baseline MEPs (MEP_{bl}): $\Delta\text{MEP} = (MEP_t - MEP_{bl})/MEP_{bl}$. For the second experiment 'tDCS-*ASL-fMRI*', the grand-average mean perfusion time course of the voxels was averaged over the time-series (CBF_t) and then normalized to the pre-stimulation baseline (CBF_{bl}): $\Delta CBF = (CBF_t - CBF_{bl})/CBF_{bl}$. In the present study, to compensate for variability between time-points, and reduce also the number of required time-points for the analysis, the neurophysiological after-stimulation measures including ΔMEP amplitudes (ten time-points) or ΔCBF values (eight time-points; excluding the scanning block during stimulation) were separately grand-averaged and pooled into two epochs of early (0-60min after stimulation) and late (75-120min after stimulation) effect.

5.2.8.2. Regions of Interest

To investigate the association between neurophysiological responses to tDCS, and the individual EF and/or anatomical factors (please see below), we defined two ROIs: 1) ROI_{HK}, and 2) ROI_{TMS}. The ROI_{HK} was selected to explore the direct tDCS effects over the hand knob motor representation area, which was defined in the cortex using a 2.5cm radius sphere centered at MNI coordinates (x=−37.4, y=−19.1,

z=52.4 mm [226]). The ROI_{TMS} was selected based on neuroanatomical and computational studies, suggesting the contribution of different neural generators of the sensorimotor network for the TMS-evoked MEP. We first extracted the respective regions (Brodmann areas corresponding to the left sensorimotor network, including the somatosensory cortex (BA1, BA3), M1 (BA4), and the premotor cortex (BA6)) from the parcellated Brodmann atlas generated by Freesurfer reconstruction of each individual T1 image. We then defined an area over this region, where the TMS-induced EF met the predefined condition $E > \frac{\sqrt{2}}{2} E_{max}$; the half power region [227-229]), Figure 5.1.D. Remote brain areas and/or regions underneath the reference electrode, were not within the scope of the current study.

5.2.8.3. Anatomical measures

The aim here was to investigate the influence of individual anatomical factors, which might affect neurophysiological responses to tDCS, by shaping the tDCS-induced EF [59, 60, 230]. To this end, we measured 1) scalp thickness, 2) skull thickness, 3) CSF thickness, 4) CSF volume (without ventricles), and 5) distance from the center of the tDCS target electrode to the individual hand motor area (ECD). The individual tissue thickness and CSF volume were obtained by respective measurement tools in Simpleware. We first selected the compartment corresponding to the target electrode (plus additional 2cm at each side; to include the area in which the target electrode exerted strong effects [60]), and extruded the layer of the thickness dimension to include the tissue regions underneath. From these individual models, we then quantified the thickness of the tissues of interest. For determination of ECD, first the center of each electrode was identified using a render view of MRIcron [216], the Euclidian distance was then calculated from this location to the individual hand motor area coordinate (MNI coordinates: x=−37.4, y=−19.1, z=52.4 mm [226]), Figure 5.1.E.

5.2.9. Statistics

Multiple linear regressions were first applied to investigate if the individual averaged EF (|E| and $\hat{n}.\vec{E}$) for the ROI_{HK} or ROI_{TMS} (as dependent variable) can be explained by respective individual anatomical factors (as explanatory variables). The same

statistical analysis was then used to test whether and to which extent the individual variability of the neurophysiological effects of tDCS (including ΔMEP and ΔCBF as dependent variables) can be explained by the respective individual EF ((|E| and $\hat{n}.\vec{E}$; for the ROI_{HK} and ROI_{TMS}), or anatomical factors. Note that, for ΔCBF, we only used EF for the ROI_{HK} because of the missing TMS condition in the MRI experiment. In addition, for each regression analysis, we further calculated Pearson's correlation coefficient to identify the directionality of the predictors. The respective p-values were adjusted for multiple comparisons via the False Discovery Rate (FDR) [231, 232].

5.3. RESULTS

5.3.1. tDCS-induced MEP and CBF alterations

The detailed results of the neurophysiological effects of tDCS are available in our former studies [75, 98]. Briefly, for the 'tDCS-TMS-MEP' experiment, a dosage-dependent effect on cortico-spinal excitability was observed, with significant facilitatory effects for all anodal active tDCS protocols relative to sham, while for cathodal tDCS, only 1.0mA resulted in a sustained excitability diminution, Figure 5.2.A (for the individual results see Figure 5.3). For the 'tDCS-fMRI' experiment, CBF increased under M1, for all active anodal tDCS conditions, while all active cathodal conditions, with the exception of 0.5mA intensity, decreased CBF (most

clearly in late epochs), with 2.0mA showing the largest change for both polarities, Figure 5.2.B (for individual results see Figure 5.4)

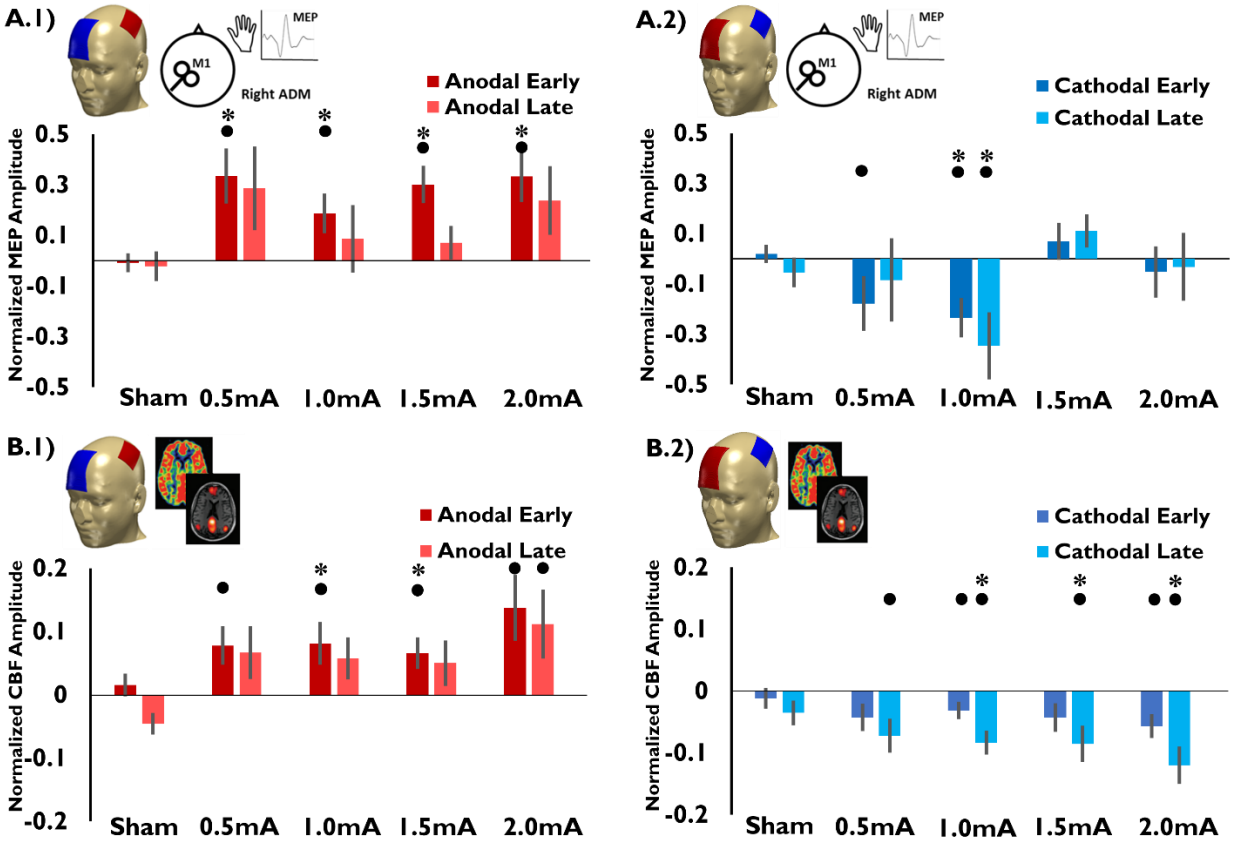

Figure 5.2 Summary of the neurophysiological effects of tDCS on cortico-spinal excitability and cerebral blood flow. Anodal or cathodal tDCS (in five sessions: sham, 0.5, 1.0, 1.5, and 2.0mA) were applied for 15min, and the effects of the interventions were obtained over the 2-h after-stimulation period. To compensate for variability between single time-points, MEP amplitudes (ten time-points) or CBF values (eight time-points) were separately grand-averaged and pooled into two epochs of early (0-60min after stimulation) and late (75-120min after stimulation) effects. **A1,2)** dosage-dependent effects of tDCS on cortico-spinal excitability were observed, with significant facilitatory effects for all anodal active tDCS protocols, relative to sham, while for cathodal tDCS, only 1.0 mA resulted in a significant excitability diminution. **B)** CBF increased under M1 for all active anodal tDCS conditions, while all active cathodal conditions, with the exception of 0.5mA intensity, showed decreased ΔCBF; with 2.0mA resulting in the largest change of CBF for both polarities. Error bars represent standard error of means. Floating symbols indicate a significant difference between stimulation after-effects and sham (*), or baseline (●) in the respective epochs. Asterisks indicate significant results. Figures adapted from [75] by permission.

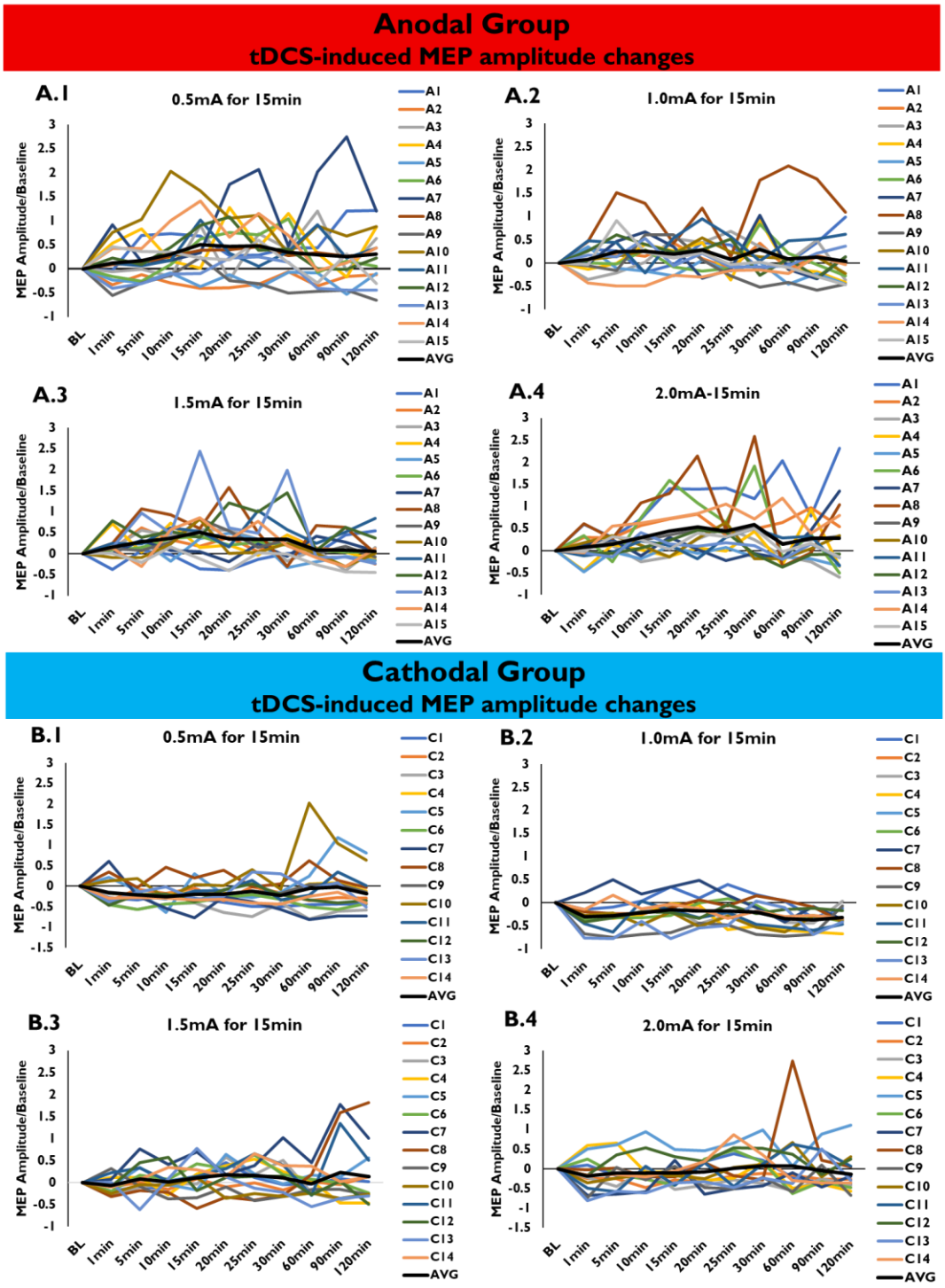

Figure 5.3. Intra-individual motor cortical excitability changes after tDCS over the primary motor cortex. The panels show individual excitability alterations after anodal tDCS (A1-4), and cathodal tDCS (B1-4), with 0.5, 1.0, 1.5, and 2mA, each intensity applied for 15min. Each colored line in each graph represents MEP values of one participant (A1–A16: anodal group; C1-C14: cathodal group). AVG: averaged across participants. MEP amplitudes are normalized to baseline values individually.

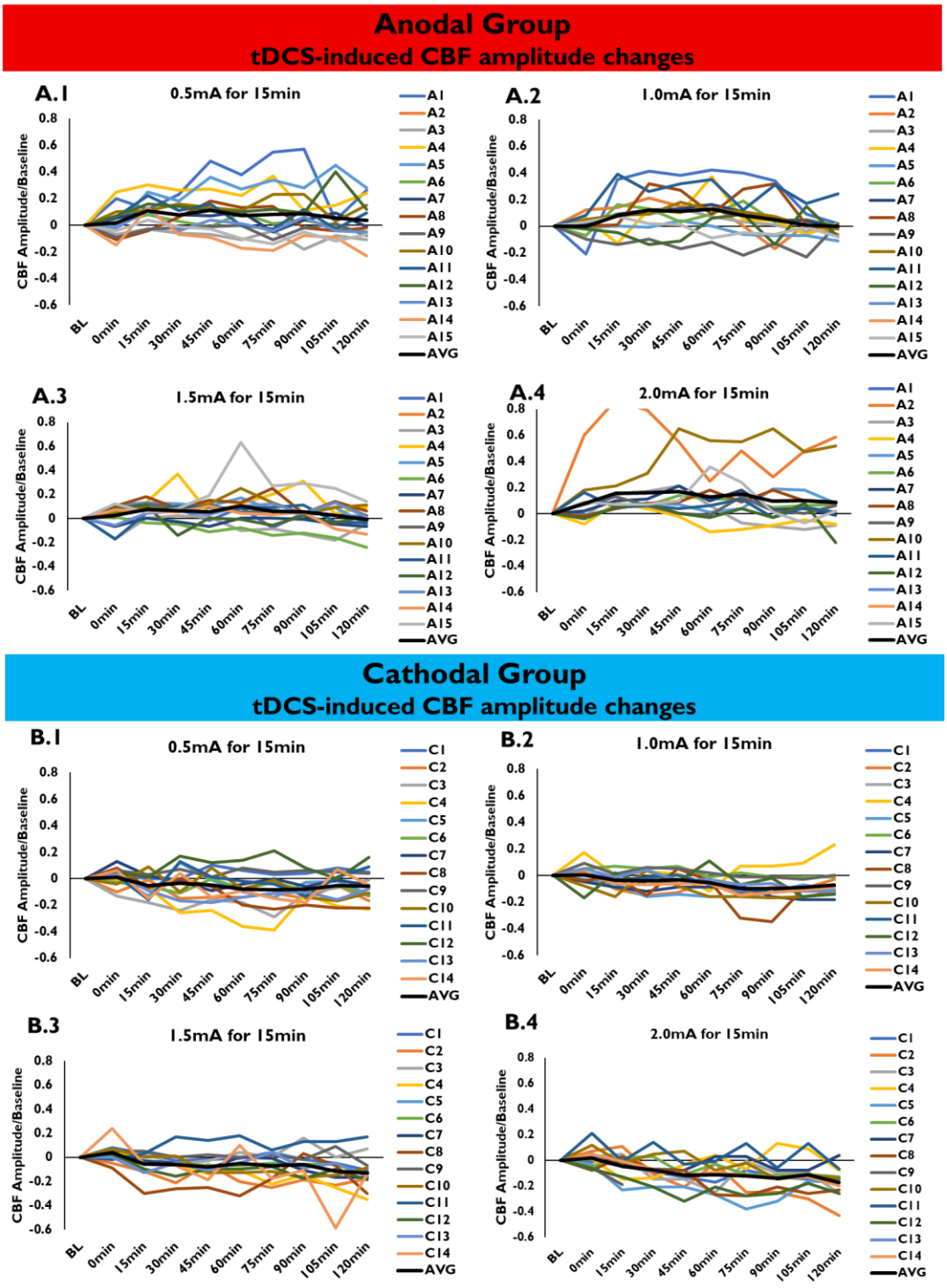

Figure 5.4. Intra-individual CBF changes after tDCS over the primary motor cortex. The panels show individual CBF alterations after anodal tDCS (A1-4), and cathodal tDCS (B1-4), with 0.5, 1.0, 1.5, and 2mA, each intensity for 15min. Each colored line in each graph represents CBF values of one participant (A1–A16: anodal group; C1-C14: cathodal group). AVG: averaged across participants. MEP amplitudes are normalized to baseline values individually.

5.3.2. tDCS- and TMS-induced Electrical Field Simulation

Figures 5.5 and 5.6 show the EF distribution ($|E|$ and $\hat{n}.\vec{E}$ for tDCS and $|E|$ for TMS) on grey matter surface, for the anodal (15 participants), and cathodal groups (14 participants), respectively.

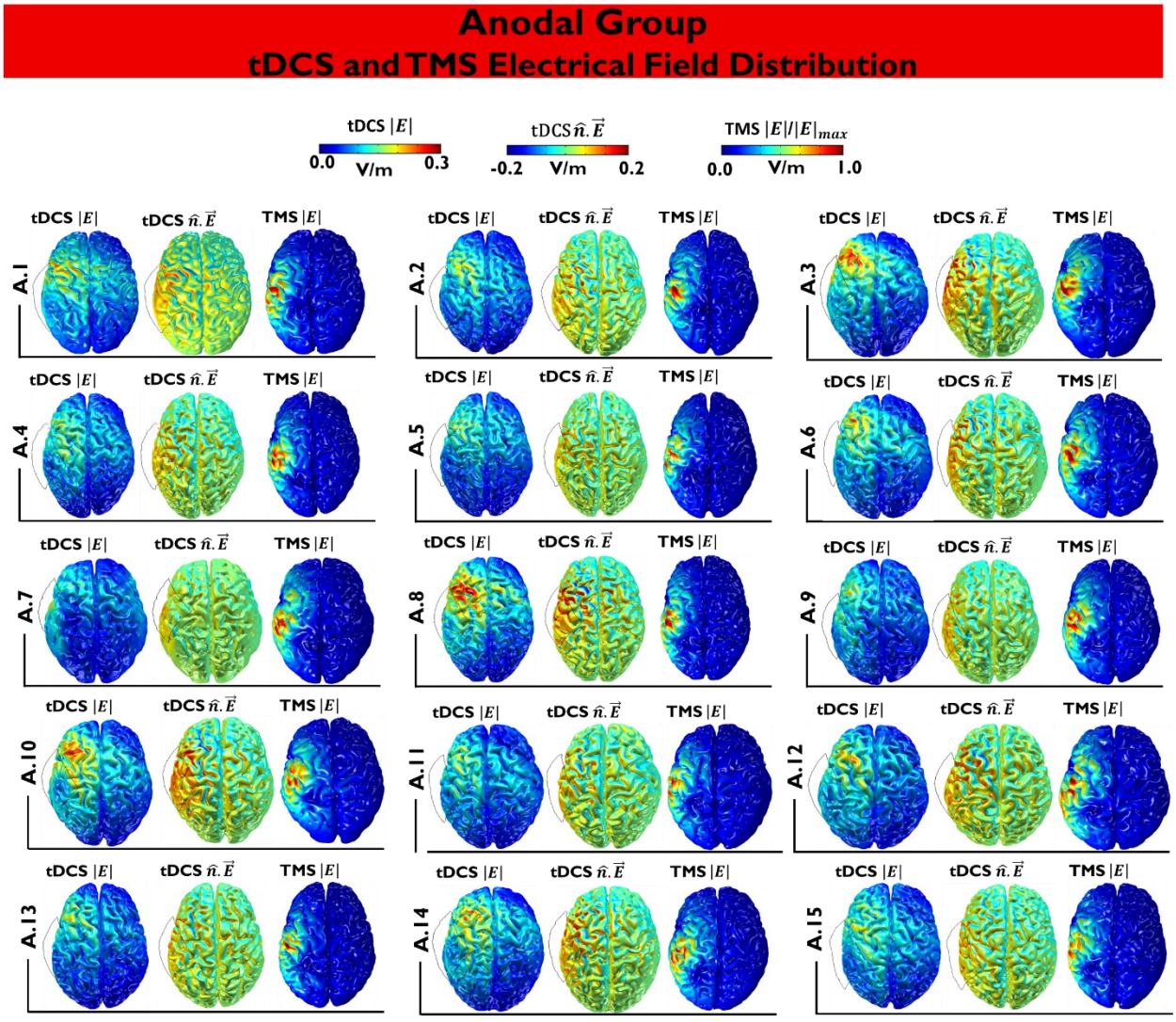

Figure 5.5 Anodal Group EF distribution. For each individual, the tDCS and TMS- induced EF were calculated. For 1mA anodal tDCS (which refers to surface inward current over the target area), the target electrode (35cm^2) was positioned over the scalp targeting the ADM muscle representation, and the reference electrode (100cm^2) placed contralaterally above the supraorbital

area. The resulting electrical fields over the gray matter surface are presented for tDCS-induced EF strength ($|E|$), -EF normal component ($\hat{n}.\vec{E}$), and EF strength of the TMS-induced EF ($|E|$).

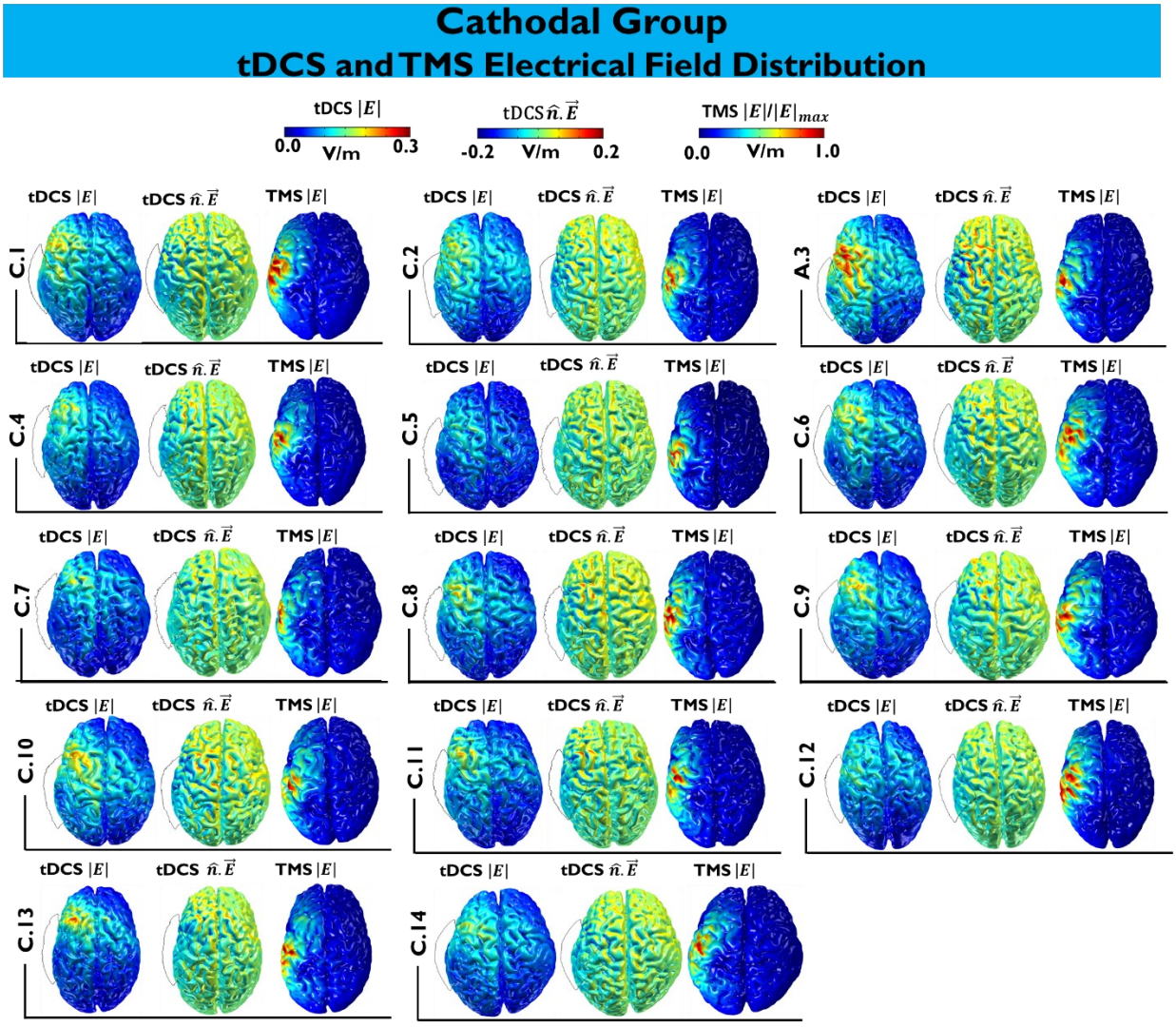

Figure 5.6 Cathodal Group EF distribution. For each individual, the tDCS- and TMS-induced EF were calculated. For 1mA cathodal tDCS (which refers to outward current over the target area), the target electrode (35cm^2) was placed over the scalp, targeting the ADM muscle representation, and the reference electrode (100cm^2) placed contralaterally above the supraorbital area. The results over the gray matter surface present the tDCS-induced EF strength ($|E|$), -EF normal component ($\hat{n}.\vec{E}$), and EF strength of TMS-induced EF ($|E|$).

5.3.3. Association between Anatomical Factors and Electrical Field

The average, standard deviation and median values of the anatomical factors, and calculated EF are listed in Table5.1. The results of the linear regression analyses, along with Pearson's correlation coefficients, which were used to test if any of the

anatomical factors explained the individual EF (strength |E|, and normal components $\hat{n}.\vec{E}$) at the two ROIs (ROI_{HK} and ROI_{TMS}), indicated that, for the anodal group, CSF thickness significantly predicted the |E| (R^2=0.476, p=0.008; r =-0.690, and ROI_{TMS}: R^2=0.620, p<0.001; r =-0.788), and $\hat{n}.\vec{E}$ at ROI_{TMS} (R^2=0.308, p_{FDR}=0.032, r=-0.555). Also ECD had significant predictive value for the |E| (ROI_{HK}:R^2=0.482, p=0.004, r=-0.695, ROI_{TMS}: R^2= 0.681, p_{FDR}<0.001, r=-0.825), and $\hat{n}.\vec{E}$ (ROI_{HK}: R^2=0.337, p_{FDR}=0.023, r=-0.581, and ROI_{TMS}: R^2= 0.339, p_{FDR}=0.012, r=-0.632). There were no significant predictive effects of the remaining anatomical factors, Figure 5.7.A, Figure 5.8.A, Table 5.2. For the cathodal group, CSF volume explained significantly the |E| at ROI_{TMS} (R^2=0.342, p_{FDR}=0.028, r=-0.585), and ECD significantly predicted the |E| (ROI_{HK} : R^2= 0.436, p_{FDR}=0.010, r=-0.660 , and ROI_{TMS}: R^2= 0.329, p_{FDR}=0.032, r=-0.574), and $\hat{n}.\vec{E}$ ($ROI_{targetElec}$: R^2= 0.379, p_{FDR}=0.020, r=-0.616, and ROI_{TMS}: R^2= 0.522, p_{FDR}=0.004, r=-0.723). The remaining anatomical factors had no significant predictive value for the EFs of the cathodal group Figure 5.7.B, Figure 5.8.B, Table 5.2.

Table 5.1. Measured anatomical and EF values. Average, standard deviation and median of the measured anatomical factors and calculated EF for the anodal, and cathodal group.

		Thickness					Electrical Field			
		Scalp (cm)	**Skull (cm)**	**CSF (cm)**	**CSF Volume (L)**	**ECD (cm)**	**|E| ROI_{HK} (V/m)**	**$\hat{n}.\vec{E}$ ROI_{HK} (V/m)**	**|E| ROI_{TMS} (V/m)**	**$\hat{n}.\vec{E}$ ROI_{TMS} (V/m)**
Anodal Group	Average± SD	0.675± 0.162	0.643± 0.163	0.161± 0.087	0.277± 0.053	3.100± 0.187	0.099± 0.044	0.058± 0.070	0.161± 0.062	0.045± 0.100
	Median	0.634	0.626	0.152	0.153	3.023	0.087	0.079	0.148	0.094
Cathodal Group	Average± SD	0.798± 0.197	0.624± 0.164	0.238± 0.123	0.282± 0.047	3.173± 0.180	0.092± 0.040	0.040± 0.062	0.175± 0.489	0.050± 0.054
	Median	0.826	0.579	0.221	0.274	3.167	0.077	0.046	0.182	0.045

Table 5.2 Association between Anatomical Factors and Electrical Field. Multiple linear regressions (*Reg*) were first applied to investigate if the individual averaged EF for the ROI_{HK} or ROI_{TMS} (as dependent variable) can be explained by respective individual anatomical factors (as explanatory variables). In addition, Pearson's correlation coefficient (*Corr*) was calculated to further identify the directionality of each regression result. The p-values were adjusted for multiple comparisons using the False Discovery Rate (FDR). Asterisks indicate significant results.

	Scalp Thickness	**Skull Thickness**	**CSF Thickness**	**CSF Volume**	**ECD**

Anodal Group	|E| **ROI_{HK}**	*Reg*	R^2	0.016	0.001	**0.476***	0.172	**0.482***
			p	0.654	0.906	**0.008***	0.124	**0.004***
		Corr	*r*	-0.126	0.033	**-0.690***	-0.415	**-0.695***
	$\hat{\mathbf{n}}.\vec{\mathbf{E}}$ **ROI_{HK}**	*Reg*	R^2	0.002	0.008	0.244	0.019	**0.337***
			p	0.932	0.750	0.085	0.624	**0.023***
		Corr	*r*	-0.013	-0.090	-0.495	0.138	**-0.581***
	|E| **ROI_{TMS}**	*Reg*	R^2	0.007	0.070	**0.620***	0.221	**0.681***
			p	0.928	0.337	**<0.001***	0.077	**<0.001***
		Corr	*r*	-0.126	-0.266	**-0.788***	-0.470	**-0.825***
	$\hat{\mathbf{n}}.\vec{\mathbf{E}}$ **ROI_{TMS}**	*Reg*	R^2	0.037	0.224	**0.308***	0.002	**0.399***
			p	0.495	0.075	**0.032***	0.871	**0.012***
		Corr	*r*	0.191	-0.473	**-0.555***	0.046	**-0.632***
Cathodal Group	|E| **ROI_{HK}**	*Reg*	R^2	0.003	0.052	0.161	0.125	**0.436***
			p	0.854	0.432	0.155	0.215	**0.010***
		Corr	*r*	0.054	0.229	-0.401	-0.353	**-0.660***
	$\hat{\mathbf{n}}.\vec{\mathbf{E}}$ **ROI_{HK}**	*Reg*	R^2	0.002	0.006	0.111	0.259	**0.379***
			p	0.961	0.802	0.245	0.063	**0.020***
		Corr	*r*	0.014	0.074	-0.333	-0.510	**-0.616***
	|E| **ROI_{TMS}**	*Reg*	R^2	0.003	0.013	0.028	**0.342***	**0.329***
			p	0.845	0.703	0.565	**0.028***	**0.032***
		Corr	*r*	0.057	0.057	-0.169	**-0.585***	**-0.574***
	$\hat{\mathbf{n}}.\vec{\mathbf{E}}$ **ROI_{TMS}**	*Reg*	R^2	0.125	0.001	0.104	0.274	**0.522***
			p	0.215	0.963	0.261	0.054	**0.004***
		Corr	*r*	-0.354	0.074	-0.333	-0.524	**-0.723***

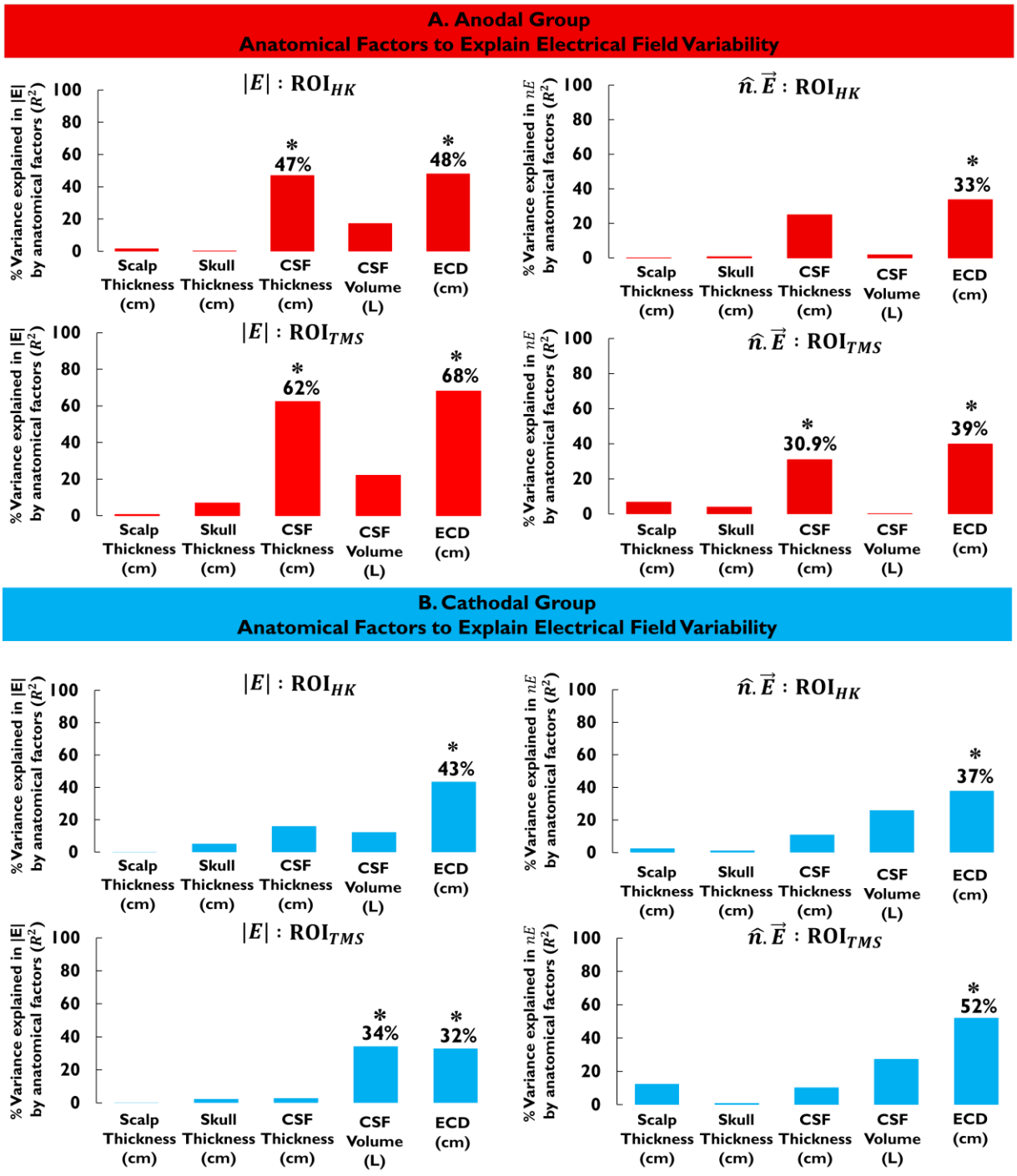

Figure 5.7 Association between Anatomical Factors and Electrical Field. Multiple linear regressions were used to test which of the obtained anatomical factors explained the individual EF (strength $|E|$, and normal components $\hat{n}.\vec{E}$) at the two ROIs (ROI_{HK} and ROI_{TMS}). The results indicate that electrode to cortex distance (ECD), explains the EFs for both ROIs, and that also CSF volume, and thickness partially explains the variability of EFs. No correlation was found however for the remaining anatomical factors. Values at the top of each bar-graph represent the percentage of explained variability (R^2), with $p<0.05$. Asterisks indicate significant results.

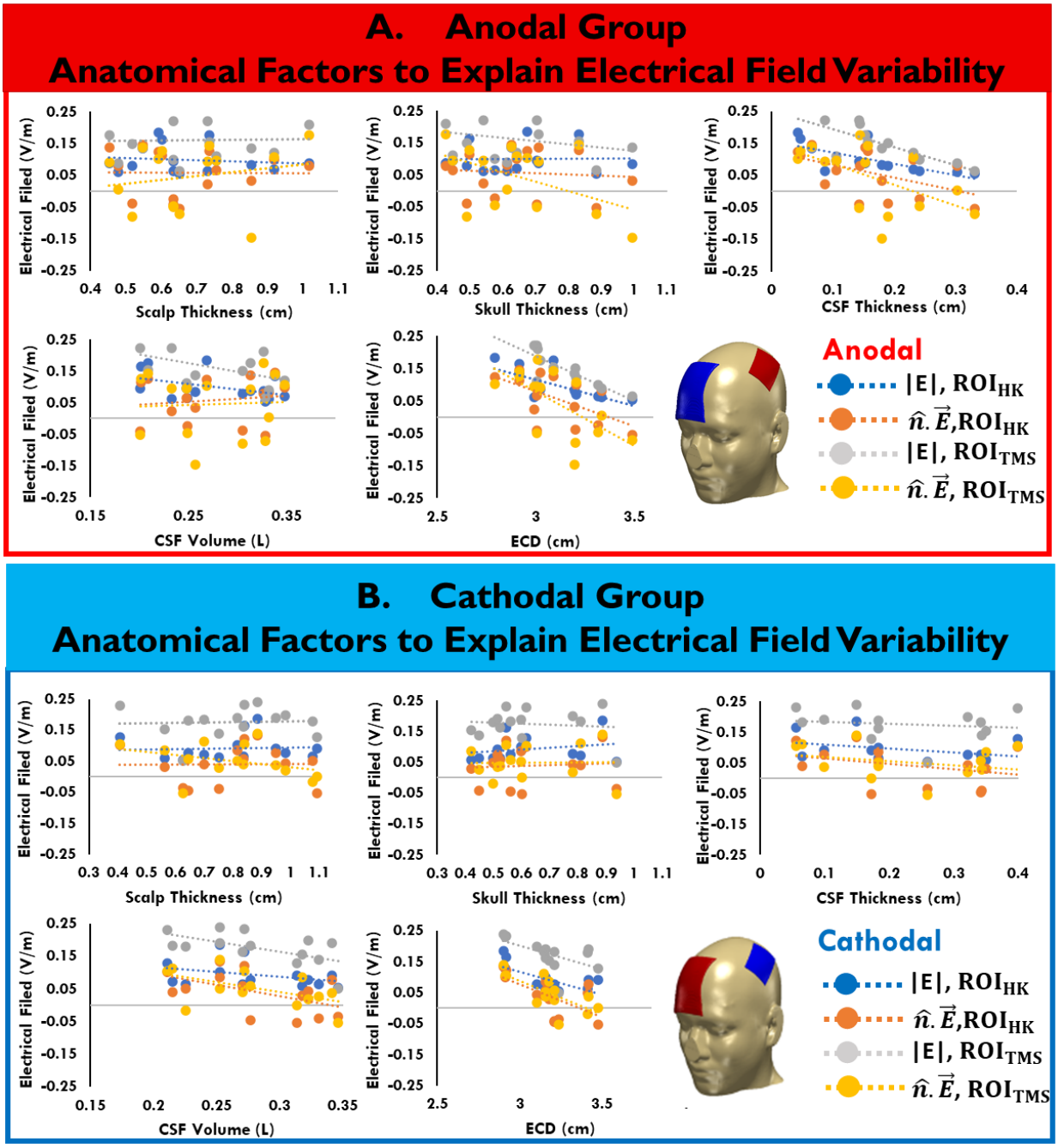

Figure 5.8. Scatterplots for the association between individual Anatomical Factors and Electrical Fields. The associations between anatomical factors including scalp, skull and CSF thickness, CSF volume and electrode to cortex distance (ECD), and averaged EFs (strength (|E|) and normal component ($\hat{n}.\vec{E}$)) extracted from two ROIs (ROI_{HK} and ROI_{TMS}), are shown for anodal and cathodal tDCS groups. The best fitting regression lines are superimposed.

5.3.4. Association between Anatomical Factors, Electrical Fields and tDCS-induced MEP Alterations

The results of linear regressions and Pearson correlation coefficients indicated that, for the anodal group, skull thickness significantly predicted the ΔMEP variance of 2.0mA-tDCS (early epoch: R^2=0.427, p_{FDR}=0.014, r=0.653). CSF thickness significantly predicted the ΔMEP variabilities of stimulation intensities at the early epoch (0.5mA-tDCS: R^2=0.409, p_{FDR}=0.042, r=-0.640, 1.0mA-tDCS: R^2= 0.364, p_{FDR}=0.041, r=-0.604, r=-0.530, and 2.0mA-tDCS: R^2=0.379, p_{FDR}=0.021, r=-0.616), and ECD had a similar predictive power (early epoch: 0.5mA-tDCS: R^2=0.302, p_{FDR}=0.045, r=-0.550, 1.0mA-tDCS: R^2=0.300, p_{FDR}=0.045, r=-0.546, 1.5mA-tDCS: R^2=0.370, p_{FDR}=0.032, r=-0.609, and 2.0mA-tDCS: R^2=0.500, p_{FDR}=0.012, r=-0.707). In addition, |E| predicted ΔMEP variance significantly at ROI_{HK} (early epoch: 0.5mA-tDCS: R^2=0.385, p_{FDR}=0.042, r=0.621, 1.0mA-tDCS: R^2=0.480, p_{FDR}=0.036, r=0.693, 1.5mA-tDCS: R^2=0.454, p_{FDR}=0.044, r=0.674), and at ROI_{TMS} (early epoch: 0.5mA-tDCS: R^2= 0.416, p_{FDR}=0.012, r=0.645, 1.0mA-tDCS: R^2= 0.361, p_{FDR}=0.040, r=0.601, and 2.0mA-tDCS: R^2= 0.421, p_{FDR}=0.014, r=0.650). Furthermore, $\hat{n}.\vec{E}$ predicted ΔMEP variance significantly at ROI_{HK} (early epoch: 0.5mA-tDCS: R^2= 0.300, p=0.048, r=0.546, 1.0mA-tDCS: R^2=0.405, p_{FDR}=0.041, r=0.636, and 2mA-tDCS: R^2=0.480, p_{FDR}=0.012, r=0.693), and at ROI_{TMS} (early epoch: 1.0mA-tDCS: R^2= 0.339, p_{FDR}=0.041, r=0.582, and 2.0mA-tDCS: R^2= 0.494, p_{FDR}=0.012, r=0.703), Figure 5.9.A.1, Figure 5.10, Table 5.3. However, none of the predictors did explain the MEP variabilities of anodal tDCS intensities at the late epoch, Figure 5.9.A.2, Figure 5.11, Table 5.3. For the cathodal group, CSF thickness only explained the ΔMEP variance of 1.0mA-tDCS (early epoch: R^2=0.553, p_{FDR}=0.009, r=-0.774; late epoch: R^2= 0.372, p_{FDR}=0.025, r=-0.609) respectively. In addition, ECD significantly explained the ΔMEP variability of only 1mA tDCS (early epoch: R^2=0.497, p_{FDR}=0.011, r=-0.705; late epoch: R^2=0.444, p_{FDR}=0.020, r=-0.666). Furthermore, the |E| and $\hat{n}.\vec{E}$, both at ROI_{HK}, predicted MEP variabilities induced by tDCS intensities of 1.0mA at the early epoch (R^2=0.444, p_{FDR}=0.015, r=0.666, R^2=0.508, p_{FDR}=0.011, r=0.712), and $\hat{n}.\vec{E}$ at ROI_{HK} predicted MEP variability for 1mA also at the late epoch (R^2=0.534, p_{FDR}=0.014, r=0.734). Moreover, at ROI_{TMS}, |E| and $\hat{n}.\vec{E}$ significantly predicted the ΔMEP variabilities of 1mA-tDCS intensity (early epoch: R^2= 0.445, p_{FDR}=0.015,

r=0.667, R^2= 0.332, p_{FDR}=0.034, r=0.568; late epoch (only |E|): R^2= 0.539, p_{FDR}=0.014, r=0.734), Figure 5.9.B.1,2, Figure 5.12, Figure 5.13, Table 5.4.

Table 5.3 Association between Anatomical Factors, Electrical Fields and anodal tDCS-induced MEP Alterations. Multiple linear regressions (Reg) were used to test whether and to which extent the individual variability of the neurophysiological effects of **anodal** tDCS (evaluated by MEP amplitude alterations) can be explained by the respective individual EF (for the (ROI_{HK} and ROI_{TMS}), or anatomical factors. In addition, Pearson's correlation coefficient (Corr) was calculated to further identify the directionality of each regression result. The p-values were adjusted for multiple comparisons using the False Discovery Rate (FDR). Asterisks indicate significant results.

				Thickness					Electrical Field			
				Scalp	**Skull**	**CSF**	**CSF Volume**	**ECD**	**|E| ROI_{HK}**	**$\hat{n}.\vec{E}$ ROI_{HK}**	**|E| ROI_{TMS}**	**$\hat{n}.\vec{E}$ ROI_{TMS}**
ΔMEP Early Epoch (0-60min)	**0.5 mA**	***Reg***	R^2	0.035	0.041	**0.409***	0.294	**0.302***	**0.385***	**0.300**	**0.416***	0.269
			p	0.502	0.502	**0.042***	0.055	**0.045***	**0.042***	**0.048***	**0.012***	0.061
		Corr	*r*	-0.188	0.202	**-0.640***	0.542	**-0.550***	**0.621***	**0.546***	**0.645***	0.518
	1.0 mA	***Reg***	R^2	0.007	0.001	**0.364***	0.022	**0.300***	**0.480***	**0.405***	**0.361***	**0.339***
			p	0.850	0.900	**0.041***	0.757	**0.045***	**0.036***	**0.041***	**0.040***	**0.041***
		Corr	*r*	-0.087	0.035	**-0.604***	0.148	**-0.547***	**0.693***	**0.636***	**0.601***	**0.582***
	1.5 mA	***Reg***	R^2	0.079	0.027	0.281	0.006	**0.370***	**0.454***	0.195	0.310	0.261
			p	0.395	0.631	0.094	0.791	**0.032***	**0.044***	0.148	0.093	0.094
		Corr	*r*	-0.282	0.163	-0.530	0.075	**-0.609***	**0.674***	0.442	0.557	0.510
	2.0 mA	***Reg***	R^2	0.012	**0.427***	**0.379***	0.149	**0.500***	0.256	**0.480***	**0.421***	**0.494***
			p	0.700	**0.014***	**0.021***	0.174	**0.012***	0.064	**0.012***	**0.014***	**0.012***
		Corr	*r*	0.108	**0.653***	**-0.616***	0.387	**-0.707***	0.507	**0.693***	**0.650***	**0.703***
ΔMEP Late Epoch (75-120min)	**0.5 mA**	***Reg***	R^2	0.002	0.211	0.055	0.244	0.099	0.035	0.062	0.033	0.061
			p	0.886	0.378	0.579	0.378	0.579	0.579	0.579	0.579	0.579
		Corr	*r*	0.041	0.456	-0.236	-0.495	-0.315	0.186	0.248	0.182	0.275
	1.0 mA	***Reg***	R^2	0.041	0.041	0.011	0.012	0.031	0.004	0.006	0.001	0.010
			p	0.873	0.897	0. 897	0. 886	0. 847	0.827	0.782	0.897	0.830
		Corr	*r*	-0.444	0.203	-0.106	0.109	-0.178	0.062	0.078	0.037	0.097
	1.5 mA	***Reg***	R^2	0.006	0.006	0.087	0.002	0.148	0.008	0.045	0.022	0.061
			p	0.865	0.775	0.745	0.865	0.721	0.754	0.746	0.798	0.773
		Corr	*r*	0.139	0.081	-0.296	-0.048	-0.385	0.089	0.213	0.148	0.249
	2.0 mA	***Reg***	R^2	0.093	0.092	0.052	0.021	0.121	0.201	0.063	0.128	0.084
			p	0.729	0.532	0.532	0.678	0.532	0.532	0.632	0.521	0.601
		Corr	*r*	-0.098	0.304	-0.228	0.146	-0.347	0.449	0.251	0.358	0.289

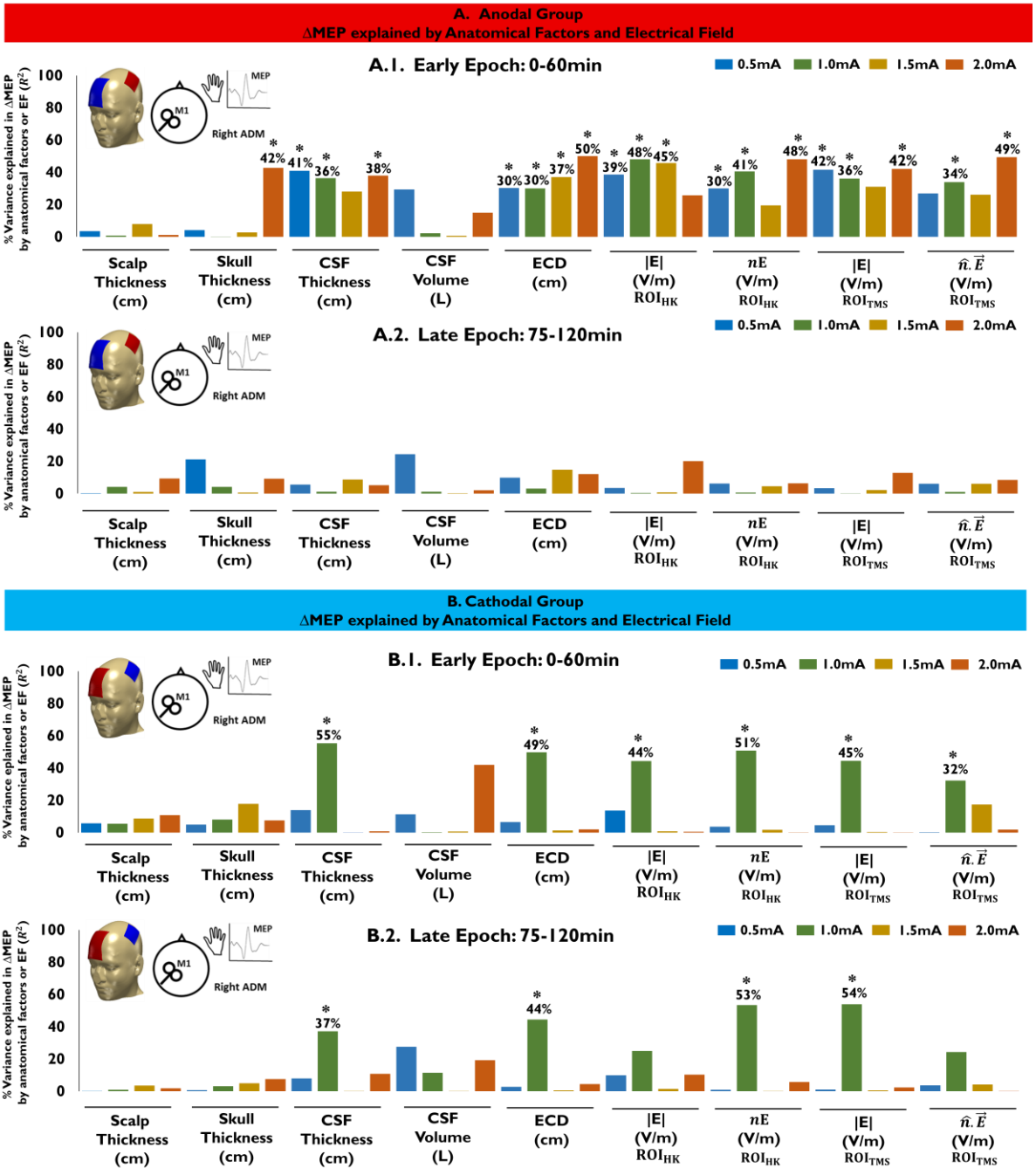

Figure 5.9 Explanatory power of anatomical factors and electrical fields for tDCS-induced MEP alterations. Anatomical factors, and individual EF (magnitude $|E|$, and normal component $\hat{n}.\vec{E}$s) at two ROIs (ROI_{HK} and ROI_{TMS}) were used to explore if these can explain MEP variabilities of four active tDCS conditions (0.5mA, 1.0mA, 1.5mA and 2.0mA) at early (0-60min) and late (75-120min) epochs after stimulation. **A) Anodal group**: the results indicate that

CSF thickness and electrode to cortex distance (ECD), and $|E|$ and $\hat{n}.\vec{E}$ for ROI_{HK} and ROI_{TMS} significantly predicted the ΔMEP variance of almost all tDCS dosages for the early, but not late epoch. **B) Cathodal group**: CSF thickness, ECD, $|E|$ and $\hat{n}.\vec{E}$ for ROI_{HK} and ROI_{TMS} significantly predicted the ΔMEP variance of only 1mA-tDCS at early and late epochs (with the exception of $|E|$ for ROI_{HK}, and $\hat{n}.\vec{E}$ for ROI_{TMS}, both at late epoch). Values at the top of each bar-graph represent the percentage of explained variability (R^2), for $p<0.05$. The p-values were adjusted for multiple comparisons using the False Discovery Rate (FDR). Asterisks indicate significant results.

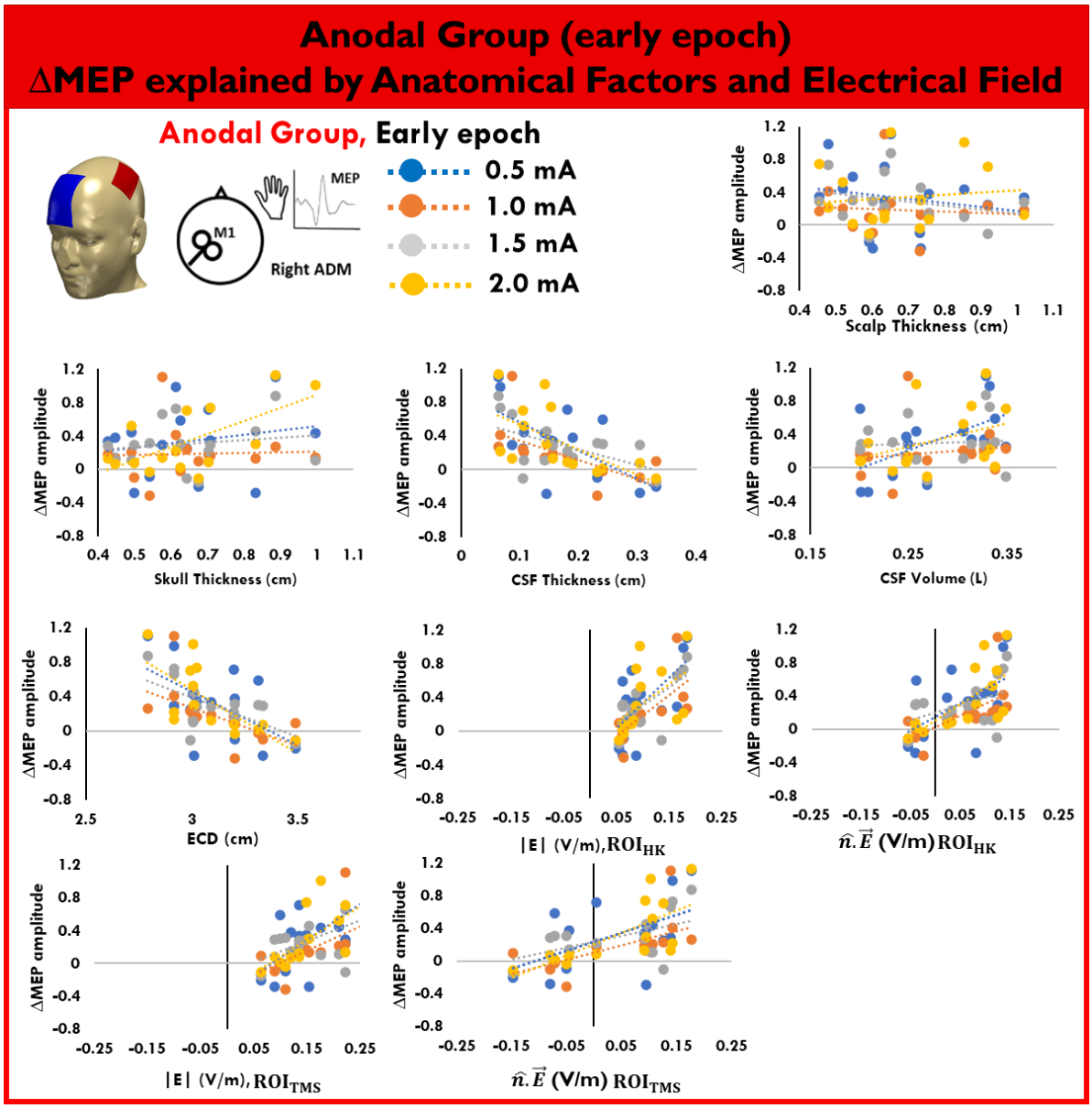

Figure 5.10. Scatterplots for the association between Anatomical Factors, Electrical Fields and anodal tDCS-induced MEP Alterations (early epoch). The associations between anatomical factors including scalp, skull and CSF thickness, CSF volume and electrode to cortex distance (ECD), averaged EFs (strength (|E|) and normal component ($\hat{n}.\vec{E}$)) extracted from two

ROIs (ROI_{HK} and ROI_{TMS}), and tDCS-induced MEP alterations are shown for anodal tDCS (early epoch). The best fitting regression lines are superimposed.

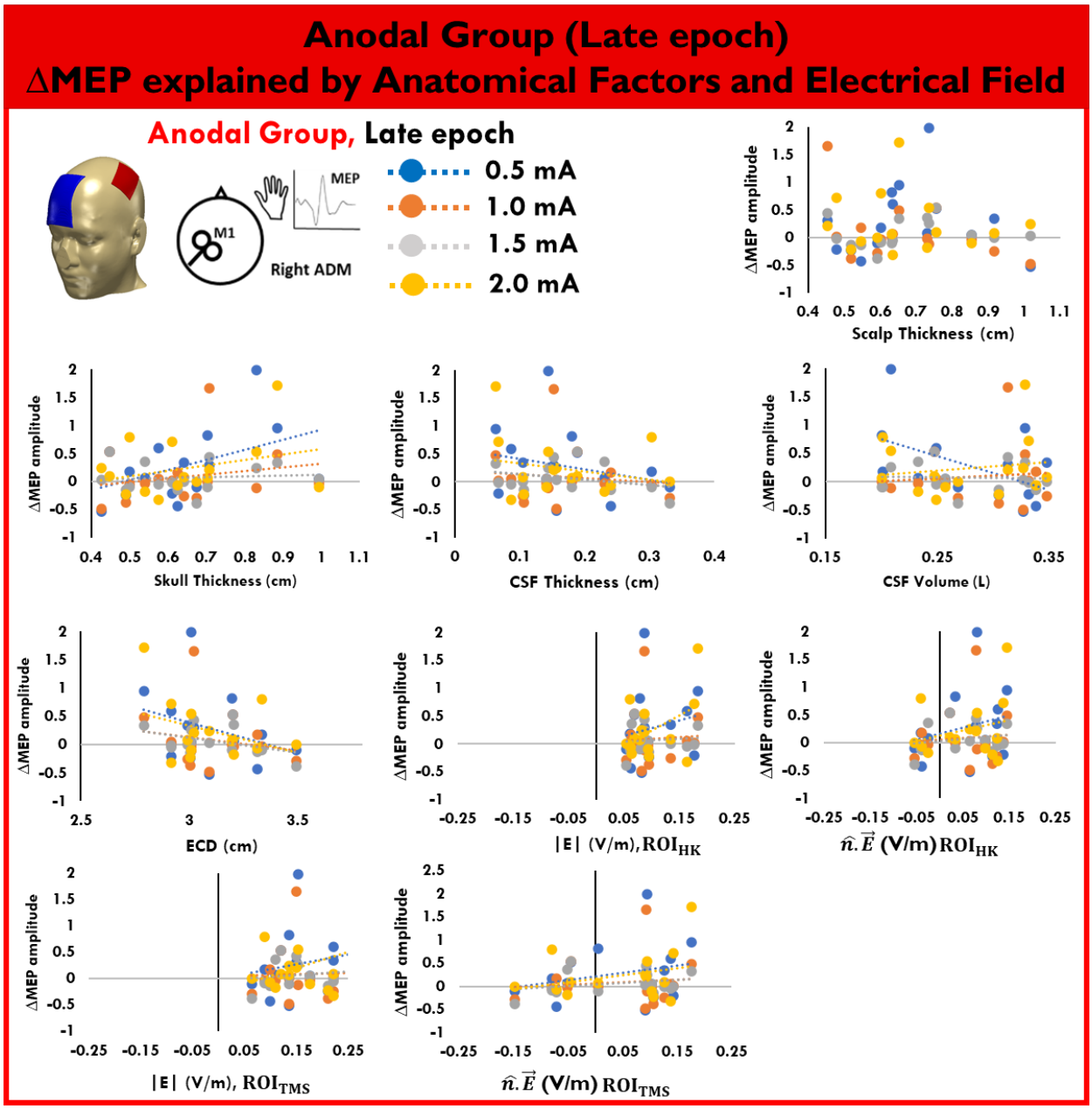

Figure 5.11. Scatterplots for the association between Anatomical Factors, Electrical Fields and anodal tDCS-induced MEP Alterations (late epoch). The associations between anatomical factors including scalp, skull and CSF thickness, CSF volume and electrode to cortex distance (ECD), averaged EFs (strength (|E|) and normal component ($\hat{n}.\vec{E}$)) extracted from two ROIs (ROI_{HK} and ROI_{TMS}), and tDCS-induced MEP alterations are shown for anodal tDCS (late epoch). The best fitting regression lines are superimposed.

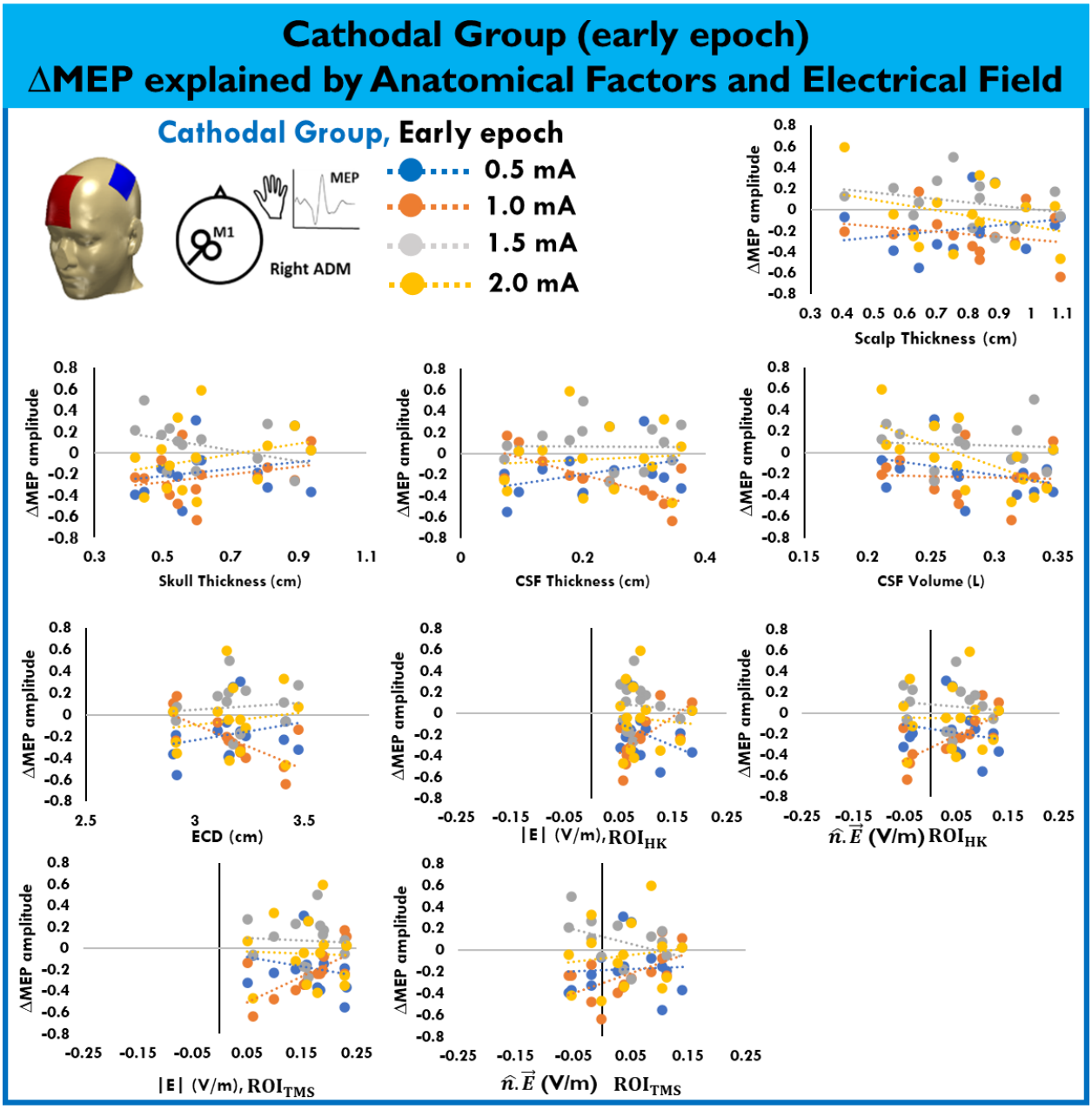

Figure 5.12. Scatterplots for the association between Anatomical Factors, Electrical Fields and cathodal tDCS-induced MEP Alterations (early epoch). The associations between anatomical factors including scalp, skull and CSF thickness, CSF volume and electrode to cortex distance (ECD), averaged EFs (strength (|E|) and normal component ($\hat{n}.\vec{E}$)) extracted from two ROIs (ROI_{HK} and ROI_{TMS}), and tDCS-induced MEP alterations are shown for cathodal tDCS (early epoch). The best fitting regression lines are superimposed.

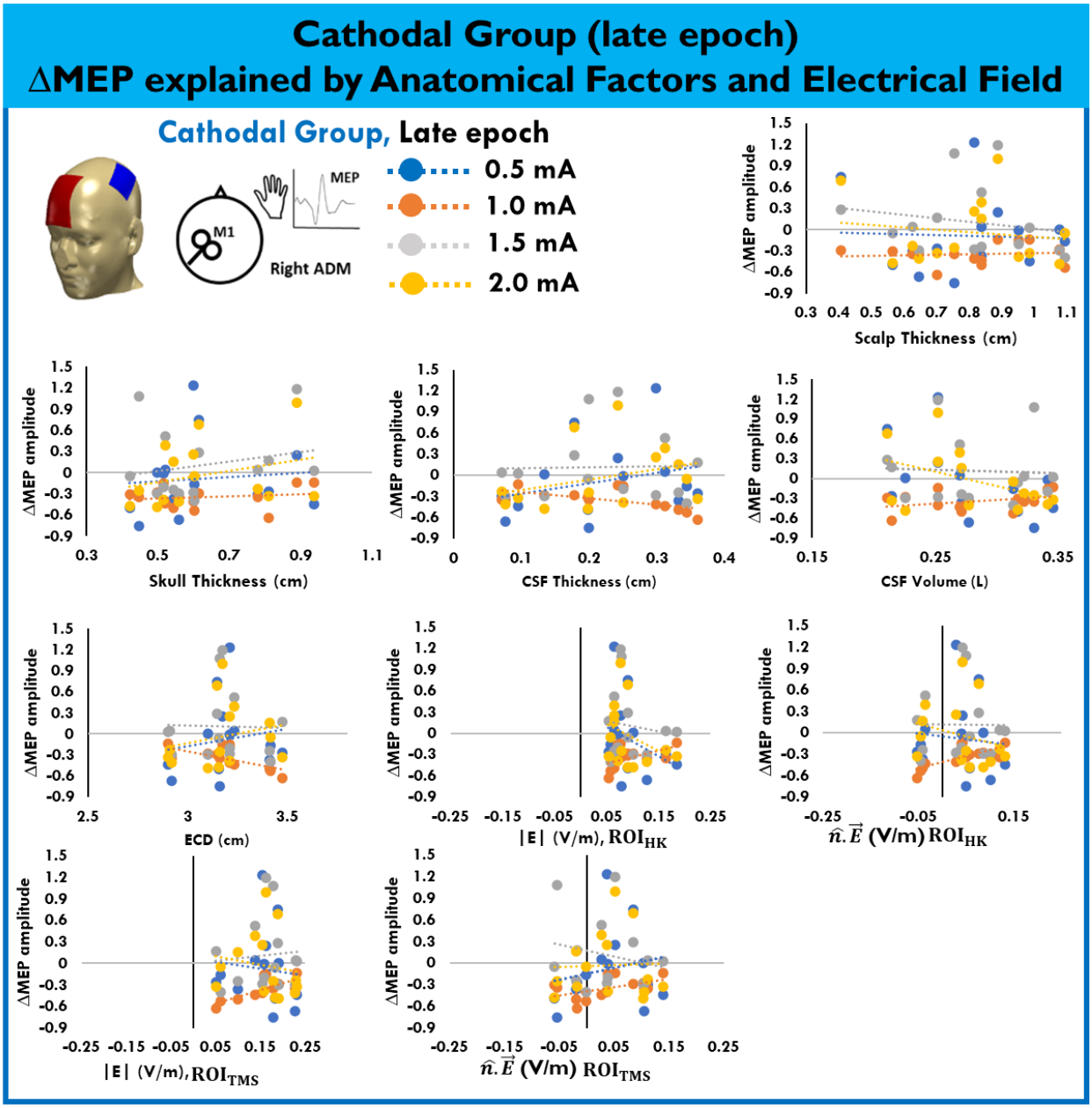

Figure 5.13. Scatterplots for the association between Anatomical Factors, Electrical Fields and cathodal tDCS-induced MEP Alterations (late epoch). The associations between anatomical factors including scalp, skull and CSF thickness, CSF volume and electrode to cortex distance (ECD), averaged EFs (strength (|E|) and normal component ($\hat{n}.\vec{E}$)) extracted from two ROIs (ROI_{HK} and ROI_{TMS}), and tDCS-induced MEP alterations are shown for cathodal tDCS (late epoch). The best fitting regression lines are superimposed.

Table 5.4 Association between Anatomical Factors, Electrical Fields and cathodal tDCS-induced MEP Alterations. Multiple linear regressions (Reg) were used to test whether and to which extent the individual variability of the neurophysiological effects of **cathodal** tDCS (evaluated by MEP amplitude alterations) can be explained by the respective individual EF (for the (ROI_{HK} and ROI_{TMS}), or anatomical factors. In addition, Pearson's correlation coefficient (Corr) was calculated to further identify the directionality of each regression result. The p-values were adjusted for multiple comparisons using the False Discovery Rate (FDR). Asterisks indicate significant results.

					Thickness					Electrical Field			
					Scalp	Skull	CSF	CSF Volume	ECD	|E| ROI_{HK}	$\hat{n}.\vec{E}$ ROI_{HK}	|E| ROI_{TMS}	$\hat{n}.\vec{E}$ ROI_{TMS}
ΔMEP Early Epoch (0-60min)	0.5 mA	*Reg*	R^2	0.057	0.049	0.139	0.113	0.065	0.136	0.036	0.046	0.003
			p	0.517	0.485	0.473	0.541	0.579	0.594	0.517	0.560	0.840
		Corr	*r*	0.239	0.220	0.374	-0.336	0.255	-0.369	-0.189	-0.215	0.059
	1.0 mA	*Reg*	R^2	0.054	0.080	**0.553***	0.003	**0.497***	**0.444***	**0.508***	**0.445***	**0.322***
			p	0.478	0.420	**0.009***	0.851	**0.011***	**0.015***	**0.011***	**0.015***	**0.034***
		Corr	*r*	-0.231	0.283	**-0.744***	-0.055	**-0.705***	**0.666***	**0.712***	**0.667***	**0.568***
	1.5 mA	*Reg*	R^2	0.087	0.178	0.001	0.006	0.013	0.008	0.017	0.004	0.174
			p	0.891	0.833	0.972	0.798	0.731	0.754	0.760	0.834	0.137
		Corr	*r*	-0.295	-0.422	-0.010	-0.075	0.115	-0.092	-0.130	-0.062	-0.417
	2.0 mA	*Reg*	R^2	0.108	0.076	0.008	0.419	0.020	0.005	0.001	0.001	0.018
			p	0.252	0.339	0.818	0.108	0.626	0.809	0.950	0.851	0.646
		Corr	*r*	-0.328	0.277	0.092	-0.647	0.143	-0.071	-0.018	-0.033	0.134
ΔMEP Late Epoch (75-120min)	0.5 mA	*Reg*	R^2	0.002	0.007	0.079	0.276	0.028	0.099	0.009	0.011	0.036
			p	0.878	0.867	0.867	0.486	0.842	0.873	0.744	0.828	0.517
		Corr	*r*	-0.045	0.086	0.281	-0.526	0.167	-0.315	-0.096	-0.102	0.189
	1.0 mA	*Reg*	R^2	0.009	0.031	**0.372***	0.115	**0.444***	0.250	**0.534***	**0.539***	0.243
			p	0.748	0.617	**0.025***	0.305	**0.020***	0.102	**0.014***	**0.014***	0.074
		Corr	*r*	0.095	0.175	**-0.609***	0.339	**-0.666***	0.500	**0.731***	**0.734***	0.493
	1.5 mA	*Reg*	R^2	0.035	0.049	0.001	0.002	0.006	0.014	0.001	0.006	0.042
			p	0.724	0.747	0.923	0.872	0.933	0.686	0.880	0.791	0.480
		Corr	*r*	-0.186	0.221	0.029	-0.047	-0.025	-0.119	-0.007	0.078	-0.206
	2.0 mA	*Reg*	R^2	0.019	0.075	0.103	0.193	0.044	0.103	0.057	0.024	0.001
			p	0.635	0.630	0.630	0.516	0.670	0.662	0.611	0.699	0.913
		Corr	*r*	-0.139	0.274	0.321	-0.439	0.210	-0.321	-0.239	-0.154	0.032

5.3.5. Association between Anatomical Factors or Electrical Fields and tDCS-induced CBF alterations

The results of the linear regressions and Pearson correlation coefficients indicate that for the anodal group, CSF thickness significantly predicted the ΔCBF variabilities (early epoch: 1.0mA-tDCS: R^2=0.403, p_{FDR}=0.047, r=-0.635). CSF volume had also significant predictive power for the early epoch (1.0mA-tDCS: R^2=0.470, p_{FDR}=0.040, r=-0.685). Furthermore, ECD significantly explained the ΔCBF variabilities for the late epoch in the 1.0mA-tDCS condition (R^2=0.448, p_{FDR}=0.040, r=-0.670). In addition, the |E| at ROI_{HK} explained the ΔCBF variance with significant predictive power (early epoch: 2.0mA-tDCS: R^2=0.770, p_{FDR}=0.007, r=0.878), and $\hat{n}.\vec{E}$ at ROI_{HK} had predictive power for the early epoch (1.0mA-tDCS: R^2=0.504, p_{FDR}=0.040, r=0.710) Figure 5.14.A.1, Figure 5.15, Table 5.5. However, none of the predictors could explain the ΔCBF variabilities at the late epoch, Figure 5.14.A.2, Figure 5.16, Table 5.5. For the cathodal group, none of the predictors could explain the ΔCBF variabilities at the early epoch, Figure 5.14.B.1, Figure 5.17, Table 5.6. However, for the late epoch, CSF thickness significantly predicted ΔCBF variabilities (1.5mA-tDCS: R^2=0.559, p_{FDR}=0.007, r=-0.774). Furthermore, ECD significantly explained the ΔCBF variabilities for the late epoch (1.5mA-tDCS: R^2=0.485, p_{FDR}=0.014, r=-0.696). In addition, the |E| at ROI_{HK} explained the ΔCBF variance with significant predictive power for the late epoch (1.5mA-tDCS: R^2=0.558, p_{FDR}=0.007, r=0.747, 2.0mA-tDCS R^2=0.504, p_{FDR}=0.014, r=0.710), and $\hat{n}.\vec{E}$ at ROI_{HK} predicted ΔCBF also for the late epoch (1.5mA-tDCS: R^2=0.608, p_{FDR}=0.007, r=0.780) Figure 5.14.B.2, Figure 5.18, Table 5.6.

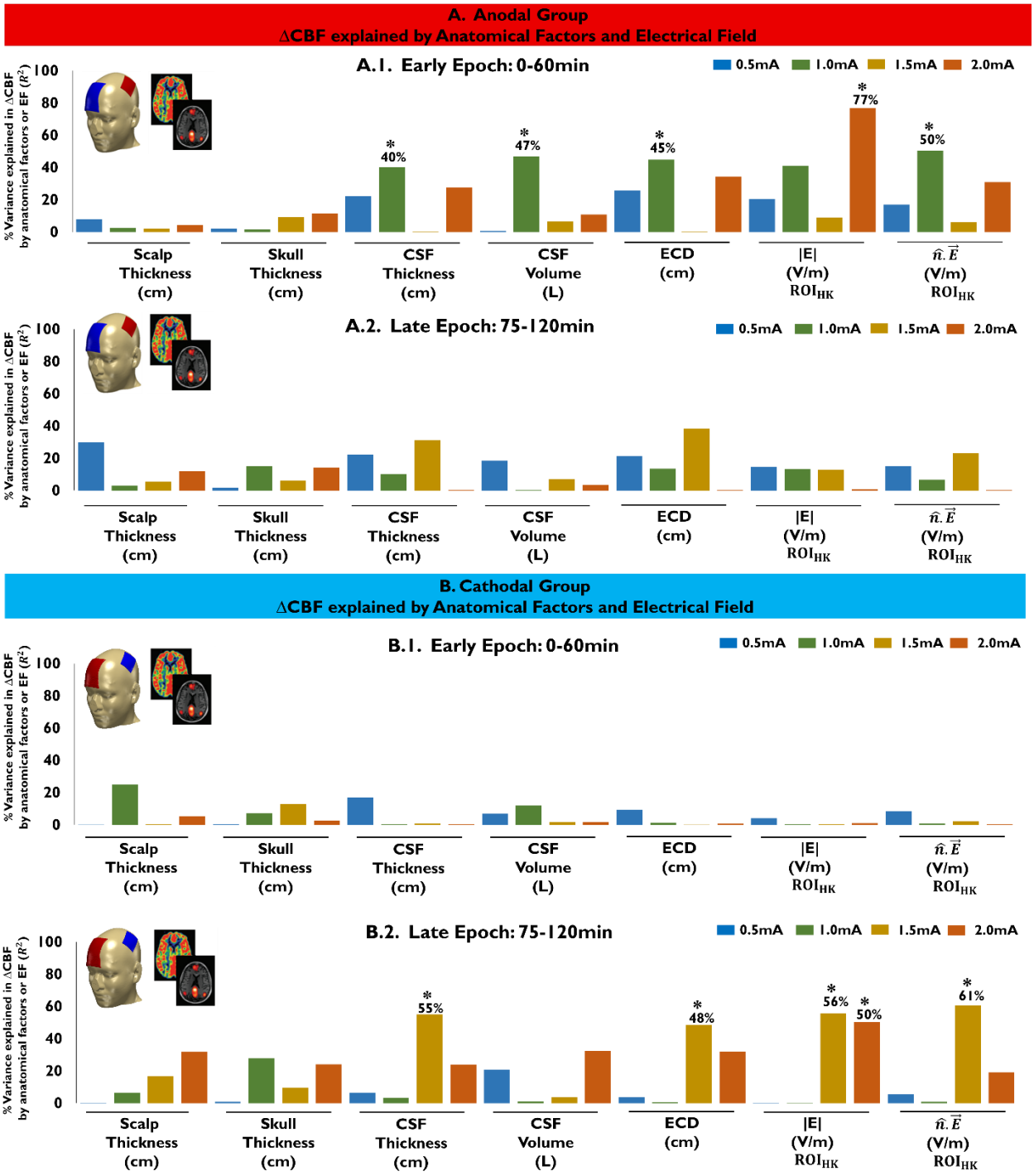

Figure 5.14 Anatomical factors and electrical field values to explain tDCS-induced CBF alterations. The impact of anatomical factors and/or individual EF (magnitude $|E|$, and normal components $\hat{n}.\vec{E}$) at ROI_{HK}, were explored with respect to their predictive power for ΔCBF variabilities, of four active tDCS conditions (0.5mA, 1.0mA, 1.5mA and 2.0mA) for early (0-60min) and late (75-120min) epochs after stimulation.. **A) Anodal group**: CSF thickness and volume, and ECD predicted ΔCBF variabilities for 1mA-tDCS at the early epoch. Moreover, the $|E|$ at ROI_{HK} significantly explained ΔCBF variability of the 2.0mA-tDCS condition at the early

epoch, and nE had significant predictive power for 1mA-tDCS at early the epoch. **B) Cathodal group**: CSF thickness, ECD, $|E|$ and nE at ROI_{HK}, predicted ΔCBF variability of 1.5mA-tDCS, with also significant predictive power of $|E|$ for 2mA-tDCS, all only at the late epoch. Values at the top of each bar-graph represent the percentage of explained variability (R^2), for $p<0.05$. The p-values were adjusted for multiple comparisons using the False Discovery Rate (FDR). Asterisks indicate significant results.

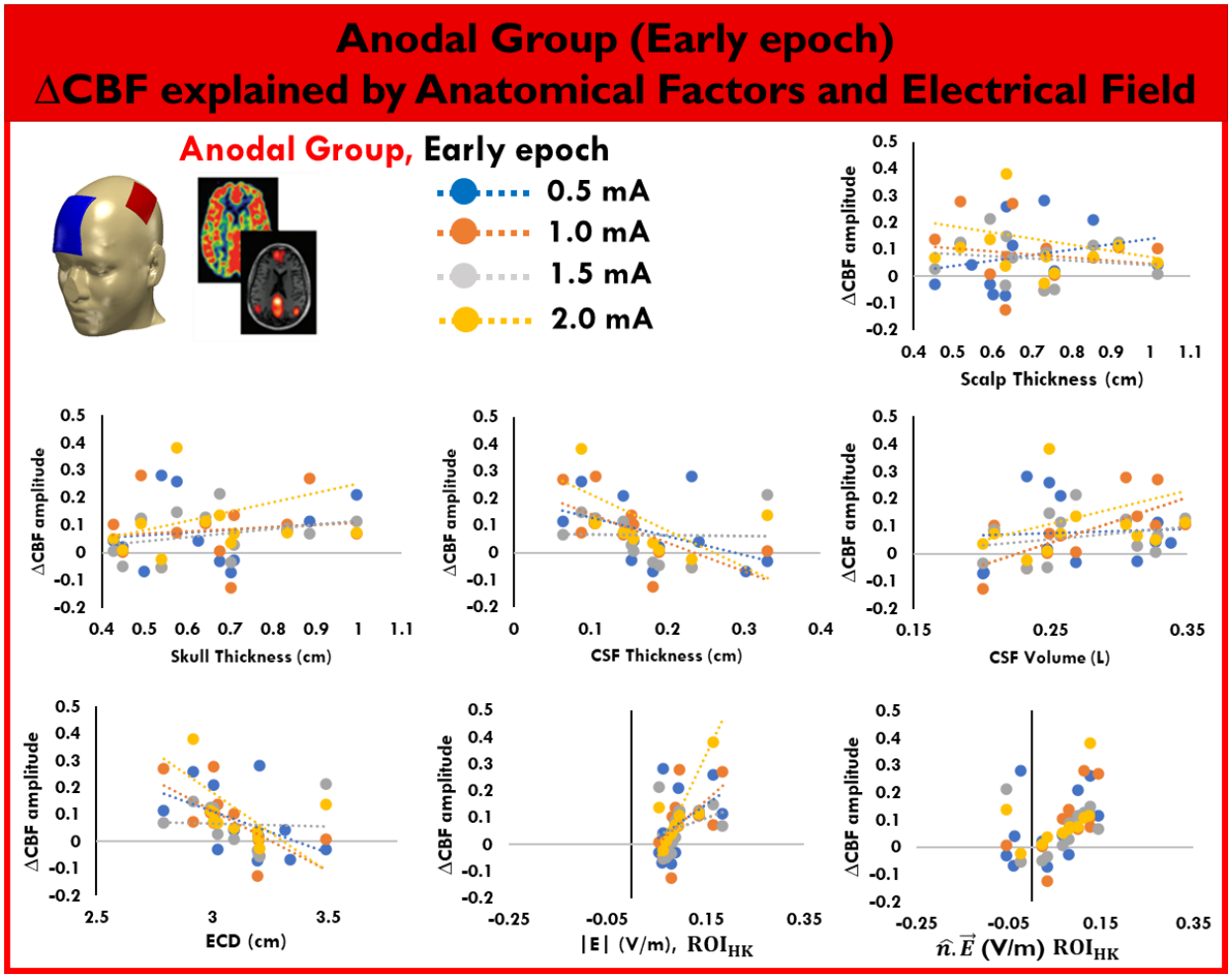

Figure 5.15. Scatterplots for the association between Anatomical Factors, Electrical Fields and anodal tDCS-induced CBF alterations (early epoch). Anatomical factors including scalp, skull and CSF thickness, CSF volume and electrode to cortex distance (ECD), and averaged EFs (strength (|E|) and normal component ($\hat{n}.\vec{E}$)) extracted from two ROIs (ROI_{HK} and ROI_{TMS}), are shown for the tDCS anodal group in relation to the tDCS effects on CBF (early epoch). The best fitting regression lines are superimposed.

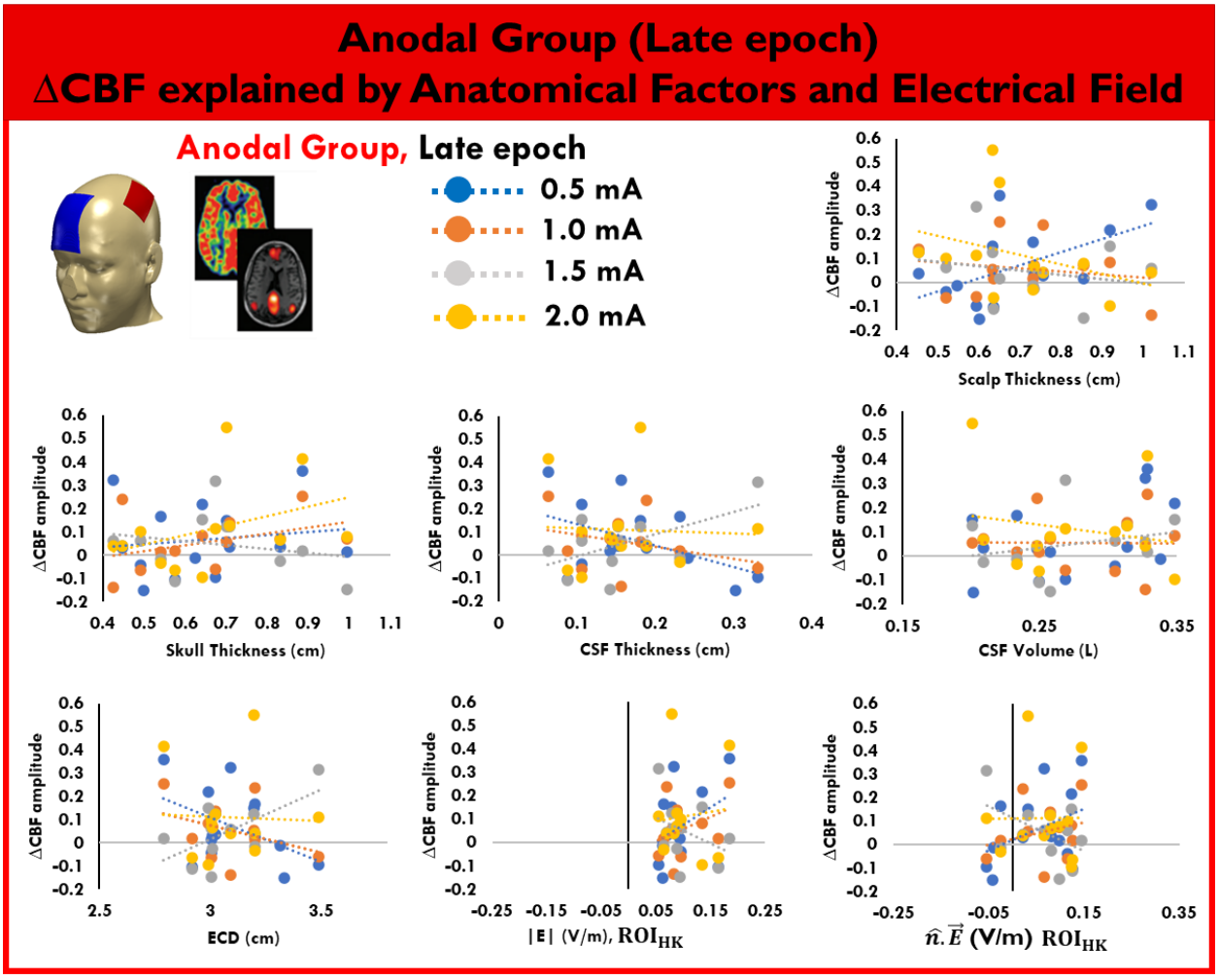

Figure 5.16. Scatterplots for the association between Anatomical Factors, Electrical Fields and anodal tDCS-induced CBF alterations (late epoch). Anatomical factors including scalp, skull and CSF thickness, CSF volume and electrode to cortex distance (ECD), and averaged EFs (strength (|E|) and normal component ($\hat{n}.\vec{E}$)) extracted from two ROIs (ROI_{HK} and ROI_{TMS}), are shown for the tDCS anodal group in relation to the tDCS effects on CBF (late epoch). The best fitting regression lines are superimposed.

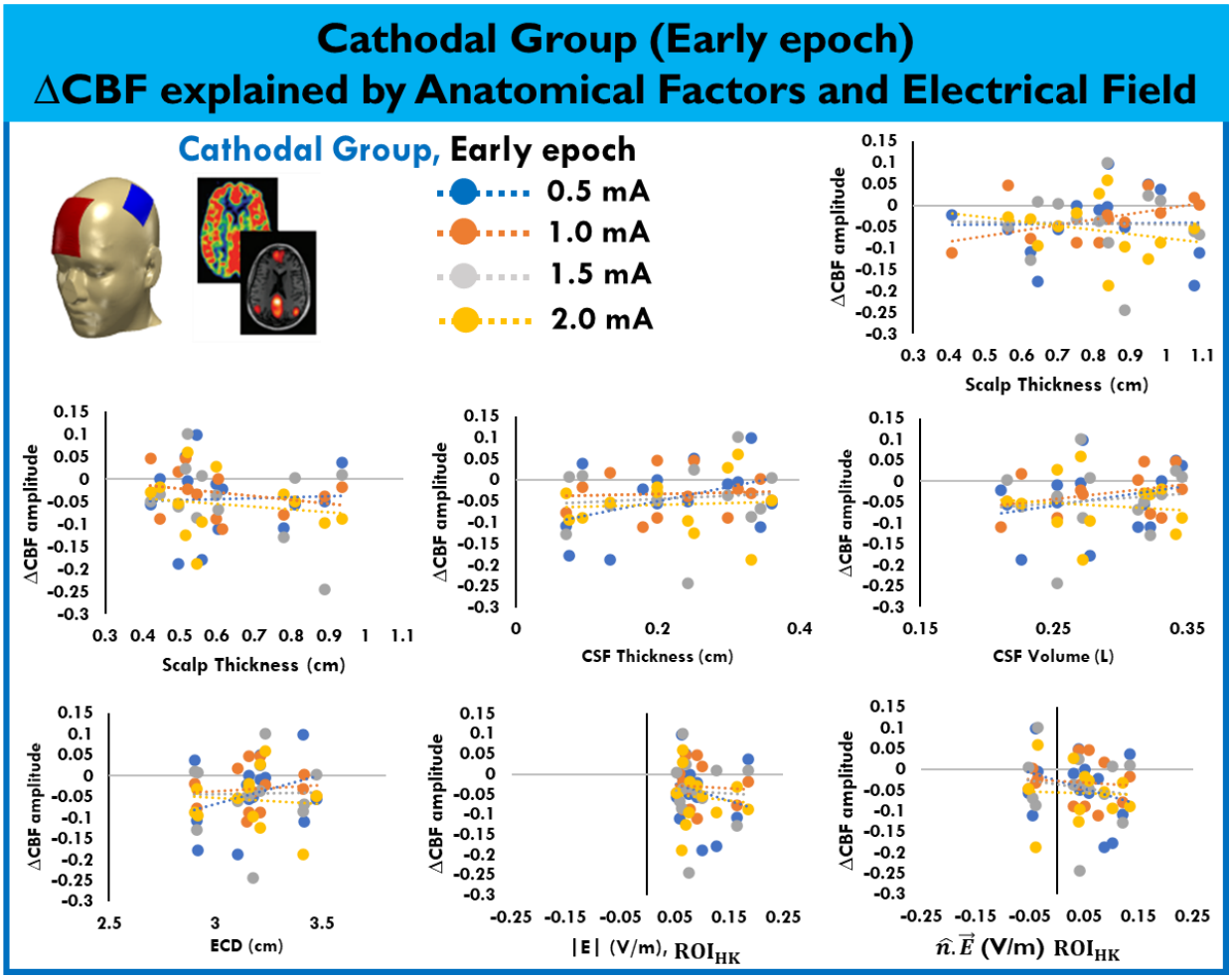

Figure 5.17. Scatterplots for the association between Anatomical Factors, Electrical Fields and cathodal tDCS-induced CBF alterations (early epoch). Anatomical factors including scalp, skull and CSF thickness, CSF volume and electrode to cortex distance (ECD), and averaged EFs (strength (|E|) and normal component ($\hat{n}.\vec{E}$)) extracted from two ROIs (ROI_{HK} and ROI_{TMS}), are shown for the tDCS cathodal group in relation to the tDCS effects on CBF (early epoch). The best fitting regression lines are superimposed.

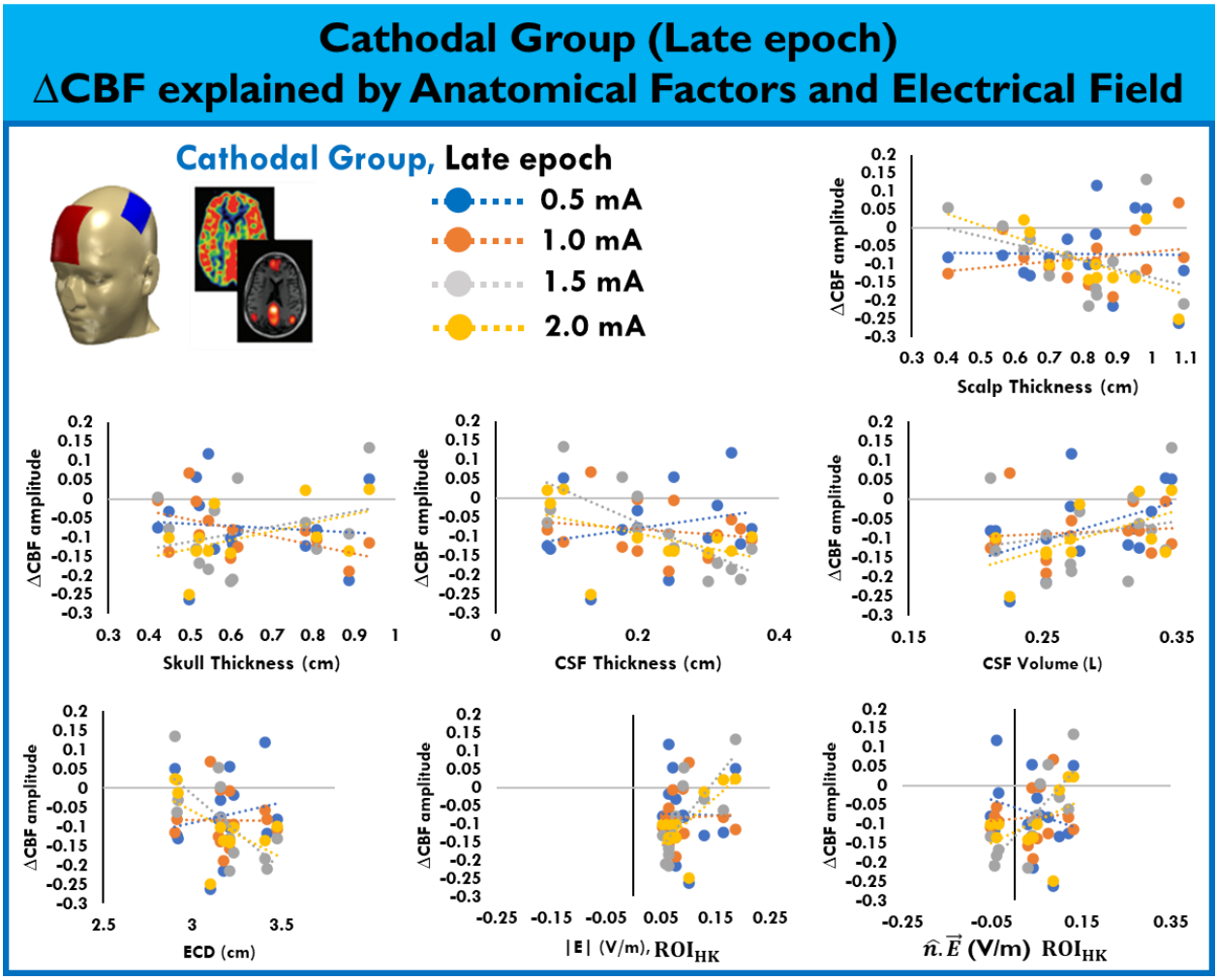

Figure 5.18. Scatterplots for the association between Anatomical Factors, Electrical Fields and cathodal tDCS-induced CBF alterations (late epoch). Anatomical factors including scalp, skull and CSF thickness, CSF volume and electrode to cortex distance (ECD), and averaged EFs (strength (|E|) and normal component ($\hat{n}.\vec{E}$)) extracted from two ROIs (ROI_{HK} and ROI_{TMS}), are shown for the tDCS cathodal group in relation to the tDCS effects on CBF (early epoch). The best fitting regression lines are superimposed.

Table 5.5 Association between Anatomical Factors, Electrical Fields and anodal tDCS-induced CBF Alterations. Multiple linear regressions (*Reg*) were used to test whether and to which extent the individual variability of the neurophysiological effects of **anodal** tDCS (evaluated by CBF amplitude alterations) can be explained by the respective individual EF (for the ROI_{HK}), or anatomical factors. In addition, Pearson's correlation coefficient (*Corr*) was calculated to further identify the directionality of each regression result. The p-values were adjusted for multiple comparisons using the False Discovery Rate (FDR). Asterisks indicate significant results.

	Thickness	Electrical Field

				Scalp	Skull	CSF	CSF Volume	ECD	$\lvert E \rvert$ ROI_{HK}	$\hat{n}.\vec{E}$ ROI_{HK}
ΔCBF Early Epoch (0-60min)	**0.5 mA**	***Reg***	R^2	0.078	0.023	0.221	0.005	0.256	0.204	0.171
			p	0.497	0.709	0.242	0.805	0.242	0.245	0.248
		Corr	***r***	0.279	0.151	-0.470	0.073	-0.506	0.452	0.413
	1.0 mA	***Reg***	R^2	0.026	0.015	**0.403***	**0.470***	**0.448***	0.310	**0.504***
			p	0.701	0.701	**0.047***	**0.040***	**0.040***	0.065	**0.040***
		Corr	***r***	-0.161	0.124	**-0.635***	**0.685***	**-0.670***	0.557	**0.710***
	1.5 mA	***Reg***	R^2	0.022	0.094	0.001	0.067	0.002	0.090	0.060
			p	0.908	0.778	0.922	0.778	0.922	0.770	0.740
		Corr	***r***	-0.147	0.307	-0.032	0.259	-0.043	0.300	0.244
	2.0 mA	***Reg***	R^2	0.043	0.113	0.277	0.108	0.342	**0.770***	0.309
			p	0.518	0.347	0.138	0.346	0.138	**0.007***	0.138
		Corr	***r***	-0.207	0.336	-0.526	0.329	-0.585	**0.878***	0.556
ΔCBF Late Epoch (75-120min)	**0.5 mA**	***Reg***	R^2	0.298	0.018	0.221	0.185	0.212	0.146	0.152
			p	0.206	0.647	0.207	0.208	0.198	0.289	0.209
		Corr	***r***	0.545	0.134	-0.470	0.430	-0.460	0.383	0.390
	1.0 mA	***Reg***	R^2	0.032	0.152	0.100	0.001	0.135	0.132	0.068
			p	0.677	0.551	0.551	0.982	0.520	0.501	0.580
		Corr	***r***	-0.178	0.390	-0.317	-0.007	-0.370	0.364	0.260
	1.5 mA	***Reg***	R^2	0.054	0.060	0.315	0.072	0.384	0.127	0.232
			p	0.464	0.443	0.151	0.168	0.154	0.357	0.198
		Corr	***r***	-0.234	-0.245	0.561	0.269	-0.620	-0.357	-0.481
	2.0 mA	***Reg***	R^2	0.118	0.143	0.002	0.034	0.001	0.007	0.001
			p	0.955	0.950	0.960	0.900	0.960	0.950	0.940
		Corr	***r***	-0.344	0.378	-0.045	-0.186	-0.032	0.082	0.006

Table 5.6 Association between Anatomical Factors, Electrical Fields and cathodal tDCS-induced CBF Alterations. Multiple linear regressions (Reg) were used to test whether and to which extent the individual variability of the neurophysiological effects of **cathodal** tDCS (evaluated by CBF amplitude alterations) can be explained by the respective individual EF (for the ROI_{HK}), or anatomical factors. In addition, Pearson's correlation coefficient (Corr) was calculated to further identify the directionality of each regression result. The p-values were adjusted for multiple comparisons using the False Discovery Rate (FDR). Asterisks indicate significant results.

				Thickness					Electrical Field	
				Scalp	Skull	CSF	CSF Volume	ECD	$\lvert E \rvert$ ROI_{HK}	$\hat{n}.\vec{E}$ ROI_{HK}
ΔCBF Early Epoch	**0.5 mA**	***Reg***	R^2	0.001	0.002	0.169	0.069	0.092	0.042	0.084
			p	0.876	0.876	0.538	0.639	0.638	0.674	0.639
		Corr	***R***	0.010	0.046	0.411	0.262	0.303	-0.205	-0.290
	1.0 mA	***Reg***	R^2	0.250	0.073	0.005	0.120	0.011	0.004	0.009
			p	0.546	0.868	0.817	0.865	0.883	0.883	0.851

		Corr	***r***	0.505	-0.270	0.072	0.346	0.103	-0.063	-0.098
	1.5 mA	***Reg***	**R^2**	0.003	0.130	0.009	0.016	0.001	0.002	0.023
			p	0.891	0.826	0.758	0.880	0.835	0.891	0.822
		Corr	***r***	-0.018	-0.361	0.095	0.127	0.024	-0.042	-0.151
	2.0 mA	***Reg***	**R^2**	0.052	0.027	0.004	0.015	0.006	0.010	0.002
			p	0.876	0.812	0.838	0.807	0.807	0.854	0.887
		Corr	***r***	-0.227	-0.164	0.066	-0.121	-0.079	-0.102	-0.046
ΔCBF Late Epoch (75-120min)	**0.5 mA**	***Reg***	**R^2**	0.001	0.008	0.066	0.207	0.036	0.001	0.056
			p	0.941	0.941	0.386	0.721	0.941	0.946	0.714
		Corr	***r***	-0.020	-0.089	0.256	0.454	0.190	-0.020	-0.237
	1.0 mA	***Reg***	**R^2**	0.063	0.278	0.034	0.011	0.005	0.002	0.008
			p	0.870	0.448	0.553	0.739	0.845	0.870	0.773
		Corr	***r***	0.250	-0.530	-0.186	0.103	-0.021	0.050	0.089
	1.5 mA	***Reg***	**R^2**	0.166	0.095	**0.559***	0.036	**0.485***	**0.558***	**0.608***
			p	0.246	0.355	**0.007***	0.536	**0.014***	**0.007***	**0.007***
		Corr	***r***	-0.408	0.309	**-0.774***	0.189	**-0.696***	**0.747***	**0.780***
	2.0 mA	***Reg***	**R^2**	0.318	0.241	0.240	0.323	0.327	**0.504***	0.192
			p	0.082	0.125	0.225	0.082	0.066	**0.014***	0.176
		Corr	***r***	-0.563	0.491	-0.490	0.568	-0.572	**0.710***	0.439

5.4. Discussion

In the present study, based on neurophysiological data obtained in former studies of our group, which explored tDCS-induced MEP (induced by TMS) and CBF (measured by ASL-fMRI) alterations, we investigated the association between individual anatomical factors and tDCS-induced EF, and the respective physiological outcomes at the level of the individual. To this end, we first explored the contribution of individual anatomical factors to EF variabilities (strength: $|\mathrm{E}|$, and normal components: $\hat{\mathrm{n}}.\vec{\mathrm{E}}$) at two ROIs (ROI_{HK} and ROI_{TMS}). At the second level, we investigated whether and to which degree the individual anatomical factors and EFs predict the tDCS-induced MEP and CBF changes. In general, of the included anatomical factors, ECD, and partially CSF parameters, significantly explained interindividual EF variabilities. Higher EF values were associated with lower ECD, and CSF thickness. In addition, apart from the observed tDCS dosage-dependent physiological effects, the results of the present study revealed that CSF thickness and ECD, as well as EFs, reliably predicted physiological effects of stimulation. These associations were however restricted to stimulation conditions which altered respective physiological measures in comparison with respective

baseline and/or sham values. In what follows, we discuss these findings in more detail, and add mechanistic explanations.

The results are in accordance with previous findings, in which CSF thickness and also ECD were suggested as key factors of EF simulations, and negatively correlated with individual EFs [59, 60]. Furthermore, with respect to the association between EFs and neurophysiological outcomes of tDCS, the results of our study are in accordance with those of another study showing a positive correlation between EF strength and physiological outcomes of the intervention [63]. An opposing finding was however reported for 1mA anodal tDCS-induced EFs and individual MEP amplitude alterations in another study, where no significant MEP modulations were observed for the active condition vs. sham [62]. The missing overall effect of tDCS in that study is however in line with our findings in which the significant association between the predictors and the neurophysiological effects were obtained only for epochs with observed physiological responses.

5.4.1. Proposed mechanism

From the amount of electrical current that is applied between two electrodes positioned on the head, a portion is shunted across the scalp [233]. The remaining current is then passed via the different tissue components of the skull, the CSF, and then reaches the brain, resulting in EF at the level of the gray matter and underlying tissues. The high inter-individual anatomical variability of respective tissues [234, 235] has been shown to strongly contribute to tDCS-induced EF variability across subjects [109].

Despite the complex interplay between tissue compartments, we found that a major part of the variance of the regional EFs can be explained by individual ECD and CSF-related parameters. With respect to the relevance of ECD, this finding is supported by reports showing that RMT, which is positively correlated with scalp-to-cortex distance [236], correlates negatively with tDCS-induced EF strength [61]. It can be thus assumed that a larger electrode-to-cortex distance results in lower current densities, and EF induced by tDCS over the targeted area. In the same vein, a thicker layer of CSF results in weaker EF at the level of the cortical target areas [59, 60]. Indeed, the significant role of CSF thickness might be due to the considerably larger electrical conductivity of CSF compared to other brain tissues,

resulting in a preferential pathway for the injected currents. The lack of predictive power of the other anatomical factors might be related to their limited volumes, and heterogeneous electrical conductivities. In principle accordance, individual CSF thickness and coil/scalp-to-cortex distance have shown to correlate strongly not only with tDCS-, but also with TMS-induced EFs [237], and TMS-evoked motor thresholds [236, 238, 239], respectively.

The principle mechanism responsible for the physiological effects of tDCS at the neuronal level is assumed to be a subthreshold alteration of neuronal membranes, whose directionality depends on the relation of EF to neuronal orientation, and subsequently alter firing rates. Prolonged stimulation modulates synaptic efficacy, which is controlled by NMDA receptors, calcium-dependent mechanisms, and downregulation of the GABAergic system [85, 169, 240]. In this line, a positive association between increased stimulation dosage, within certain limits, and tDCS efficacy enhancement has been reported [20, 96]. It has however also been shown that exceeding stimulation dosage beyond respective limits with respect to stimulation intensity, and duration results in non-linear effects, which depend on calcium concentration [65, 67, 68, 82, 89]. The observed positive correlation between the individual EFs, and anodal tDCS after-effects in the present study fits nicely with these prior findings, indicating stimulation intensity-dependent increased efficacy of anodal tDCS to enhance MEP amplitudes [19], and CBF changes, as far as these can be dedicated to neuronal effects. The relatively lower predictive power of EF values for anodal tDCS effects on CBF, as compared to MEP, might be due to the mixed effects of tDCS on vessels, and neural excitability [241, 242].

In contrast, our results showed a more limited predictive power of CSF thickness, ECD, and EF for explaining intensity-dependent cathodal tDCS-induced MEP alterations. This might be caused to some degree by the non-linear physiological effects of motor cortex cathodal tDCS within the tested dosage range. While anodal tDCS shows a linear dosage-effect relationship for a relatively broad range of stimulation intensities, non-linear effects were observed for cathodal tDCS, with higher intensities converting the effects of cathodal tDCS into an excitability enhancement, or no effects [64, 65, 98, 183]. This was also observed in the present study, where only 1 mA stimulation resulted in a clear excitability diminution. In accordance, the clearest effects with respect to the association of EF, and MEP size

were seen for a stimulation intensity of 1.0 mA. For CSF, furthermore for 1.5 mA stimulation intensity such an association was revealed. These results further support previous findings that an association between EF, and physiological effects of tDCS can only be identified if the latter do emerge, which is the case for 1.0 mA stimulation intensity for MEP, and additionally 1.5 mA stimulation intensity for CSF measures. Furthermore, in difference to associations between EF and MEP, which did already emerge in the early epoch, respective EF associations with CSF were visible only in the later epoch. On the one hand, this fits to the assumption that clear physiological effects should be present to identify such an association, because CSF effects of cathodal tDCS were larger in the late epoch. On the other hand, the missing predictive power of explanatory variables for the early epoch of cathodal tDCS-altered CBF amplitudes could be explained by non-homogeneous effects of cathodal tDCS on neural excitability, and vessels, as well as different temporal dynamics of the respective contributions [88, 241, 242]. At present, these explanations are speculative, and should be explored in future studies directly.

In general, the model developed in this study showed relatively good predictions of tDCS-induced physiological effects, it explained about 50% of the observed variability. Beyond the physical factors, which were explored in the present study, however other confounding factors might also contribute to inter-individual variability of tDCS effects, including brain state, neurotransmitter and modulator availability [45, 109, 243], as well as network effects of locally induced plasticity [87, 244-247], which have already been shown to affect tDCS outcome. Moreover, for predicting the neuromodulatory effects of NIBS, nonlinearities of neuroplastic responses have to be taken into account, which also differ inter-individually, as shown in a recent study for theta burst stimulation [175]. Therefore, advanced computational approaches, which incorporate realistic neuronal models, are required to approximate the effects of the intervention on different neural circuits, in addition to respective EF simulations [197, 198]. Finally, the models developed in this study might be relevant for other NIBS modes beyond tDCS, such as TMS, where stimulation intensity with respect to various cortical targets is individualized based on motor cortex reactivity, which however might has limited value for stimulation of other brain areas, such as the dorsolateral prefrontal cortex, a hub for cognitive processes, and target for therapeutic stimulation approaches in neuropsychiatric disorders.

5.4.2. Limitation and future directions

In the present study, we used a well-stablished computational modeling pipeline to simulate tDCS-induced EF, which has been shown to predict *in-vivo* intra-cranial EF recordings well [187]. However, this modeling approach might be improved by considering several issues in future studies. The first issue is related to the validity of the estimated EF. Efforts have been made to validate and/or evaluate the accuracy of ′ modelling results by comparing measurements from electroencephalography (EEG) surface recordings [192], physiological effects in vivo in simians [248], and humans [249, 250], in vivo intracranial recordings from humans [251], and magnetic resonance current density imaging (MRCDI) [252, 253]. Model predictions from scalp surface voltages face however limitations, as the induced scalp voltages can prove the accuracy of the high-resolution individualized model at the level of the scalp, but not directly validate the model prediction of current flow at the level of the *brain* [187, 192]. On the other hand, direct in vivo measurements of EF are strongly sensitive to experimental procedures, resulting in measurement errors which can under- or overestimate the distributed EF inside the brain [46], and compared to MRCDI measurements, simulations underestimate current densities on average by 24% [252, 253]. There is therefore a strong need to improve the validity and accuracy of computational modeling, which should be considered in future studies.

Furthermore, in this study we segmented the head tissues into seven major compartments, in line with recent studies [63, 187]. Other works have however highligheted the importance of including additional head tissues to improve the accuracy of predicted EF results. For example, subcutaneous fat and muscle tissues have been suggested to profoundly affect the magnitude and distribution pattern of induced current density in some studies [254, 255]. Other studies have however suggested only a small contribution of these tissues (e.g. differences in head fat thickness are assumed to contribute only to ~10% additional variability with respect to peak cortical current density [256]). Likewise, skull compartments have been shown to influence the estimated EF in some studies [60, 257, 258], but suggested to be negligble in another study [187]. In addition, we treated all internal tissues of the brain as WM; other studies have however further subdivided internal brain tissues for the reconstructed head model (e.g 40 head compartments [259], or 20 anatomical regions [197]). Despite increasing the cost and complexity of

computation, this might improve the accuracy of the estimated EF. Furthemore, brain tissue anisotropic conductivity, specially of WM, has been shown to influence EF directionality, especially within the sulci [257], and EF magnitude [260], but again other studies suggested that its effects might be negligble [187, 197]. Moreover, there are still uncertainties related to *individual* tissue electrical conductivity [261, 262], as conductivity is usually determined based on an average of a range of values found in the literature based on ex-vivo measurements in animal and human tissues. Reliable measurements of these conductivities at the level of the individual are difficult to obtain, and the results vary considerably between subjects [56]. Recently developed MR-based methods of conductivity and curent density measurements such as MRCDI or magnetic resonance electrical impedance tomography [252, 253, 263, 264] might open of a window to address these uncertainities, and should be considered in future studies.

In addition, due to limited MRI resolution ($1mm^3$), image noise, and low contrast in some areas, automatic tissue segmentation might suffer from inherent errors, including discontinuities in the CSF, and unassigned/ disconnected voxels, among others (for detail please see [214, 265]). In this study, we tried to correct these errors via two steps: 1) automatic correction (in Matlab), and 2) manual correction (via Simpleware, +ScanIP) by comparing the original and automatically corrected head tissue masks [187, 214]. Despite these, some parts of brain tissues (e.g. thin layers of CSF) might not have been accurately be reconstructed due to low resolution of conventional 1 mm^3 MRI, which might then influence the measured anatomical factors, as well as the resulting EF simulation [46, 201, 265]. Furthermore, MRI studies have shown that CSF thickness changes when a subject moves from prone to supine position [266, 267]. This has been shown to affect the magnitude of EEG signals [267], is suggested also to influence cortical activity [268], and has an impact of about 10% on simulations of tDCS-induced EF [269]. This might be important, as tDCS is applied usually when subjects are in an upright position, whereas MR images, which are the main materials used of realistic head models, are typically acquired with the subject lying in a supine position. This causes concerns about the extent to which the individual MR-derived EF simulations represent the tDCS-generated EF distribution in real-life, and should be considered in future studies.

Moreover, the target population in this study was healthy young humans. However, the neurophysiological effects of tDCS can be affected by stimulation protocol, age,

gender as well as neurological and neupsychiatric disorders [113, 115, 184, 270-273]. These confounding factors, which also affect tDCS-induced EFs, should be taken into consideration for the extension of the results obtained in this study to other populations. Finally, we mainly focused on regional effects of tDCS, but not on network effects; considering these in future studies might further improve our understanding of intervention effects.

5.5. Conclusions

This study shows that individual anatomical factors (including CSF thickness and electrode-to-cortex distance (ECD)), significantly explain inter-individual EF variabilities. In addition, CSF thickness, and ECD were negatively correlated, whereas EFs were positively correlated with tDCS-induced physiological changes. It general, our study demonstrates the usefulness of computational modeling, similar to the one used in this study, for the prediction of EF, and physiological effects induced by tDCS. However, considering other relevant head tissues, anisotropic conductivity, as well as individual electrical conductivity, and neuronal models might improve modeling accuracy and potentially the predictive power for the neurophysiolocal effects of tDCS. In addition, the transferability of these results to other cortical areas, age, and patient populations should be considered in future studies. This study provides further insights into the dependency of neuromodulatory effects of tDCS from individual anatomy, and the usefulness of electrical field simulations, and therefore delivers crucial information for future applications.

6 Study 5: Transferability of tDCS effects from the primary motor to the dorsolateral prefrontal cortex: a multimodal TMS-EEG study

6.1. Introduction

Neuroplasticity, an important foundation of cognitive processes such as learning and memory formation, is the property of the brain to adjust the strength and/or the efficacy of neural connections in response to environmental changes or injuries [11, 12]. Non-invasive brain stimulation (NIBS) protocols, in humans, have been shown to induce and modulate brain plasticity, and thus open a window to shed light on the underlying brain functions [76, 181], to explore the physiological foundation of cognitive processes, and to improve symptoms of associated neurological and psychiatric disorders [17, 18].

One of those tools, transcranial direct current stimulation (tDCS), has been shown to bidirectionally induce neuroplasticity in the targeted area, by delivering weak direct electrical currents through the scalp via two electrodes placed on the head. For the primary motor cortex, anodal tDCS, which refers to surface inward current over the target area, results in enhancement of cortical excitability, whereas cathodal tDCS, which refers to outward current over the target area, reduces it. The direction, and strength of effects depends on the stimulation parameters, such as polarity and intensity/duration [20, 96, 116].

tDCS-induced neuroplastic after-effects have so far been most extensively investigated for the primary motor cortex, and less often in other cortical areas, such as visual, auditory and somatosensory areas [72, 73, 274]. The results obtained for the primary motor cortex, as indicated by transcranial magnetic stimulation (TMS)-induced motor evoked potentials (MEP), suggest a positive association of the obtained excitability alterations with increased stimulation dosage within certain limits [20, 96]. Stimulation dosage-dependent non-linear after-effects were however observed when stimulation settings exceed the limits of conventional protocols [65, 67, 68, 82, 89]. Notwithstanding, it remains unclear to what extent motor tDCS effects transfer to other brain regions, as the number of available studies is limited. Over the sensorimotor cortex, anodal tDCS increased the amplitude of somatosensory potentials, whereas cathodal tDCS had no effects in one study [73],

while another study showed excitability-diminishing effects of only cathodal tDCS [74]. For the effects of tDCS on visual evoked potentials, anodal tDCS enhanced, and cathodal tDCS reduced cortical excitability, however, the duration of the effects was relevantly shorter as compared to motor cortex stimulation with otherwise identical protocols [72]. The results of these studies show only a gradual comparability of stimulation effects. Taking anatomical, as well as receptor, and neurotransmitter distribution differences of distinct cortical areas into account, these gradual differences of effects are plausible, and require direct physiological tests of tDCS over respective target areas [22].

This is of critical importance, since tDCS has been probed not only to improve symptoms of motor-related neurological disorders [18], and/or to explore the physiological foundation of motor functions [22], but its neuromodulatory effects have been also extensively explored for the treatment of neuropsychiatric diseases [21], and physiological mechanisms underlying cognitive functions, including working memory (WM), and mood and emotional states, with the dorsolateral prefrontal cortex (DLPFC) as target region [32, 35, 275]. However, the neurophysiological effects of tDCS on this area have been much less explored. A recently developed multimodal neuroimaging technique, which combines TMS and electroencephalography (EEG), opened up a window to address modulatory effects of tDCS, and other NIBS techniques, on cortical excitability of different brain regions, as indexed by TMS-evoked potentials (TEPs) recorded from scalp EEG electrodes [276].

Few studies have employed TMS-EEG so far to evaluate tDCS effects. Anodal and cathodal tDCS with 1mA for 13min applied ***over the primary motor cortex*** have been shown to induce a bidirectional 'anodal-enhancement cathodal-inhibition' modulation of early TEP amplitudes. ***For the prefrontal cortex***, anodal tDCS with 1mA for 20min, applied with bipolar and high-definition tDCS (HD-tDCS), induced likewise an increase of local early TEP peaks, and a decrease of TMS-evoked beta and gamma oscillatory power over posterior EEG channels [277, 278]. In another study, with a newly developed electrode configuration, tDCS with 1.5mA for 14min, targeting the left DLPFC with the anode, and the right DLPFC with the cathode, however showed a reduction of late TEPs (about 120ms after the TMS pulse) over only the parietal cortex, accompanied by a reduction of TMS-evoked power of theta and gamma oscillations at the global scalp level, whereas tDCS with opposite

electrode positions had no effects [279]. Thus, most TMS-EEG studies so far indicated qualitatively comparable results of tDCS over the motor and prefrontal cortex, however the number of studies is scarce, and results are partially heterogeneous. A systematic comparative investigation of the neuroplastic effects of tDCS over these different brain regions is therefore required.

In a foregoing study, we systematically explored the dosage-dependent impact of cathodal tDCS on motor cortex excitability, as explored by TMS-generated MEP. In that study, we combined different stimulation intensities (1, 2, and 3mA, electrode size 35 cm^2), and durations (15, 20 and 30min). MEP amplitudes were reduced by low and high intensity protocols, whereas an excitability enhancement was observed after medium intensity tDCS [65]. In the present study, we aimed to explore the transferability of these results from the primary motor to the dorsolateral prefrontal cortex. In eight randomized sessions, four cathodal tDCS dosages of low, medium and high intensity, as well as sham stimulation were applied over the primary motor, and dorsolateral prefrontal cortex, with current densities at the scalp-electrode interface identical to our foregoing study. tDCS-induced after-effects were then evaluated using the TMS-EEG, and TMS-MEP approaches at the regional level for TMS-evoked cortical reactivity, oscillations, and MEP alterations. Based on previous findings, we hypothesized that all active protocols would modulate TEP amplitudes compared to the respective baseline and/or sham conditions. We also anticipated dosage-dependent nonlinear TEP and MEP amplitude modulations for motor cortex tDCS. Furthermore, based on anatomical, pharmacological and functional differences between motor and prefrontal cortex, we expected gradually different patterns of the neurophysiological effects of tDCS over the prefrontal cortex, as compared to motor cortex tDCS.

6.2. Material and Methods

6.2.1. Participants

Eighteen healthy, non-smoking participants (11 males, mean age 26.61±3.56 years) completed the entire study. All participants were right-handed according to the Edinburgh handedness inventory [93] and had no history of neurological and psychiatric diseases, or fulfilled exclusion criteria for noninvasive electrical or magnetic brain stimulation [94, 95]. The study conformed to the Declaration of Helsinki, and was approved by the local Ethics Committee. All participants gave

written informed consent before starting the study, and were financially compensated for participation.

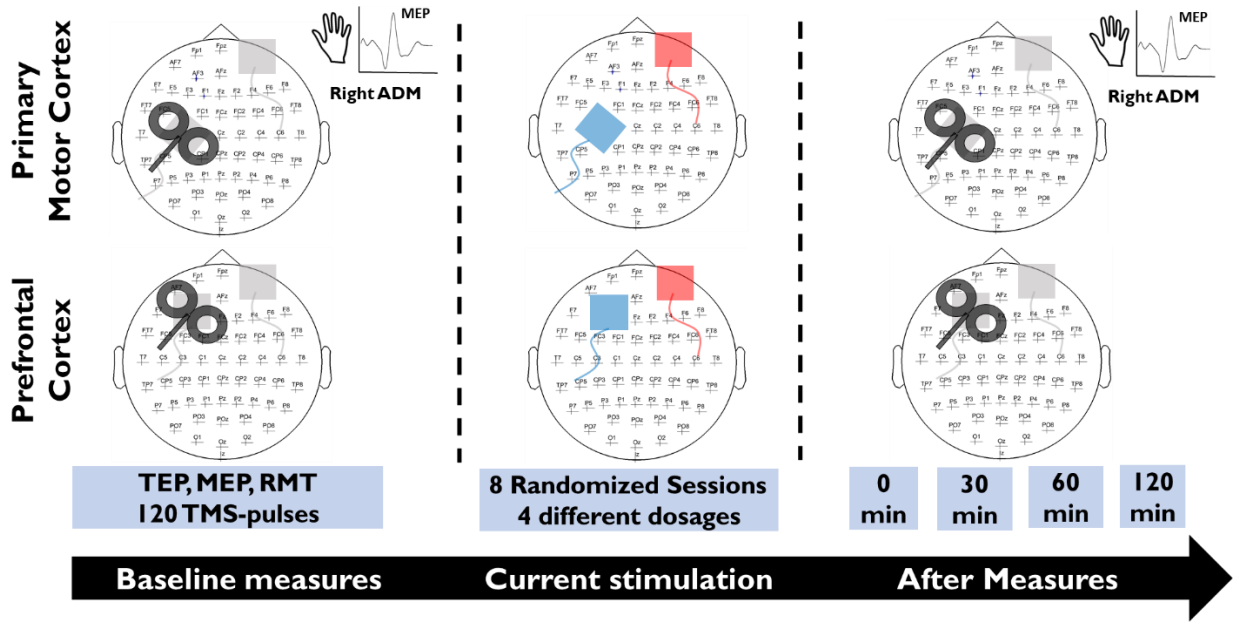

Figure 6.1. Course of the Study. Eighteen participants were included in this complete cross-over single-blinded, sham-controlled study, in which eight randomized sessions with four cathodal tDCS dosages of low, medium, and high intensities, and sham, were applied over the stimulation site primary motor (M1) and dorsolateral prefrontal cortex (F3). To evaluate the neuromodulatory effects of tDCS, TMS-evoked cortical reactivity, and TMS-elicited MEP (only for tDCS applied over the primary motor cortex), were recorded before tDCS, and immediately, 30min, 60min and 120min after tDCS. The recorded data were then evaluated at the regional level, for TMS-evoked potentials (TEPs), oscillations, and MEP alterations.

6.2.2. Neuro-navigated TMS-EEG and -MEP Measures

6.2.2.1. Transcranial Magnetic Stimulation

Single-pulse TMS at 0.33 Hz ± 30% (random) delivered by a PowerMag magnetic stimulator (Mag&More, Munich, Germany) with a figure-of-eight coil (PMD70) which was held tangentially over the EEG cap, with the handle pointing backwards and laterally at 45° from the midline, were applied. For the motor cortex stimulation site (PMCSS), TMS pulses were first applied to determine the representational area of the right abductor digiti minimi (ADM) muscle, in which the largest MEPs were produced by a given medium TMS intensity. At this stimulation site, the resting motor threshold (RMT) was then determined by the TMS-Motor-Threshold-Assessment Tool (MTAT 2.0) [280]. For the prefrontal cortex stimulation site (PFCSS), the TMS coil was placed over the F3 position, with the handle pointing backwards and laterally at 45° from the midline, to approximate the scalp location

overlaying the left DLPFC [277, 281, 282]. At each stimulation site, and for each time-point, 120 single TMS pulses were applied with a stimulation intensity of 100% of RMT, Figure 6.1.

6.2.2.2. EEG Recording

A TMS-compatible EEG system (NeurOne, BittiumCorporation, Finland) was used to continuously record TMS-elicited TEP at DC with a sampling frequency of 5kHz. EEG signals were captured by a TMS compatible Ag/AgCl C-ring 64 electrode EEG cap (EasyCap, Herrsching, Germany) according to the 10-20 International EEG Standard[1]. Electrodes were online referenced and grounded to external electrodes placed on the forehead (above the nasion). Two additional electrodes were used to record horizontal and vertical eye movements (one on the orbital ridge centered directly below the left eye and the other one at the lateral junction of the upper and lower right eyelids) [283]. Impedances at all electrodes were kept below 5kΩ during the experiment.

6.2.2.3. Neuronavigation

Following the individual TMS stimulation site identification, an MR-based 3D-neuronavigation system (PowerMAG View, Mag&More, Munich, Germany) was employed to store and display online the position and orientation of the TMS coil with respect to the participant's head and fiducials based on an individual structural MRI scan, assuring accuracy and reproducibility of the stimulation outcome throughout the experiment [276].

All imaging data were acquired in a 3T Philips Achieva scanner (Best, Netherlands) with a 32-channel head coil. Anatomical images were recorded based on T1-weighted fast 3D gradient echo pulse sequences (repetition-time= 8179 ms, echo-time= 3.7 ms, flip-angle= 8°, 220 slices, matrix-size= 240x240, and resolution= 1x1x1 mm^3).

6.2.2.4. MEP Recording

Surface EMG was recorded from the right ADM in a belly-tendon montage. The signals were amplified, and filtered (1000; 3 Hz–3 kHz) using D440-2

[1] AF3, AF4, F5, F1, F2, F4, F6, F8, FC5, FC3, FC1, FCZ, FC2, FC4, FC6, T7, C5, C1, CZ, C2, C4, C6, T8, CP5, CP3, CP1, CP2, CP4, CP6, P3, P5, P7, PZ, P1, P2, P4, P6, P8, PO3, POZ, PO4, O1, OZ, O2.

(Digitimer, WelwynGardenCity, UK), and were digitized (sampling rate: 5 kHz) with a micro 1401 AD converter (CED, Cambridge, UK), controlled by Signal Software (CED, v. 2.13).

6.2.3. Transcranial direct current stimulation

tDCS was applied with a constant-current battery-powered stimulator (neuroCare, Ilmenau, Germany), through a pair of surface rubber electrodes (25cm^2) attached on the scalp using conductive paste (Ten20®, Weaver). For the motor cortex stimulation sessions, the target electrode was centered over C3, according to the International EEG 10-20 system, and rotated 45^0 towards the midline. For the prefrontal cortex stimulation sessions, the target electrode was centered over the F3 position, parallel to the midline. The anodal return electrode, for both stimulation targets, was located on the contralateral supraorbital region. Prior to electrode placement, a topical anesthetic cream (EMLA®, AstraZeneca, UK) was applied to the respective stimulation sites, in order to decrease somatosensory sensations and sufficiently blind the participants [97]. In eight randomized sessions, four cathodal tDCS dosage of low (for 15min), medium (for 20min), and high (for 20min) intensities, and sham, were applied over the two stimulation sites, the primary motor (M1) and dorsolateral prefrontal cortex (F3). We chose stimulation parameters (intensity and duration) based on the results of our former study [65]; but with smaller stimulation electrodes (25cm^2) to sacrifice less EEG channels around tDCS targeted sites. Therefore, the same current densities at the scalp-electrode interface as in the previous study were applied for low (0.028mA/cm^2), medium (0.057mA/cm^2), and high (0.085mA/cm^2) dosage tDCS. For sham stimulation, low dosage tDCS was delivered for 15 seconds, with a 10sec ramp up and down followed by 15min with 0.0mA stimulation.

6.2.4. Experimental procedures

The study was performed in a cross-over single-blinded sham-controlled repeated measures design. At the beginning of each session, participants were seated in a comfortable chair with head- and arm-rests. Afterwards, the topical anesthetic cream was applied over the scalp at the identified corresponding stimulation sites. Then the tDCS electrodes were attached onto the head with conductive paste, followed by the set-up of the EEG cap. The participant's head was then co-registered to the individual head model within the neuronavigation system. Thereafter, TMS

stimulation sites (motor cortex representation area of the right ADM (motor hot-spot) and F3 (prefrontal hot-spot)) were identified for motor and prefrontal stimulation, and stored to the neuronavigation system, to be used throughout the experiment. Subsequently, TMS intensity was adjusted to identify the RMT, as explained above. Then, for the motor cortex stimulation site, baseline cortical excitability was determined by applying 120 TMS pulses over the motor hot-spot, with simultaneous recording of MEP, and TEP. For the prefrontal stimulation site, baseline cortical excitability was likewise determined by applying 120 TMS pulses over the prefrontal hot-spot. Afterwards, the respective tDCS protocol (as outlined above), was applied. After intervention, cortical excitability was monitored by applying 120 TMS pulses immediately (POST0), 30min (POST30), 60min (POST60) and 120min (POST120) after tDCS, Figure 6.1. Concurrent with TEP recording, white noise was implemented through headphones to minimize contamination of the EEG signal by auditory evoked potentials, induced by the TMS-related clicking sound [284, 285].
The tDCS sessions were applied in randomized order with a minimum of seven days between sessions to avoid carry-over effects [85].

6.2.5. Calculations

Offline data processing was performed with custom scripts in MATLAB (R2019b, Mathworks, USA), and the Fieldtrip toolbox [286].

6.2.5.1. MEP and TEP preprocessing

MEP amplitudes were first visually inspected to exclude MEP trials: 1) in which background electromyographic activity was present, and 2) with respective bad TEP trials (see below). Then, the individual means of peak-to-peak MEP amplitudes, recorded at each time-point, were separately calculated for all subjects and all conditions.
TEP waveforms were first segmented into epochs around the TMS pulses (−1000 to 1500 ms), down-sampled to 1kHz, visually inspected to remove bad trials/channels [287], and referenced to the average of all electrodes. Then, a time-period (−5 to +15ms) around each TMS pulse was removed and interpolated. Afterwards, the data were high-pass filtered ($1\text{Hz}; 4\text{th} - \text{order zero} - \text{phase Butterworth}$) and preprocessed with the 'signal-space projection with source-informed reconstruction' algorithm, which has been shown to efficiently suppresses TMS-related muscle artifacts [288], and minimize the contribution of peripherally-evoked sensory inputs

to TEPs [289]. For the SSP-SIR algorithm, we formed subject-specific, realistic leadfield matrices, by first automatically segmenting the individual T1-weighted MRI images using Freesurfer software [290], which were then imported to Brainstorm toolboxes [291], to generate leadfields, based on the three-layer symmetric boundary element method via OpenMEEG [292] (tissue conductivity values (S/m): scalp = 0.33, skull = 0.0033 and brain = 0.33). Data were then low-pass filtered ($100Hz; 4th-order\ zero-phase\ Butterworth$) following an independent component analysis (FastICA) to remove remaining noise components [293-296]. Finally, the decomposed data were filtered (lowpass: 45Hz; bandstop: 49-51Hz; 4th-order, zero-phase Butterworth), and baseline-corrected (−100 to −50ms to the TMS onset).

6.2.5.2. TMS-evoked Potentials- TEP

To evaluate the local effects of tDCS, we extracted the TEP deflections from the averaged FC1 and CP1 electrodes (for tDCS over the motor cortex; region of interest (ROI_{motor})), and from the averaged FC1 and Fz electrodes (for tDCS over the prefrontal cortex; $ROI_{prefront}$). These ROIs were selected to capture the regional effects of tDCS, as they are located close to the tDCS target electrode, and are distant from cranial muscles, to reduce the TMS-related artifacts [277, 297]. For these ROIs, the known TEP peaks were first identified by searching the maximum (for positive) or minimum (for negative) TEP deflections over the time-periods of: 20-40ms (P30), 35-55ms (N45), 45-75ms (P60), 85-135ms (N100) and 170-230ms (P200) [276, 298-300]. A 10ms window (±5ms) around each identified TEP peak was then averaged to calculate the respective TEP amplitude, and used for further statistical analysis.

6.2.5.3. TMS-evoked Oscillations

To test if tDCS modulated TMS-related neural oscillations, time-frequency representations (TFRs) of oscillatory power were calculated, for ROI_{motor} and $ROI_{prefront}$, on single trials (Morlet wavelet; wavelet width=3.5 cycles, steps of 1Hz between 2 and 45Hz), and then normalized relative to the respective baseline (−300 to −100ms) [301-303]. Finally, frequency power estimates were calculated, for four separate frequency bands (FBs), including of Theta (θ; 4-7Hz), Alpha (α; 8-13Hz), Beta (β; 14-29Hz) and Gamma (γ; 30-45Hz).

6.2.5.4. Discriminability and qualitative assessment of tDCS protocols

After finishing each session, participants were asked to fill in a questionnaire which contained: 1. Guessed intensity of tDCS (none, low, medium, high) 2. Rating scales

for the presence and amount of visual phenomena, itching, tingling and pain during stimulation, and 3. Rating scales for the presence and amount of skin redness, headache, fatigue, concentration difficulties, nervousness and sleep problems within 24 hours after stimulation. The side-effects were rated on a numerical scale from zero to five, zero representing no and five extremely strong sensations.

6.2.6. Statistics

All statistical analyses were performed using SPSS (IBM Corp. v.26.0), custom scripts in MATLAB and the Fieldtrip toolbox [286].

6.2.6.1. Baseline measures

At the regional level (ROI_{motor}, $ROI_{prefrontal}$), to test if baseline measures differed between sessions, within and or between stimulation sites, two-way repeated-measures ANOVAs (rmANOVA) were performed, with condition (4 levels) and stimulation site (2 levels) as within-subject factors, and baseline of TEP peak, or TFRs of FB as dependent variables. In addition, two separate one-way rmANOVAs were performed with condition (8 levels for TMS_{RMT}, or 4 levels for baseline MEP) as within-subject factor, and TMS_{RMT} intensity, or baseline MEP as dependent variables, respectively.

6.2.6.2. Regional effects of tDCS and motor-to-prefrontal transferability

At the regional level ($ROI_{prefront}$, ROI_{motor}), we investigated if 1) within each stimulation site, the tDCS after-effects differed vs. respective sham, and baseline values and/or between each other, and 2) effects of the stimulation protocols differed between tDCS motor and prefrontal stimulation. To this end, individual means of the after tDCS measures: TEP peaks, TFRs of each frequency band, and MEP amplitudes, were first normalized (Δ) to the respective individual mean baseline: $(post.tDCS - baseline) \,/\, |baseline|$. Then, three-way rmANOVAs were calculated with condition (4 levels), time-point (5 levels) and stimulation site (2 levels) as within-subject factors, and each normalized TEP peak (ΔP30, ΔN45, ΔP60, ΔN100, ΔP200), TFRs of each normalized FB (ΔTheta, ΔAlpha, ΔBeta, and ΔGamma) as dependent variable. Another two-way rmANOVA with condition (4 levels), and time point (5 levels) as within-subject factors, and ΔMEP as dependent variable, was calculated to test if MEP amplitudes differed between conditions and/or baseline.

6.2.6.3. Qualitative assessment of tDCS protocols

To identify if participants correctly guessed tDCS intensities correctly, chi-square tests were conducted. Side-effects during and after tDCS were analyzed by a repeated measure ANOVA with condition (8 levels) as within-subject factor and rating scores (0-5) as dependent variable. In case of significant effects, follow-up exploratory post-hoc paired t-tests were conducted to examine if an active session resulted in a significantly different sensation relative to sham.

For all ANOVAs, Mauchly's test of sphericity was conducted, and the Greenhouse-Geisser correction was applied when necessary. The critical significance level was set at $p \leq 0.05$. Post hoc t-tests were Bonferroni-corrected for multiple comparisons.

6.3. Results

6.3.1. Baseline measures

Baseline measures, at the regional level (ROI_{motor} and $ROI_{prefrontal}$), are listed in Table 6.1. For the baseline TEP peaks, the respective rmANOVAs showed no significant differences for each stimulation site, however, significant differences between stimulation sites were observed for P30 and N100. Post-hoc tests indicated a lower amplitude of P30 and N100 over the prefrontal cortex, as compared to the primary motor cortex. Also, for baseline TFRs of each FBs, the respective rmANOVAs showed no significant differences, within each stimulation site. However, significant differences were identified between stimulation sites for Theta and Alpha frequency bands, with lower power over PFCSS, as compared to PMCSS. No significant differences were also observed for either TMS_{RMT}, or baseline MEP amplitudes, between stimulation conditions, Table 6.2.

Table 6.1. Baseline measurements. TEP peaks, Frequency bands (FBs), MEP and TMS intensity for RMT. Data are presented as mean ± standard error of mean (SEM).

	Stim-sites	tDCS Protocol	P30 (μV)	N45 (μV)	P60 (μV)	N100 (μV)	P200 (μV)
TEPs	**Motor Cortex**	**Sham**	1.96 ± 0.38	-1.07 ± 0.52	1.52 ± 0.43	-5.31 ± 0.31	4.45 ± 0.64
		Low dosage	2.14 ± 0.35	-1.03 ± 0.49	0.91 ± 0.40	-5.03 ± 0.29	3.78 ± 0.55
		Medium dosage	1.53 ± 0.33	-1.78 ± 0.42	1.16 ± 0.41	-5.29 ± 0.47	3.95 ± 0.67
		High dosage	2.04 ± 0.38	-1.38 ± 0.33	1.46 ± 0.33	-5.42 ± 0.31	4.23 ±0.52
		Sham	0.42 ± 0.29	-1.21 ± 0.29	1.33 ± 0.25	-4.15 ± 0.32	4.22 ± 0.36

	Prefrontal Cortex	**Low dosage**	0.40 ± 0.26	-0.98 ± 0.26	1.38 ± 0.26	-4.05 ± 0.31	4.14 ± 0.31
		Medium dosage	0.46 ± 0.24	-1.25 ± 0.29	1.44 ± 0.23	-4.22 ± 0.44	4.30 ± 0.31
		High dosage	0.44 ± 0.33	-1.57 ± 0.33	1.27 ± 0.23	-4.07 ± 0.39	4.53 ± 0.31
			Theta (θ; μV^2/Hz)	Alpha (α; μV^2/Hz)	Beta (β; μV^2/Hz)	Gamma (γ; μV^2/Hz)	
FBs	**Motor Cortex**	**Sham**	2.51 ± 0.31	1.33 ± 0.10	1.44 ± 0.05	1.56 ± 0.09	
		Low dosage	2.48 ± 0.19	1.26 ± 0.08	1.34 ± 0.05	1.52 ± 0.08	
		Medium dosage	2.47 ± 0.27	1.28 ± 0.08	1.53 ± 0.10	1.55 ± 0.08	
		High dosage	2.45 ± 0.24	1.32 ± 0.12	1.45 ± 0.11	1.55 ± 0.12	
	Prefrontal Cortex	**Sham**	1.67 ± 0.11	1.03 ± 0.16	1.39 ± 0.13	1.43 ± 0.12	
		Low dosage	2.04 ± 0.17	1.03 ± 0.07	1.48 ± 0.13	1.51 ± 0.11	
		Medium dosage	1.98 ± 0.27	1.07 ± 0.19	1.38 ± 0.13	1.42 ± 0.08	
		High dosage	1.81 ± 0.12	1.14 ± 0.20	1.39 ± 0.16	1.37 ± 0.10	
			TMS_{RMT} (%; stimulator output)				
TMS_{RMT}	**Motor Cortex**	**Sham**	57.44 ± 1.91				
		Low dosage	56.86 ±1.87				
		Medium dosage	56.94 ± 2.06				
		High dosage	58.52 ± 1.97				
	Prefrontal Cortex	**Sham**	56.22 ± 1.91				
		Low dosage	57.50 ± 1.79				
		Medium dosage	57.16 ± 2.15				
		High dosage	56.50 ± 1.95				
			MEP (μV)				
MEP	**Motor Cortex**	**Sham**	53.25 ± 4.98				
		Low dosage	46.52 ± 4.13				
		Medium dosage	43.53 ± 2.49				
		High dosage	52.01 ± 4.83				

Table 6.2. Results of ANOVAs conducted to evaluate baseline measurements. The ANOVAs showed no significant differences of baseline measures within stimulation sites; however, significant differences were observed for the TEP P30 and N100 between stimulation sites, and FBs for theta and alpha frequency bands. Asterisks indicate significant effects ($p < .05$), d.f. = degrees of freedom, η_p^2 = partial eta squared.

Baseline Measures	**Factors**	**d.f., Error**	**F value**	***p* Value**	$\boldsymbol{\eta_p^2}$

TEPs	**P30**	**Condition**	3, 51	0.541	0.656	0.031
		Stimulation site	1, 17	25.815	<0.001*	0.603
		Condition × Stimulation site	3, 51	0.804	0.491	0.045
	N45	**Condition**	3, 51	1.291	0.288	0.071
		Stimulation site	1, 17	0.080	0.780	0.005
		Condition × Stimulation site	3, 51	0.681	0.568	0.039
	P60	**Condition**	3, 51	0.363	0.780	0.021
		Stimulation site	1, 17	0.175	0.681	0.010
		Condition × Stimulation site	3, 51	0.767	0.518	0.043
	N100	**Condition**	3, 51	0.212	0.888	0.012
		Stimulation site	1, 17	16.161	0.001*	0.487
		Condition × Stimulation site	3, 51	0.184	0.907	0.011
	P200	**Condition**	1.970, 33.488	0.436	0.728	0.025
		Stimulation site	1, 17	0.266	0.613	0.015
		Condition × Stimulation site	3, 51	0.358	0.783	0.021
FBs	**Theta (θ)**	**Condition**	3, 45	1.048	0.381	0.065
		Stimulation site	1, 15	9.999	0.006*	0.400
		Condition× Stimulation site	3, 45	0.393	0.759	0.026
	Alpha (α)	**Condition**	3, 48	0.215	0.886	0.013
		Stimulation site	1, 16	14.001	0.002*	0.467
		Condition× Stimulation site	1.856, 29.693	1.226	0.310	0.071
	Beta (β)	**Condition**	2.207, 37.516	0.119	0.905	0.007
		Stimulation site	1, 17	0.187	0.671	0.011
		Condition× Stimulation site	2.060, 35.024	1.020	0.373	0.057
	Gamma (γ)	**Condition**	3, 39	0.452	0.718	0.034
		Stimulation site	1, 13	3.439	0.086	0.209
		Condition× Stimulation site	3, 39	0.125	0.945	0.010
TMS_{RMT}	**TMS_{RMT}**	**Condition**	3.724, 63.315	1.466	0.226	0.079
MEP	**MEP**	**Condition**	3, 51	1.453	0.238	0.079

6.3.2. TMS-evoked Potentials- TEPs; Regional Level

For the ΔP30 TEP, the rmANOVA indicated significant main effects of condition ($F_{(3,15)} = 11.798, p < 0.001, \eta_p^2 = 0.702$), time-point ($F_{(4,20)} = 3.131, p = 0.038, \eta_p^2 = 0.385$), interactions of condition and time-point ($F_{(12,60)} = 2.947, p = 0.003, \eta_p^2 = 0.371$), condition and stimulation site ($F_{(3,15)} = 6.278, p = 0.006, \eta_p^2 = 0.557$), time-point and stimulation site ($F_{(4,20)} = 3.469, p = 0.025, \eta_p^2 = 0.412$), and condition, time-point and stimulation site ($F_{(12,60)} = 3.143, p = 0.037, \eta_p^2 = 0.386$), but no main effect of stimulation site Figure 6.2.D, Table 6.3. For the PMCSS, post-hoc tests comparing

conditions revealed a significant increase of the ΔP30 amplitude for the medium dosage (POST0), as compared to sham, low- and high-dosage tDCS. In addition, post-hoc tests comparing tDCS after-effects to baseline indicated a significant ΔP30 amplitude reduction for high-dosage stimulation (POST0, POST30, POST60), while the medium dosage increased the TEP amplitude (only POST0). For the PFCSS, post-hoc tests comparing conditions revealed a significant reduction of the ΔP30 amplitude for medium- (POST0, POST30) and high-dosage (POST0, POST30, POST60) tDCS, in comparison with sham. Furthermore, post-hoc tests comparing baseline with after intervention time-points showed a significant ΔP30 amplitude reduction for medium- (POST0, POST30) and high-dosage (POST0, POST30, POST60) tDCS. Finally, post-hoc test comparisons of conditions between stimulation sites indicated a significant difference for the medium dosages (POST0, POST30), with a larger ΔP30 amplitude over the motor cortex, as compared to the prefrontal cortex, Figure 6.2.D, Table 6.3.

For the ΔN45 TEP, the rmANOVA indicated no significant effects of the main effects condition, stimulation site, and time-point, nor their respective interactions, Figure 6.2.D, Table 6.3.

For the ΔP60 TEP, the rmANOVA resulted in a significant main effect of condition ($F_{(3,15)} = 3.441, p = 0.034, \eta_p^2 = 0.408$), and a significant interaction of condition and time-point ($F_{(12,43)} = 3.667, p = 0.041, \eta_p^2 = 0.442$), but no significant main effect of stimulation site, or significances of other interactions, Figure 6.2.D, Table 6.3. For the PMCSS, post-hoc tests comparing conditions revealed a significant decrease of the ΔP60 amplitude for low- (POST0, POST30) and high-dosage (POST30, POST60) tDCS, as compared to sham. In addition, post-hoc tests comparing baseline TEPs with after affects within conditions showed a significant ΔP60 amplitude reduction for low- (POST0, POST30) and high-dosage (POST0, POST30, POST60) tDCS. For PFCSS, post-hoc tests comparing conditions revealed a significant reduction of the ΔP60 amplitude for low- (only POST30) and high-dosage (POST30, POST60) tDCS, compared to sham. Furthermore, post-hoc tests comparing baseline with time-points after tDCS within conditions indicated a significant ΔP60 amplitude reduction for low-, medium- and high-dosage tDCS (all protocols: POST30, POST60), Figure 6.2.D, Table 6.3.

For the ΔN100 TEP, the the results of the rmANOVA show a significant main effect of time-point ($F_{(4,20)} = 2.782, p = 0.046, \eta_p^2 = 0.284$), and significant interactions of condition and time-point ($F_{(12,84)} = 3.270, p = 0.025, \eta_p^2 = 0.284$),

and time-point and stimulation site ($F_{(4,31)} = 4.021, p = 0.040, \eta_p^2 = 0.410$), but no significant main effects of condition, stimulation site, or other respective interactions, Figure 6.2.D, Table 6.3. Post-hoc tests revealed a significant increase of the ΔN100 amplitude for low-dosage tDCS (POST0, POST30), in comparison with sham, and baseline, for PFCSS, Figure 6.2.D, Table 6.3.
For the ΔP200 TEP, the rmANOVA showed no significant main effects, or interactions, Figure 6.2.D, Table 6.3.

Table 6.3. Results of the ANOVAs conducted for tDCS-induced ΔTEP alterations. The statistical results indicate tDCS-induced effects for the early (ΔP30 and ΔP60) and late (ΔN100) TEP peaks, with no one-to-one transferability of tDCS effects from the motor to the prefrontal cortex. Asterisks indicate significant effects (where p < .05), d.f. = degrees of freedom, η_p^2 = partial eta squared.

	Factors	d.f., Error	F Value	*p* Value	η_p^2
ΔP30	**Condition**	3, 15	11.798	<0.001*	0.702
	Time-point	4, 20	3.131	0.038*	0.385
	Stimulation site	1, 5	4.501	0.087	0.474
	Condition × Time-point	12, 60	2.947	0.003*	0.371
	Condition × Stimulation site	3, 15	6.278	0.006*	0.557
	Time-point × Stimulation site	4, 20	3.496	0.025*	0.412
	Condition × Time-point × Stimulation site	12, 60	3.143	0.037*	0.386
ΔN45	**Condition**	3, 45	1.027	0.390	0.064
	Time-point	4, 60	1.061	0.384	0.066
	Stimulation site	1, 15	0.795	0.387	0.050
	Condition × Time-point	12, 180	0.436	0.947	0.028
	Condition × Stimulation site	3, 45	1.945	0.136	0.115
	Time-point × Stimulation site	4, 60	0.725	0.524	0.046
	Condition × Time-point × Stimulation site	12, 180	0.894	0.554	0.056
ΔP60	**Condition**	3, 15	3.441	0.034*	0.408
	Time-point	4, 20	1.054	0.405	0.174
	Stimulation site	1, 5	0.001	0.994	0.002
	Condition × Time-point	12, 43	3.667	0.041*	0.442
	Condition × Stimulation site	3, 15	0.560	0.740	0.138
	Time-point × Stimulation site	4, 20	0.158	0.957	0.031
	Condition × Time-point × Stimulation site	12, 60	0.853	0.597	0.146
ΔN100	**Condition**	3, 21	1.158	0.349	0.142
	Time-point	4, 20	2.782	0.046*	0.284
	Stimulation site	1, 7	1.522	0.284	0.345
	Condition × Time-point	12, 84	3.270	0.025*	0.246
	Condition × Stimulation site	3, 21	0.744	0.741	0.052
	Time-point × Stimulation site	4, 31	4.021	0.040*	0.410
	Condition × Time-point × Stimulation site	12, 70	1.723	0.240	0.159

ΔP200	**Condition**	3, 33	2.095	0.120	0.160
	Time-point	4, 44	0.913	0.465	0.077
	Stimulation site	1, 11	0.127	0.728	0.011
	Condition × Time-point	12, 132	1.593	0.101	0.126
	Condition × Stimulation site	3, 33	2.729	0.199	0.060
	Time-point × Stimulation site	4, 44	0.197	0.939	0.018
	Condition × Time-point × Stimulation site	12, 80	1.671	0.117	0.103

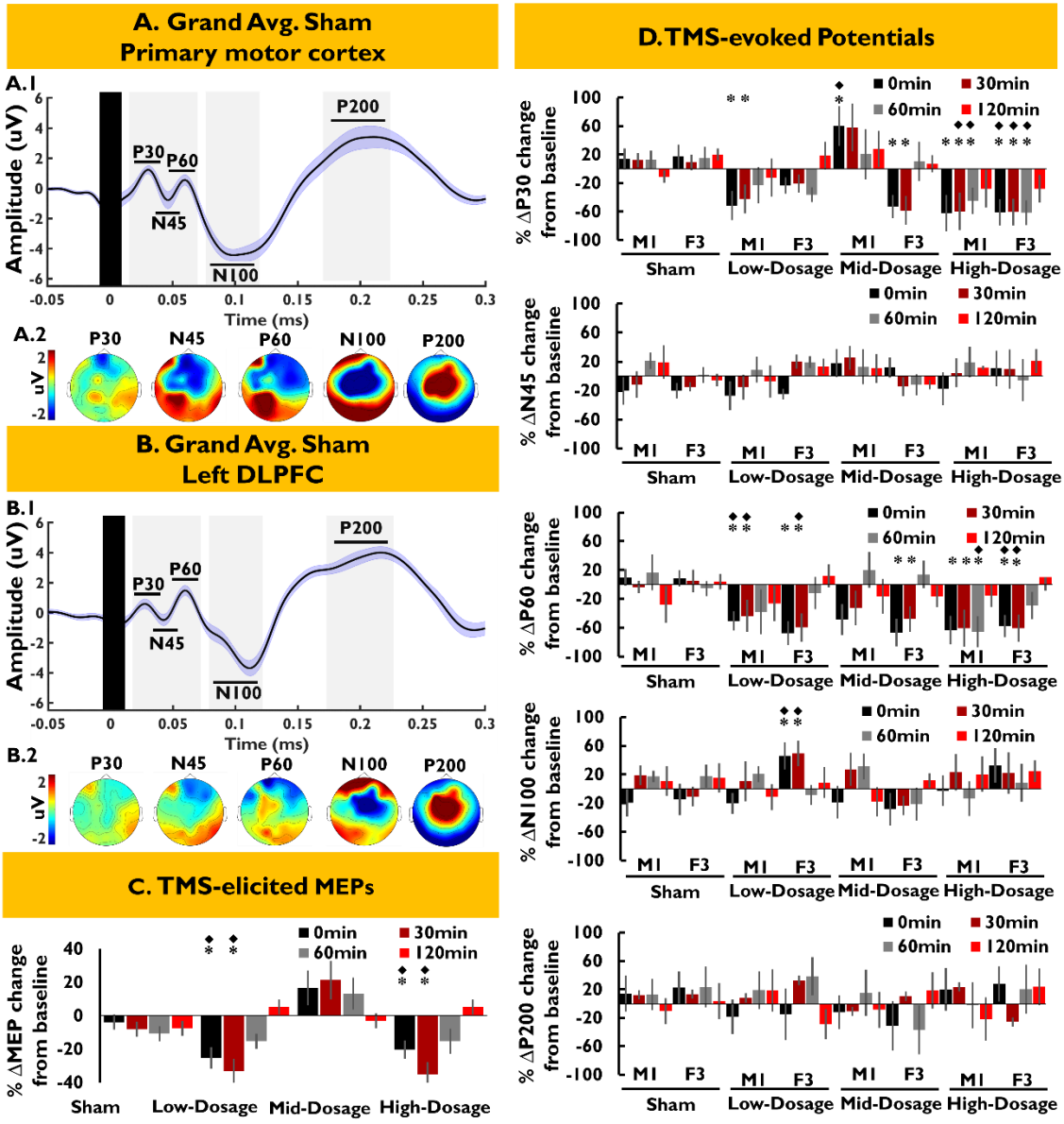

Figure 6.2. Local neuromodulatory effects of tDCS. Cathodal tDCS dosages of low, medium, and high intensities, and sham, were applied over the stimulation site primary motor (M1) and dorsolateral prefrontal cortex (F3). The local tDCS effects were then evaluated, every 30min,

immediately for up to two hours after stimulation, over the ROI_{motor} (averaged FC1 and CP1 electrodes) and $ROI_{prefront}$ (averaged FC1 and Fz electrodes). **A, B)** grand average across all subjects following sham stimulation over the left primary motor cortex (ROI_{motor}; **A.1**) and left DLPFC ($ROI_{prefront}$; **B.1**), and topographic plots displaying voltage distributions across the scalp for each TEP peak at the respective stimulation sites (**A.2, B.2**); Grey bars, together with the horizontal lines, correspond to the latency window of TEP components, and curve shadings are standard error of mean (SEM). **C)** ***TMS-elicited MEPs***: Low and high dosages significantly reduced the tDCS-induced MEP amplitudes, while a trend-wise cortico-spinal excitability enhancement was observed after medium dosage tDCS. Error bars represent standard error of mean (SEM). **D)** ***TMS-evoked potentials*** (ΔP30, ΔN45, ΔP60, ΔN100, ΔP200): tDCS generated a dosage-dependent, partially non-linear modulation of TEP over the different stimulation sites, as shown by the amplitude alterations of early (P30 and P60) and late (N100) TEP peaks. Floating symbols show a significant difference of real tDCS conditions vs. sham (◆), and real tDCS vs. respective baseline values (*****).

6.3.3. TMS-evoked Oscillations

For all frequency bands (Δθ, Δα, Δβ, Δγ), the rmANOVAs showed no significant effects of either the main effects condition, time-point and stimulation site, or their respective interactions, Table 6.4.

Table 6.4. Results of the ANOVAs conducted for tDCS-induced alterations of cortical oscillations. The rmANOVAs showed no significant effect of tDCS at the regional level on cortical oscillatory activities. FB: frequency band, d.f. = degrees of freedom, η_p^2 = partial eta squared.

	Factors		d.f., Error	F Value	*p* Value	η_p^2
FBs	**Δθ**	**Condition**	3, 12	0.383	0.767	0.087
		Time-point	4, 16	2.170	0.119	0.352
		Stimulation site	1, 4	0.049	0.835	0.012
		Condition × Time-point	12, 48	0.902	0.552	0.184
		Condition × Stimulation site	3, 12	1.143	0.371	0.222
		Time-point × Stimulation site	4, 16	0.735	0.581	0.155
		Condition × Time-point × Stimulation site	12, 48	1.287	0.257	0.243
	Δα	**Condition**	3, 21	1.006	0.410	0.126
		Time-point	4, 28	1.520	0.223	0.178
		Stimulation site	1, 7	0.847	0.388	0.108
		Condition × Time-point	12, 48	1.543	0.125	0.181
		Condition × Stimulation site	3, 21	1.960	0.151	0.219
		Time-point × Stimulation site	4, 28	1.086	0.382	0.134
		Condition × Time-point × Stimulation site	12, 84	1.142	0.339	0.140
	Δβ	**Condition**	3, 27	1.112	0.310	0.168
		Time-point	4, 36	1.623	0.190	0.153
		Stimulation site	1, 9	0.167	0.692	0.018
		Condition × Time-point	12, 108	0.697	0.752	0.072

		Condition × Stimulation site	3, 27	1.055	0.384	0.105
		Time-point × Stimulation site	4, 36	0.463	0.763	0.049
		Condition × Time-point × Stimulation site	12, 108	1.040	0.419	0.104
	Δγ	**Condition**	3, 18	2.353	0.106	0.282
		Time-point	4, 24	1.772	0.167	0.228
		Stimulation site	1, 6	0.031	0.21	0.852
		Condition × Time-point	12, 72	0.666	0.778	0.100
		Condition × Stimulation site	3, 18	2.466	0.095	0.291
		Time-point × Stimulation site	4, 24	0.050	0.875	0.010
		Condition × Time-point × Stimulation site	12, 72	0.661	0.783	0.099

6.3.4. TMS-elicited MEPs

The 2-factorial ANOVA (condition-4 levels, and time point-5 levels), conducted for the ΔMEP amplitudes, revealed significant main effects of tDCS condition ($F_{(3,51)} = 17.853, p < 0.001, \eta_p^2 = 0.512$), and time-point ($F_{(1.992,32.748)} = 10.467, p < 0.001, \eta_p^2 = 0.381$), and a significant interaction ($F_{(4.893,83.186)} = 7.491, p < 0.001, \eta_p^2 = 0.306$). Post hoc tests comparing sham tDCS with the respective active conditions revealed that low-, and high-dosage tDCS significantly reduced MEP amplitudes (both protocols: $(\mathrm{POST0}, \mathrm{POST30})$, while a trend-wise cortico-spinal excitability enhancement was observed after medium-dosage cathodal tDCS (only POST60; p=0.067). Similar results were found by comparing after effects with respective baselines, Figure 6.2.C, Table 6.5.

Table 6.5. Results of the ANOVA conducted for tDCS-generated alterations of TMS-elicited MEP. The statistical results indicate significant main effects of stimulation condition, time-point and the respective interaction. Asterisks indicate significant effects (p < .05), d.f. = degrees of freedom, η_p^2 = partial eta squared.

Factors		**d.f., Error**	**F Value**	***p* Value**	$\boldsymbol{\eta_p^2}$
ΔMEP	**Condition**	3, 51	17.853	< 0.001*	0.512
	Time-point	1.926, 32.748	10.467	< 0.001*	0.381
	Condition × Time-point	4.893, 83.186	7.491	< 0.001*	0.306

6.3.5. Qualitative assessment of tDCS protocols

Participants' guesses of received stimulation intensity are shown in Table 6.6. The Chi-square tests indicated no significant heterogeneity for any of the tDCS dosages (sham: χ^2=0.111, p=0.739; low-dosage: χ^2=2.778, p=0.096; medium-dosage: χ^2=1.778, p=0.182; high-dosage: $\chi^2$1.000, p=0.317), which shows successful

blinding. Ratings of the presence and intensity of side-effects are documented in Table 6.7. The ANOVAs conducted for the side-effects showed also no significant effect either during, or 24h after stimulation (Table 6.8).

Guessed intensity of tDCS (none, low, medium, high) 2. Rating scales for the presence and amount of visual phenomena

Table 6.6. Frequency table of participants' guesses of received stimulation intensity. In each session, participants were asked to guess the intensity of tDCS (none, low, medium, high). Note that the study included four tDCS dosages applied over two different stimulation sites. The table contrasts actually applied intensity (rows) with perceived intensity (columns).

	Stimulation site		Intensity guessed by participants			
			none	Low	Medium	High
Actual tDCS intensity	Motor Cortex	none	6	7	3	2
		Low	6	8	3	1
		Medium	3	7	5	3
		High	1	4	6	7
	Prefrontal Cortex	None	6	7	4	1
		Low	6	8	4	0
		Medium	2	6	7	3
		High	2	5	5	6

Table 6.7. Participant ratings of the presence and intensity of side-effects. Visual phenomena, itching, tingling and pain during stimulation. Skin redness, headache, fatigue, concentration difficulties, nervousness and sleep problems within 24 hours after stimulation. The presence and intensity of the side-effects were rated in a numerical scale from zero to five, zero representing no and five extremely strong sensations. Data are presented as mean ± SD.

		Motor Cortex Stimulation-site				Prefrontal Cortex Stimulation-site			
	Side-effects	Sham	Low Dosage	Medium Dosage	High Dosage	Sham	Low Dosage	Medium Dosage	High Dosage
During stimulation	Visual Phenomenon	0.33 ± 0.68	0.61 ± 0.69	0.61 ± 1.03	0.05 ± 0.23	0.94 ± 1.05	0.88 ± 0.90	0.33 ± 0.68	0.61 ± 0.69
	Itching	0.33 ± 0.48	0.50 ± 0.98	0.55 ± 0.92	0.22 ± 0.54	0.33 ± 0.68	0.66 ± 0.69	0.33 ± 0.48	0.44 ± 0.78
	Tingling	0.66 ± 0.84	0.50 ± 0.51	0.38 ± 0.84	1.00 ± 0.90	0.33 ± 0.48	0.50 ± 0.98	0.66 ± 0.84	0.55 ± 0.61
	Pain	0.27 ± 0.46	0.38 ± 0.77	0.50 ± 0.98	0.66 ± 1.08	0.66 ± 0.84	0.50 ± 0.51	0.27 ± 0.46	0.38 ± 0.77
24 hours after stimulation	Redness	0.27 ± 0.95	0.22 ± 0.54	0.22 ± 0.54	0.44 ± 0.85	0.27 ± 0.46	0.38 ± 0.77	0.27 ± 0.95	0.16 ± 0.38
	Headache	0.27 ± 0.46	0.27 ± 0.57	0.44 ± 0.70	0.66 ± 1.13	0.27 ± 0.95	0.22 ± 0.54	0.27 ± 0.46	0.27 ± 0.57

	Fatigue	0.66 ± 0.76	0.33 ± 0.48	0.50 ± 0.85	0.72 ± 1.17	0.27 ± 0.51	0.27 ± 0.57	0.66 ± 0.76	0.33 ± 0.48
	Concentration	0.33 ± 0.84	0.33 ± 0.76	0.33 ± 0.84	0.38 ± 0.60	0.66 ± 0.76	0.33 ± 0.48	0.33 ± 0.84	0.33 ± 0.76
	Nervousness	0.00 ± 0.00	0.16 ± 0.51	0.05 ± 0.23	0.50 ± 0.70	0.33 ± 0.84	0.33 ± 0.76	0.00 ± 0.00	0.16 ± 0.51
	Sleep Problem	0.00 ± 0.00	0.05 ± 0.23	0.11 ± 0.47	0.44 ± 0.61	0.00 ± 0.00	0.16 ± 0.51	0.00 ± 0.00	0.05 ± 0.23

Table 6.8. The presence and intensity of side-effects were analyzed by one-way repeated-measures ANOVAs. No significant effects of side-effects were identified either during or 24h after stimulation. d.f.= degrees of freedom. η_p^2 = partial eta squared.

	Side-effects	**d.f., Error**	**F Value**	η_p^2	**p Value**
During stimulation	**Visual Phenomena**	7, 119	1.567	0.084	0.152
	Itching	7, 119	0.765	0.043	0.618
	Tingling	7, 119	1.780	0.095	0.098
	Pain	3.106, 52.800	1.041	0.058	0.384
24 hours after stimulation	**Redness**	7, 119	0.363	0.021	0.922
	Headache	2.432, 41.342	1.157	0.064	0.332
	Fatigue	7, 119	1.560	0.084	0.154
	Concentration	3.038, 51.650	1.129	0.062	0.346
	Nervousness	3.100, 52.706	2.209	0.115	0.096
	Sleep Problem	7, 119	1.630	0.087	0.133

6.4. Discussion

In this study, we explored the dosage-dependent neuroplastic effects of cathodal tDCS at two targeted stimulation sites, the primary motor and dorsolateral prefrontal cortex. In a single-blind and sham-controlled repeated measures design, four cathodal tDCS dosages of low, medium, high intensity, and sham stimulation, were applied over the primary motor and dorsolateral prefrontal cortex. The after-effects were then tested by TMS-EEG and TMS-MEP techniques, at the regional level, for TMS-evoked cortical reactivity, oscillations, and MEP amplitude alterations. In general, we observed a nonlinear dosage-dependent effect of motor cortex tDCS (for TMS-evoked early positive TEPs, and MEPs), whereas prefrontal tDCS decreased almost uniformly the early positive TEP peaks. Furthermore, blinding was successful, and all participants tolerated tDCS well.

tDCS over the Primary Motor Cortex: for the *effects on early TEPs,* the results showed a significant reduction of the ΔP30 amplitude for low- and high-dosage tDCS, as compared to baseline, but a significant enhancement of the ΔP30 amplitude after medium dosage tDCS, in comparison with baseline and sham stimulation

values. No significant effects were however found for the ΔN45 TEP at this stimulation site. For the ΔP60, the results showed a significant reduction after low- and high-dosage tDCS, as compared to baseline, and sham stimulation conditions. For the *effects on late TEPs*, no significant differences were observed for the ΔN100 and ΔP200. In addition, the results showed no *effects of tDCS on TMS-evoked oscillations*. Furthermore, for the *TMS-elicited MEPs*, tDCS resulted in significant MEP amplitude reductions after low- and high-dosage tDCS, and a trendwise enhancement of MEP amplitudes after medium-dosage tDCS.

tDCS over the Dorsolateral Prefrontal Cortex: for the *effects on early TEPs,* the results revealed a significant reduction of the ΔP30 amplitude after medium- and high-dosage tDCS. No significant effects were however found for the ΔN45 TEP peak. For the ΔP60, significant TEP amplitude reductions were observed after low-, medium-, and high-dosage tDCS, as compared to baseline, and sham (the latter however not for medium dosage tDCS). For the *effects on late TEPs*, the results showed a significant enhancement of the ΔN100 only after low-dosage tDCS, as compared to baseline and sham conditions. No significant differences were observed for the P200 amplitude. In addition, the results revealed no impact of tDCS *on TMS-evoked oscillations*.

Comparison of tDCS effects on Motor and Prefrontal Cortex excitability: for *baseline TMS-evoked TEPs*, the results show a lower amplitude of the P30 and N100 over the prefrontal cortex, as compared to the primary motor cortex. For *baseline TMS-evoked oscillations*, significant differences were identified for theta and alpha frequencies, with lower power over the prefrontal, as compared to the primary motor cortex. In addition, the results of tDCS *after-effects on early and late TEPs show* a larger ΔP30 amplitude over the motor cortex, as compared to the prefrontal cortex, only for the medium dosage, in which an enhancement of the ΔP30 amplitude was observed for M1 stimulation. No significant differences were however observed for other TEP peaks. In what follows, we discuss these findings in more detail, and add mechanistic explanations.

The results of local TMS-evoked TEPs for low-dosage motor cortex tDCS are in accordance with the only available other tDCS-TMS-EEG study, in which significant reductions of only early positive TEP peaks, as compared to baseline, were observed after cathodal tDCS with 1mA for 13min over the primary motor cortex [304]. However, no sham-controlled TMS-EEG-evaluated neurophysiological data were so far available for different dosages of cathodal tDCS.

Moreover, the results of the present study are compatible with those obtained for other NIBS protocols. Continuous theta burst stimulation (cTBS) applied over M1, which reduces cortico-spinal excitability, decreased the P30 amplitude [305]. For the cathodal prefrontal tDCS TMS-EEG response, only one other study is available, in which, with a newly developed electrode configuration, bipolar tDCS, targeting cathodal-left and anodal-right DLPFC with 1.5 mA for 14min generated no effects on either TMS-evoked TEPs or oscillations. However, the electrode configuration and placement, as well as tDCS dosage were different, as compared to the present study, which might explain this disparity of outcomes. For other NIBS protocols, no significant effects of cTBS over F3, targeting the left DLPFC, have been reported for late TEP peaks (N120 and P200), and this stimulation protocol did also not alter oscillatory power [306]. Except for the N100 enhancement after low dosage tDCS over the prefrontal cortex in the present study, these results are in accordance with our findings. In addition, the dosage-dependent TMS-induced MEP amplitude reduction after low and high dosages of tDCS, together with the trend-wise enhancement of cortico-spinal excitability after medium dosage tDCS fit well with previous findings for tDCS [64, 65], and other NIBS modalities [307, 308].

6.4.1. Proposed Mechanisms

Over the ***primary motor cortex***, a significant reduction of the P30 amplitude was observed after *low dosage motor cathodal tDCS.* Several lines of indirect evidence suggest that early TEP peaks (≤ 30ms) might reflect excitatory neurotransmission *at the stimulation site* [309], and be a putative marker of excitability of the corticospinal system [310]. This assumption is supported by the fact that 1) after stimulating M1, motor cortical areas responded within the first 28 ms [311], 2) MEP amplitudes correlated with the N15/P30 complex, or the P25 amplitude [312, 313], 3), this TEP peak is similarly affected as MEPs by TMS intensity [314], coil angle [315], and paired pulse protocols [316], 4) MEP generation is suggested to depend on the predominance of excitatory postsynaptic potentials (EPSPs) in corticospinal pyramidal neurons [300], and 5) In animal models, EPSPs generated by NMDA receptor activation peak at ~15–40 ms, following electrical stimulation of the neocortex [317, 318], a time window which is similar to the P30 TEP peak. Taking this into account, reduction of the P30 amplitude by *low dosage motor cathodal tDCS* likely reflects the direct cathodal tDCS-induced neural excitability diminution at the stimulation site, which is driven by a reduction of glutamate, and NMDA receptor activity, and gated by reduced GABA activity [86, 100, 143]. This effect is

furthermore similar to the impact of this stimulation protocol on MEPs, which stresses the tight association of these parameters.
Furthermore, a reduction of the P60 amplitude was observed after *low dosage motor cathodal tDCS*. This propagated positive peak (P60) is suggested to reflect a fluctuation between EPSP and inhibitory postsynaptic (IPSP) activities mediated by AMPA, NMDA, and GABA receptors *in the stimulated cortical network,* as shown by paired-pulse and pharmaco-TMS-EEG studies [300, 313, 319, 320]. Therefore, with the known GABA and glutamate reduction after cathodal tDCS (see above), the reduction of P60 after this tDCS dosage is likely caused by reduction of glutamate, as the effects are equivalent to the P30 peak.
Moreover, in the current study, the N100, and later amplitudes did not change after *low dosage cathodal motor cortex tDCS*. Previous TMS-EEG studies linked the N100 peak to changes of local GABA-related activity [319, 321, 322], but a further contribution of also interhemispheric excitatory-inhibitory activity of motor networks or other long-range connections was also described [321, 323-325]. Taken this, and the known GABA and glutamate reduction after cathodal tDCS into account, it might be speculated that local GABA reduction, which would decrease this potential, would be counteracted upon by glutamate reduction-related enhancement of the N100, which would then result in a zero net effect of tDCS on the N100, in accordance with previous tDCS-TMS-EEG findings.

In contrast to low dosage tDCS, an enhancement of the P30 amplitude was observed after *medium dosage cathodal motor cortex tDCS*. This fits well with the MEP results, and shows stimulation intensity-dependent non-linear effects of tDCS also at the intrinsic level of the motor cortex, which, based on the neurophysiological foundations of the P30, are likely driven by the glutamatergic system. For mechanisms of glutamatergic synaptic plasticity, it is known that calcium concentration, which involve NMDA receptors, determines the increase or decrease of synaptic weight, i.e. long term potentiation (LTP) and long term depression (LTD) [101, 121]. Low and prolonged Ca^{2+} influx causes LTD, a moderate increase of calcium influx induces no synaptic modulation, and larger calcium increases result in LTP [101, 121, 153]. In accordance, also for tDCS in humans, pharmacological and neuroimaging studies showed that a glutamatergic process involving NMDA receptors contributes strongly to tDCS-induced plasticity [86, 143, 167, 168]. Therefore, the enhancement of the P30 amplitude after *medium dosage cathodal motor cortex stimulation* reflects likely a switch from LTD- to LTP-like plasticity due to an enhancement of Ca2+ influx at a level sufficient for induction of LTP-like

plasticity. However, apart from these presumed calcium-dependent effects, increasing tDCS intensity might affect also neurons in deeper cortical layers [105], and increase also the contribution of neighbored networks to a larger degree [112, 247]. A network effect is however unlikely. Such an impact would be more likely observed for the P60 amplitude, which more strongly depends on network effects than the P30. The P60 was however not affected by medium dose motor cortex tDCS. The missing effect of this intervention on the N100, and later potentials further support the spatial restrictedness of the stimulation effects.

For *high dosage cathodal motor tDCS*, the results show again a reduction of the P30, and P60 amplitudes. Taken the relatedness of the P30 TEP to MEPs, together with the involvement of calcium channel dynamics, into account, animal studies showed that calcium influx beyond the LTP-inducing level again results in no or excitability-diminishing plasticity due to counterregulatory mechanisms, which activate potassium channels [102]. In accordance, we have confirmed an involvement of calcium channel dynamics to the nonlinear high dosage tDCS-induced LTD-like plasticity in an MEP study in humans [326]. Therefore, *high dosage motor cathodal tDCS* reduced the P30, and also the P60 amplitude, likely by respective counterregulatory mechanisms. The missing effect of this intervention protocol on later potentials supports again the spatial restrictedness of its effects, similar to medium and low dosage motor cortex tDCS protocols (see above).

Moreover, the observed pattern of tDCS effects on MEP amplitudes, with a reduction after low and high dosages tDCS, and enhancement after medium dosage tDCS, is similar to the impact of stimulation on early TEP, and thus likely caused by ssimilar mechanisms, as explained above.

Over the prefrontal cortex, the results for the different tDCS dosages are, in general, relatively uniform, with the exception of the P30 and N100 amplitude after *low dosage cathodal prefrontal tDCS*. Based on knowledge about cathodal motor cortex tDCS effects (see explanation for the P30 TEP alteration obtained by low dosage cathodal motor tDCS), the P30 amplitude diminution observed with medium and high dosages of tDCS is compatible with reduced local glutamatergic activity induced by cathodal tDCS. The only numerical, but non-significant reduction of this amplitude by low-dosage tDCS might hint to an insufficient efficacy of this dosage to alter this potential with this prefrontal stimulation protocol. For more widespread effects of the stimulation, which are monitored by the P60, however also low dosage tDCS seemed to be efficient to alter excitability.

The P60 amplitude decreased significantly after *low, medium and high dosage cathodal prefrontal tDCS*. Prefrontal paired-pulse TMS-EEG studies have shown that the P60 amplitude is reduced by short interval cortical inhibition (SICI) protocols, which are mainly associated with GABA receptor activity, while this peak is enhanced via intra-cortical facilitation (ICF) protocols, which are attributed to glutamatergic-related NMDA-receptor activities. It is therefore suggested that this TEP peak reflects a balance of excitatory-inhibitory mechanisms [313], similar to the situation in the primary motor cortex. In addition, based on the proposed reduction of GABA and glutamate after motor tDCS, a GABA reduction would enhance P60, but glutamate reduction might reduce it. Thus, taken the proposed mechanisms, together with the alteration pattern of this peak, into consideration, the contribution of glutamate is the more likely cause for the P60 reduction after low, medium, as well as high dosage prefrontal tDCS.

Moreover, the results unaltered N100 and later peaks after *medium and high dosage of stimulation,* but an enhancement of N100 after *low dosage prefrontal tDCS*. Regarding mechanisms of these effects, several studies have reported that late TEPs, especially at periods~100ms and ~200ms, might represent similar underlying cortical sources, regardless of the target site following stimulation [309, 327]. In addition, over the left prefrontal cortex, GABA positively and glutamate negatively correlated with the N100 peak, as shown by magnetic resonance spectroscopy [328], suggesting that the N100 amplitude is linked to the balance of local inhibition-excitation. Therefore, with the known reduction of GABA and glutamate after cathodal tDCS, we would speculate that the GABA-reduction caused diminution, and glutamate-reduction caused enhancement of the N100 resulted in a null effect after medium and low dosage cathodal tDCS. For the enhancement of the N100 after low dosage tDCS, considering the effects of this protocol on the P60 amplitude, reduced glutamate seems to be the most likely cause. Therefore, it can be speculated that this specific low dosage tDCS is more selective for glutamate neurons, than for GABA, whereas with higher intensity tDCS protocols, GABA reduction would counteract the glutamate-reduction caused enhancement of the N100, resulting in no alterations of the N100 after medium and high dosage tDCS.

In comparison with the effects of motor tDCS, early positive TEP peaks were almost uniformly decreased following all prefrontal tDCS dosages. This might be explained by anatomical cytoarchitectonic, pharmacological and functional differences of these two areas [329, 330], which could result in a broader range of LTD induction in the prefrontal cortex. From a pharmacological point of view, dopamine is more

prevalent in the prefrontal cortex [331], and has been shown to strengthen cathodal tDCS-induced LTD-like plasticity; but converted anodal tDCS-induced LTP- to LTD-like plasticity [147]. Therefore, the higher amount of dopamine might have enhanced efficacy of cathodal tDCS-induced LTD-like plasticity relevantly in prefrontal areas, and prevented conversion effects into LTP-like plasticity. In addition, from a physical point of view, computational studies have shown that inter-electrode distance (iED; by affecting the amount of shunting current through the scalp), and scalp-to-cortex distance highly influence the tDCS-induced electrical field (EF) [59, 60, 332]. Here, with the same tDCS dosage applied over the motor, and prefrontal cortex, the lower iED and higher scalp-to-cortex distance in case of prefrontal stimulation [236, 238] might have resulted in lower prefrontal tDCS-induced EF over the targeted cortical area, and potentially therefore explains the missing effects of P30 after low dosage prefrontal tDCS, but also lack of prefrontal tDCS-induced plasticity conversion, compare to what was observed after increasing tDCS dosage over the motor cortex.

6.4.2. Limitations and future directions

In this study, we aimed to explore the transferability of regional effects of cathodal tDCS protocols from the primary motor cortex to a non-motor region. The investigation of whole brain effects was not within the scope of the present study, but will be tackled in future. In addition, we probed the neurophysiological effects of tDCS at the group level, but inter-individual variability has been shown to affect the outcome of tDCS and other NIBS protocols [43, 108]. In accordance, the data obtained in the present experiment show some variability, as can be seen in Figure 6.3 and Figure 6.4. Potential contributing factors are anatomical and biophysical differences of individual brains, genetics, age, gender, time of day, and brain state [109, 114, 149]. Thus, to improve stimulation efficacy at the level of the individual, an important next step would now be to understand/control for individual factors affecting the physiological and behavioral outcomes of tDCS [45].

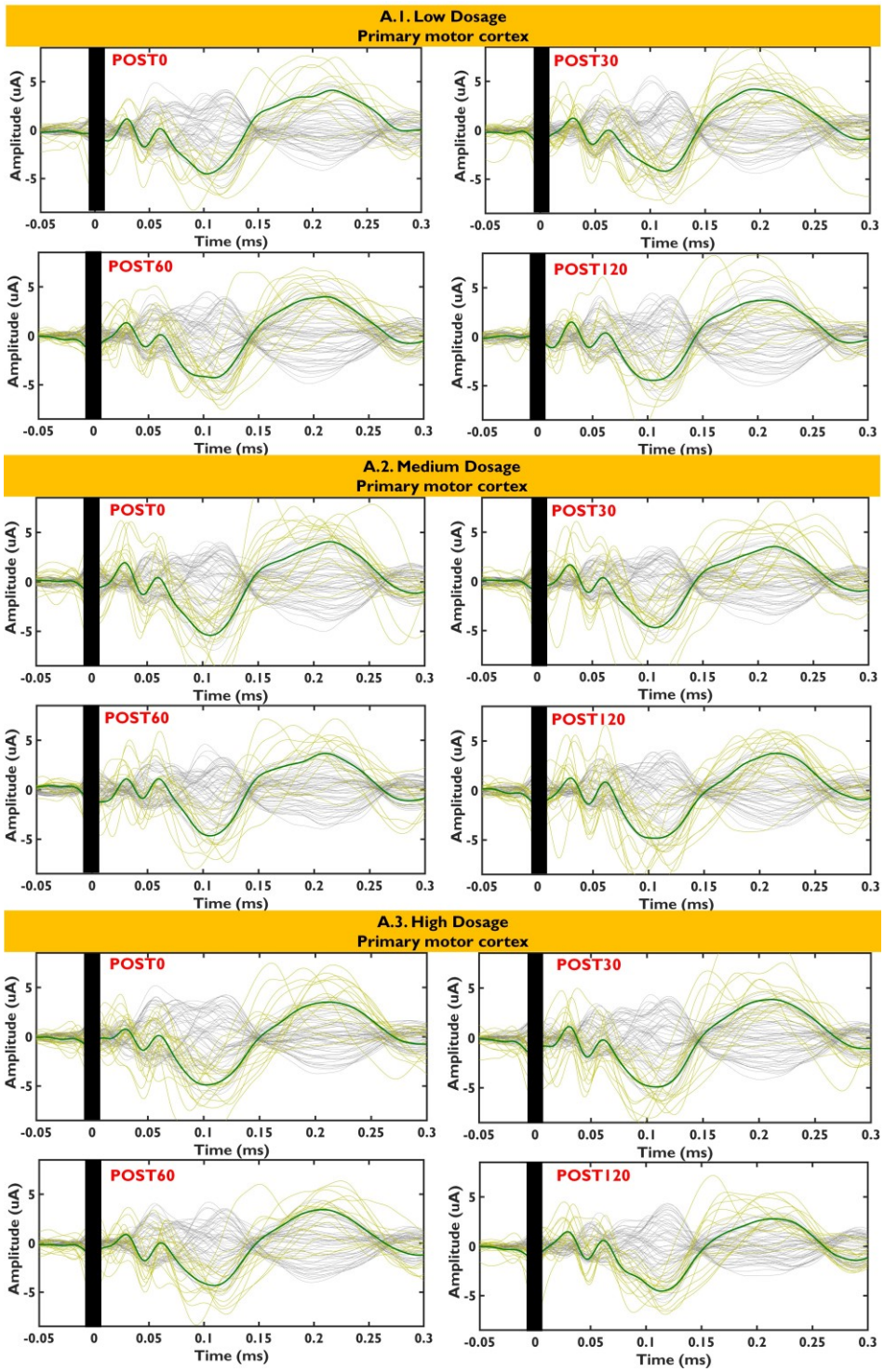

Figure 6.3. Individual TMS-evoked cortical reactivity after low, medium and high dosage of cathodal tDCS over the primary motor cortex. In each graph, the green line denotes averaged reactivity over the FC1 and CP1 electrodes used for ROI analyses, while each yellow trace is an individual TEP at the ROI, and the gray lines show activity over all electrodes, averaged across all subjects (n = 18) at the respective time point. POST0, POST30, POST60, POST120, are the TEP measures 0min, 30min, 60min, and 120min after tDCS.

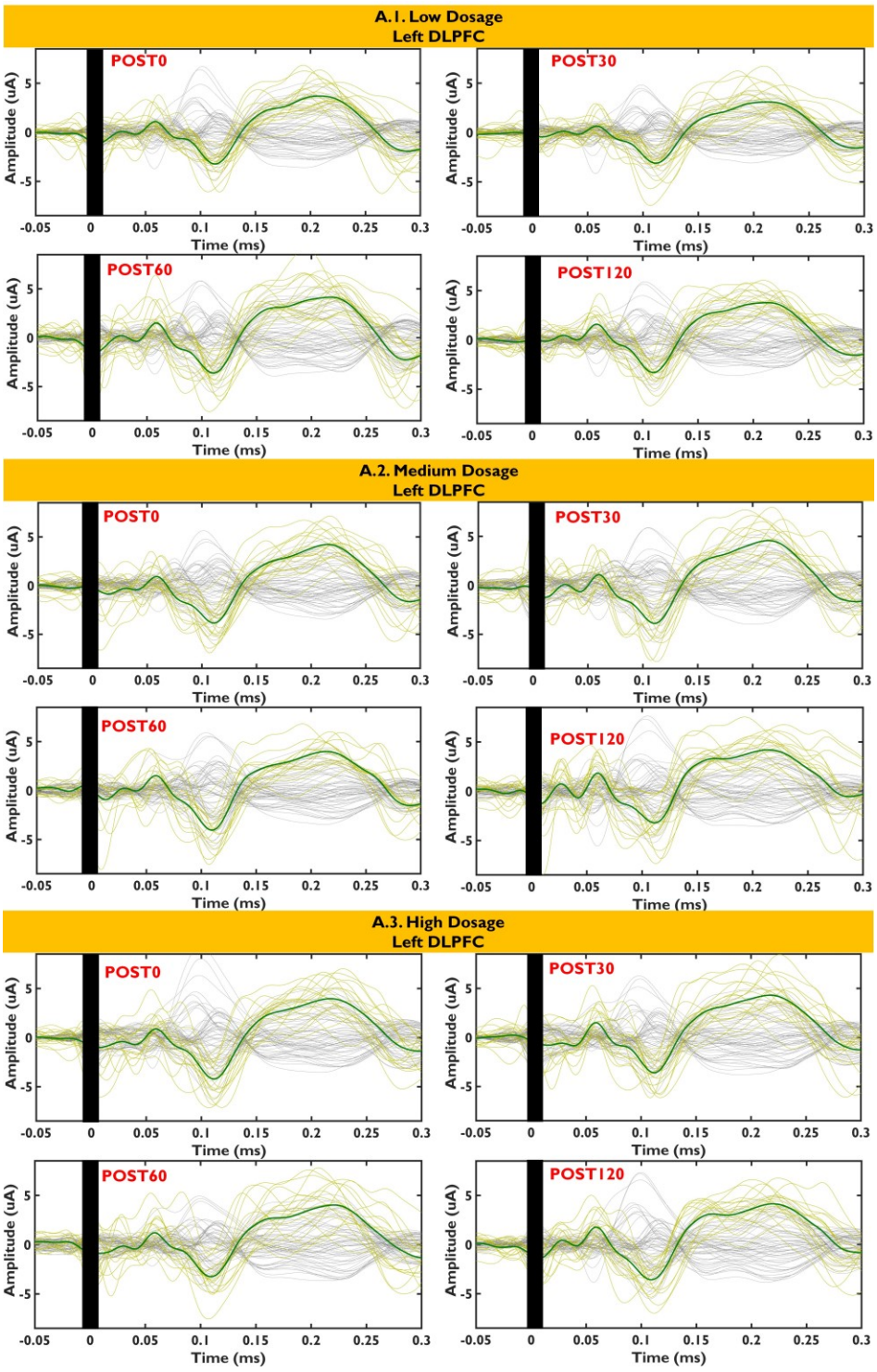

Figure 6.4. Individual TMS-evoked cortical reactivity after low, medium and high dosage of cathodal tDCS over the left DLPFC. In each graph, the green line denotes the averaged reactivity over the FC1 and Fz electrodes used for ROI analyses, while each yellow trace is an individual TEP at the ROI, and the gray lines show activity over all electrodes, averaged across all subjects (n = 18) at the respective time point. POST0, POST30, POST60, POST120, are the TEP measures 0min, 30min, 60min, and 120min after tDCS.

Furthermore, the neurophysiological data obtained in this study, which were based on healthy young participants, might not be one-to-one transferable to other cortical areas, other populations, as well as task-based motor or prefrontal tDCS applications. Moreover, the physiological effects of tDCS are not only determined by stimulation duration and intensity, but also by repetition intervals [68, 184], and electrode configuration [272], amongst other factors, which were beyond the scope of the present study, but might be important for shaping optimal stimulation protocols in future. Furthermore, the different effects obtained by prefrontal and motor cortex stimulation, as identified in this study, should be carefully evaluated in future studies, as it is not clear if these are due to biological differences between respective areas, or different current density at the cortical level, due to anatomical differences. Further work, including computational modeling, might help to clarify this issue.

6.5. Conclusion

The results of this study show modulatory effects of motor cortex tDCS on TMS-evoked cortical reactivity, which are comparable to respective cortico-spinal excitability effects, measured by TMS-MEP. Low- and high-dosage motor cortex tDCS reduced early positive TEP peak and MEP amplitudes, whereas an amplitude enhancement was observed for the medium dosage of motor cortex tDCS. In contrast, prefrontal low-, medium- and high-dosage tDCS almost uniformly reduced the early positive TEP peak amplitudes. Furthermore, over both cortical areas, neuromodulatory effects of tDCS were not observed for late TEP peaks (except for low-dosage prefrontal tDCS), and TMS-evoked oscillations. The specific differences of the effects of tDCS might be related to physiological, anatomical and pharmacological differences of motor and non-motor areas. The overall results provide the first direct comparison of tDCS effects on different brain areas at the physiological level, which will further consolidate the rationale for the extension of tDCS applications at both, basic and clinical levels.

7 Summary and Outlook

In this section, we first summarize the main outcomes of the conducted studies, and at the end, we will provide suggestions for future research directions.

7.1. Summary

The main goal of this thesis was to address the current challenge regarding the limited neuroplastic efficacy of cathodal tDCS, aiming to empower cathodal tDCS outcome. To this end, from the infinite parameter space, we selected electrical current intensity, duration and repetition rate, and then manipulated these factors to test if they can increase tDCS-induced neuroplastic after-effects. We further addressed the Ca^{2+} dependency of cathodal tDCS-induced neuroplastic effects, aiming to explain the observed stimulation dosage-dependent nonlinearity, which might be another source of limited/heterogeneous efficacy. It has been moreover shown that the effects of tDCS are restricted by the inter-individual physical variability. We therefore investigated, by a computational modeling approach, whether and to which extent the neurophysiological outcome of tDCS, at the individual level, can be explained by considering individual physical factors, which affect the tDCS-induced electrical field and therefore potentially its neuroplastic effects. In addition, the target region of the aforementioned studies was the primary motor cortex, much less is however known for its effects over the prefrontal cortex, which is associated with executive functions, including working memory and selective attention, and an important area for clinical application of brain stimulation. We thus finally explored the transferability of motor cortex cathodal tDCS-induced neuroplasticity results to the prefrontal cortex. In what follows, we give, based on each study, an overview of these findings.

Study 1: Titrating the neuroplastic effects of cathodal transcranial direct current stimulation (tDCS) over the primary motor cortex

> **Background:** clinical applications of tDCS with encouraging results have been reported in several pilot studies, but optimal stimulation protocols remain to be determined. This is also important because the efficacy and directionality of tDCS effects follow non-linear rules regarding neuroplastic effects for the stimulation parameters duration and intensity.
>
> **Method:** in this study, we systemically explored the association between tDCS, these parameters and induced after-effects on motor cortex excitability. Cathodal tDCS was applied at four different intensities (sham, 1, 2 and 3mA),

and three durations (15, 20 and 30mins) in 16 young healthy subjects and the after-effects were monitored with TMS-induced MEP until the next day evening after stimulation.

Results: the statistical results conducted to disentangle the effects of tDCS intensity and duration show a main effect of intensity, in which 1 mA and 3 mA stimulation intensities induced a reduction of MEP amplitudes, but 2 mA resulted in an excitability enhancement. In addition, the statistical results conducted to compare if active stimulation effects differ from those of sham stimulation revealed a significant main effect of tDCS condition, in which stimulation with 1 mA for 15 min, and 1 mA for 30 min induced a significant MEP amplitude diminution, while stimulation with 2 mA for 20 min resulted in a significant cortico-spinal excitability enhancement. Protocols with higher stimulation intensity (specifically stimulation with 3 mA for 20 min) induced again a significant excitability diminution lasting for about one and half hour after stimulation, and thus were more efficient than the other protocols.

Conclusions: our study thus provides further insights on the dependency of tDCS -induced neuroplasticity from specific stimulation parameters, and therefore delivers crucial information for future applications.

Study 2: Probing the relevance of repeated cathodal tDCS over the primary motor cortex for prolongation of after-effects

Background: tDCS has promising results in pilot studies as therapeutic intervention in disorders of the central nervous system, more sustained effects are however required for clinical application. To address this issue, one possible solution is the use of repeated stimulation protocols. Previous studies indicated the capability of extending single intervention-generated cathodal tDCS after-effects with repeated tDCS protocols, with a superiority of relatively short intervals.

Method: in this study, we thus investigated the effects of repeated stimulation protocols with short, and long intervals for a conventional (1mA for 15min) and an optimized tDCS protocol (3mA for 20min). In 16 healthy participants, we compared single interventions of conventional and optimized protocols with repeated application of these protocols with intervals of 20 min and 24 hours, and a sham tDCS session. tDCS-induced neuroplastic after-effects were then monitored with TMS-induced MEPs until the next day evening after stimulation.

Results: the results revealed that the duration of after-effects of repeated conventional and optimized protocols with short intervals remained nearly unchanged, as compared to the respective single intervention protocols. For the long interval (24 h), stimulation with the conventional protocol did not significantly alter respective after-effects, while it reduced the efficacy of the optimized protocol, as compared with respective single interventions. Thus late-phase plasticity could not be induced by a single repetition of stimulation in this study, but repetition reduced the efficacy of stimulation protocols with higher intensities.

Conclusions: this study provides further insights on the dependency of tDCS-induced neuroplasticity from stimulation parameters, and therefore delivers crucial information for future tDCS applications.

Study 3: Ca2+ channel dynamics explain the nonlinear neuroplasticity induction by cathodal transcranial direct current stimulation over the primary motor cortex

Background: tDCS induces polarity-dependent neuroplasticity: with conventional protocols, anodal tDCS results in excitability enhancement while cathodal stimulation reduces excitability. However, partially non-linear responses are observed with increased stimulation intensity and/or duration. Cathodal tDCS with 2mA for 20min reverses the excitability-diminishing plasticity induced by stimulation with 1mA into excitation, while cathodal tDCS with 3mA again results in excitability diminution. Since tDCS generates NMDA receptor-dependent neuroplasticity, such non-linearity could be explained by different levels of calcium concentration changes, which have been demonstrated in animal models to control for the directionality of plasticity.

Method: in this study, we tested the calcium dependency of non-linear cortical plasticity induced by cathodal tDCS in human subjects in a placebo controlled, double-blind and randomized design. The calcium channel blocker flunarizine was applied in low (2.5 mg), medium (5 mg) or high (10 mg) dosages before 20min cathodal motor cortex tDCS with 3mA in 12 young healthy subjects. After-effects of stimulation were monitored with TMS-induced MEPs until 2 hours after stimulation.

Results: the results show that motor cortical excitability-diminishing after-effects of stimulation were unchanged, diminished, or converted to excitability enhancement with low, medium and high dosages of flunarizine.

Conclusion: These results suggest a calcium-dependency of the directionality of tDCS-induced neuroplasticity, which may have relevant implications for future basic and clinical research.

Study 4: A Comprehensive Study of the Association Between Individual Electrical Field and Anatomical Factors on the Neurophysiological Outcomes of tDCS: a TMS-MEP and MRI Study

Background: tDCS has shown promising results in basic and clinical studies. The known interindividual variability of the effects restrict however the efficacy of the technique. Recently we reported neurophysiological effects of tDCS applied over the primary motor cortex at the group level, based on data from twenty-nine participants, who received 15min of either sham, 0.5, 1.0, 1.5 or 2.0 mA anodal, or cathodal tDCS. The neurophysiological effects were evaluated via changes in: 1) TMS-MEP, and 2) cerebral blood flow (CBF) measured by functional magnetic resonance imaging (MRI) via arterial spin labeling (ASL). At the group level, dosage-dependent effects of the intervention were obtained, which showed however interindividual variability.

Method: In this study, we investigated the cause of the observed inter-individual variability. To this end, for each participant, a MRI-based realistic head model was designed to 1) calculate anatomical factors and 2) simulate the tDCS- and TMS-induced electrical fields (EF). We then investigated at the regional level which individual anatomical factors explain the simulated EFs (strength and normal component). Finally, we explored which specific anatomical and/or EF factors predicted the neurophysiological outcomes of tDCS.

Results: The results showed a significant negative correlation between electrode to cortex distance (ECD), and CSF thickness, and the individual EFs. In addition, CSF thickness, and ECD were negatively correlated, whereas EFs were positively correlated with tDCS-induced physiological changes.

Conclusion: These results provide novel insights into the dependency of the neuromodulatory effects of tDCS from individual physical factors.

Study 5: Transferability of tDCS effects from the primary motor to the prefrontal cortex: a multimodal TMS-EEG study

Background: Neurophysiological effects of transcranial direct current stimulation (tDCS) have been extensively studied over the primary motor cortex. Much less is however known for its effects over non-motor areas, such as the prefrontal cortex, which is the neuronal foundation for many high-level cognitive functions, and involved in neuropsychiatric disorders.

Method: In this study eighteen healthy participants were involved in eight randomized sessions, in which four cathodal tDCS dosages, low, medium, and high, as well as sham stimulation, were applied over the primary motor and dorsolateral prefrontal cortex. After-effects of tDCS were evaluated via transcranial magnetic stimulation (TMS)-electroencephalography (EEG), and TMS-elicited motor evoked potentials (MEP) at the regional level, for the outcome parameters TMS-evoked potentials (TEP), TMS-evoked oscillations, and MEP amplitude alterations.

Results: The results indicate a dosage-dependent nonlinear neurophysiological effect of motor cortex tDCS, which is not one-to-one transferable to prefrontal tDCS. Low and high dosages of motor cortex tDCS reduced early positive TEP peaks (P30, P60), and MEP amplitudes, while an enhancement was observed for medium dosage motor cortex tDCS (P30 and MEP amplitudes). In contrast, prefrontal low, medium and high dosage tDCS uniformly reduced the early positive TEP peak amplitudes. Furthermore, for both cortical areas, tDCS-induced neuromodulatory effects were not observed for late TEP peaks (with the exception of low-dosage prefrontal tDCS), nor TMS-evoked oscillations.

Conclusion: This study provides the first direct physiological comparison of tDCS effects applied over different brain areas, and therefore delivers crucial information for future tDCS applications.

In summary, we showed that manipulating stimulation intensity and duration can enhance neuroplastic effects induced by cathodal tDCS over the motor cortex, but results also in stimulation dosage-dependent nonlinearity at the group level, with

relevant interindividual variability of the outcome. In addition, we showed that repetition with an intensified protocol might potentially decrease the after effects of cathodal tDCS over the motor cortex. Moreover, we showed that the nonlinear intensity-dependent after-effects of stimulation can be explained by calcium channel dynamics. Furthermore, computational approaches revealed that individual anatomical factors and tDCS-induced EFs can help to explain the inter-individual variability of tDCS effects. Finally, we showed that the observed dosage-dependent nonlinear neurophysiological effect of motor cortex tDCS was not one-to-one transferable to prefrontal tDCS.

7.2. Outlook

The results of the studies included in this thesis should be interpreted within the context of some limitations, which should be considered in future studies. ***First***, we explored only the intensity, duration and repetition rate of cathodal tDCS, for the aim to enhance its efficacy, over only primary motor cortex. However, brain regions do not operate in isolation, but interact with other regions through networks. Accordingly, a new multifocal tDCS protocol targeting the resting state motor network, showed promising results for enhancing tDCS effects [272]. Therefore, a promising way of enhancing stimulation efficacy might be the use of multisite network-based stimulation, which might be considered in future studies. ***Second***, the neurophysiological and computational data obtained in this thesis which were based on healthy young participants, might not be one-to-one transferable to task-based tDCS applications, and to other cortical areas as well as different age populations and patient groups, and should therefore be directly tested with respect to these parameters. ***Third***, we showed that calcium channel dynamics are involved in the non-linear after-effects of high intensity cathodal motor tDCS. However, detailed mechanisms of this nonlinearity are largely unexplored, but might be important for the informed development of more efficient stimulation protocols, and should be explored in future studies. ***Fourth***, we used a well-stablished computational modeling pipeline to simulate tDCS-induced EF, which has been shown to correlate with in-vivo intra-cranial EF recordings [187]. However, despite increasing sophistication of simulation techniques for the estimation of individual current distribution achieved by tDCS, that support the usefulness of individualized head models, this approach showed high sensitivity to modeling differences in the pipelines [46], including the addition of other relevant head tissues [256, 333], as well as individual head tissue electrical conductivity characteristics [56], leading to notable differences in the simulated tDCS-induced EF

that might be large enough to change the results regarding the dose distribution or strength in the brain. In this line, important progress has been made over the last few years in the field of MR-based current density imaging (MRCDI), which makes it now possible to reconstruct current density distributions in the human body using the weak current injection MRI technique [252]. This tool might be considered to improve the accuracy of modeling results via physical validation of simulations, which is crucial for the aim to adapt stimulation parameters, including electric field dose and electrode montage at the level of the individual to achieve inter-individually similar, and/or optimized neurophysiological or behavioral effects. ***Fifth***, our results showed a strong correlation between individual anatomical and electrical field factors, and tDCS-generated neurophysiological responses. An important next step would now be to test if modeling-based individual dosage adjustment can reduce interindividual variability, leading to more homogeneous and sustained effects of stimulation, across individuals. ***Finally***, we, throughout the thesis, mainly focused on regional effects of tDCS, but not on distributed/network effects; considering these in future studies might further improve our understanding of intervention effects.

List of Figures

List of Tables

Glossary of Acronyms

MDD major depression disorder

NIBS non-invasive brain stimulation

tDCS transcranial direct current stimulation

TMS transcranial magnetic stimulation

EEG electroencephalography

MRI magnetic resonance imaging

MRS magnetic resonance spectroscopy

fMRI functional magnetic resonance imaging

ASL arterial spin label

SICI short-interval intracortical inhibition

ICF intracortical facilitation

MSO maximum stimulator output

EF electrical field

FEM finite element method

M1 primary motor cortex

DLPFC dorsolateral prefrontal cortex

CSF cerebrospinal fluid

GM gray matter

WM white matter

MEP motor evoked potential

CBF cerebral blood flow

TEP transcranial evoked potential

FLU flunarizine

NMDA N-methyl-D-aspartate

AMPA α-amino-3-hydroxy-5-methyl-4-isoxazolepropionic acid

ECD electrode-to-cortex distance

ROI region of interest

HK hand motor knob

Bibliography

[1] H. U. Wittchen, F. Jacobi, J. Rehm, A. Gustavsson, M. Svensson, B. Jönsson, J. Olesen, C. Allgulander, J. Alonso, C. Faravelli, L. Fratiglioni, P. Jennum, R. Lieb, A. Maercker, J. van Os, M. Preisig, L. Salvador-Carulla, R. Simon, and H. C. Steinhausen, "The size and burden of mental disorders and other disorders of the brain in Europe 2010," *Eur Neuropsychopharmacol,* vol. 21, no. 9, pp. 655-79, Sep, 2011.

[2] J. Zimmermann, A. Wolter, N. R. Krischke, U. W. Preuss, T. Wobrock, and P. Falkai, "[Response and remission in schizophrenic subjects]," *Nervenarzt,* vol. 82, no. 11, pp. 1440-8, Nov, 2011.

[3] S. M. Hendriks, J. Spijker, C. M. Licht, A. T. Beekman, and B. W. Penninx, "Two-year course of anxiety disorders: different across disorders or dimensions?," *Acta Psychiatr Scand,* vol. 128, no. 3, pp. 212-21, Sep, 2013.

[4] M. B. Keller, G. L. Klerman, P. W. Lavori, W. Coryell, J. Endicott, and J. Taylor, "Long-term outcome of episodes of major depression. Clinical and public health significance," *Jama,* vol. 252, no. 6, pp. 788-92, Aug 10, 1984.

[5] F. Fregni, and A. Pascual-Leone, "Technology insight: noninvasive brain stimulation in neurology-perspectives on the therapeutic potential of rTMS and tDCS," *Nat Clin Pract Neurol,* vol. 3, no. 7, pp. 383-93, Jul, 2007.

[6] D. Edwards, H. Krebs, A. Rykman, J. Zipse, G. Thickbroom, F. Mastaglia, A. Pascual-Leone, and B. Volpe, "Raised corticomotor excitability of M1 forearm area following anodal tDCS is sustained during robotic wrist therapy in chronic stroke," *Restorative Neurology and Neuroscience,* vol. 27, no. 3, pp. 199-207, 2009.

[7] S. C. Cramer, "Repairing the human brain after stroke. II. Restorative therapies," *Ann Neurol,* vol. 63, no. 5, pp. 549-60, May, 2008.

[8] S. C. Cramer, "Changes in motor system function and recovery after stroke," *Restor Neurol Neurosci,* vol. 22, no. 3-5, pp. 231-8, 2004.

[9] F. Fregni, D. K. Simon, A. Wu, and A. Pascual-Leone, "Non-invasive brain stimulation for Parkinson's disease: a systematic review and meta-analysis of the literature," *J Neurol Neurosurg Psychiatry,* vol. 76, no. 12, pp. 1614-23, Dec, 2005.

[10] W. H. Organization, *Prevention of mental disorders: Effective interventions and policy options: Summary report*: World Health Organization, 2004.

[11] M.-S. Rioult-Pedotti, D. Friedman, and J. P. Donoghue, "Learning-induced LTP in neocortex," *Science,* vol. 290, no. 5491, pp. 533-536, 2000.

[12] R. C. Malenka, and M. F. Bear, "LTP and LTD: an embarrassment of riches," *Neuron,* vol. 44, no. 1, pp. 5-21, 2004.

[13] A. R. Brunoni, L. Valiengo, A. Baccaro, T. A. Zanão, J. F. de Oliveira, A. Goulart, P. S. Boggio, P. A. Lotufo, I. M. Benseñor, and F. Fregni, "The sertraline vs electrical current therapy for treating depression clinical study: results from a factorial, randomized, controlled trial," *JAMA Psychiatry,* vol. 70, no. 4, pp. 383-391, 2013.

[14] K. D'Ostilio, and G. Garraux, "The network model of depression as a basis for new therapeutic strategies for treating major depressive disorder in Parkinson's disease," *Frontiers in Human Neuroscience,* vol. 10, 2016.

[15] D. G. Nair, S. Hutchinson, F. Fregni, M. Alexander, A. Pascual-Leone, and G. Schlaug, "Imaging correlates of motor recovery from cerebral infarction and their physiological significance in well-recovered patients," *Neuroimage,* vol. 34, no. 1, pp. 253-263, 2007.

[16] S. Grimm, J. Beck, D. Schuepbach, D. Hell, P. Boesiger, F. Bermpohl, L. Niehaus, H. Boeker, and G. Northoff, "Imbalance between left and right dorsolateral prefrontal cortex in major depression is

linked to negative emotional judgment: an fMRI study in severe major depressive disorder," *Biological Psychiatry,* vol. 63, no. 4, pp. 369-376, 2008.

[17] J. P. Lefaucheur, N. Andre-Obadia, A. Antal, S. S. Ayache, C. Baeken, D. H. Benninger, R. M. Cantello, M. Cincotta, M. de Carvalho, D. De Ridder, H. Devanne, V. Di Lazzaro, S. R. Filipovic, F. C. Hummel, S. K. Jaaskelainen, V. K. Kimiskidis, G. Koch, B. Langguth, T. Nyffeler, A. Oliviero, F. Padberg, E. Poulet, S. Rossi, P. M. Rossini, J. C. Rothwell, C. Schonfeldt-Lecuona, H. R. Siebner, C. W. Slotema, C. J. Stagg, J. Valls-Sole, U. Ziemann, W. Paulus, and L. Garcia-Larrea, "Evidence-based guidelines on the therapeutic use of repetitive transcranial magnetic stimulation (rTMS)," *Clin Neurophysiol,* vol. 125, no. 11, pp. 2150-2206, Nov, 2014.

[18] J. P. Lefaucheur, A. Antal, S. S. Ayache, D. H. Benninger, J. Brunelin, F. Cogiamanian, M. Cotelli, D. De Ridder, R. Ferrucci, B. Langguth, P. Marangolo, V. Mylius, M. A. Nitsche, F. Padberg, U. Palm, E. Poulet, A. Priori, S. Rossi, M. Schecklmann, S. Vanneste, U. Ziemann, L. Garcia-Larrea, and W. Paulus, "Evidence-based guidelines on the therapeutic use of transcranial direct current stimulation (tDCS)," *Clin Neurophysiol,* vol. 128, no. 1, pp. 56-92, Jan, 2017.

[19] M. A. Nitsche, and W. Paulus, "Excitability changes induced in the human motor cortex by weak transcranial direct current stimulation," *The Journal of Physiology,* vol. 527, no. 3, pp. 633-639, 2000.

[20] M. A. Nitsche, and W. Paulus, "Sustained excitability elevations induced by transcranial DC motor cortex stimulation in humans," *Neurology,* vol. 57, no. 10, pp. 1899-1901, 2001.

[21] M.-F. Kuo, P.-S. Chen, and M. A. Nitsche, "The application of tDCS for the treatment of psychiatric diseases," *International Review of Psychiatry,* vol. 29, no. 2, pp. 146-167, 2017.

[22] F. Yavari, A. Jamil, M. Mosayebi Samani, L. P. Vidor, and M. A. Nitsche, "Basic and functional effects of transcranial Electrical Stimulation (tES)—An introduction," *Neuroscience & Biobehavioral Reviews,* vol. 85, pp. 81-92, 2018/02/01/, 2018.

[23] S. T. Grafton, J. C. Mazziotta, S. Presty, K. J. Friston, R. S. Frackowiak, and M. E. Phelps, "Functional anatomy of human procedural learning determined with regional cerebral blood flow and PET," *J Neurosci,* vol. 12, no. 7, pp. 2542-8, Jul, 1992.

[24] R. D. Seidler, "Neural correlates of motor learning, transfer of learning, and learning to learn," *Exerc Sport Sci Rev,* vol. 38, no. 1, pp. 3-9, Jan, 2010.

[25] J. Reis, H. M. Schambra, L. G. Cohen, E. R. Buch, B. Fritsch, E. Zarahn, P. A. Celnik, and J. W. Krakauer, "Noninvasive cortical stimulation enhances motor skill acquisition over multiple days through an effect on consolidation," *Proceedings of the National Academy of Sciences,* vol. 106, no. 5, pp. 1590-1595, 2009.

[26] J. Reis, and B. Fritsch, "Modulation of motor performance and motor learning by transcranial direct current stimulation," *Current Opinion in Neurology,* vol. 24, no. 6, pp. 590-596, 2011.

[27] C. J. Stagg, G. Jayaram, D. Pastor, Z. T. Kincses, P. M. Matthews, and H. Johansen-Berg, "Polarity and timing-dependent effects of transcranial direct current stimulation in explicit motor learning," *Neuropsychologia,* vol. 49, no. 5, pp. 800-804, 2011/04/01/, 2011.

[28] M. A. Nitsche, A. Schauenburg, N. Lang, D. Liebetanz, C. Exner, W. Paulus, and F. Tergau, "Facilitation of implicit motor learning by weak transcranial direct current stimulation of the primary motor cortex in the human," *Journal of Cognitive Neuroscience,* vol. 15, no. 4, pp. 619-626, 2003.

[29] F. Dolcos, K. S. LaBar, and R. Cabeza, "Dissociable effects of arousal and valence on prefrontal activity indexing emotional evaluation and subsequent memory: an event-related fMRI study," *NeuroImage,* vol. 23, no. 1, pp. 64-74, 2004/09/01/, 2004.

[30] F. M. Mottaghy, B. J. Krause, L. J. Kemna, R. Töpper, L. Tellmann, M. Beu, A. Pascual-Leone, and H. W. Müller-Gärtner, "Modulation of the neuronal circuitry subserving working memory in

healthy human subjects by repetitive transcranial magnetic stimulation," *Neurosci Lett,* vol. 280, no. 3, pp. 167-70, Feb 25, 2000.

[31] B. R. Mull, and M. Seyal, "Transcranial magnetic stimulation of left prefrontal cortex impairs working memory," *Clinical Neurophysiology,* vol. 112, no. 9, pp. 1672-1675, 2001.

[32] M. Nitsche, J. Koschack, H. Pohlers, S. Hullemann, W. Paulus, and S. Happe, "Effects of Frontal Transcranial Direct Current Stimulation on Emotional State and Processing in Healthy Humans," *Frontiers in Psychiatry,* vol. 3, no. 58, 2012-June-18, 2012.

[33] A. Mungee, P. Kazzer, M. Feeser, M. A. Nitsche, D. Schiller, and M. Bajbouj, "Transcranial direct current stimulation of the prefrontal cortex: a means to modulate fear memories," *Neuroreport,* vol. 25, no. 7, pp. 480-484, 2014.

[34] K. E. Hoy, M. R. L. Emonson, S. L. Arnold, R. H. Thomson, Z. J. Daskalakis, and P. B. Fitzgerald, "Testing the limits: Investigating the effect of tDCS dose on working memory enhancement in healthy controls," *Neuropsychologia,* vol. 51, no. 9, pp. 1777-1784, 2013/08/01/, 2013.

[35] E. A. Karuza, Z. Z. Balewski, R. H. Hamilton, J. D. Medaglia, N. Tardiff, and S. L. Thompson-Schill, "Mapping the Parameter Space of tDCS and Cognitive Control via Manipulation of Current Polarity and Intensity," *Frontiers in Human Neuroscience,* vol. 10, no. 665, 2016-December-27, 2016.

[36] F. Fregni, P. S. Boggio, C. G. Mansur, T. Wagner, M. J. Ferreira, M. C. Lima, S. P. Rigonatti, M. A. Marcolin, S. D. Freedman, and M. A. Nitsche, "Transcranial direct current stimulation of the unaffected hemisphere in stroke patients," *Neuroreport,* vol. 16, no. 14, pp. 1551-1555, 2005.

[37] F. Hummel, P. Celnik, P. Giraux, A. Floel, W.-H. Wu, C. Gerloff, and L. G. Cohen, "Effects of non-invasive cortical stimulation on skilled motor function in chronic stroke," *Brain,* vol. 128, no. 3, pp. 490-499, 2005.

[38] P. S. Boggio, R. Ferrucci, S. P. Rigonatti, P. Covre, M. Nitsche, A. Pascual-Leone, and F. Fregni, "Effects of transcranial direct current stimulation on working memory in patients with Parkinson's disease," *J Neurol Sci,* vol. 249, no. 1, pp. 31-8, Nov 1, 2006.

[39] P. S. Boggio, S. P. Rigonatti, R. B. Ribeiro, M. L. Myczkowski, M. A. Nitsche, A. Pascual-Leone, and F. Fregni, "A randomized, double-blind clinical trial on the efficacy of cortical direct current stimulation for the treatment of major depression," *International Journal of Neuropsychopharmacology,* vol. 11, no. 2, pp. 249-254, 2008.

[40] C. Andrade, "Transcranial direct current stimulation for refractory auditory hallucinations in schizophrenia," *J Clin Psychiatry,* vol. 74, no. 11, pp. e1054-8, Nov, 2013.

[41] P. Shiozawa, A. P. Leiva, C. D. Castro, M. E. da Silva, Q. Cordeiro, F. Fregni, and A. R. Brunoni, "Transcranial direct current stimulation for generalized anxiety disorder: a case study," *Biol Psychiatry,* vol. 75, no. 11, pp. e17-8, Jun 1, 2014.

[42] E. M. Khedr, N. F. E. Gamal, N. A. El-Fetoh, H. Khalifa, E. M. Ahmed, A. M. Ali, M. Noaman, A. A. El-Baki, and A. A. Karim, "A double-blind randomized clinical trial on the efficacy of cortical direct current stimulation for the treatment of Alzheimer's disease," *Frontiers in aging neuroscience,* vol. 6, pp. 275-275, 2014.

[43] S. Wiethoff, M. Hamada, and J. C. Rothwell, "Variability in response to transcranial direct current stimulation of the motor cortex," *Brain Stimulation,* vol. 7, no. 3, pp. 468-475, 2014.

[44] W. Strube, T. Bunse, M. A. Nitsche, A. Nikolaeva, U. Palm, F. Padberg, P. Falkai, and A. Hasan, "Bidirectional variability in motor cortex excitability modulation following 1 mA transcranial direct current stimulation in healthy participants," *Physiological reports,* vol. 4, no. 15, pp. e12884, 2016.

[45] Y. Z. Huang, M. K. Lu, A. Antal, J. Classen, M. Nitsche, U. Ziemann, M. Ridding, M. Hamada, Y. Ugawa, S. Jaberzadeh, A. Suppa, W. Paulus, and J. Rothwell, "Plasticity induced by non-invasive

transcranial brain stimulation: A position paper," *Clin Neurophysiol,* vol. 128, no. 11, pp. 2318-2329, Nov, 2017.

[46] O. Puonti, G. B. Saturnino, K. H. Madsen, and A. Thielscher, "Value and limitations of intracranial recordings for validating electric field modeling for transcranial brain stimulation," *NeuroImage,* vol. 208, pp. 116431, 2020/03/01/, 2020.

[47] G. Ruffini, F. Wendling, I. Merlet, B. Molaee-Ardekani, A. Mekonnen, R. Salvador, A. Soria-Frisch, C. Grau, S. Dunne, and P. C. Miranda, "Transcranial current brain stimulation (tCS): models and technologies," *IEEE Trans Neural Syst Rehabil Eng,* vol. 21, no. 3, pp. 333-45, May, 2013.

[48] P. C. Miranda, M. A. Callejón-Leblic, R. Salvador, and G. Ruffini, "Realistic modeling of transcranial current stimulation: The electric field in the brain," *Current Opinion in Biomedical Engineering,* vol. 8, pp. 20-27, 2018/12/01/, 2018.

[49] A. Y. Kabakov, P. A. Muller, A. Pascual-Leone, F. E. Jensen, and A. Rotenberg, "Contribution of axonal orientation to pathway-dependent modulation of excitatory transmission by direct current stimulation in isolated rat hippocampus," *J Neurophysiol,* vol. 107, no. 7, pp. 1881-9, Apr, 2012.

[50] A. Rahman, D. Reato, M. Arlotti, F. Gasca, A. Datta, L. C. Parra, and M. Bikson, "Cellular effects of acute direct current stimulation: somatic and synaptic terminal effects," *J Physiol,* vol. 591, no. 10, pp. 2563-78, May 15, 2013.

[51] A. Rahman, B. Lafon, L. C. Parra, and M. Bikson, "Direct current stimulation boosts synaptic gain and cooperativity in vitro," *The Journal of Physiology,* vol. 595, no. 11, pp. 3535-3547, 2017.

[52] F. Fröhlich, and D. A. McCormick, "Endogenous electric fields may guide neocortical network activity," *Neuron,* vol. 67, no. 1, pp. 129-143, 2010.

[53] D. Reato, A. Rahman, M. Bikson, and L. C. Parra, "Low-intensity electrical stimulation affects network dynamics by modulating population rate and spike timing," *J Neurosci,* vol. 30, no. 45, pp. 15067-79, Nov 10, 2010.

[54] A. Llera, T. Wolfers, P. Mulders, and C. F. Beckmann, "Inter-individual differences in human brain structure and morphology link to variation in demographics and behavior," *eLife,* vol. 8, pp. e44443, 2019/07/03, 2019.

[55] M. L. Seghier, and C. J. Price, "Interpreting and Utilising Intersubject Variability in Brain Function," *Trends in Cognitive Sciences,* vol. 22, no. 6, pp. 517-530, 2018.

[56] H. McCann, G. Pisano, and L. Beltrachini, "Variation in Reported Human Head Tissue Electrical Conductivity Values," *Brain Topography*, 2019/05/03, 2019.

[57] S. I. Gonçalves, J. C. de Munck, J. P. Verbunt, F. Bijma, R. M. Heethaar, and F. Lopes da Silva, "In vivo measurement of the brain and skull resistivities using an EIT-based method and realistic models for the head," *IEEE Trans Biomed Eng,* vol. 50, no. 6, pp. 754-67, Jun, 2003.

[58] A. V. Peterchev, T. A. Wagner, P. C. Miranda, M. A. Nitsche, W. Paulus, S. H. Lisanby, A. Pascual-Leone, and M. Bikson, "Fundamentals of transcranial electric and magnetic stimulation dose: definition, selection, and reporting practices," *Brain stimulation,* vol. 5, no. 4, pp. 435-453, 2012.

[59] I. Laakso, S. Tanaka, S. Koyama, V. De Santis, and A. Hirata, "Inter-subject Variability in Electric Fields of Motor Cortical tDCS," *Brain Stimul,* vol. 8, no. 5, pp. 906-13, Sep-Oct, 2015.

[60] A. Opitz, W. Paulus, S. Will, A. Antunes, and A. Thielscher, "Determinants of the electric field during transcranial direct current stimulation," *Neuroimage,* vol. 109, pp. 140-50, Apr 1, 2015.

[61] M. Mikkonen, I. Laakso, M. Sumiya, S. Koyama, A. Hirata, and S. Tanaka, "TMS Motor Thresholds Correlate With TDCS Electric Field Strengths in Hand Motor Area," *Frontiers in Neuroscience,* vol. 12, no. 426, 2018-June-25, 2018.

[62] I. Laakso, M. Mikkonen, S. Koyama, A. Hirata, and S. Tanaka, "Can electric fields explain inter-individual variability in transcranial direct current stimulation of the motor cortex?," *Scientific Reports,* vol. 9, no. 1, pp. 626, 2019/01/24, 2019.

[63] D. Antonenko, A. Thielscher, G. B. Saturnino, S. Aydin, B. Ittermann, U. Grittner, and A. Flöel, "Towards precise brain stimulation: Is electric field simulation related to neuromodulation?," *Brain Stimulation*, 2019/03/22/, 2019.

[64] G. Batsikadze, V. Moliadze, W. Paulus, M. F. Kuo, and M. Nitsche, "Partially non-linear stimulation intensity-dependent effects of direct current stimulation on motor cortex excitability in humans," *The Journal of Physiology,* vol. 591, no. 7, pp. 1987-2000, 2013.

[65] M. Mosayebi Samani, D. Agboada, A. Jamil, M.-F. Kuo, and M. A. Nitsche, "Titrating the neuroplastic effects of cathodal transcranial direct current stimulation (tDCS) over the primary motor cortex," *Cortex,* vol. 119, pp. 350-361, 2019/10/01/, 2019.

[66] K. Monte-Silva, M.-F. Kuo, D. Liebetanz, W. Paulus, and M. A. Nitsche, "Shaping the optimal repetition interval for cathodal transcranial direct current stimulation (tDCS)," *Journal of Neurophysiology,* vol. 103, no. 4, pp. 1735-1740, 2010.

[67] D. J. Kidgell, R. M. Daly, K. Young, J. Lum, G. Tooley, S. Jaberzadeh, M. Zoghi, and A. J. Pearce, "Different current intensities of anodal transcranial direct current stimulation do not differentially modulate motor cortex plasticity," *Neural Plasticity,* vol. 2013, 2013.

[68] M. Mosayebi Samani, D. Agboada, M. F. Kuo, and M. A. Nitsche, "Probing the relevance of repeated cathodal transcranial direct current stimulation over the primary motor cortex for prolongation of after-effects," *The Journal of Physiology,* vol. 598, no. 4, pp. 805-816, Feb, 2020.

[69] M. Hassanzahraee, M. A. Nitsche, M. Zoghi, and S. Jaberzadeh, "Determination of anodal tDCS duration threshold for reversal of corticospinal excitability: An investigation for induction of counter-regulatory mechanisms," *Brain Stimulation,* vol. 13, no. 3, pp. 832-839, 2020/05/01/, 2020.

[70] S. Weller, M. A. Nitsche, and C. Plewnia, "Cognitive control training and transcranial direct current stimulation: a systematic approach to optimisation," *Brain Stimulation*, 2020/07/18/, 2020.

[71] G. S. Shekhawat, and S. Vanneste, "Optimization of Transcranial Direct Current Stimulation of Dorsolateral Prefrontal Cortex for Tinnitus: A Non-Linear Dose-Response Effect," *Scientific Reports,* vol. 8, no. 1, pp. 8311, 2018/05/29, 2018.

[72] A. Antal, T. Z. Kincses, M. A. Nitsche, O. Bartfai, and W. Paulus, "Excitability changes induced in the human primary visual cortex by transcranial direct current stimulation: direct electrophysiological evidence," *Invest Ophthalmol Vis Sci,* vol. 45, no. 2, pp. 702-7, Feb, 2004.

[73] K. Matsunaga, M. A. Nitsche, S. Tsuji, and J. C. Rothwell, "Effect of transcranial DC sensorimotor cortex stimulation on somatosensory evoked potentials in humans," *Clin Neurophysiol,* vol. 115, no. 2, pp. 456-60, Feb, 2004.

[74] A. Dieckhöfer, T. D. Waberski, M. Nitsche, W. Paulus, H. Buchner, and R. Gobbelé, "Transcranial direct current stimulation applied over the somatosensory cortex – Differential effect on low and high frequency SEPs," *Clinical Neurophysiology,* vol. 117, no. 10, pp. 2221-2227, 2006/10/01/, 2006.

[75] A. Jamil, G. Batsikadze, H. I. Kuo, R. L. Meesen, P. Dechent, W. Paulus, and M. A. Nitsche, "Current intensity-and polarity-specific online and aftereffects of transcranial direct current stimulation: An fMRI study," *Human Brain Mapping*, 2019.

[76] E. Dayan, N. Censor, E. R. Buch, M. Sandrini, and L. G. Cohen, "Noninvasive brain stimulation: from physiology to network dynamics and back," *Nature Neuroscience,* vol. 16, no. 7, pp. 838-844, 2013.

[77] P. M. Rossini, and S. Rossi, "Transcranial magnetic stimulation Diagnostic, therapeutic, and research potential," *Neurology,* vol. 68, no. 7, pp. 484-488, 2007.

[78] A. Flöel, "tDCS-enhanced motor and cognitive function in neurological diseases," *Neuroimage,* vol. 85, pp. 934-947, 2014.

[79] M.-F. Kuo, W. Paulus, and M. A. Nitsche, "Therapeutic effects of non-invasive brain stimulation with direct currents (tDCS) in neuropsychiatric diseases," *Neuroimage,* vol. 85, pp. 948-960, 2014.

[80] P. B. Fitzgerald, K. Hoy, S. McQueen, J. J. Maller, S. Herring, R. Segrave, M. Bailey, G. Been, J. Kulkarni, and Z. J. Daskalakis, "A randomized trial of rTMS targeted with MRI based neuro-navigation in treatment-resistant depression," *Neuropsychopharmacology,* vol. 34, no. 5, pp. 1255, 2009.

[81] Z. J. Daskalakis, B. Möller, B. K. Christensen, P. B. Fitzgerald, C. Gunraj, and R. Chen, "The effects of repetitive transcranial magnetic stimulation on cortical inhibition in healthy human subjects," *Experimental Brain Research,* vol. 174, no. 3, pp. 403-412, 2006.

[82] K. Monte-Silva, M.-F. Kuo, S. Hessenthaler, S. Fresnoza, D. Liebetanz, W. Paulus, and M. A. Nitsche, "Induction of late LTP-like plasticity in the human motor cortex by repeated non-invasive brain stimulation," *Brain Stimulation,* vol. 6, no. 3, pp. 424-432, 2013.

[83] M. A. Nitsche, S. Doemkes, T. Karakose, A. Antal, D. Liebetanz, N. Lang, F. Tergau, and W. Paulus, "Shaping the effects of transcranial direct current stimulation of the human motor cortex," *Journal of Neurophysiology,* vol. 97, no. 4, pp. 3109-3117, 2007.

[84] C. J. Stagg, and M. A. Nitsche, "Physiological basis of transcranial direct current stimulation," *The Neuroscientist,* vol. 17, no. 1, pp. 37-53, 2011.

[85] M. A. Nitsche, L. G. Cohen, E. M. Wassermann, A. Priori, N. Lang, A. Antal, W. Paulus, F. Hummel, P. S. Boggio, and F. Fregni, "Transcranial direct current stimulation: state of the art 2008," *Brain Stimulation,* vol. 1, no. 3, pp. 206-223, 2008.

[86] C. J. Stagg, J. G. Best, M. C. Stephenson, J. O'Shea, M. Wylezinska, Z. T. Kincses, P. G. Morris, P. M. Matthews, and H. Johansen-Berg, "Polarity-sensitive modulation of cortical neurotransmitters by transcranial stimulation," *Journal of Neuroscience,* vol. 29, no. 16, pp. 5202-5206, 2009.

[87] R. Polanía, W. Paulus, and M. A. Nitsche, "Modulating cortico-striatal and thalamo-cortical functional connectivity with transcranial direct current stimulation," *Human Brain Mapping,* vol. 33, no. 10, pp. 2499-2508, 2012.

[88] X. Zheng, D. C. Alsop, and G. Schlaug, "Effects of transcranial direct current stimulation (tDCS) on human regional cerebral blood flow," *Neuroimage,* vol. 58, no. 1, pp. 26-33, 2011.

[89] A. Bastani, and S. Jaberzadeh, "Differential modulation of corticospinal excitability by different current densities of anodal transcranial direct current stimulation," *PLoS One,* vol. 8, no. 8, pp. e72254, 2013.

[90] K.-A. Ho, J. L. Taylor, T. Chew, V. Gálvez, A. Alonzo, S. Bai, S. Dokos, and C. K. Loo, "The effect of transcranial direct current stimulation (tDCS) electrode size and current intensity on motor cortical excitability: evidence from single and repeated sessions," *Brain Stimulation,* vol. 9, no. 1, pp. 1-7, 2016.

[91] R. Lindenberg, V. Renga, L. Zhu, D. Nair, and G. Schlaug, "Bihemispheric brain stimulation facilitates motor recovery in chronic stroke patients," *Neurology,* vol. 75, no. 24, pp. 2176-2184, 2010.

[92] F. Yavari, A. Jamil, M. M. Samani, L. P. Vidor, and M. A. Nitsche, "Basic and functional effects of transcranial Electrical Stimulation (tES)—An introduction," *Neuroscience & Biobehavioral Reviews*, 2017.

[93] R. C. Oldfield, "The assessment and analysis of handedness: the Edinburgh inventory," *Neuropsychologia,* vol. 9, no. 1, pp. 97-113, 1971.

[94] S. Rossi, M. Hallett, P. M. Rossini, A. Pascual-Leone, and S. o. T. C. Group, "Safety, ethical considerations, and application guidelines for the use of transcranial magnetic stimulation in clinical practice and research," *Clinical Neurophysiology,* vol. 120, no. 12, pp. 2008-2039, 2009.

[95] M. Bikson, P. Grossman, C. Thomas, A. L. Zannou, J. Jiang, T. Adnan, A. P. Mourdoukoutas, G. Kronberg, D. Truong, and P. Boggio, "Safety of transcranial direct current stimulation: evidence based update 2016," *Brain Stimulation,* vol. 9, no. 5, pp. 641-661, 2016.

[96] M. A. Nitsche, M. S. Nitsche, C. C. Klein, F. Tergau, J. C. Rothwell, and W. Paulus, "Level of action of cathodal DC polarisation induced inhibition of the human motor cortex," *Clinical Neurophysiology,* vol. 114, no. 4, pp. 600-604, 2003.

[97] J. L. McFadden, J. J. Borckardt, M. S. George, and W. Beam, "Reducing procedural pain and discomfort associated with transcranial direct current stimulation," *Brain Stimulation,* vol. 4, no. 1, pp. 38-42, 2011.

[98] A. Jamil, G. Batsikadze, H. I. Kuo, L. Labruna, A. Hasan, W. Paulus, and M. A. Nitsche, "Systematic evaluation of the impact of stimulation intensity on neuroplastic after-effects induced by transcranial direct current stimulation," *The Journal of Physiology,* vol. 595, no. 4, pp. 1273-1288, 2017.

[99] D. Liebetanz, M. A. Nitsche, F. Tergau, and W. Paulus, "Pharmacological approach to the mechanisms of transcranial DC-stimulation-induced after-effects of human motor cortex excitability," *Brain,* vol. 125, no. 10, pp. 2238-2247, 2002.

[100] M. A. Nitsche, D. Liebetanz, A. Schlitterlau, U. Henschke, K. Fricke, K. Frommann, N. Lang, S. Henning, W. Paulus, and F. Tergau, "GABAergic modulation of DC stimulation-induced motor cortex excitability shifts in humans," *European Journal of Neuroscience,* vol. 19, no. 10, pp. 2720-2726, 2004.

[101] J. E. Lisman, "Three Ca2+ levels affect plasticity differently: the LTP zone, the LTD zone and no man's land," *The Journal of Physiology,* vol. 532, no. 2, pp. 285-285, 2001.

[102] H. Misonou, D. P. Mohapatra, E. W. Park, V. Leung, D. Zhen, K. Misonou, A. E. Anderson, and J. S. Trimmer, "Regulation of ion channel localization and phosphorylation by neuronal activity," *Nature Neuroscience,* vol. 7, no. 7, pp. 711-718, 2004.

[103] H. Monai, M. Ohkura, M. Tanaka, Y. Oe, A. Konno, H. Hirai, K. Mikoshiba, S. Itohara, J. Nakai, and Y. Iwai, "Calcium imaging reveals glial involvement in transcranial direct current stimulation-induced plasticity in mouse brain," *Nature Communications,* vol. 7, pp. 11100, 2016.

[104] M. D. M. V. Lugon, G. Batsikadze, S. Fresnoza, J. Grundey, M.-F. Kuo, W. Paulus, E. M. Nakamura-Palacios, and M. A. Nitsche, "Mechanisms of nicotinic modulation of glutamatergic neuroplasticity in humans," *Cerebral Cortex,* vol. 27, no. 1, pp. 544-553, 2015.

[105] D. P. Purpura, and J. G. McMurtry, "Intracellular activities and evoked potential changes during polarization of motor cortex," *Journal of Neurophysiology,* vol. 28, no. 1, pp. 166-185, 1965.

[106] P. Y. Chhatbar, R. Chen, R. Deardorff, B. Dellenbach, S. A. Kautz, M. S. George, and W. Feng, "Safety and tolerability of transcranial direct current stimulation to stroke patients–a phase I current escalation study," *Brain Stimulation: Basic, Translational, and Clinical Research in Neuromodulation,* vol. 10, no. 3, pp. 553-559, 2017.

[107] B. Guleyupoglu, N. Febles, P. Minhas, C. Hahn, and M. Bikson, "Reduced discomfort during high-definition transcutaneous stimulation using 6% benzocaine," *Frontiers in Neuroengineering,* vol. 7, 2014.

[108] M. Ridding, and U. Ziemann, "Determinants of the induction of cortical plasticity by non-invasive brain stimulation in healthy subjects," *The Journal of Physiology,* vol. 588, no. 13, pp. 2291-2304, 2010.

[109] L. M. Li, K. Uehara, and T. Hanakawa, "The contribution of interindividual factors to variability of response in transcranial direct current stimulation studies," *Frontiers in Cellular Neuroscience,* vol. 9, pp. 181, 2015.

[110] P. Minhas, M. Bikson, A. J. Woods, A. R. Rosen, and S. K. Kessler, "Transcranial direct current stimulation in pediatric brain: a computational modeling study." pp. 859-862.

[111] A. Datta, J. M. Baker, M. Bikson, and J. Fridriksson, “Individualized model predicts brain current flow during transcranial direct-current stimulation treatment in responsive stroke patient,” *Brain Stimulation,* vol. 4, no. 3, pp. 169-174, 2011.
[112] A. Datta, V. Bansal, J. Diaz, J. Patel, D. Reato, and M. Bikson, “Gyri-precise head model of transcranial direct current stimulation: improved spatial focality using a ring electrode versus conventional rectangular pad,” *Brain Stimulation,* vol. 2, no. 4, pp. 201-207. e1, 2009.
[113] V. Moliadze, E. Lyzhko, T. Schmanke, S. Andreas, C. Freitag, and M. Siniatchkin, “Transcranial direct current stimulation in healthy children and adolescents: Does age matter,” *Brain Stimulation: Basic, Translational, and Clinical Research in Neuromodulation,* vol. 10, no. 2, pp. 515, 2017.
[114] V. Moliadze, E. Lyzhko, T. Schmanke, S. Andreas, C. M. Freitag, and M. Siniatchkin, “1 mA cathodal tDCS shows excitatory effects in children and adolescents: Insights from TMS evoked N100 potential,” *Brain Research Bulletin,* vol. 140, pp. 43-51, Jun, 2018.
[115] H. Fujiyama, J. Hyde, M. R. Hinder, S.-J. Kim, G. H. McCormack, J. C. Vickers, and J. J. Summers, “Delayed plastic responses to anodal tDCS in older adults,” *Frontiers in Aging Neuroscience,* vol. 6, pp. 115, 2014.
[116] M. A. Nitsche, and W. Paulus, “Excitability changes induced in the human motor cortex by weak transcranial direct current stimulation,” *J Physiol,* vol. 527 Pt 3, pp. 633-9, Sep 15, 2000.
[117] C. Allman, U. Amadi, A. M. Winkler, L. Wilkins, N. Filippini, U. Kischka, C. J. Stagg, and H. Johansen-Berg, “Ipsilesional anodal tDCS enhances the functional benefits of rehabilitation in patients after stroke,” *Science translational medicine,* vol. 8, no. 330, pp. 330re1-330re1, 2016.
[118] A. Schoellmann, M. Scholten, B. Wasserka, R. B. Govindan, R. Krüger, A. Gharabaghi, C. Plewnia, and D. Weiss, “Anodal tDCS modulates cortical activity and synchronization in Parkinson's disease depending on motor processing,” *NeuroImage: Clinical,* vol. 22, pp. 101689, 2019/01/01/, 2019.
[119] A. R. Brunoni, A. H. Moffa, B. Sampaio-Junior, L. Borrione, M. L. Moreno, R. A. Fernandes, B. P. Veronezi, B. S. Nogueira, L. V. M. Aparicio, L. B. Razza, R. Chamorro, L. C. Tort, R. Fraguas, P. A. Lotufo, W. F. Gattaz, F. Fregni, and I. M. Benseñor, “Trial of Electrical Direct-Current Therapy versus Escitalopram for Depression,” *New England Journal of Medicine,* vol. 376, no. 26, pp. 2523-2533, 2017.
[120] J.-P. Lefaucheur, A. Antal, S. S. Ayache, D. H. Benninger, J. Brunelin, F. Cogiamanian, M. Cotelli, D. De Ridder, R. Ferrucci, B. Langguth, P. Marangolo, V. Mylius, M. A. Nitsche, F. Padberg, U. Palm, E. Poulet, A. Priori, S. Rossi, M. Schecklmann, S. Vanneste, U. Ziemann, L. Garcia-Larrea, and W. Paulus, “Evidence-based guidelines on the therapeutic use of transcranial direct current stimulation (tDCS),” *Clinical Neurophysiology,* vol. 128, no. 1, pp. 56-92, 2017/01/01/, 2017.
[121] J. Lisman, “A mechanism for the Hebb and the anti-Hebb processes underlying learning and memory,” *Proceedings of the National Academy of Sciences,* vol. 86, no. 23, pp. 9574-9578, 1989.
[122] K. G. Reymann, and J. U. Frey, “The late maintenance of hippocampal LTP: requirements, phases, 'synaptic tagging', 'late-associativity' and implications,” *Neuropharmacology,* vol. 52, no. 1, pp. 24-40, Jan, 2007.
[123] C. A. Vickers, K. S. Dickson, and D. J. Wyllie, “Induction and maintenance of late-phase long-term potentiation in isolated dendrites of rat hippocampal CA1 pyramidal neurones,” *J Physiol,* vol. 568, no. Pt 3, pp. 803-13, Nov 1, 2005.
[124] T. Ahmed, D. Blum, S. Burnouf, D. Demeyer, V. Buee-Scherrer, R. D'Hooge, L. Buee, and D. Balschun, “Rescue of impaired late-phase long-term depression in a tau transgenic mouse model,” *Neurobiol Aging,* vol. 36, no. 2, pp. 730-9, Feb, 2015.

[125] K. Fricke, A. A. Seeber, N. Thirugnanasambandam, W. Paulus, M. A. Nitsche, and J. C. Rothwell, "Time course of the induction of homeostatic plasticity generated by repeated transcranial direct current stimulation of the human motor cortex," *Journal of Neurophysiology,* vol. 105, no. 3, pp. 1141-1149, 2011.

[126] K. K. Monte-Silva, M.-F. Kuo, D. Liebetanz, W. Paulus, and M. A. Nitsche, "Shaping the optimal repetition interval for cathodal transcranial direct current stimulation (tDCS)," *Journal of neurophysiology*, 2010.

[127] T. V. Perneger, "What's wrong with Bonferroni adjustments," *Bmj,* vol. 316, no. 7139, pp. 1236-1238, 1998.

[128] Y. Y. Huang, C. Pittenger, and E. R. Kandel, "A form of long-lasting, learning-related synaptic plasticity in the hippocampus induced by heterosynaptic low-frequency pairing," *Proc Natl Acad Sci U S A,* vol. 101, no. 3, pp. 859-64, Jan 20, 2004.

[129] O. L. Gamboa, A. Antal, B. Laczo, V. Moliadze, M. A. Nitsche, and W. Paulus, "Impact of repetitive theta burst stimulation on motor cortex excitability," *Brain Stimul,* vol. 4, no. 3, pp. 145-51, Jul, 2011.

[130] M. R. Goldsworthy, J. B. Pitcher, and M. C. Ridding, "The application of spaced theta burst protocols induces long-lasting neuroplastic changes in the human motor cortex," *Eur J Neurosci,* vol. 35, no. 1, pp. 125-34, Jan, 2012.

[131] M. R. Goldsworthy, J. B. Pitcher, and M. C. Ridding, "Neuroplastic modulation of inhibitory motor cortical networks by spaced theta burst stimulation protocols," *Brain Stimul,* vol. 6, no. 3, pp. 340-5, May, 2013.

[132] T. Nyffeler, P. Wurtz, H. R. Luscher, C. W. Hess, W. Senn, T. Pflugshaupt, R. von Wartburg, M. Luthi, and R. M. Muri, "Extending lifetime of plastic changes in the human brain," *Eur J Neurosci,* vol. 24, no. 10, pp. 2961-6, Nov, 2006.

[133] T. Nyffeler, D. Cazzoli, C. W. Hess, and R. M. Müri, "One session of repeated parietal theta burst stimulation trains induces long-lasting improvement of visual neglect," *Stroke,* vol. 40, no. 8, pp. 2791-2796, 2009.

[134] D. Cazzoli, R. M. Muri, R. Schumacher, S. von Arx, S. Chaves, K. Gutbrod, S. Bohlhalter, D. Bauer, T. Vanbellingen, M. Bertschi, S. Kipfer, C. R. Rosenthal, C. Kennard, C. L. Bassetti, and T. Nyffeler, "Theta burst stimulation reduces disability during the activities of daily living in spatial neglect," *Brain,* vol. 135, no. Pt 11, pp. 3426-39, Nov, 2012.

[135] Y. Shinoda, Y. Kamikubo, Y. Egashira, K. Tominaga-Yoshino, and A. Ogura, "Repetition of mGluR-dependent LTD causes slowly developing persistent reduction in synaptic strength accompanied by synapse elimination," *Brain Res,* vol. 1042, no. 1, pp. 99-107, Apr 25, 2005.

[136] M. A. Nitsche, F. Muller-Dahlhaus, W. Paulus, and U. Ziemann, "The pharmacology of neuroplasticity induced by non-invasive brain stimulation: building models for the clinical use of CNS active drugs," *J Physiol,* vol. 590, no. 19, pp. 4641-62, Oct 1, 2012.

[137] A. R. Brunoni, F. Fregni, and R. L. Pagano, "Translational research in transcranial direct current stimulation (tDCS): a systematic review of studies in animals," *Rev Neurosci,* vol. 22, no. 4, pp. 471-81, 2011.

[138] S. Sajikumar, and J. U. Frey, "Anisomycin inhibits the late maintenance of long-term depression in rat hippocampal slices in vitro," *Neurosci Lett,* vol. 338, no. 2, pp. 147-50, Feb 27, 2003.

[139] S. J. Pelletier, and F. Cicchetti, "Cellular and molecular mechanisms of action of transcranial direct current stimulation: evidence from in vitro and in vivo models," *The international journal of neuropsychopharmacology,* vol. 18, no. 2, pp. pyu047, 2014.

[140] D. Manahan-Vaughan, A. Kulla, and J. U. Frey, "Requirement of Translation But Not Transcription for the Maintenance of Long-Term Depression in the CA1 Region of Freely Moving Rats," *The Journal of Neuroscience,* vol. 20, no. 22, pp. 8572-8576, 2000.

[141] G. L. Collingridge, S. Peineau, J. G. Howland, and Y. T. Wang, "Long-term depression in the CNS," *Nat Rev Neurosci,* vol. 11, no. 7, pp. 459-73, Jul, 2010.
[142] J. Lisman, "Glutamatergic synapses are structurally and biochemically complex because of multiple plasticity processes: long-term potentiation, long-term depression, short-term potentiation and scaling," *Philosophical transactions of the Royal Society of London. Series B, Biological sciences,* vol. 372, no. 1715, pp. 20160260, 2017.
[143] M. Nitsche, K. Fricke, U. Henschke, A. Schlitterlau, D. Liebetanz, N. Lang, S. Henning, F. Tergau, and W. Paulus, "Pharmacological modulation of cortical excitability shifts induced by transcranial direct current stimulation in humans," *The Journal of Physiology,* vol. 553, no. 1, pp. 293-301, 2003.
[144] E. M. Wexler, and P. K. Stanton, "Priming of homosynaptic long-term depression in hippocampus by previous synaptic activity," *Neuroreport: An International Journal for the Rapid Communication of Research in Neuroscience*, 1993.
[145] E. L. Bienenstock, L. N. Cooper, and P. W. Munro, "Theory for the development of neuron selectivity: orientation specificity and binocular interaction in visual cortex," *J Neurosci,* vol. 2, no. 1, pp. 32-48, Jan, 1982.
[146] H. R. Siebner, N. Lang, V. Rizzo, M. A. Nitsche, W. Paulus, R. N. Lemon, and J. C. Rothwell, "Preconditioning of Low-Frequency Repetitive Transcranial Magnetic Stimulation with Transcranial Direct Current Stimulation: Evidence for Homeostatic Plasticity in the Human Motor Cortex," *The Journal of Neuroscience,* vol. 24, no. 13, pp. 3379-3385, 2004.
[147] M. F. Kuo, W. Paulus, and M. A. Nitsche, "Boosting focally-induced brain plasticity by dopamine," *Cereb Cortex,* vol. 18, no. 3, pp. 648-51, Mar, 2008.
[148] S. Fresnoza, W. Paulus, M. A. Nitsche, and M.-F. Kuo, "Nonlinear Dose-Dependent Impact of D1 Receptor Activation on Motor Cortex Plasticity in Humans," *The Journal of Neuroscience,* vol. 34, no. 7, pp. 2744-2753, 2014.
[149] M. F. Kuo, W. Paulus, and M. A. Nitsche, "Sex differences in cortical neuroplasticity in humans," *Neuroreport,* vol. 17, no. 16, pp. 1703-7, Nov 6, 2006.
[150] M.-S. Rioult-Pedotti, D. Friedman, G. Hess, and J. P. Donoghue, "Strengthening of horizontal cortical connections following skill learning," *Nature Neuroscience,* vol. 1, no. 3, 1998.
[151] D. E. Feldman, "Synaptic mechanisms for plasticity in neocortex," *Annual Review of Neuroscience,* vol. 32, pp. 33-55, 2009.
[152] A. J. Woods, A. Antal, M. Bikson, P. S. Boggio, A. R. Brunoni, P. Celnik, L. G. Cohen, F. Fregni, C. S. Herrmann, and E. S. Kappenman, "A technical guide to tDCS, and related non-invasive brain stimulation tools," *Clinical neurophysiology,* vol. 127, no. 2, pp. 1031-1048, 2016.
[153] K. Cho, J. P. Aggleton, M. Brown, and Z. Bashir, "An experimental test of the role of postsynaptic calcium levels in determining synaptic strength using perirhinal cortex of rat," *The Journal of Physiology,* vol. 532, no. 2, pp. 459-466, 2001.
[154] M. Mosayebi Samani, D. Agboada, A. Jamil, M.-F. Kuo, and M. A. Nitsche, "Titrating the neuroplastic effects of cathodal transcranial direct current stimulation (tDCS) over the primary motor cortex " *Cortex,* vol. In Press, 2019.
[155] B. Holmes, R. Brogden, R. Heel, T. Speight, and G. Avery, "Flunarizine," *Drugs,* vol. 27, no. 1, pp. 6-44, 1984.
[156] T. V. Perneger, "What's wrong with Bonferroni adjustments," *Bmj,* vol. 316, no. 7139, pp. 1236-8, Apr 18, 1998.
[157] L. J. Bindman, O. Lippold, and J. Redfearn, "The action of brief polarizing currents on the cerebral cortex of the rat (1) during current flow and (2) in the production of long-lasting after-effects," *The Journal of physiology,* vol. 172, no. 3, pp. 369-382, 1964.

[158] L. J. Bindman, O. C. J. Lippold, and J. W. T. Redfearn, “Long-lasting Changes in the Level of the Electrical Activity of the Cerebral Cortex produced by Polarizing Currents,” *Nature,* vol. 196, no. 4854, pp. 584-585, 1962/11/01, 1962.
[159] C. A. Terzuolo, and T. H. Bullock, “MEASUREMENT OF IMPOSED VOLTAGE GRADIENT ADEQUATE TO MODULATE NEURONAL FIRING,” *Proceedings of the National Academy of Sciences of the United States of America,* vol. 42, no. 9, pp. 687-694, 1956.
[160] D. Reato, A. Rahman, M. Bikson, and L. C. Parra, “Low-intensity electrical stimulation affects network dynamics by modulating population rate and spike timing,” *The Journal of neuroscience : the official journal of the Society for Neuroscience,* vol. 30, no. 45, pp. 15067-15079, 2010.
[161] M. Bikson, M. Inoue, H. Akiyama, J. K. Deans, J. E. Fox, H. Miyakawa, and J. G. Jefferys, “Effects of uniform extracellular DC electric fields on excitability in rat hippocampal slices in vitro,” *J Physiol,* vol. 557, no. Pt 1, pp. 175-90, May 15, 2004.
[162] O. D. Creutzfeldt, G. H. Fromm, and H. Kapp, “Influence of transcortical d-c currents on cortical neuronal activity,” *Experimental Neurology,* vol. 5, no. 6, pp. 436-452, 1962/06/01/, 1962.
[163] N. Islam, M. Aftabuddin, A. Moriwaki, Y. Hattori, and Y. Hori, “Increase in the calcium level following anodal polarization in the rat brain,” *Brain Res,* vol. 684, no. 2, pp. 206-8, Jul 3, 1995.
[164] V. A. Aroniadou, and A. Keller, “Mechanisms of LTP induction in rat motor cortex in vitro,” *Cerebral Cortex,* vol. 5, no. 4, pp. 353-362, 1995.
[165] M. A. Castro-Alamancos, J. P. Donoghue, and B. W. Connors, “Different forms of synaptic plasticity in somatosensory and motor areas of the neocortex,” *Journal of Neuroscience,* vol. 15, no. 7, pp. 5324-5333, 1995.
[166] M. Bennett, “The concept of long term potentiation of transmission at synapses,” *Progress in neurobiology,* vol. 60, no. 2, pp. 109-137, 2000.
[167] M. A. Nitsche, W. Jaussi, D. Liebetanz, N. Lang, F. Tergau, and W. Paulus, “Consolidation of human motor cortical neuroplasticity by D-cycloserine,” *Neuropsychopharmacology,* vol. 29, no. 8, pp. 1573-8, Aug, 2004.
[168] V. P. Clark, B. A. Coffman, M. C. Trumbo, and C. Gasparovic, “Transcranial direct current stimulation (tDCS) produces localized and specific alterations in neurochemistry: a (1)H magnetic resonance spectroscopy study,” *Neurosci Lett,* vol. 500, no. 1, pp. 67-71, Aug 1, 2011.
[169] C. J. Stagg, J. G. Best, M. C. Stephenson, J. O'Shea, M. Wylezinska, Z. T. Kincses, P. G. Morris, P. M. Matthews, and H. Johansen-Berg, “Polarity-sensitive modulation of cortical neurotransmitters by transcranial stimulation,” *J Neurosci,* vol. 29, no. 16, pp. 5202-6, Apr 22, 2009.
[170] D. Antonenko, A. Thielscher, G. B. Saturnino, S. Aydin, B. Ittermann, U. Grittner, and A. Flöel, “Towards precise brain stimulation: Is electric field simulation related to neuromodulation?,” *Brain Stimulation: Basic, Translational, and Clinical Research in Neuromodulation*, 2019.
[171] M. A. Nitsche, A. Seeber, K. Frommann, C. C. Klein, C. Rochford, M. S. Nitsche, K. Fricke, D. Liebetanz, N. Lang, A. Antal, W. Paulus, and F. Tergau, “Modulating parameters of excitability during and after transcranial direct current stimulation of the human motor cortex,” *The Journal of physiology,* vol. 568, no. Pt 1, pp. 291-303, 2005.
[172] M. Biabani, M. Aminitehrani, M. Zoghi, M. Farrell, G. Egan, and S. Jaberzadeh, “The effects of transcranial direct current stimulation on short-interval intracortical inhibition and intracortical facilitation: a systematic review and meta-analysis,” *Rev Neurosci,* vol. 29, no. 1, pp. 99-114, Jan 26, 2018.
[173] S. N. Yang, Y. G. Tang, and R. S. Zucker, “Selective induction of LTP and LTD by postsynaptic [Ca2+]i elevation,” *J Neurophysiol,* vol. 81, no. 2, pp. 781-7, Feb, 1999.

[174] S. H. Doeltgen, and M. C. Ridding, "Low-intensity, short-interval theta burst stimulation modulates excitatory but not inhibitory motor networks," *Clin Neurophysiol,* vol. 122, no. 7, pp. 1411-6, Jul, 2011.
[175] T. Sasaki, S. Kodama, N. Togashi, Y. Shirota, Y. Sugiyama, S.-i. Tokushige, S. Inomata-Terada, Y. Terao, Y. Ugawa, and M. Hamada, "The intensity of continuous theta burst stimulation, but not the waveform used to elicit motor evoked potentials, influences its outcome in the human motor cortex," *Brain Stimulation,* vol. 11, no. 2, pp. 400-410, 2018/03/01/, 2018.
[176] V. Moliadze, D. Atalay, A. Antal, and W. Paulus, "Close to threshold transcranial electrical stimulation preferentially activates inhibitory networks before switching to excitation with higher intensities," *Brain Stimul,* vol. 5, no. 4, pp. 505-11, Oct, 2012.
[177] M. Wischnewski, M. Engelhardt, A. Salehinejad, D. Schutter, M. Kuo, and M. Nitsche, "Motor cortex plasticity induced by beta transcranial alternating current stimulation," *Brain Stimulation: Basic, Translational, and Clinical Research in Neuromodulation,* vol. 12, no. 2, pp. 446-447, 2019.
[178] U. Ziemann, W. Paulus, M. A. Nitsche, A. Pascual-Leone, W. D. Byblow, A. Berardelli, H. R. Siebner, J. Classen, L. G. Cohen, and J. C. Rothwell, "Consensus: motor cortex plasticity protocols," *Brain stimulation,* vol. 1, no. 3, pp. 164-182, 2008.
[179] T. Kunze, A. Hunold, J. Haueisen, V. Jirsa, and A. Spiegler, "Transcranial direct current stimulation changes resting state functional connectivity: A large-scale brain network modeling study," *Neuroimage,* vol. 140, pp. 174-87, Oct 15, 2016.
[180] A. Datta, V. Bansal, J. Diaz, J. Patel, D. Reato, and M. Bikson, "Gyri-precise head model of transcranial direct current stimulation: improved spatial focality using a ring electrode versus conventional rectangular pad," *Brain Stimul,* vol. 2, no. 4, pp. 201-7, 207.e1, Oct, 2009.
[181] R. Polanía, M. A. Nitsche, and C. C. Ruff, "Studying and modifying brain function with non-invasive brain stimulation," *Nature Neuroscience,* vol. 21, no. 2, pp. 174-187, 2018/02/01, 2018.
[182] K. E. Hoy, S. L. Arnold, M. R. Emonson, Z. J. Daskalakis, and P. B. Fitzgerald, "An investigation into the effects of tDCS dose on cognitive performance over time in patients with schizophrenia," *Schizophr Res,* vol. 155, no. 1-3, pp. 96-100, May, 2014.
[183] D. Agboada, M. Mosayebi Samani, A. Jamil, M.-F. Kuo, and M. A. Nitsche, "Expanding the parameter space of anodal transcranial direct current stimulation of the primary motor cortex," *Scientific Reports,* vol. 9, no. 1, pp. 18185, 2019/12/03, 2019.
[184] D. Agboada, M. Mosayebi-Samani, M.-F. Kuo, and M. A. Nitsche, "Induction of long-term potentiation-like plasticity in the primary motor cortex with repeated anodal transcranial direct current stimulation – better effects with intensified protocols?," *Brain Stimulation*, 2020/04/21/, 2020.
[185] M. Hamada, N. Murase, A. Hasan, M. Balaratnam, and J. C. Rothwell, "The role of interneuron networks in driving human motor cortical plasticity," *Cereb Cortex,* vol. 23, no. 7, pp. 1593-605, Jul, 2013.
[186] A. Opitz, A. Falchier, C. G. Yan, E. M. Yeagle, G. S. Linn, P. Megevand, A. Thielscher, A. R. Deborah, M. P. Milham, A. D. Mehta, and C. E. Schroeder, "Spatiotemporal structure of intracranial electric fields induced by transcranial electric stimulation in humans and nonhuman primates," *Sci Rep,* vol. 6, pp. 31236, Aug 18, 2016.
[187] Y. Huang, A. A. Liu, B. Lafon, D. Friedman, M. Dayan, X. Wang, M. Bikson, W. K. Doyle, O. Devinsky, and L. C. Parra, "Measurements and models of electric fields in the in vivo human brain during transcranial electric stimulation," vol. 6, Feb 7, 2017.
[188] C. Evans, C. Bachmann, J. S. A. Lee, E. Gregoriou, N. Ward, and S. Bestmann, "Dose-controlled tDCS reduces electric field intensity variability at a cortical target site," *Brain Stimulation,* vol. 13, no. 1, pp. 125-136, 2020/01/01/, 2020.

[189] M. Ferdjallah, F. X. Bostick, Jr., and R. E. Barr, "Potential and current density distributions of cranial electrotherapy stimulation (CES) in a four-concentric-spheres model," *IEEE Trans Biomed Eng,* vol. 43, no. 9, pp. 939-43, Sep, 1996.
[190] S. Rush, and D. A. Driscoll, "Current distribution in the brain from surface electrodes," *Anesth Analg,* vol. 47, no. 6, pp. 717-23, Nov-Dec, 1968.
[191] P. C. Miranda, A. Mekonnen, R. Salvador, and G. Ruffini, "The electric field in the cortex during transcranial current stimulation," *Neuroimage,* vol. 70, pp. 48-58, Apr 15, 2013.
[192] A. Datta, X. Zhou, Y. Su, L. C. Parra, and M. Bikson, "Validation of finite element model of transcranial electrical stimulation using scalp potentials: implications for clinical dose," *J Neural Eng,* vol. 10, no. 3, pp. 036018, Jun, 2013.
[193] M. Windhoff, A. Opitz, and A. Thielscher, "Electric field calculations in brain stimulation based on finite elements: an optimized processing pipeline for the generation and usage of accurate individual head models," *Hum Brain Mapp,* vol. 34, no. 4, pp. 923-35, Apr, 2013.
[194] Y.-J. Jung, J.-H. Kim, and C.-H. Im, "COMETS: A MATLAB toolbox for simulating local electric fields generated by transcranial direct current stimulation (tDCS)," *Biomedical Engineering Letters,* vol. 3, no. 1, pp. 39-46, 2013/03/01, 2013.
[195] F. S. Salinas, J. L. Lancaster, and P. T. Fox, "3D modeling of the total electric field induced by transcranial magnetic stimulation using the boundary element method," *Phys Med Biol,* vol. 54, no. 12, pp. 3631-47, Jun 21, 2009.
[196] S. Turovets, and V. Volkov, "A 3D finite-difference BiCG iterative solver with the Fourier-Jacobi preconditioner for the anisotropic EIT/EEG forward problem," vol. 2014, pp. 426902, 2014.
[197] S. S. Shahid, M. Bikson, H. Salman, P. Wen, and T. Ahfock, "The value and cost of complexity in predictive modelling: role of tissue anisotropic conductivity and fibre tracts in neuromodulation," *Journal of Neural Engineering,* vol. 11, no. 3, pp. 036002, 2014.
[198] A. S. Aberra, B. Wang, W. M. Grill, and A. V. Peterchev, "Simulation of transcranial magnetic stimulation in head model with morphologically-realistic cortical neurons," *Brain Stimulation,* vol. 13, no. 1, pp. 175-189, 2020/01/01/, 2020.
[199] S. Joucla, A. Glière, and B. Yvert, "Current approaches to model extracellular electrical neural microstimulation," *Frontiers in Computational Neuroscience,* vol. 8, no. 13, 2014-February-19, 2014.
[200] H. S. Suh, W. H. Lee, and T. S. Kim, "Influence of anisotropic conductivity in the skull and white matter on transcranial direct current stimulation via an anatomically realistic finite element head model," *Phys Med Biol,* vol. 57, no. 21, pp. 6961-80, Nov 7, 2012.
[201] Y. Huang, A. Datta, M. Bikson, and L. C. Parra, "Realistic volumetric-approach to simulate transcranial electric stimulation-ROAST-a fully automated open-source pipeline," *J Neural Eng,* vol. 16, no. 5, pp. 056006, Jul 30, 2019.
[202] S. Wagner, S. M. Rampersad, U. Aydin, J. Vorwerk, T. F. Oostendorp, T. Neuling, C. S. Herrmann, D. F. Stegeman, and C. H. Wolters, "Investigation of tDCS volume conduction effects in a highly realistic head model," *J Neural Eng,* vol. 11, no. 1, pp. 016002, Feb, 2014.
[203] G. Saturnino, A. Antunes, J. Stelzer, and A. Thielscher, "SimNIBS: a versatile toolbox for simulating fields generated by transcranial brain stimulation."
[204] J. H. Kim, D. W. Kim, W. H. Chang, Y. H. Kim, K. Kim, and C. H. Im, "Inconsistent outcomes of transcranial direct current stimulation may originate from anatomical differences among individuals: electric field simulation using individual MRI data," *Neurosci Lett,* vol. 564, pp. 6-10, Apr 3, 2014.
[205] S. Bestmann, and J. W. Krakauer, "The uses and interpretations of the motor-evoked potential for understanding behaviour," *Exp Brain Res,* vol. 233, no. 3, pp. 679-89, Mar, 2015.

[206] J. Reis, O. B. Swayne, Y. Vandermeeren, M. Camus, M. A. Dimyan, M. Harris-Love, M. A. Perez, P. Ragert, J. C. Rothwell, and L. G. Cohen, "Contribution of transcranial magnetic stimulation to the understanding of cortical mechanisms involved in motor control," *The Journal of physiology,* vol. 586, no. 2, pp. 325-351, 2008.
[207] K. Weise, O. Numssen, A. Thielscher, G. Hartwigsen, and T. R. Knösche, "A novel approach to localize cortical TMS effects," *NeuroImage,* vol. 209, pp. 116486, 2020/04/01/, 2020.
[208] R. Salvador, C. Wenger, and P. C. Miranda, "Investigating the cortical regions involved in MEP modulation in tDCS," *Frontiers in cellular neuroscience,* vol. 9, pp. 405-405, 2015.
[209] R. Salvador, S. Silva, P. J. Basser, and P. C. Miranda, "Determining which mechanisms lead to activation in the motor cortex: A modeling study of transcranial magnetic stimulation using realistic stimulus waveforms and sulcal geometry," *Clinical Neurophysiology,* vol. 122, no. 4, pp. 748-758, 2011/04/01/, 2011.
[210] S. K. Esser, S. L. Hill, and G. Tononi, "Modeling the effects of transcranial magnetic stimulation on cortical circuits," *J Neurophysiol,* vol. 94, no. 1, pp. 622-39, Jul, 2005.
[211] G. G. Ambrus, H. Al-Moyed, L. Chaieb, L. Sarp, A. Antal, and W. Paulus, "The fade-in--short stimulation--fade out approach to sham tDCS--reliable at 1 mA for naive and experienced subjects, but not investigators," *Brain Stimul,* vol. 5, no. 4, pp. 499-504, Oct, 2012.
[212] P. C. Gandiga, F. C. Hummel, and L. G. Cohen, "Transcranial DC stimulation (tDCS): a tool for double-blind sham-controlled clinical studies in brain stimulation," *Clin Neurophysiol,* vol. 117, no. 4, pp. 845-50, Apr, 2006.
[213] J. Ashburner, K. Friston, and W. Penny, "Chapter 35 - Image Segmentation," *Human Brain Function (Second Edition)*, R. S. J. Frackowiak, K. J. Friston, C. D. Frith, R. J. Dolan, C. J. Price, S. Zeki, J. T. Ashburner and W. D. Penny, eds., pp. 695-706, Burlington: Academic Press, 2004.
[214] Y. Huang, J. P. Dmochowski, Y. Su, A. Datta, C. Rorden, and L. C. Parra, "Automated MRI segmentation for individualized modeling of current flow in the human head," *J Neural Eng,* vol. 10, no. 6, pp. 066004, Dec, 2013.
[215] J. J. Timmons, E. Lok, P. San, K. Bui, and E. T. Wong, "End-to-end workflow for finite element analysis of tumor treating fields in glioblastomas," *Phys Med Biol,* vol. 62, no. 21, pp. 8264-8282, Oct 12, 2017.
[216] C. Rorden, and M. Brett, "Stereotaxic display of brain lesions," *Behav Neurol,* vol. 12, no. 4, pp. 191-200, 2000.
[217] T. Wagner, F. Fregni, S. Fecteau, A. Grodzinsky, M. Zahn, and A. Pascual-Leone, "Transcranial direct current stimulation: A computer-based human model study," *NeuroImage,* vol. 35, no. 3, pp. 1113-1124, 2007/04/15/, 2007.
[218] Z. D. Deng, S. H. Lisanby, and A. V. Peterchev, "Electric field depth-focality tradeoff in transcranial magnetic stimulation: simulation comparison of 50 coil designs," *Brain Stimul,* vol. 6, no. 1, pp. 1-13, Jan, 2013.
[219] A. Thielscher, and T. Kammer, "Electric field properties of two commercial figure-8 coils in TMS: calculation of focality and efficiency," *Clinical Neurophysiology,* vol. 115, no. 7, pp. 1697-1708, 2004/07/01/, 2004.
[220] P. C. Miranda, L. Correia, R. Salvador, and P. J. Basser, "Tissue heterogeneity as a mechanism for localized neural stimulation by applied electric fields," *Phys Med Biol,* vol. 52, no. 18, pp. 5603-17, Sep 21, 2007.
[221] F. S. Salinas, J. L. Lancaster, and P. T. Fox, "Detailed 3D models of the induced electric field of transcranial magnetic stimulation coils," *Physics in Medicine and Biology,* vol. 52, no. 10, pp. 2879-2892, 2007/05/01, 2007.
[222] B. J. Roth, L. G. Cohen, and M. Hallett, "The electric field induced during magnetic stimulation," *Electroencephalogr Clin Neurophysiol Suppl,* vol. 43, pp. 268-78, 1991.

[223] T. Kammer, S. Beck, A. Thielscher, U. Laubis-Herrmann, and H. Topka, "Motor thresholds in humans: a transcranial magnetic stimulation study comparing different pulse waveforms, current directions and stimulator types," *Clin Neurophysiol,* vol. 112, no. 2, pp. 250-8, Feb, 2001.
[224] A. Thielscher, and T. Kammer, "Linking physics with physiology in TMS: a sphere field model to determine the cortical stimulation site in TMS," *Neuroimage,* vol. 17, no. 3, pp. 1117-30, Nov, 2002.
[225] T. A. Wagner, M. Zahn, A. J. Grodzinsky, and A. Pascual-Leone, "Three-dimensional head model simulation of transcranial magnetic stimulation," *IEEE Trans Biomed Eng,* vol. 51, no. 9, pp. 1586-98, Sep, 2004.
[226] M. A. Pimentel, P. Vilela, I. Sousa, and P. Figueiredo, "Localization of the hand motor area by arterial spin labeling and blood oxygen level-dependent functional magnetic resonance imaging," *Hum Brain Mapp,* vol. 34, no. 1, pp. 96-108, Jan, 2013.
[227] R. Carbunaru, and D. M. Durand, "Toroidal coil models for transcutaneous magnetic simulation of nerves," *IEEE Transactions on Biomedical Engineering,* vol. 48, no. 4, pp. 434-441, 2001.
[228] D. H. Kim, G. E. Georghiou, and C. Won, "Improved field localization in transcranial magnetic stimulation of the brain with the utilization of a conductive shield plate in the stimulator," *IEEE Trans Biomed Eng,* vol. 53, no. 4, pp. 720-5, Apr, 2006.
[229] R. Salvador, P. C. Miranda, Y. Roth, and A. Zangen, "High permeability cores to optimize the stimulation of deeply located brain regions using transcranial magnetic stimulation," *Phys Med Biol,* vol. 54, no. 10, pp. 3113-28, May 21, 2009.
[230] A. Datta, D. Truong, P. Minhas, L. C. Parra, and M. Bikson, "Inter-Individual Variation during Transcranial Direct Current Stimulation and Normalization of Dose Using MRI-Derived Computational Models," *Front Psychiatry,* vol. 3, pp. 91, 2012.
[231] D. Yekutieli, and Y. Benjamini, "Resampling-based false discovery rate controlling multiple test procedures for correlated test statistics," *Journal of Statistical Planning and Inference,* vol. 82, no. 1, pp. 171-196, 1999/12/01/, 1999.
[232] Y. Benjamini, and Y. Hochberg, "Controlling the False Discovery Rate: A Practical and Powerful Approach to Multiple Testing," *Journal of the Royal Statistical Society: Series B (Methodological),* vol. 57, no. 1, pp. 289-300, 1995.
[233] A. Datta, M. Elwassif, F. Battaglia, and M. Bikson, "Transcranial current stimulation focality using disc and ring electrode configurations: FEM analysis," *J Neural Eng,* vol. 5, no. 2, pp. 163-74, Jun, 2008.
[234] M. A. Frost, and R. Goebel, "Measuring structural-functional correspondence: spatial variability of specialised brain regions after macro-anatomical alignment," *Neuroimage,* vol. 59, no. 2, pp. 1369-81, Jan 16, 2012.
[235] C. Song, D. S. Schwarzkopf, R. Kanai, and G. Rees, "Reciprocal anatomical relationship between primary sensory and prefrontal cortices in the human brain," *J Neurosci,* vol. 31, no. 26, pp. 9472-80, Jun 29, 2011.
[236] F. A. Kozel, Z. Nahas, C. deBrux, M. Molloy, J. P. Lorberbaum, D. Bohning, S. C. Risch, and M. S. George, "How coil-cortex distance relates to age, motor threshold, and antidepressant response to repetitive transcranial magnetic stimulation," *J Neuropsychiatry Clin Neurosci,* vol. 12, no. 3, pp. 376-84, Summer, 2000.
[237] J. D. Bijsterbosch, A. T. Barker, K.-H. Lee, and P. W. R. Woodruff, "Where does transcranial magnetic stimulation (TMS) stimulate? Modelling of induced field maps for some common cortical and cerebellar targets," *Medical & Biological Engineering & Computing,* vol. 50, no. 7, pp. 671-681, 2012/07/01, 2012.
[238] K. A. McConnell, Z. Nahas, A. Shastri, J. P. Lorberbaum, F. A. Kozel, D. E. Bohning, and M. S. George, "The transcranial magnetic stimulation motor threshold depends on the distance from

coil to underlying cortex: a replication in healthy adults comparing two methods of assessing the distance to cortex," *Biol Psychiatry,* vol. 49, no. 5, pp. 454-9, Mar 1, 2001.
[239] M. G. Stokes, C. D. Chambers, I. C. Gould, T. R. Henderson, N. E. Janko, N. B. Allen, and J. B. Mattingley, "Simple metric for scaling motor threshold based on scalp-cortex distance: application to studies using transcranial magnetic stimulation," *J Neurophysiol,* vol. 94, no. 6, pp. 4520-7, Dec, 2005.
[240] C. J. Stagg, and M. A. Nitsche, "Physiological basis of transcranial direct current stimulation," *Neuroscientist,* vol. 17, no. 1, pp. 37-53, Feb, 2011.
[241] S. Durand, B. Fromy, P. Bouye, J. L. Saumet, and P. Abraham, "Vasodilatation in response to repeated anodal current application in the human skin relies on aspirin-sensitive mechanisms," *J Physiol,* vol. 540, no. Pt 1, pp. 261-9, Apr 1, 2002.
[242] M. N. Berliner, "Skin microcirculation during tapwater iontophoresis in humans: cathode stimulates more than anode," *Microvasc Res,* vol. 54, no. 1, pp. 74-80, Jul, 1997.
[243] C. J. Stagg, A. Antal, and M. A. Nitsche, "Physiology of Transcranial Direct Current Stimulation," *J ect,* vol. 34, no. 3, pp. 144-152, Sep, 2018.
[244] N. Lang, H. Siebner, N. Ward, L. Lee, M. Nitsche, W. Paulus, J. Rothwell, R. Lemon, and R. Frackowiak, "How does transcranial DC stimulation of the primary motor cortex alter regional neuronal activity in the human brain?," *Eur J Neurosci,* vol. 22, no. 2, pp. 495-504, Jul 1, 2005.
[245] S. Bestmann, J. Baudewig, H. Siebner, J. Rothwell, and J. Frahm, "BOLD MRI responses to repetitive TMS over human dorsal premotor cortex," *Neuroimage,* vol. 28, no. 1, pp. 22-9, Oct 15, 2005.
[246] D. E. Callan, B. Falcone, A. Wada, and R. Parasuraman, "Simultaneous tDCS-fMRI Identifies Resting State Networks Correlated with Visual Search Enhancement," *Frontiers in human neuroscience,* vol. 10, pp. 72-72, 2016.
[247] R. Polanía, M. A. Nitsche, and W. Paulus, "Modulating functional connectivity patterns and topological functional organization of the human brain with transcranial direct current stimulation," *Human Brain Mapping,* vol. 32, no. 8, pp. 1236-1249, 2011.
[248] W. H. Lee, S. H. Lisanby, A. F. Laine, and A. V. Peterchev, "Electric Field Model of Transcranial Electric Stimulation in Nonhuman Primates: Correspondence to Individual Motor Threshold," *IEEE Trans Biomed Eng,* vol. 62, no. 9, pp. 2095-105, Sep, 2015.
[249] D. Edwards, M. Cortes, A. Datta, P. Minhas, E. M. Wassermann, and M. Bikson, "Physiological and modeling evidence for focal transcranial electrical brain stimulation in humans: a basis for high-definition tDCS," *Neuroimage,* vol. 74, pp. 266-75, Jul 1, 2013.
[250] A. Opitz, W. Legon, A. Rowlands, W. K. Bickel, W. Paulus, and W. J. Tyler, "Physiological observations validate finite element models for estimating subject-specific electric field distributions induced by transcranial magnetic stimulation of the human motor cortex," *Neuroimage,* vol. 81, pp. 253-264, Nov 1, 2013.
[251] Y. Huang, A. A. Liu, B. Lafon, D. Friedman, M. Dayan, X. Wang, M. Bikson, W. K. Doyle, O. Devinsky, and L. C. Parra, "Measurements and models of electric fields in the in vivo human brain during transcranial electric stimulation," *eLife,* vol. 6, pp. e18834, 2017/02/07, 2017.
[252] C. Goksu, L. G. Hanson, H. R. Siebner, P. Ehses, K. Scheffler, and A. Thielscher, "Human in-vivo brain magnetic resonance current density imaging (MRCDI)," *Neuroimage,* vol. 171, pp. 26-39, May 1, 2018.
[253] C. Göksu, K. Scheffler, H. R. Siebner, A. Thielscher, and L. G. Hanson, "The stray magnetic fields in Magnetic Resonance Current Density Imaging (MRCDI)," *Physica Medica,* vol. 59, pp. 142-150, 2019/03/01/, 2019.

[254] S. Shahid, P. Wen, and T. Ahfock, "Effects of model complexity and tissue anisotropic conductivity on cortical modulation during transcranial direct current stimulation," *IET Science, Measurement & Technology,* vol. 6, no. 6, pp. 464-473, 2012.
[255] D. Q. Truong, G. Magerowski, A. Pascual-Leone, M. Alonso-Alonso, and M. Bikson, "Finite Element study of skin and fat delineation in an obese subject for transcranial Direct Current Stimulation," *Conf Proc IEEE Eng Med Biol Soc,* vol. 2012, pp. 6587-90, 2012.
[256] D. Q. Truong, G. Magerowski, G. L. Blackburn, M. Bikson, and M. Alonso-Alonso, "Computational modeling of transcranial direct current stimulation (tDCS) in obesity: Impact of head fat and dose guidelines," *NeuroImage: Clinical,* vol. 2, pp. 759-766, 2013/01/01/, 2013.
[257] M. K. Metwally, S. M. Han, and T. S. Kim, "The effect of tissue anisotropy on the radial and tangential components of the electric field in transcranial direct current stimulation," *Med Biol Eng Comput,* vol. 53, no. 10, pp. 1085-101, Oct, 2015.
[258] J. D. Nielsen, K. H. Madsen, O. Puonti, H. R. Siebner, C. Bauer, C. G. Madsen, G. B. Saturnino, and A. Thielscher, "Automatic skull segmentation from MR images for realistic volume conductor models of the head: Assessment of the state-of-the-art," *Neuroimage,* vol. 174, pp. 587-598, Jul 1, 2018.
[259] M. Parazzini, S. Fiocchi, E. Rossi, A. Paglialonga, and P. Ravazzani, "Transcranial direct current stimulation: estimation of the electric field and of the current density in an anatomical human head model," *IEEE Trans Biomed Eng,* vol. 58, no. 6, pp. 1773-80, Jun, 2011.
[260] M. Mosayebi Samani, S. M. Firoozabadi, and H. Ekhtiari, "Consideration of Individual Brain Geometry and Anisotropy on the Effect of tDCS," *Iranian Journal of Medical Physics,* vol. 14, no. 4, pp. 203-218, 2017.
[261] O. Puonti, G. B. Saturnino, K. H. Madsen, and A. Thielscher, "Comparing and Validating Automated Tools for Individualized Electric Field Simulations in the Human Head," *bioRxiv*, pp. 611962, 2019.
[262] G. B. Saturnino, A. Thielscher, K. H. Madsen, T. R. Knösche, and K. Weise, "A principled approach to conductivity uncertainty analysis in electric field calculations," *NeuroImage,* vol. 188, pp. 821-834, 2019/03/01/, 2019.
[263] M. V. Jog, R. X. Smith, K. Jann, W. Dunn, B. Lafon, D. Truong, A. Wu, L. Parra, M. Bikson, and D. J. Wang, "In-vivo imaging of magnetic fields induced by transcranial direct current stimulation (tDCS) in human brain using MRI," *Scientific reports,* vol. 6, pp. 34385, 2016.
[264] M. Chauhan, A. Indahlastari, A. K. Kasinadhuni, M. Schär, T. H. Mareci, and R. J. Sadleir, "Low-Frequency Conductivity Tensor Imaging of the Human Head In Vivo Using DT-MREIT: First Study," *IEEE Transactions on Medical Imaging,* vol. 37, no. 4, pp. 966-976, 2018.
[265] Y. Huang, A. Datta, M. Bikson, and L. C. Parra, "ROAST: An Open-Source, Fully-Automated, Realistic Volumetric-Approach-Based Simulator For TES," *Conf Proc IEEE Eng Med Biol Soc,* vol. 2018, pp. 3072-3075, Jul, 2018.
[266] F. Wallois, M. Mahmoudzadeh, A. Patil, and R. Grebe, "Usefulness of simultaneous EEG–NIRS recording in language studies," *Brain and Language,* vol. 121, no. 2, pp. 110-123, 2012/05/01/, 2012.
[267] J. K. Rice, C. Rorden, J. S. Little, and L. C. Parra, "Subject position affects EEG magnitudes," *Neuroimage,* vol. 64, pp. 476-84, Jan 1, 2013.
[268] C. Spironelli, J. Busenello, and A. Angrilli, "Supine posture inhibits cortical activity: Evidence from Delta and Alpha EEG bands," *Neuropsychologia,* vol. 89, pp. 125-131, Aug, 2016.
[269] M. Mikkonen, and I. Laakso, "Effects of posture on electric fields of non-invasive brain stimulation," *Phys Med Biol,* vol. 64, no. 6, pp. 065019, Mar 14, 2019.
[270] M.-F. Kuo, W. Paulus, and M. A. Nitsche, "Sex differences in cortical neuroplasticity in humans," *Neuroreport,* vol. 17, no. 16, pp. 1703-1707, 2006.

[271] A. Indahlastari, A. Albizu, A. O'Shea, M. A. Forbes, N. R. Nissim, J. N. Kraft, N. D. Evangelista, H. K. Hausman, and A. J. Woods, "Modeling transcranial electrical stimulation in the aging brain," *Brain Stimul,* vol. 13, no. 3, pp. 664-674, May-Jun, 2020.

[272] D. B. Fischer, P. J. Fried, G. Ruffini, O. Ripolles, R. Salvador, J. Banus, W. T. Ketchabaw, E. Santarnecchi, A. Pascual-Leone, and M. D. Fox, "Multifocal tDCS targeting the resting state motor network increases cortical excitability beyond traditional tDCS targeting unilateral motor cortex," *Neuroimage,* vol. 157, pp. 34-44, Aug 15, 2017.

[273] M. Mosayebi Samani, D. Agboada, M.-F. Kuo, and M. A. Nitsche, "Probing the relevance of repeated cathodal tDCS over the primary motor cortex for prolongation of after-effects," *The Journal of Physiology,* vol. In Press, no. n/a, 2019.

[274] T. Zaehle, M. Beretta, L. Jancke, C. S. Herrmann, and P. Sandmann, "Excitability changes induced in the human auditory cortex by transcranial direct current stimulation: direct electrophysiological evidence," *Exp Brain Res,* vol. 215, no. 2, pp. 135-40, Nov, 2011.

[275] J. Dedoncker, A. R. Brunoni, C. Baeken, and M.-A. Vanderhasselt, "A Systematic Review and Meta-Analysis of the Effects of Transcranial Direct Current Stimulation (tDCS) Over the Dorsolateral Prefrontal Cortex in Healthy and Neuropsychiatric Samples: Influence of Stimulation Parameters," *Brain Stimulation,* vol. 9, no. 4, pp. 501-517, 2016/07/01/, 2016.

[276] S. Tremblay, N. C. Rogasch, I. Premoli, D. M. Blumberger, S. Casarotto, R. Chen, V. Di Lazzaro, F. Farzan, F. Ferrarelli, P. B. Fitzgerald, J. Hui, R. J. Ilmoniemi, V. K. Kimiskidis, D. Kugiumtzis, P. Lioumis, A. Pascual-Leone, M. C. Pellicciari, T. Rajji, G. Thut, R. Zomorrodi, U. Ziemann, and Z. J. Daskalakis, "Clinical utility and prospective of TMS–EEG," *Clinical Neurophysiology,* vol. 130, no. 5, pp. 802-844, 2019/05/01/, 2019.

[277] A. T. Hill, N. C. Rogasch, P. B. Fitzgerald, and K. E. Hoy, "Effects of prefrontal bipolar and high-definition transcranial direct current stimulation on cortical reactivity and working memory in healthy adults," *Neuroimage,* vol. 152, pp. 142-157, May 15, 2017.

[278] A. T. Hill, N. C. Rogasch, P. B. Fitzgerald, and K. E. Hoy, "Impact of concurrent task performance on transcranial direct current stimulation (tDCS)-Induced changes in cortical physiology and working memory," *Cortex,* vol. 113, pp. 37-57, Apr, 2019.

[279] P. C. Gordon, C. Zrenner, D. Desideri, P. Belardinelli, B. Zrenner, A. R. Brunoni, and U. Ziemann, "Modulation of cortical responses by transcranial direct current stimulation of dorsolateral prefrontal cortex: A resting-state EEG and TMS-EEG study," *Brain Stimul,* vol. 11, no. 5, pp. 1024-1032, Sep - Oct, 2018.

[280] F. Awiszus, and J. Borckardt, "TMS Motor Threshold Assessment Tool 2.0 2012. Available from: http://clinicalresearcher. org/software. htm [accessed 19.10. 2012]," 2012.

[281] W. Beam, J. J. Borckardt, S. T. Reeves, and M. S. George, "An efficient and accurate new method for locating the F3 position for prefrontal TMS applications," *Brain stimulation,* vol. 2, no. 1, pp. 50-54, 2009.

[282] U. Herwig, P. Satrapi, and C. Schonfeldt-Lecuona, "Using the international 10-20 EEG system for positioning of transcranial magnetic stimulation," *Brain Topogr,* vol. 16, no. 2, pp. 95-9, Winter, 2003.

[283] M. Fecchio, A. Pigorini, A. Comanducci, S. Sarasso, S. Casarotto, I. Premoli, C.-C. Derchi, A. Mazza, S. Russo, F. Resta, F. Ferrarelli, M. Mariotti, U. Ziemann, M. Massimini, and M. Rosanova, "The spectral features of EEG responses to transcranial magnetic stimulation of the primary motor cortex depend on the amplitude of the motor evoked potentials," *PloS one,* vol. 12, no. 9, pp. e0184910-e0184910, 2017.

[284] V. Nikouline, J. Ruohonen, and R. J. Ilmoniemi, "The role of the coil click in TMS assessed with simultaneous EEG," *Clin Neurophysiol,* vol. 110, no. 8, pp. 1325-8, Aug, 1999.

[285] E. M. ter Braack, C. C. de Vos, and M. J. van Putten, "Masking the Auditory Evoked Potential in TMS-EEG: A Comparison of Various Methods," *Brain Topogr,* vol. 28, no. 3, pp. 520-8, May, 2015.
[286] R. Oostenveld, P. Fries, E. Maris, and J.-M. Schoffelen, "FieldTrip: open source software for advanced analysis of MEG, EEG, and invasive electrophysiological data," *Computational intelligence and neuroscience,* vol. 2011, 2011.
[287] R. J. Ilmoniemi, and D. Kicic, "Methodology for combined TMS and EEG," *Brain Topogr,* vol. 22, no. 4, pp. 233-48, Jan, 2010.
[288] T. P. Mutanen, M. Kukkonen, J. O. Nieminen, M. Stenroos, J. Sarvas, and R. J. Ilmoniemi, "Recovering TMS-evoked EEG responses masked by muscle artifacts," *Neuroimage,* vol. 139, pp. 157-166, Oct 1, 2016.
[289] M. Biabani, A. Fornito, T. P. Mutanen, J. Morrow, and N. C. Rogasch, "Characterizing and minimizing the contribution of sensory inputs to TMS-evoked potentials," *Brain Stimulation,* vol. 12, no. 6, pp. 1537-1552, 2019/11/01/, 2019.
[290] A. M. Dale, B. Fischl, and M. I. Sereno, "Cortical surface-based analysis. I. Segmentation and surface reconstruction," *Neuroimage,* vol. 9, no. 2, pp. 179-94, Feb, 1999.
[291] F. Tadel, S. Baillet, J. C. Mosher, D. Pantazis, and R. M. Leahy, "Brainstorm: a user-friendly application for MEG/EEG analysis," *Comput Intell Neurosci,* vol. 2011, pp. 879716, 2011.
[292] A. Gramfort, T. Papadopoulo, E. Olivi, and M. Clerc, "OpenMEEG: opensource software for quasistatic bioelectromagnetics," *BioMedical Engineering OnLine,* vol. 9, no. 1, pp. 45, 2010/09/06, 2010.
[293] J. C. Hernandez-Pavon, J. Metsomaa, T. Mutanen, M. Stenroos, H. Maki, R. J. Ilmoniemi, and J. Sarvas, "Uncovering neural independent components from highly artifactual TMS-evoked EEG data," *J Neurosci Methods,* vol. 209, no. 1, pp. 144-57, Jul 30, 2012.
[294] N. C. Rogasch, R. H. Thomson, F. Farzan, B. M. Fitzgibbon, N. W. Bailey, J. C. Hernandez-Pavon, Z. J. Daskalakis, and P. B. Fitzgerald, "Removing artefacts from TMS-EEG recordings using independent component analysis: Importance for assessing prefrontal and motor cortex network properties," *NeuroImage,* vol. 101, pp. 425-439, 2014/11/01/, 2014.
[295] N. C. Rogasch, C. Sullivan, R. H. Thomson, N. S. Rose, N. W. Bailey, P. B. Fitzgerald, F. Farzan, and J. C. Hernandez-Pavon, "Analysing concurrent transcranial magnetic stimulation and electroencephalographic data: A review and introduction to the open-source TESA software," *Neuroimage,* vol. 147, pp. 934-951, Feb 15, 2017.
[296] A. Hyvärinen, and E. Oja, "Independent component analysis: algorithms and applications," *Neural Networks,* vol. 13, no. 4, pp. 411-430, 2000/06/01/, 2000.
[297] T. Mutanen, H. Maki, and R. J. Ilmoniemi, "The effect of stimulus parameters on TMS-EEG muscle artifacts," *Brain Stimul,* vol. 6, no. 3, pp. 371-6, May, 2013.
[298] P. Lioumis, D. Kicic, P. Savolainen, J. P. Makela, and S. Kahkonen, "Reproducibility of TMS-Evoked EEG responses," *Hum Brain Mapp,* vol. 30, no. 4, pp. 1387-96, Apr, 2009.
[299] S. Komssi, and S. Kahkonen, "The novelty value of the combined use of electroencephalography and transcranial magnetic stimulation for neuroscience research," *Brain Res Rev,* vol. 52, no. 1, pp. 183-92, Aug 30, 2006.
[300] N. C. Rogasch, and P. B. Fitzgerald, "Assessing cortical network properties using TMS-EEG," *Hum Brain Mapp,* vol. 34, no. 7, pp. 1652-69, Jul, 2013.
[301] C. Tallon-Baudry, and O. Bertrand, "Oscillatory gamma activity in humans and its role in object representation," *Trends Cogn Sci,* vol. 3, no. 4, pp. 151-162, Apr, 1999.
[302] M. X. Cohen, *Analyzing neural time series data: theory and practice*: MIT press, 2014.
[303] A. R. Vandenbroucke, I. G. Sligte, J. G. de Vries, M. X. Cohen, and V. A. Lamme, "Neural Correlates of Visual Short-term Memory Dissociate between Fragile and Working Memory Representations," *J Cogn Neurosci,* vol. 27, no. 12, pp. 2477-90, Dec, 2015.

[304] M. C. Pellicciari, D. Brignani, and C. Miniussi, "Excitability modulation of the motor system induced by transcranial direct current stimulation: a multimodal approach," *Neuroimage,* vol. 83, pp. 569-80, Dec, 2013.
[305] M. Vernet, S. Bashir, W.-K. Yoo, J. M. Perez, U. Najib, and A. Pascual-Leone, "Insights on the neural basis of motor plasticity induced by theta burst stimulation from TMS-EEG," *The European journal of neuroscience,* vol. 37, no. 4, pp. 598-606, 2013.
[306] S. W. Chung, B. P. Lewis, N. C. Rogasch, T. Saeki, R. H. Thomson, K. E. Hoy, N. W. Bailey, and P. B. Fitzgerald, "Demonstration of short-term plasticity in the dorsolateral prefrontal cortex with theta burst stimulation: A TMS-EEG study," *Clin Neurophysiol,* vol. 128, no. 7, pp. 1117-1126, Jul, 2017.
[307] S. H. Doeltgen, and M. C. Ridding, "Low-intensity, short-interval theta burst stimulation modulates excitatory but not inhibitory motor networks," *Clinical Neurophysiology,* vol. 122, no. 7, pp. 1411-1416, 2011.
[308] V. Moliadze, D. Atalay, A. Antal, and W. Paulus, "Close to threshold transcranial electrical stimulation preferentially activates inhibitory networks before switching to excitation with higher intensities," *Brain Stimulation,* vol. 5, no. 4, pp. 505-511, Oct, 2012.
[309] N. C. Rogasch, C. Zipser, G. Darmani, T. P. Mutanen, M. Biabani, C. Zrenner, D. Desideri, P. Belardinelli, F. Müller-Dahlhaus, and U. Ziemann, "The effects of NMDA receptor blockade on TMS-evoked EEG potentials from prefrontal and parietal cortex," *Scientific Reports,* vol. 10, no. 1, pp. 3168, 2020/02/21, 2020.
[310] G. Darmani, T. O. Bergmann, C. Zipser, D. Baur, F. Müller-Dahlhaus, and U. Ziemann, "Effects of antiepileptic drugs on cortical excitability in humans: A TMS-EMG and TMS-EEG study," vol. 40, no. 4, pp. 1276-1289, Mar, 2019.
[311] R. J. Ilmoniemi, J. Virtanen, J. Ruohonen, J. Karhu, H. J. Aronen, R. Näätänen, and T. Katila, "Neuronal responses to magnetic stimulation reveal cortical reactivity and connectivity," *Neuroreport,* vol. 8, no. 16, pp. 3537-40, Nov 10, 1997.
[312] H. Mäki, and R. J. Ilmoniemi, "The relationship between peripheral and early cortical activation induced by transcranial magnetic stimulation," *Neurosci Lett,* vol. 478, no. 1, pp. 24-8, Jun 30, 2010.
[313] R. F. H. Cash, Y. Noda, R. Zomorrodi, N. Radhu, F. Farzan, T. K. Rajji, P. B. Fitzgerald, R. Chen, Z. J. Daskalakis, and D. M. Blumberger, "Characterization of Glutamatergic and GABAA-Mediated Neurotransmission in Motor and Dorsolateral Prefrontal Cortex Using Paired-Pulse TMS–EEG," *Neuropsychopharmacology,* vol. 42, no. 2, pp. 502-511, 2017/01/01, 2017.
[314] S. Komssi, S. Kähkönen, and R. J. Ilmoniemi, "The effect of stimulus intensity on brain responses evoked by transcranial magnetic stimulation," *Hum Brain Mapp,* vol. 21, no. 3, pp. 154-64, Mar, 2004.
[315] C. Bonato, C. Miniussi, and P. M. Rossini, "Transcranial magnetic stimulation and cortical evoked potentials: A TMS/EEG co-registration study," *Clinical Neurophysiology,* vol. 117, no. 8, pp. 1699-1707, 2006/08/01/, 2006.
[316] N. C. Rogasch, Z. J. Daskalakis, and P. B. Fitzgerald, "Mechanisms underlying long-interval cortical inhibition in the human motor cortex: a TMS-EEG study," *J Neurophysiol,* vol. 109, no. 1, pp. 89-98, Jan, 2013.
[317] B. Sutor, and J. J. Hablitz, "EPSPs in rat neocortical neurons in vitro. I. Electrophysiological evidence for two distinct EPSPs," *J Neurophysiol,* vol. 61, no. 3, pp. 607-20, Mar, 1989.
[318] B. Sutor, and J. J. Hablitz, "EPSPs in rat neocortical neurons in vitro. II. Involvement of N-methyl-D-aspartate receptors in the generation of EPSPs," *J Neurophysiol,* vol. 61, no. 3, pp. 621-34, Mar, 1989.

[319] F. Ferreri, P. Pasqualetti, S. Maatta, D. Ponzo, F. Ferrarelli, G. Tononi, E. Mervaala, C. Miniussi, and P. M. Rossini, “Human brain connectivity during single and paired pulse transcranial magnetic stimulation,” *Neuroimage,* vol. 54, no. 1, pp. 90-102, Jan 1, 2011.
[320] F. König, P. Belardinelli, C. Liang, D. Desideri, F. Müller-Dahlhaus, P. C. Gordon, C. Zipser, C. Zrenner, and U. Ziemann, “TMS-EEG signatures of glutamatergic neurotransmission in human cortex,” *bioRxiv*, pp. 555920, 2019.
[321] I. Premoli, N. Castellanos, D. Rivolta, P. Belardinelli, R. Bajo, C. Zipser, S. Espenhahn, T. Heidegger, F. Müller-Dahlhaus, and U. Ziemann, “TMS-EEG Signatures of GABAergic Neurotransmission in the Human Cortex,” *The Journal of Neuroscience,* vol. 34, no. 16, pp. 5603, 2014.
[322] B. W. Connors, R. C. Malenka, and L. R. Silva, “Two inhibitory postsynaptic potentials, and GABAA and GABAB receptor-mediated responses in neocortex of rat and cat,” *J Physiol,* vol. 406, pp. 443-68, Dec, 1988.
[323] G. Darmani, and U. Ziemann, “Pharmacophysiology of TMS-evoked EEG potentials: A mini-review,” *Brain Stimul,* vol. 12, no. 3, pp. 829-831, May-Jun, 2019.
[324] V. V. Nikulin, D. Kicić, S. Kähkönen, and R. J. Ilmoniemi, “Modulation of electroencephalographic responses to transcranial magnetic stimulation: evidence for changes in cortical excitability related to movement,” *Eur J Neurosci,* vol. 18, no. 5, pp. 1206-12, Sep, 2003.
[325] S. Bender, K. Basseler, I. Sebastian, F. Resch, T. Kammer, R. Oelkers-Ax, and M. Weisbrod, “Electroencephalographic response to transcranial magnetic stimulation in children: evidence for giant inhibitory potentials,” *Annals of neurology,* vol. 58, no. 1, pp. 58-67, 2005.
[326] M. Mosayebi-Samani, L. Melo, D. Agboada, M. F. Kuo, and M. A. Nitsche, “Ca2+ channel dynamics explain the nonlinear neuroplasticity induction by cathodal transcranial direct current stimulation over the primary motor cortex,” *work submitted for publication*, 2020.
[327] X. Du, F. S. Choa, A. Summerfelt, L. M. Rowland, J. Chiappelli, P. Kochunov, and L. E. Hong, “N100 as a generic cortical electrophysiological marker based on decomposition of TMS-evoked potentials across five anatomic locations,” *Exp Brain Res,* vol. 235, no. 1, pp. 69-81, Jan, 2017.
[328] X. Du, L. M. Rowland, A. Summerfelt, A. Wijtenburg, J. Chiappelli, K. Wisner, P. Kochunov, F.-S. Choa, and L. E. Hong, “TMS evoked N100 reflects local GABA and glutamate balance,” *Brain stimulation,* vol. 11, no. 5, pp. 1071-1079, Sep-Oct, 2018.
[329] K. Zilles, and K. Amunts, “Centenary of Brodmann's map—conception and fate,” *Nature Reviews Neuroscience,* vol. 11, no. 2, pp. 139-145, 2010.
[330] P. A. Chouinard, and T. Paus, “The primary motor and premotor areas of the human cerebral cortex,” *The neuroscientist,* vol. 12, no. 2, pp. 143-152, 2006.
[331] P. Gaspar, B. Bloch, and C. Le Moine, “D1 and D2 receptor gene expression in the rat frontal cortex: cellular localization in different classes of efferent neurons,” *Eur J Neurosci,* vol. 7, no. 5, pp. 1050-63, May 1, 1995.
[332] P. Faria, M. Hallett, and P. C. Miranda, “A finite element analysis of the effect of electrode area and inter-electrode distance on the spatial distribution of the current density in tDCS,” *Journal of neural engineering,* vol. 8, no. 6, pp. 066017-066017, 2011.
[333] S. Shahid, P. Wen, and T. Ahfock, "Effect of fat and muscle tissue conductivity on cortical currents - a tDCS study." pp. 211-215.

Erklärung

Ich versichere, dass ich die vorliegende Arbeit ohne unzulässige Hilfe Dritter und ohne Benutzung anderer als der angegebenen Hilfsmittel angefertigt habe. Die aus anderen Quellen direkt oder indirekt übernommenen Daten und Konzepte sind unter Angabe der Quelle gekennzeichnet.

Bei der Auswahl und Auswertung folgenden Materials haben mir die nachstehend aufgeführten Personen in der jeweils beschriebenen Weise unentgeltlich geholfen:

1) Unterstützung bei der Interpretation der Ergebnisse der gesamten Arbeit.
Prof. Dr.-Ing. habil. Jens Haueisen, Technische Universität Ilmenau, Fakultät für Informatik und Automatisierung, Deutschland

2) Unterstützung bei der Interpretation der Ergebnisse der gesamten Arbeit.
Prof. Dr. med. Michael A. Nitsche, Leibniz-Institut für Arbeitsforschung an der TU Dortmund (IfADo), Deutschland

Weitere Personen waren an der inhaltlich-materiellen Erstellung der vorliegenden Arbeit nicht beteiligt. Insbesondere habe ich hierfür nicht die entgeltliche Hilfe von Vermittlungs- bzw. Beratungsdiensten (Promotionsberater oder anderer Personen) in Anspruch genommen. Niemand hat von mir unmittelbar oder mittelbar geldwerte Leistungen für Arbeiten erhalten, die im Zusammenhang mit dem Inhalt der vorgelegten Dissertation stehen.

Die Arbeit wurde bisher weder im In- noch im Ausland in gleicher oder ähnlicher Form einer Prüfungsbehörde vorgelegt.

Ich bin darauf hingewiesen worden, dass die Unrichtigkeit der vorstehenden Erklärung als Täuschungsversuch angesehen wird und gemäß § 7 Abs. 10 der Promotionsordnung den Abbruch des Promotionsverfahrens zur Folge hat.

24.08.2020 Mohsen Mosayebi Samani